UNIVERSITA' DELLA CALABRIA

Dipartimento di Ingegneria per l'Ambiente e il Territorio e Ingegneria Chimica

Dottorato di Ricerca in

Ingegneria Chimica e dei Materiali

CICLO

XXVI

DEVELOPMENT OF MEMBRANE BIOREACTOR (MBR) PROCESS APPLYING NOVEL LOW FOULING MEMBRANES

Settore Scientifico Disciplinare CHIM/07 Fondamenti chimici delle tecnologie

Coordinatore: Ch.mo Prof. Raffaele Molinari

Supervisori: Ch.mo Prof. Enrico Drioli

Dott. Alberto Figoli

Prof. Jan Hoinkis

Dottorando: Dott. Shamim Ahmed Deowan

UNIVERSITÀ DELLA CALABRIA

UNIVERSITA' DELLA CALABRIA

Dipartimento di Ingegneria per l'Ambiente e il Territorio e Ingegneria Chimica

Dottorato di Ricerca in

Ingegneria Chimica e dei Materiali

CICLO

XXVI

DEVELOPMENT OF MEMBRANE BIOREACTOR (MBR) PROCESS APPLYING NOVEL LOW FOULING MEMBRANES

Settore Scientifico Disciplinare CHIM/07 Fondamenti chimici delle tecnologie

Coordinatore: Ch.mo Prof. Raffaele Molinari

Supervisori: Ch.mo Prof. Enrico Drioli

Dott. Alberto Figoli

Prof. Jan Hoinkis

Dottorando: Dott. Shamim Ahmed Deowan

Summary

Water is a part and parcel of human life. Water contaminated from industry and agriculture with heavy metal ions, pesticides, organic compounds, endocrine disruptive compounds, nutrients (phosphates, nitrates, nitrites) has to be efficiently treated to protect humans from being intoxicated with these compounds or with bacteria. Clean water as basis for health and good living conditions is too far out of reach for the majority of the population in the world (Bionexgen, 2013). Water recycling is now widely accepted as a sustainable option to respond to the general increase of the fresh water demand, water shortages and for environmental protection. Water recycling is commonly seen as one of the main options to provide remedy for water shortage caused by the increase of the water demand and draughts as well as a response to some economical and environmental drivers. The main options for wastewater recycling are industrial, irrigation, aquifer recharge and urban reuse (Pidou, M., 2006).

Among the industrial wastewaters, the textile industry is long regarded as a water intensive sector, due to its high demand of water for all parts of its procedures. Accordingly, textile wastewater includes quite a large variety of contents, chemicals, additives and different kinds of dyestuffs. The main environmental concern with this waste water is about the quantity and quality of the water discharged and the chemical load it carries. To illustrate, for each ton of fabric products, 20 – 350 m^3 of water are consumed, which differs from the color and procedure used. The quality of the textile wastewater depends much on the employed coloring matters, dyestuffs, accompanying chemicals, as well as the process itself (Brik et al., 2006).

MBR technology is recognised as a promising technology to provide water with reliable quality for reuse. It provides safely reuse water for non-potable use. But the treated textile wastewater by MBR technology alone can't comply with the reuse or discharge standard in many countries due to its colouring matters and dyestuffs remained in the effluent, if otherwise, MBR is associated with other technology like NF, RO, other processes or the applied membrane is modified or a **novel MBR** is applied. **Fouling** is another limiting factor for worldwide application of MBR technology especially in high-strength industrial wastewater like textile wastewater. Moreover, membrane fouling is regarded as the most important bottleneck for further development of MBR technology. It is the main limitation for faster development of this process, particularly when it leads to flux losses that cleaning cannot restore (Howell et al. 2004).

In this thesis work, a novel membrane bioreactor (MBR) process was developed by modifying a applied commercial PES UF membrane in MBR module by nano-structured novel coating through polymerisable bicontinuous microemulsion (PBM) process with the purpose of having higher hydrophilicity and low fouling propensity. Before starting the MBR experiments, some characterisation tests such as SEM, AFM images analysis, roughness measurements, pore geometry, contact angel, standard salt rejections, model textile dye rejections were performed. In addition, fouling tests using two laboratory cross flow testing units were conducted as well. To reach the ultimate goal of research, 6 sheets of novel coated membranes with size of 30 cm × 30 cm were prepared and these were used to prepare a three-envelope MBR module of 25 cm × 25 cm in size (total membrane area 0.33 m^2) similar to that of a commercially available three-envelope PES UF MBR module. This novel MBR module was tested in a submerged lab-scale MBR pilot plant (tank volume ca. 60 L) for about 6 months using model textile dye wastewater (MTDW) as test media for all experiments with the aim of having uniform compositions with respect to time. The tests were done based on carefully selected operation conditions. Prior to testing of the novel membrane module MBR, experiments were carried out with a commercial PES UF MBR module using the same pilot plant set up and the same selected operating conditions for about 10 months. After completion of trials with the novel coated MBR module, similar experiments were carried out again with a commercial PES UF MBR module to check the similarity of the biological sludge conditions and other operation conditions as well. In short, the sequences of the experiments were as follows:

Commercial PES UF MBR (10 months) →novel membrane coated MBR (6 months)→PES UF MBR (1.5 months)

The ultimate goal of the experiments was to compare the results between the commercial MBR and novel coated MBR module in order to demonstrate improvement regarding fouling propensity and permeate water quality.

The performance analysis shows that the novel coated MBR module compared to the commercial MBR module has 7% points higher COD removal efficiency, 20% points higher blue dye removal efficiency, high antifouling/antimicrobial properties, resulting in a very low-fluctuating and highly robust MBR process which looks promising with regard to economic viability.

Since the newly developed MBR module worked excellent on laboratory scale it consequently should be deployed at an industrial site to be tested with real

wastewater. Therefore, this novel three-envelope MBR module is on the way to be tested with real wastewater in a textile factory in Tunisia. The findings of these on-site pilot trials will serve as a basis for further improvement and eventually pilot trails with larger membrane area will be addressed.

References

BioNexGen, www.bionexgen.eu, accessed on September 6, 2013

Pidou, M., Hybrid membrane processes for water reuse, PhD thesis, 2006, School of applied science, department of sustainable systems, centre for water science, Cranfield University, UK

Brik, M., Schoeberl, P. Chamam, B., Braun, R., Fuchs, W., Advanced treatment of textile wastewater towards reuse using a membrane bioreactor, Process Biochemistry 41 (2006) 1751 – 1757

Howell, J.A., Chua, H.C., Arnot, T.C (2004), In situ manipulation of critical flux in a submerged membrane bioreactor using variable aeration rates and effects of membrane history, Journal of Membrane Science, Vol 242 (2004) 13-19

Riassunto

Il riciclo dell'acqua è comunemente visto come una delle principali soluzioni al problema della scarsità dell'acqua causata dall'aumento della sua richiesta e come risposta a ragioni economiche ed ambientali (Pidou, M., 2006). Le acque di scarico prodotte in processi industriali spesso contengono sostanze nocive per la salute umana e per l'ambiente. Perciò al fine di poter riutilizzare tali correnti, è necessario un loro trattamento. Tra i processi industriali, quello tessile presenta la più alta intensità di utilizzo di acqua. Ad esempio, per ogni tonnellata di tessuto prodotto, sono consumati 20-350 m^3 di acqua a seconda della procedura utilizzata (Brik et al., 2006). Nel sistema produttivo, tali acque vengono a contatto con una serie di sostanze inquinanti che vanno dai prodotti chimici e additivi a differenti tipi di coloranti che rendono necessaria la loro purificazione prima di essere scaricate nell'ambiente o riutilizzate.

La tecnologia MBR (bioreattori a membrana) è riconosciuta come una tra le più promettenti per la produzione di acqua, potenzialmente riutilizzabile. Tuttavia, il trattamento delle acque di scarico tessili mediante tecnologia MBR non può soddisfare da sola gli standard di riciclo o di scarico richiesti in molti paesi, a causa delle sostanze coloranti che rimangono nel filtrato. Perciò la tecnologia MBR viene di solito integrata con altre tecnologie come la nanofiltrazione (NF) o osmosi inversa (RO), ecc. Lo sporcamento (**fouling**) è un altro fattore limitante della tecnologia MBR specialmente in acque di scarico difficili da trattare come quelle tessili. A causa dello sporcamento, si registra una riduzione drastica delle prestazioni in termini di flusso difficilmente ripristinabili anche con trattamenti chimici (Howell et al. 2004).

Nel presente lavoro di tesi, il processo MBR è stato migliorato attraverso la modifica, mediante un coating, ottenuto tramite polimerizzazione di microemulsione bicontinua (PBM), di membrane commerciali da ultrafiltrazione in PES, con lo scopo di produrre membrane altamente idrofiliche e con una bassa tendenza allo sporcamento (**innovative low fouling membrane**). Le nuove membrane prodotte sono state caratterizzate mediante analisi di immagini al microscopio Eletrronico a Scansione (SEM), a Forza Atomica (AFM), misure di rugosità della superficie, geometria dei pori, angolo di contatto, reiezione ai sali, reiezione a coloranti modello. Inoltre, i test di sporcamento sono stati eseguiti attraverso l'utilizzo di due celle a flusso tangenziale (cross-flow) da ultrafiltrazione (UF) impiegando anche membrane commerciali in PES per 10

mesi. Le nuove membrane in PBM sono state utilizzate per assemblare 3 moduli MBR aventi una superfice di membrana pari a (0.33 m^2).

I moduli MBR prodotti, contenenti membrane con e senza coating (PES commerciali), sono stati testati su scala di laboratorio per circa 6 e 1,5 mesi, rispettivamente, utilizzando acque di scarico tessili modello (MTDW). I test sono stati eseguiti mantenendo costanti le condizioni operative.

Test MBR con membrane commerciali in PES da UF (10 mesi) →MBR ibrido (6 mesi) → MBR PES UF (1,5 mesi)
Scopo ultimo degli esperimenti è stato quello di comparare i risultati MBR ottenuti con le membrane commerciali con quelli ottenuti con le membrane PBM.

Le analisi dei risultati mostrano che il modulo MBR preparato con le membrane PBM, rispetto a quello con le membrane commerciali, ha un'efficienza di rimozione dei COD (carbon oxygen demand) maggiore del 7%, una rimozione del colorante blu maggiore del 20%, alte proprietà anti-sporcamento e antimicrobiche. Il processo risulta essere inoltre più semplice e robusto e maggiormente sostenibile economicamente (riduzione dei tempi di lavaggio e sostituzione nuove membrane). L'insieme di tutti questi benefici ha permesso di raggiungere gli obbiettivi prefigurati, ovvero lo sviluppo di un innovativo processo MBR.

Il nuovo MBR realizzato e testato su scala di laboratorio può essere quindi prontamente sviluppato su scala industriale per essere collaudato in condizioni reali. A tal riguardo. in Tunisia, sono in corso esperimenti su più larga scala e su acque reflue reali tessili.

References

BioNexGen, www.bionexgen.eu, accessed on September 6, 2013

Pidou, M., Hybrid membrane processes for water reuse, PhD thesis, 2006, School of applied science, department of sustainable systems, centre for water science, Cranfield University, UK

Brik, M., Schoeberl, P. Chamam, B., Braun, R., Fuchs, W., Advanced treatment of textile wastewater towards reuse using a membrane bioreactor, Process Biochemistry 41 (2006) 1751 – 1757

Howell, J.A., Chua, H.C., Arnot, T.C (2004), In situ manipulation of critical flux in a submerged membrane bioreactor using variable aeration rates and effects of membrane history, Journal of Membrane Science, Vol 242 (2004) 13-19

Zusammenfassung

Wasser ist ein wesentlicher Bestandteil des menschlichen Lebens. Die Abwässer aus der Industrie und Landwirtschaft, welche mit Schwermetallionen, Pestiziden, organischen Verbindungen , endokrinen Verbindungen und Nährstoffen (Phosphate , Nitrate, Nitrite) belastet sein können, müssen effizient behandelt werden, um die Umwelt vor einer Verschmutzung zu schützen. Sauberes Wasser, welches als Grundlage für die Gesundheit und das Wohlbefinden einer Gesellschaft dient, ist für die Mehrheit der Weltbevölkerung nicht zugänglich (BIONEXGEN, 2013). Die Aufbereitung und Wiederverwendung von Abwasser wird heute als Antwort auf die zunehmende Wasserknappheit und steigende Nachfrage nach Frischwasser als nachhaltige Möglichkeit zum Schutz der Umwelt akzeptiert. Deshalb wird das Recycling von aufbereitetem Abwasser allgemein als eine der wichtigsten Optionen zur Beseitigung von Wassermangel - verursacht durch den starken Anstieg der Nachfrage und den damit verbundenen steigenden Wasserpreisen - betrachtet. Die wichtigsten Bereiche für Abwasser-Recycling sind Industrieanwendungen, Bewässerung , Grundwasserneubildung und urbane Wiederverwendung (Pidou, M. , 2006).

Die Textilindustrie ist im Bereich industrieller Abwässer traditionell ein wasserintensiver Bereich und hat deshalb einen hohen Bedarf an Frischwasser für alle Produktionsverfahren. Textilabwässer enthalten eine große Vielfalt von Inhaltstoffen, wie Prozesschemikalien, Hilfsstoffe und verschiedene Arten von Farbstoffen. Aus ökologischer und ökonomischer Sicht sind die Menge und Qualität des Abwassers, d.h die chemischen Belastungen die es trägt, von großer Bedeutung. So werden für die Herstellung jeder Tonne textiler Produkte 20 bis 350 m^3 Wasser verbraucht, wobei sich die angewendeten Produktionsverfahren deutlich unterscheiden können und sich damit die Qualität der Abwässer entsprechend ändern können (hinsichtlich verwendeter Farbstoffe, Hilfschemikalien etc.) (Brik et al. , 2006).

Die Membranbioreaktor (MBR)-Technologie wird als eine vielversprechende Technologie betrachtet, um Wasser mit hoher Qualität zur Wiederverwendung in Bereichen bereitzustellen, in denen keine Trinkwasserqualität erforderlich ist. Allerdings hat sich bei der Behandlung von Textilabwässern durch MBR-Technologie gezeigt, dass sich die erforderlichen Wasserqualitätstandards für eine Einleitung in Gewässer bzw. Wiederverwendung - insbesondere aufgrund seiner Farbigkeit - nicht einhalten lassen, falls nicht zusätzliche Behandlungsverfahren zum Einsatz kommen (z.B. Umkehrosmose oder Nanofiltration).

Fouling ist ein weiterer limitierender Faktor für den weltweiten Einsatz von MBR-Technologie vor allem in Industrieabwässern mit schwer abbaubaren Inhaltsstoffen, wie Textilabwasser. Insbesondere wird Membranfouling als entscheidender Engpass für die weitere Entwicklung der MBR-Technologie betrachtet. Es ist die wichtigste Einschränkung für eine schnellere Verbreitung dieser Technologie, insbesondere da Fouling häufig zu einer irreversiblen Reduktion des Wasserfluxes führt, der auch durch Reinigungsmaßnahmen nicht behoben werden kann (Howell et al. 2004).

In dieser Arbeit wurde durch Verwendung einer neuartigen nanostrukturierten Membran ein neuer Membran-Bioreaktor (MBR)-Prozess entwickelt. Diese Membran wurde durch das Verfahren der Polymerisation von bikontinuierlichen Mikroemulsionen (PBM) durch Beschichtung von kommerziellen Ultratfiltrations- (UF) Flachmembranen (PES) hergestellt mit dem Ziel eine hydrophile Membran mit geringerem Foulingpotential zu erhalten. Vor Beginn der eigentlichen MBR Versuche wurde die neuartige Membran mittels verschiedener Verfahren untersucht und charakterisiert: SEM-, AFM-Aufnahmen, Rauhigkeitsmessungen, Porengeometrie, Kontaktwinkel, Standard-Salzrückhaltung und Rückhalt an Modellfarbstoffen. Darüber hinaus wurden Fouling-Tests unter Verwendung von zwei Laborversuchsanlagen mit Querstrommembranmodulen durchgeführt. Zur Untersuchung des Verhaltens in einem Labor-Membranbioreaktor wurde aus sechs mittels PBM Verfahren beschichteten Membranblättern (30 cm × 30 cm) ein kleines MBR-Modul mit drei Membrantaschen hergestellt (25 cm × 25 cm, gesamte Membranfläche ca. 0,3 m^2). Ein Modul mit diesen Abmessungen war bereits als kommerzielles UF MBR-Modul erhältlich.
Dieses MBR-Modul wurde als getauchte Membran in einer Labor-Pilotanlage (Tankvolumen ca. 60 L) über einen Zeitraum von etwa 6 Monaten getestet. Für diese Versuche wurde ein Modell-Textilabwasser unter sorgfältig ausgewählten Versuchsbedingungen eingesetzt, um über die gesamte Versuchsdauer eine konstante Zusammensetzung im Zulauf und damit möglichst konstante Versuchsbedingungen zu gewährleisten. Zum Vergleich wurden vor dem Test mit dem neuartigen MBR-Modul Versuche mit einem kommerziellen PES UF MBR-Modul mit der gleichen Pilotanlage und den gleichen Betriebsbedingungen über eine Versuchsperiode von 10 Monate durchgeführt. Nach Abschluss der Pilotversuche mit dem neuartigen MBR-Modul wurde die Versuchsreihe wieder mit einem kommerziellen PES UF MBR-Modul unter gleichen Versuchsbedingungen fortgeführt, um Einflüsse eventueller Veränderungen in der Belebtschlammbiologie zu überprüfen. Damit war der Ablauf der Versuchsreihen wie folgt :

Kommerzielles PES UF MBR-Modul (10 Monate) → Neuartiges MBR-Modul (6 Monate) → Kommerzielles PES UF MBR-Modul (1.5 Monate)
Insgesamt war es das Ziel der Versuchsreihen die Ergebnisse zwischen dem kommerziellen MBR und neuartigen MBR-Modul zu vergleichen, um eine Verbesserung hinsichtlich Fouling-Neigung sowie Permeat-Wasserqualität aufzuzeigen.

Die Auswertung der Versuchsreihen hat gezeigt, dass das neuartige, durch PBM beschichtete, MBR-Modul im Vergleich zu dem kommerziellen Modul eine um 7 %-Punkte höhere Effizienz des CSB-Abbaus und eine 20%-Punkte höhere Effizienz beim Abbau des blauen Farbstoff aufweist. Außerdem weist die neuartige Membran geringeres Fouling sowie auch nach Ende der Versuchsreihe noch deutlich antimikrobielle Eigenschaften auf. Dadurch ergibt sich im Vergleich mit dem kommerziellen Modul ein wesentlich stabilerer Prozess mit geringeren Schwankungen in der Permeatqualität und damit lässt sich auch eine Verbesserung der Wirtschaftlichkeit erwarten.

Der im Labormaßstab mit einem Modellwasser erfolgreich getestete MBR-Prozess sollte nun an einem industriellen Standort mit realem Abwasser pilotiert werden. Deshalb sind bereits erste Versuche mit dem Drei-Membrantaschenmodul in einer Textilfabrik in Tunesien vorbereitet worden. Die Ergebnisse dieser Pilotierung sollen dann als Grundlage für eine weitere Verbesserung der neuartigen Membran dienen, um anschließend MBR-Module mit größerer Membranfläche herzustellen und zu testen.

References

BioNexGen, www.bionexgen.eu, accessed on September 6, 2013

Pidou, M., Hybrid membrane processes for water reuse, PhD thesis, 2006, School of applied science, department of sustainable systems, centre for water science, Cranfield University, UK

Brik, M., Schoeberl, P. Chamam, B., Braun, R., Fuchs, W., Advanced treatment of textile wastewater towards reuse using a membrane bioreactor, Process Biochemistry 41 (2006) 1751 – 1757

Howell, J.A., Chua, H.C., Arnot, T.C (2004), In situ manipulation of critical flux in a submerged membrane bioreactor using variable aeration rates and effects of membrane history, Journal of Membrane Science, Vol 242 (2004) 13-19

Contents

1. Chapter 1: Introduction

1.1 General Introduction

Water is another synonym of life. According to the World Health Organisation (WHO), the most dangerous threat for health of mankind emerging within the next years is polluted water. In under developed countries the shortage of clean freshwater will be the most important cause of death for children under 5 years. The low quantities of fresh water for industrial, agricultural and municipal usage have to be well preserved by efficient, sustainable and cost-effective technologies. Water contaminated from industry and agriculture with heavy metal ions, pesticides, organic compounds, endocrine disruptive compounds, nutrients (phosphates, nitrates, nitrites) has to be efficiently treated to protect humans from being intoxicated with these compounds or with bacteria. Furthermore, incidental sludge of industrial wastewater treatment facilities is commonly highly contaminated with toxic compounds (Bionexgen, 2013).

Clean water as basis for health and good living conditions is too far out of reach for the majority of the population in the world. Thus neither sustainable consumption nor reinforcement of governmental regulations are effective drivers to force the industry to adopt sustainability policies. Though polluted water and water shortages demand for a sustainable water usage and recycling of waste water, the barriers are high to adopt these (Bionexgen, 2013).

Water recycling is now widely accepted as a sustainable option to respond to the general increase of the fresh water demand, water shortages and for environment protection. Water recycling is commonly seen as one of the main options to provide remedy for water shortage caused by the increase of the water demand and draughts as well as a response to some economical and environmental drivers. The main options for wastewater recycling are industrial, irrigation, aquifer recharge and urban reuse (Pidou, M., 2006).

Among the industrial wastewaters, the textile industry is long regarded as a water intensive sector, due to its high demand of water for all parts of its procedures. Accordingly, textile wastewater includes quite a large variety of contents, chemicals, additives, different kinds of dyestuffs, and so on. The main environmental concern with this waste water is about the quantity and quality of the water discharged and the chemical loads it carries. To illustrate, for each

ton of fabric products, 20 – 350 m^3 of water are consumed, which differs from the color and procedure used (Brik et al., 2006).

The consumption of water during the production process in textile industry is shown in Table 1.1:

*Table 1.1 Constituent ratio of water in textile industry (*Eswaramoorthi et al., 2009)

Process	Consumption of water (%)
Spinning	6
Weaving	9
Bleaching, finishing	38
Dyeing	16
Printing	8
Boiler	14
Others	9

The quality of the textile wastewater depends much on the employed coloring matters, dyestuffs, accompanying chemicals, as well as the process itself. Moreover, from season to season, the fashion changes, which also lead to a different demand of coloring. On the other hand, the process itself changes from time to time with the latest technology. In the field applications, about 8000 kinds of coloring matters and 6900 additives are currently used (Brik et al., 2006), which lead to a content of both organic and inorganic pollution in the textile wastewater.

In order to treat these kinds of textile wastewater, two concerns are important. One is to remove the highly biodegradable organics within the wastewater. The other concern is to remove the colouring matters and dyestuffs, which are low biodegradable (Rott and Minke, 1999).

MBR technology is recognised as a promising technology to provide water with reliable quality for reuse. Today, MBRs are robust, simple to operate and even more affordable. They take up little space, need modest technical support and can remove any contaminants in one step. This makes it practical to provide safely reuse water for non-potable use. But the treated textile wastewater by MBR technology alone can't comply with the re-use or discharge standard in many countries due to its colouring matters and dyestuffs remained in the effluent, if otherwise, MBR is associated with other technology like NF, RO, other processes or the applied membrane is modified. Fouling is another limit-

ing factor for worldwide application of MBR technology especially in high-strength industrial wastewater like textile wastewater. However, membrane fouling is regarded as the most important bottleneck for further development of MBR technology. It is the main limitation for faster development of this process, particularly when it leads to flux losses that cleaning cannot restore (Howell et al. 2004).

The target of this thesis was to develop a membrane bioreactor focusing on novel low fouling membrane towards developing upgraded or novel or hybrid MBR process. Generally the term "hybrid" means the combination of two different things resulting in the development of a modified thing which has the superior characteristics compared to its origin. In terms of MBR, hybrid or upgraded MBR means improved or novel MBR process which has higher performances like better permeate quality and lower fouling propensity compared to conventional MBR process. Many researchers have developed novel MBR process integrating conventional MBR with other technologies like NF, RO, PAC, biofilm carriers, porous suspended carriers etc. (Mulder et al., 2007; Ravindran et al., 2009; Liu et al., 2010 and Yang et al., 2009).

To develop the MBR process in this thesis work, commercial UF membrane was modified by a nano-structured functionalised novel coating using polymerisable bicontinuous microemulsion (PBM) process. This modified novel coated membrane is associated with anti-fouling properties through cationic surfactant, acryloyloxyundecyltriethyl ammonium bromide (AUTEAB) used in the preparation process. The surface smoothness and hydrophilicity of the novel coated membrane was much higher than the unmodified commercial membranes. Higher hydrophilicity and anti-fouling properties of the modified membrane showed higher fouling resistant which was revealed from different tests (physical and biological) with model foulant in cross-flow ultrafiltration testing cells and biological sludge treatment in a lab scale – MBR plant carried throughout this thesis work. This kind of low fouling novel coated modified membrane applied in MBR application looks promising in terms of economic viability of the process for textile wastewater treatment.

1.2 Research Objectives

The aim of this PhD thesis is to develop a novel MBR process preparing nano-structured functionalised novel MBR membranes with a focus on reducing fouling propensities. The main objectives of the thesis workare as follows:

- To prepare nano-structured functionalised novel coating by polymerisable bicontinuous microemulsion process onto commercial UF membranes following the protocol developed by ITM-CNR, Italy
- To characterise the prepared novel membranes in terms of pore geometry, hydrophilicity, surface smoothness, water permeablities, model foulant tests, etc..
- To define the antifouling effect (reversible and irreversible) of the prepared novel membranes applying model foulant (humic acid) and textile dyestuffs (Remazol Brilliant Blue R and Acid Red 4) with ultrafiltration cross-flow testing cells
- To carry out long term lab scale MBR experiment applying commercial PES UF MBR module for benchmarking
- To carry out long term lab scale MBR experiment applying novel coated PBM MBR module
- To compare the results of PES UF MBR and PBM MBR modules and illustrate the process benefits

1.3 Thesis outline

This PhD thesis was formulated based on the development steps and is structurized into 8 chapters which are shown in Fig.1.1.

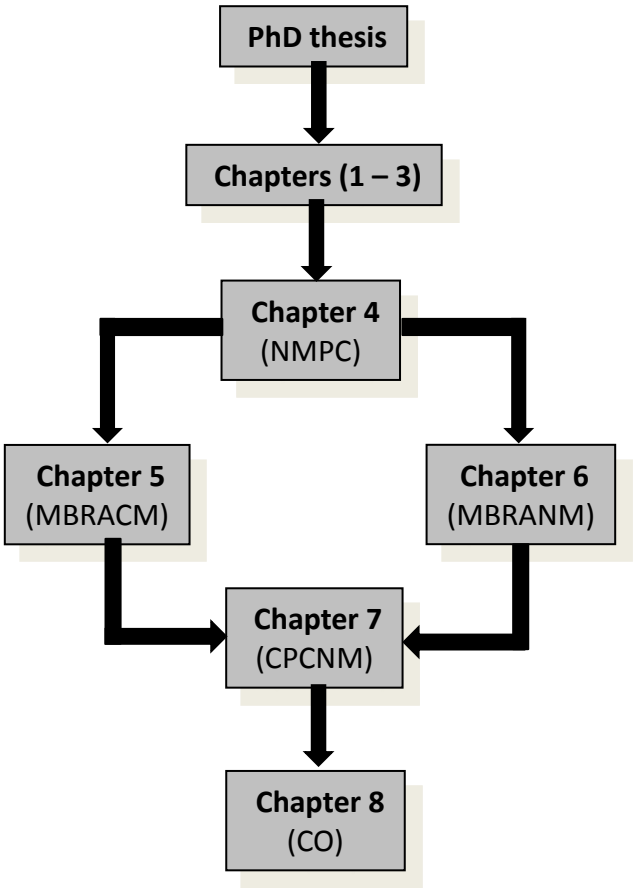

Fig. 1.1: Outline of the thesis structure

N.B.:

NMPC	*: Novel Membrane Preparations and Characterisation*
MBRACM	*: MBR Applying Commercial Membranes*
MBRANM	*: MBR Applying Novel membranes*
CPCNM	*: Comparison of Performances between Commercial and Novel Membranes*
CO	*: Conclusion and Outlook*

The chapters (Chapter 2 - Chapter 8) of this thesis are also divided into two parts: Part I and Part II. Part I describes the theoretical aspects and it includes Chapter 2 and Chapter 3. The rest of the chapters (Chapter 4 - Chapter 8) belong to Part II and discusses the experimental aspects and results.

The following section summarises the content of all chapters (Chapter 1 - Chapter 8) of this thesis:

Chapter 1

Chapter 1 is the introductory chapter of this thesis. The research objectives and outline of the thesis are also shown in this section.

Chapter 2

A literature review on membrane bioreactor (MBR) in general and MBR for textile wastewater treatment is illustrated in Chapter 2. The basic aspects of MBR, its configurations, filtration processes, biological aspects, hydraulic geometry and fouling mechanisms were discussed in this section. An outline on how to control MBR fouling was also provided. Different conventional technologies for wastewater treatment are also discussed in this part. The emphasis is given on MBR technology for textile wastewater treatment; its current status and future prospects. It is also discussed on how the objectives of this thesis contributed in MBR technology for textile wastewater treatment. Part of this chapter was the basis of a scientific paper entitled as "Membrane Bioreactor (MBR) Technology – A Promising Approach for Industrial Wastewater Reuse" published in Journal of Procedia Engineering in 2012.

Chapter 3

In Chapter 3, materials and methods applied in this thesis are discussed. A short description of the applied materials and methods including their operating ranges and accuracy are provided.

Chapter 4

The process of preparing novel membrane by polymerisable bicontinuous microemulsion (PBM) and its characterisation in detail are discussed in chapter 4. The antifouling/antimicrobial effects of the PBM coated membranes under different test conditions in different experimental set ups are also discussed in this chapter. The critical operating conditions which are needed to be optimised for preparing high performing PBM coated membrane are discussed in this chapter as well.

Chapter 5

In Chaper 5, a MBR system incorporated with commercial MBR module that was applied for textile wastewater treatment is discussed. The entire range of the applied MBR system starting from start up until the final results obtained is covered by this part. The results obtained from chapter 5 are used as reference for Chapter 6.

Chapter 6

In Chapter 6, the MBR system wherein PBM coated novel MBR module was applied for textile wastewater treatment and the results have been discussed. The test conditions of the experiments were similar to that of chapter 5. The basis for this chapter is based on scientific publication entitled as "Submerged Membrane Bioreactor (SMBR) for treatment of Textile Dye Wastewater towards Developing Nobel MBR Process" published in journal of APCBEE Procedia in 2013 and a patent "BICONTINUOUS MICROEMULSION POLYMERIZED COATING FOR WATER TREATMENT", registration number IT GE2013A000096, filed on 27.09.2013.

Chapter 7

In Chapter 7, the results obtained from commercial MBR and PBM/novel coated MBR systems have been compared. The results have been analysed based on product quality, organic stuff degradation/rejection, fouling properties, process robustness etc.. The techno-economical analysis of the obtained results concludes that the objectives of the thesis have been achieved.

Chapter 8

In Chapter 8, overall conclusions are provided and the future prospective of the developed MBR process is discussed in detail. In addition, some recommendations for process optimisations and real-field application of the technology in an industrial site are presented.

References

BioNexGen, www.bionexgen.eu, accessed on September 6, 2013

Brik, M., Schoeberl, P. Chamam, B., Braun, R., Fuchs, W., Advanced treatment of textile wastewater towards reuse using a membrane bioreactor, Process Biochemistry 41 (2006) 1751 – 1757

Eswaramoorthi, S., Dhanapal, K. andChauhan, D.S., Textile Waste Water Treatment With Membrane Bioreactor, 2009, environmental technology awareness series, India.

Howell, J.A., Chua, H.C., Arnot, T.C (2004), In situ manipulation of critical flux in a submerged membrane bioreactor using variable aeration rates and effects of membrane history, Journal of Membrane Science, Vol 242 (2004) 13-19

Jan Hoinkis, Shamim A. Deowan, Volker Panten, Alberto Figoli, Rong Rong Huang and Enrico Drioli, Membrane Bioreactor (MBR) Technology –

A Promising Approach for Industrial Wastewater Reuse, Procedia Engineering 33 (2012) 234-241

Liu, Q, Wang, X.C., Liu, Y, Yuan, H., Du, Y., Performance of a hybrid membrane bioreactor in municipal wastewater treatment, Desalination 258 (2010) 143 - 147

Mulder, J. W., Braunersreuther, M., Schonewille, H., Jager, R. D. and Veraart, A., Hybrid MBR for industrial reuse of domestic wastewater in the Nederlands, 2007

Pidou, M., Hybrid membrane processes for water reuse, PhD thesis, 2006, School of applied science, department of sustainable systems, centre for water science, Cranfield University, UK.

Ravindran, V., Tsai, H.H., Williams, M.D., Pirbazari, M., Hybrid membrane bioreactor technology for small water treatment utilities: Process evaluation and primordial considerations, Journal of Membrane Science 244 (2009) 39 - 54

Rott, U. and Minke, R., Overview of wastewater treatment and recycling in the textile processing industry, Water Sci. Technol. 1999, 40(1):137 - 144.

Shamim Ahmed Deowan, Francesco Galiano, Jan Hoinkis, Alberto Figoli, Enrico Drioli, Submerged Membrane Bioreactor (SMBR) for Treatment of Textile Dye Wastewater towards Developing Nobel MBR Process, APCBEE Procedia 5 (2013) 259-264

Yang Q., Y., Yang, T., Wang, H., J. and Liu, K. Q., Filtration characteristics of activated sludge in hybrid membrane bioreactor with porous suspended carriers (HMBR), Desalination 249 (2009) 507 – 514

2. Chapter 2 : Literature Review

2.1 Section I: The State of the Art of Membrane Bioreactor (MBR) Technology

2.1.1 Basic aspects of Membrane Bioreactor

Basic aspects of membrane bioreactor (MBR) such as its definition, history, its configuration, materials etc. are discussed in the following sections.

2.1.1.1 Definition of MBR

Membrane bioreactor (MBR) technology is a combination of the conventional biological sludge process, a wastewater treatment process characterised by a suspended growth of biomass, with a micro- or ultrafiltration membrane system (Judd, 2006, p.55). The biological unit is responsible for the biodegradation of the waste compounds and the membrane module for the physical separation of the treated water from the mixed liquor. The pore diameter of the membranes is in the range between 0.01 – 0.1 µm so that particulates and bacteria can be kept out of permeate and the membrane system replaces the traditional gravity sedimentation unit (clarifier) in the biological sludge process. Hence, the MBR offers the advantage of higher product water quality and low footprint. Due to its advantages, membrane bioreactor technology has great potential in wide ranging applications including municipal and industrial wastewater treatment and process water recycling. By 2006, around 100 municipal full scale plants (>500 p.e.) and around 300 industrial large scale plants (> 20 m^3/d) were in operation in Europe (Lesjean *et al.*, 2008). MBR installations capacity grew in 2007, but declined in 2008 and 2009. The market was impacted by lower industrial spending due to the economic downturun. However, there was an increase in demand for large size plants during the past 2 – 3 years. Installations of MBR increased significantly in the years of 2010 and early 2011 (GIA, 2013).

The main industrial applications are in food and beverage, chemical, pharmaceutical and cosmetics, textile industry as well as in laundries. The technical

feasibility of this technology has been demonstrated through a large number of small and large scale applications.

2.1.1.2 History of MBR development

The first membrane bioreactors were developed commercially by Dorr-Oliver in the late 1960s (Bemberis *et al*., 1971), with application to ship-board sewage treatment (Bailey *et al*., 1971). Other bench–scale membrane separation systems linked with an activated sludge process were reported at around the same time (Hardt *et. al.,* 1970; Smith *et al.,* 1969). These systems were all based on what have become to be known as "sidestream" configuration (sMBR), as opposed to the now more commercially significant "submerged or immersed" configuration (iMBR). The Dorr-Oliver membrane sewage treatment (MST) process was based on flat-sheet (FS) ultrafiltration (UF) membranes operated at what would now be considered excessive pressures (3.5 bar inlet pressure) and low fluxes (17 $L/m^2 \cdot h$), yielding permeabilities of less than 10 $L/m^2 \cdot h \cdot bar$. Nonetheless, the Dorr-Oliver system succeeded in establishing the principle of coupling an activated sludge process with a membrane to concentrate simultaneously the biomass whilst generating a clarified, disinfected product. The system was marketed in Japan under license to Sanki Engineering, with some success up until the early 1990s. Developments were also underway in South Africa which led to the commercialisation of an anaerobic digester UF (ADUF) MBR by Weir Envig (Botha *et al*., 1992), for use on high-strength industrial wastewaters.

At around this time, from the late 1980s, to early 1990s, other important commercial developments were taking place. In the USA, Thetford Systems were developing their Cycle-Let® process, another sidestream process, for wastewater recycling duties. Zenon Environmental, a company formed in 1980, were developing an MBR system which eventually led to the introduction of the first ZenoGem® iMBR process in the early 1990s. The company acquired Thetford Systems in 1993. Meanwhile, in Japan, the government –instigated Aqua Renaissance programme prompted the development of an FS-microfiltration iMBR by the agricultural machinery company Kubota. This subsequently underwent demonstration at pilot scale, first at Hiroshima in 1990 with capacity of 0.025 million liters per day (MLD) and then at the company's own site at Sakai-Rinkai in 1992 (0.110 MLD). By the end of 1996, there were already 60 Kubota plants installed in Japan for night soil, domestic wastewater (i.e. sewage) and, latter, industrial effluent treatment, providing a total installed capacity of 5.5 MLD.

In the early 1990s, only one Kubota plant for sewage treatment had been installed outside of Japan, this being the pilot plant at Kingston Seymour operated by Wesex Water in the UK. Within Japan, however, the Kubota process dominated the market in the 1990s, effectively displacing the older side stream systems, such as that of Rhodia-Orelis (now Novasep Orelis). To this day, Kubota continues to dominate the Japanese membrane wastewater treatment market and also provides the largest number of MBRs worldwide, although around 86% of these are for flows of less than 0.2 MLD.

In the late 1980s, development of a hollow fibre (HF) UF iMBR was taking place both in Japan, with pioneering work by Kazuo Yamamoto and his co-workers (1989), and also in the US. By the early 1990s, the ZenoGem® process had been patented (Tonelli and Behmann, 1996; Tonelli and Canning, 1993), and the total installed capacity had reached 2.8 MLD from installations in North America. Zenon introduced its first immersed HF ZeeWeeD® module in 1993, this being the ZW 145 (145 square feet), quickly followed by the ZW130 and 150 modules. These were in time superceded by the first of the ZW500 series in 1997. The company introduced the ZW500b, c and d modules in 1990, 2001 and 2003 respectively, the design changing to increase the overall process efficiency and cyclic aeration in 2000. Over this period, Kubota also developed products with improved overall energy efficiency, introducing a double decker design in 2003.

The cumulative capacity of both Zenon and Kubota has increased exponentially since the immersed products were first introduced. These two systems dominate the MBR market today, with a very large number of small-scale Kubota systems and the largest MBR systems tending to be Zenon. The largest MBR worldwide is currently at Kaarst in Germany (50 MLD), though there is actually a larger membrane wastewater recycling facility in Kuwait (The Sulaibiya plant), which has a design capacity of 375 MLD (Judd, 2006, p. 12).

2.1.1.3 MBR Configurations

According to MBR configurations, MBRs can be divided into two classes as side-stream MBR (sMBR) and submerged or immersed MBR (iMBR) (Fig.2.1).

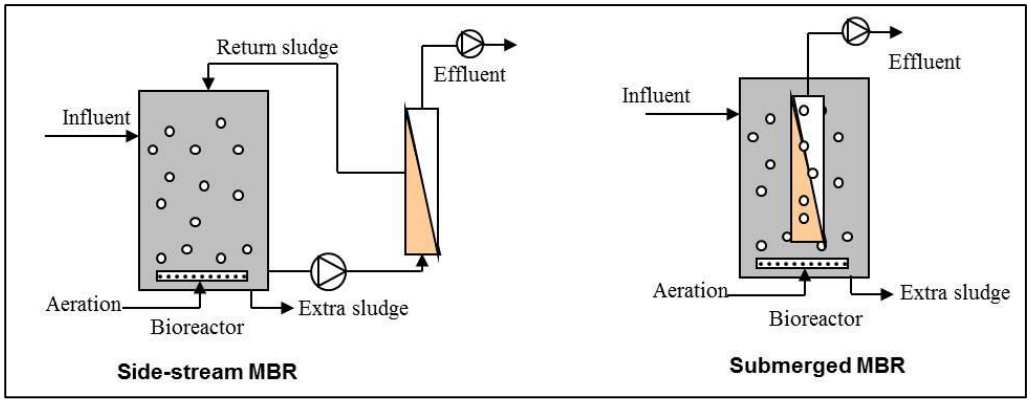

Fig. 2.1 : Configuration of side-stream and submerged MBR (modified from Jiang, 2007)

In side-stream MBRs, membrane module is placed outside of the MBR reactor. The sludge from the MBR reactor is pumped to the membrane module which creates cross-flow at the membrane surface and permeate is generated. The concentrated sludge rejected by the membrane is recycled to the MBR reactor. This is a pressure driven membrane filtration process. In the early development of side-stream MBRs, both of the transmembrane pressure (TMP) and cross flow velocity were generated by the recirculation pump. However, a few modifications were made to reduce the high energy consumption associated with the side-stream configuration. Firstly, a suction pump was added on the permeate side, which increased the operation flexibility and decreased the cross flow rate and energy consumption (Shimizu *et al*., 1996). The latest side-stream MBRs even introduced an air flow in the membrane module, which intensified the turbulence in the feed side of the membrane and reduced the fouling and operational costs (Jiang, 2007).

In submerged MBRs, membrane module is directly submerged in the reactor. A suction pump or a vacuum pump is needed to create transmembrane pressure for permeate production. In this case, no circulation pump is needed since cross flow is created by aeration. This concept was first developed by Yamamoto *et al.* (1989) to reduce energy consumption compared to side-stream MBR configuration. In some circumstances (e.g. MF membrane and very low filtration fluxes), the permeate side is placed in a lower position, and the gravity itself is the only driving force for the filtration (Ueda and Hata, 1999, p.10).

The comparison between the side-stream and submerged MBRs is summarized in Table 2.1. The submerged MBR has a simpler configuration, since it needs

less equipment. The coarse bubble aeration in the membrane tank is multifunctional. In addition to the membrane fouling control, it also supplies oxygen to the biological process (although the oxygen utilisation efficiency is low). The biggest advantage of submerged over side-stream configuration is the energy saving by using coarse bubble aeration, instead of high rate recirculation pump in side-stream MBRs. The capillary and hollow fibre membranes used in many submerged MBRs have very high packing density and low cost, which make it feasible to use more membranes. However, typical tubular membranes used in side-stream MBRs have low packing density and they are very expensive. Gander *et al*. (2000) reviewed 4 side-stream and 4 submerged MBR systems and concluded that the side-stream MBRs have a higher total energy cost, by up to two orders of magnitude, mainly due to the high recycle flow velocity (1-3 m/s) and head loss within the membrane module. In addition, the submerged MBRs suffered fouling and could be cleaned easier than the side-stream MBRs (Gander *et at.,* 2000).

Table. 2.1 : The comparison of side-stream MBRs and submerged MBRs (Jiang, 2007, p.11).

Comparing parameters	Side-stream	Submerged
Complexity	Complicated	Simple
Flexibility	Flexible	Less flexible
Robustness	Robust	Less robust
Flux	High (40-100 L/m^2·h)	Low (10-30 L/m^2·h)
Fouling reducing methods	• Crossflow • Airlift • Backwashing • Chemical cleaning	• Air bubble agitation • Backwashing (not always possible) • Chemical cleaning
Membrane packing density	Low	High
Energy consumption with filtration	**High** (2-10 kWh/m^3)	**Low** (0.2-0.4 kWh/m^3)

However, the side-stream MBRs have the advantage of having more robust physical strength, more flexible cross-flow velocity control and hydraulic loading. They are now mostly used in industrial wastewater treatment and small scale WWTPs, where influent flow rate and composition has larger variation and operational conditions are tough (e.g., at high temperature conditions) (Jiang, 2007).

2.1.1.4 Configurations of membrane module

The configuration of the membrane, i.e. its geometry and the way it is mounted and oriented in relation to the flow of water, is crucial in determining the overall process performance (Judd, 2006, p.26). Large membrane areas are normally required when membranes have to be applied on an industrial scale. The smallest unit into which the membranes are packed is called module (Mulder, 1996, p.465). The practical considerations concern the way in which the membrane elements, that is the individual discrete membrane units themselves, are housed in "shells" to produce modules, the complete vessels through which the water flows. Ideally, the membrane should be configured so as to have (Judd, 2006, p.26) :

(a) a high membrane area to module bulk volume ratio,
(b) a high degree of turbulence for mass transfer promotion on the feed side,
(c) a low energy expenditure per unit product water volume,
(d) a low cost per unit membrane area,
(e) a design that facilitates cleaning,
(f) a design that permits modularisation

The simplest design is the one in which a single module is used as shown in Fig 2.2.

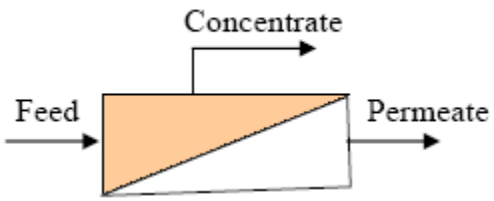

Fig. 2.2 : Schematic drawing of a module

Of the above mentioned configurations, only flat sheet (FS), hollow fiber (HF) and multitubular (MT) membranes modules are suited to MBR technologies (Judd, 2006, p.26). The flat sheet, capillary and hollow fiber membranes are applied in iMBR and typical tubular membranes are used in sMBR (Gander *et al*., 2000). Geometric structure of a membrane is valuable if it is capable of

minimizing fouling during filtration process, and, contemporarily, of having a good specific surface of the module, where, for "specific surface" the filtering surface per unity of occupied volume is intended. Also structural simplicity, management flexibility and modularity are important factors while deciding if a membrane module is valuable. A very important parameter often taken into account while considering the membrane filtration process is the molecular weight of the compound that can be retained by the membrane. This is called Molecular Weight Cut Off (MWCO); it refers to molecular cut off of the solute at which 90% rejection takes place and it is expressed in Dalton (Manigas, 2008).

Since plate and frame membrane from flat sheet membrane module and hollow fiber membrane from tubular membrane module are most suited to MBR technologies, these are described in sections 2.1.1.4.1 and 2.1.1.4.2 elaborately.

2.1.1.4.1 Flat sheet membrane module

Plate and frame membrane module

The plate-and-frame module is used on industrial scale for various membrane separation processes such as ultrafiltration, reverse osmosis and gas separation. Its design has its origin in the conventional filter press-concept. Membrane, feed spacers, and product spacers are layered together between two end-plates and placed in housing. A flat sheet MBR module is shown in Fig. 2.3.

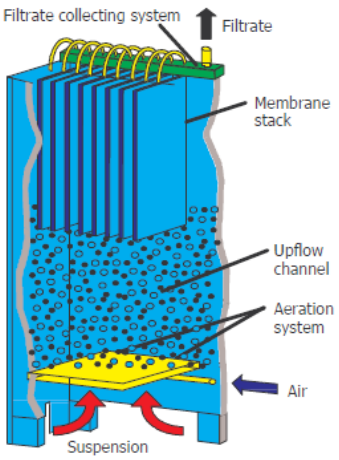

*Fig. 2.3 **:** Schematic diagram of the plate-and-frame MBR module (Aggerwasser, 2011).*

Plate and frame membranes from flat sheet configuration are most suited to submerged membrane bioreactor. An overview of different membrane configurations for MBR has been outlined in Table 2.2.

Table 2.2 : Membrane product catagories (Judd, 2006, p.201)

	Process configuration	
	Immersed	Sidestream
Membrane configuration		
FS	A3	Novasep-
	Orelis	
	Colloide	
	Brightwater	
	Huber[a]	
	ITRINWF	
	Kubota	
	Microdyn-Nadir (MN)	
HF	Toray	
	Asahi Kasei	Polymem
	Han-S Environmental	Ultraflo
	ITT	
	Koch-Puron	
	Kolon	
	Mitsubishi Rayon	
	Motimo	
	Siemens-Memcor	
MT	Zenon	
	Millenniumpore	Berghof[b]
		Millenniumpore
		Norit X-Flow[b]

a:Rotating membrane

b:MT membrane products used by process suppliers such as Aquabio, Dynatec, Triqua, Wehrle

2.1.1.4.2 Tubular membrane module

Hollow fiber membrane module

The hollow fiber membranes are generally used in iMBR but there are some some applications for sMBR as well (Table 2.2). The hollow fiber modules are formed of two basic geometries as shown in Fig. 2.4. In the first case, the shell-side feed design (Fig. 2.4a), the system is pressurised from the shell side, the permeate passes through the fiber wall and it is collected at the open fiber ends. This design is easy to make and allows using very large membrane areas. For this reason, the fibers usually have small diameters and thick walls, typically 50 µm inner diameter and 100 to 200 µm outer diameters. These types of modules are generally applied in iMBR.

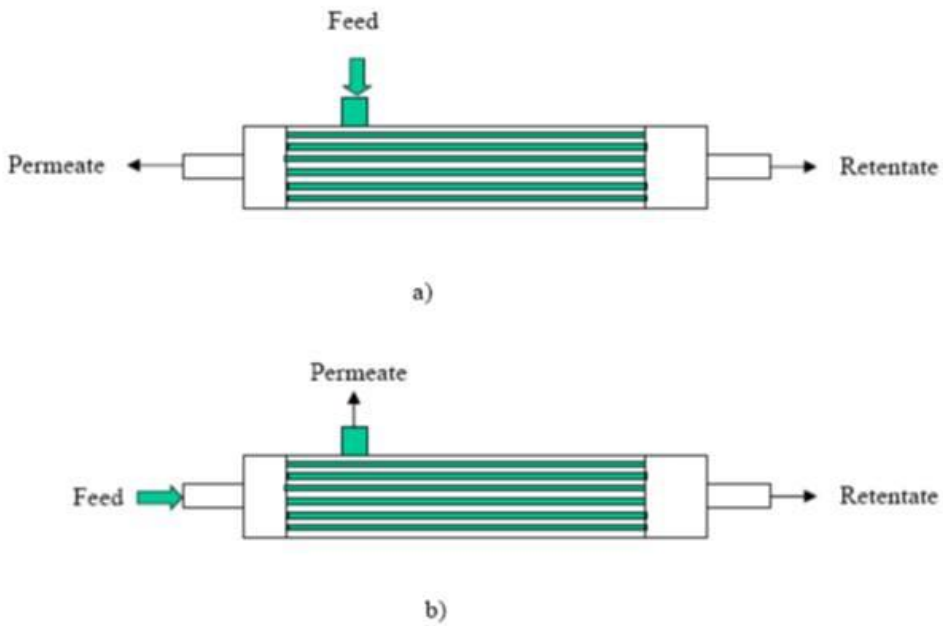

Fig. 2.4 : The two types of hollow fiber modules typically used: a) shell-side feed b) bore-side feed.

In the second case (Fig. 2.4b), the bore side feed, the fibers are open at both ends and the feed fluid circulates through the bore of the fibers. To minimise the pressure drop inside the fibers, the diameters are usually larger than those of fine fibers used in the other case and are generally made by spinning solu-

tion. This type of module is mainly applied with tubular membranes in sMBR. A hollow fiber cross section is shown in Fig.2.5.

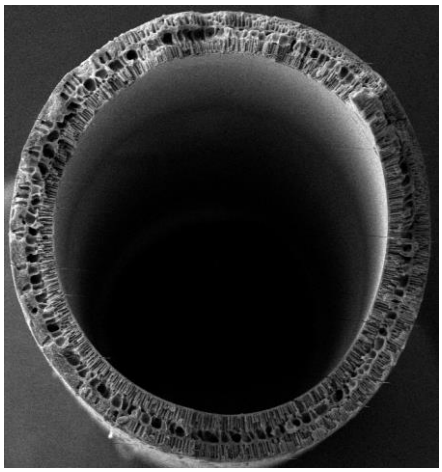

*Fig. 2.5 : Cross section of a Hollow fiber membrane (*Figoli, et al. 2005)

Concentration polarisation is well controlled in bore side-feed modules while in shell-side feed this is difficult to avoid. A method to minimise the concentration polarisation is to direct the feed flow normal to the direction of the hollow fibers. The hollow fiber module has the highest packing density of all modules types available on the market today. Expensive, sophisticated and very high speed automated spinning machine, fiber handling and module fabrication equipment is required to produce these modules (Baker, 2000, p.148).

2.1.1.5 Membrane materials and pore size

Membrane materials and pore size are important criteria to select membranes for MBR application. There are two different types of membrane materials, these being polymeric and ceramic. Metallic membrane filters also exist, but these have very specific applications which do not relate to membrane bioreactor (MBR) technology. The membrane material, to be made useful, must then be formed (or configured) in such a way as to allow water to pass through it. In MBRs, a tight microfiltration or a loose ultrafiltration membrane is often applied. The range of membrane filtration with particle size is shown in Fig. 2.6.

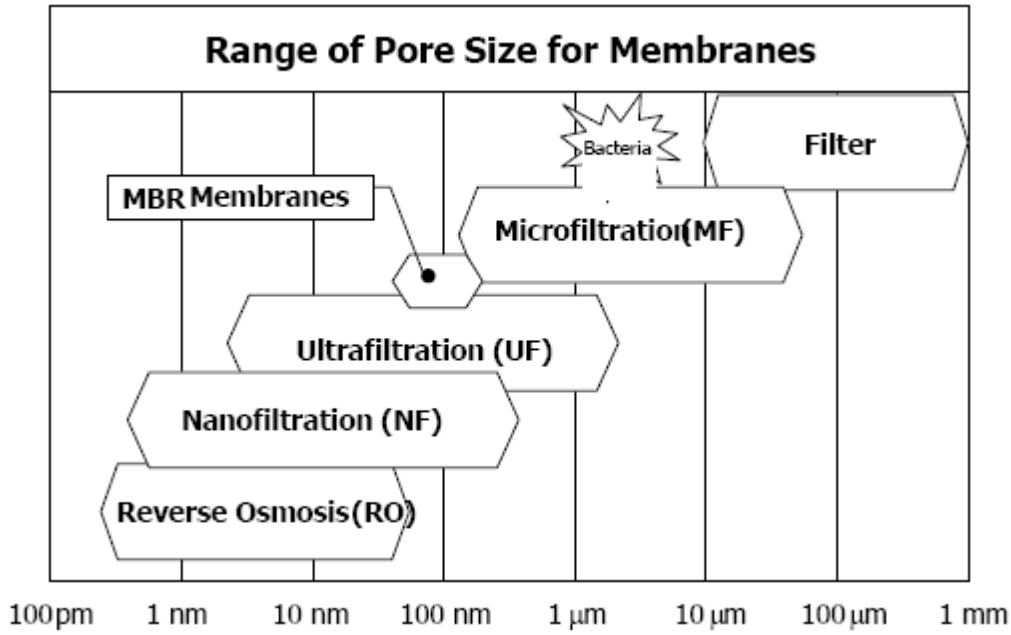

Fig. 2.6 : Range of pore size for MBR membranes (Adapted from Aggerwasser, Kubota, 2005)

A number of different polymeric and ceramic materials are used to form membranes, but generally nearly always comprise a thin surface layer which provides the required permselectivity on top of a more open, thicker porous support which provides mechanical stability. A classical membrane is thus anisotropic in structure, having symmetry only in the plane orthogonal to the membrane surface. Polymeric membranes are also usually fabricated both to have a high surface porosity, or % total surface pore cross-sectional area, and narrow pore size distribution to provide as high a throughput and as selective a degree of rejection as possible. The membrane must also be mechanically strong (i.e. to have structural integrity). Lastly, the material will normally have some resistance to thermal and chemical attack, that is, extremes of temperature, pH and/or oxidant concentrations that normally arise when the membrane is chemically cleaned, and should ideally offer some resistance fouling (Judd, 2006, p.24).

Whilst, in principal, any polymer can be used to form a membrane, only a limited number of materials are suitable for the duty of membrane separation, the most common being:

- Polyvinylidene difluoride (PVDF)
- Polyethylsulphone (PES)
- Polyethylene (PE)
- Polypropylene (PP)
- Polysulfon (PS)

The most often used membrane materials in MBRs are organic polymers, e.g., PE, PP and PVDF membranes (Judd, 2006, p.25). Some of them are blended with other materials to change their surface charge or hydrophobicity (Mulder, 1996, p.49). Nowadays ceramic materials have been shown suitable for MBR technology due to their thermal, chemical and mechanical stability.

All the above polymers can be formed, through specific manufacturing techniques, into membrane materials having desirable physical properties, and they each have reasonable chemical resistance (Judd, 2006, p.25). Based on the common membrane materials the principle types of membrane are shown in Fig. 2.7.

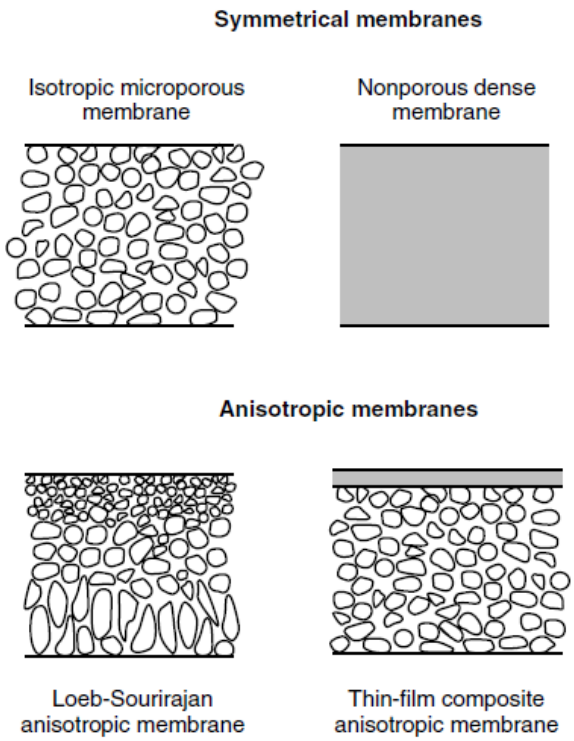

Fig. 2.7 : Principle types of membranes (Baker, 2004, p.4)

Membrane hydrophobicity has shown in some studies to play a significant role (Chang and Lee, 1998; Chang *et al.*, 1999; Choo *et al.*, 2000a; Stephenson *et al.*, 2000). Hydrophobic protein residues can form strong attachments to hydrophobic membranes resulting in strong fouling (Howell and Nystrom,1993; Russotti *et al.*, 2001). Indeed, surface modification of hydrophobic polymeric membranes by chemical oxidation, chemical reaction, plasma treatment (Judd, 2006, p.25) or grafting more hydrophilic polymers can reduce fouling and improve flux (Choo *et al.*, 2000b; Russotti *et al.*, 2001; Sainbayar *et al.*, 2001). Membrane materials may also determine the applicable fluxes. Kang *et al.* (2002) compared the filtration characteristics of organic and inorganic membranes, observing that flux was determined by internal fouling in inorganic membranes and the formation of a cake layer over the organic membrane. Ghyoot and Verstraete (1997) also achieved higher fluxes using a ceramic microfiltration membrane, in comparison with a polymeric ultrafiltration membrane. However, these differences in membrane performances may also be the result of structural differences between the membranes, like surface roughness. (Bérubé *et al.*, 2006).

Membrane pore sizes used in wastewater treatment applications are in the range of 0.02-0.5 μm (Stephenson *et al.*, 2000). Several authors have observed the existence of an optimum membrane pore size (Choo and Lee, 1996; Elmaleh and Abdelmoumni, 1997). This suggests that higher pore sizes may foul more rapidly as a result of blocking by macrocolloids or cells, while those smaller are expected to foul more readily as a result of clogging by microcolloids that can adsorb to the internal surface of the pores (Bérubé *et al.*, 2006). It should also be considered that membrane rejection properties are not only defined by membrane pore size but also by the formation of a gel or cake layer, which acts as a secondary dynamic membrane. This phenomenon has been observed in both anaerobic and aerobic MBRs (Harada *et al.*, 1994; Pillay *et al.*, 1994; Choi *et al.*, 2005b). When long term operation is considered, the formation of cake or gel layers may also reduce the influence of membrane properties over filtration performance, since the membrane is not anymore in direct contact with the suspension.

2.1.2 Filtration processes of MBRs

2.1.2.1 Membrane filtration process in general

A membrane is an interphase that restricts the passage of different components in a specific manner and over a wide range of particle sizes and molecular weights, from ions to macromolecules (Drioli, *et al*. 2005, p.8).

The influent to the membrane is called “feed” and the solvent passes through the membrane is called “permeate”. It is measured as a flow rate per surface unit. The liquid that is retained by the membrane and remained in the feed stream is called “concentrate or retentate”. The basic principle of a membrane operation is shown in Fig. 2.8.

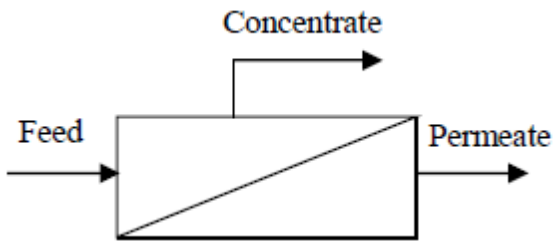

Fig. 2.8 : Basic principle of membrane operation

The efficiency of a membrane basically is determined by two parameters: permeability (the rate at which a given component is transferred through the membrane) and selectivity (the ability to separate in a specific way a given component from others). The transport of different species through a membrane is a non-equilibrium process, and the separation of the different components results from difference in their transport rate. In a membrane separation process, the transport rate of a component through the membrane is activated by various driving forces such as gradients in concentration, pressure, temperature or electrical potential.

2.1.2.2 Pressure driven membrane process

In pressure driven membrane processes the solvent and solute molecules permeate through the membrane as a result of the applied pressure, whereas other molecules or particles are rejected to various extents depending on the structure of the membrane. If the pore size is considered for membranes from microfiltration to ultrafiltration, nanofiltration and reverse osmosis, the pore sizes in

the membrane diminishes and consequently becomes smaller the size (or molecular weight) of the particles or molecules separated. This implies that the resistance of the membranes to mass transfer increases and hence the applied pressure has to be increased to obtain the same flux (Table 2.3).

*Table 2.3 : Typical pore size and driving force applied in pressure driven membrane processe (IUPAC definition of pore diameter: Macropores: ∅ > 50 nm; Mesopores: ∅ range 2 nm – 50 nm; Micropores: ∅ < 2 nm (*Drioli, *et al*. 2005, p.9*).*

Membrane process	**Typical pore size**		**Pressure applied**
	Pore diameter	IUPAC classification	
Microfiltration	50 – 10000 nm	macropores	<2 bar
Ultrafiltration	1 – 100 nm	mesopores	1 – 10 bar
Nanofiltration	< 2 nm	micropores	10 – 25 bar
Reverse Osmosis	< 2 nm	micropores	15 – 80 bar

Filtration systems, which membranes belong to, can be divided primarily into "depth filters", in which all the depth of filtering element contributes to retain the particles from the flow, and "screen filters", in which particles whose dimensions are larger than pores are retained on a single side of the filter. Membranes (e.g. MBR) belong to this last category, the one of screen filters (Manigas, 2008).

Microfiltration and ultrafiltration processes are mainly related to porous membranes and are used in MBR technology. A large variety of pore geometries is possible.

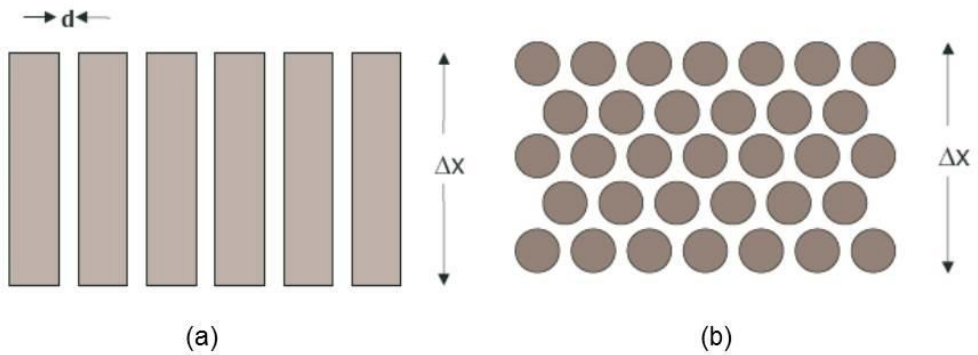

Fig. 2.9 : Simplified schematic pore geometries in porous membranes : a) cylindrical b) spherical (UNSW, 2005, aaflowsystem, 2005, tu-freiburg, 2011)

Fig. 2.9 gives two simplified schematic pore geometries found in porous membranes. The existence of these pore geometries implies that different models have been developed to describe mass transport adequately.

Since MBR technology represents microfiltration or ultrafiltration processes, the models based on these processes have been taken into account. These transport models indicate which structural parameters are important and how membrane performance can be improved by variation of specific parameters.

There are mainly two basic models (Mulder, 1996, p.224):

- Model A
- Model B

These models are discussed in the following sections.

Model A

The simplest representation is one in which the membrane is considered as a number of parallel cylindrical pores perpendicular to the membrane surface (Fig. 2.9 a).

The length of each cylindrical pore is in simplest equal to membrane thickness. The volume flux can be described by the Hagen-Poiseuille law. Assuming that all pores have the same diameter the liquid flow through a pore is given by:

$$\dot{q} = \frac{\pi d^4}{128\eta} \frac{\Delta p}{\Delta x} \qquad (2.1)$$

Where Δp is the pressure difference across the pore length Δx, η is the liquid viscosity and d is the diameter of the pore. The flux, or flow per unit membrane area, is the sum of all flows through the individual pores and so given by:

$$\dot{V} = N \frac{\pi d^4}{128\eta} \frac{\Delta p}{\Delta x} \qquad (2.2)$$

Where N is the number of pores per square unit of membrane. For membranes of equal pore area and surface porosity ε_s, the number of pores per square unit, N is:

$$N = \varepsilon_s \frac{4}{\pi d^2} \qquad (2.3)$$

By combining Eq. (2.2) and Eq. (2.3) it follows:

$$\dot{V} = \frac{\varepsilon_s d^2}{32\eta} \frac{\Delta p}{\Delta x} \qquad (2.4)$$

The most important properties characterizing a microporous membrane are the pore diameter *d* and the surface porosity ε_s (Fig. 2.10). The pore diameter is typically in the range of 0.01-10 μm, the porosity is about 0.3 - 0.7. Although microporous membranes are usually characterized by a single pore diameter value, most membranes actually contain a range of pore size distribution.

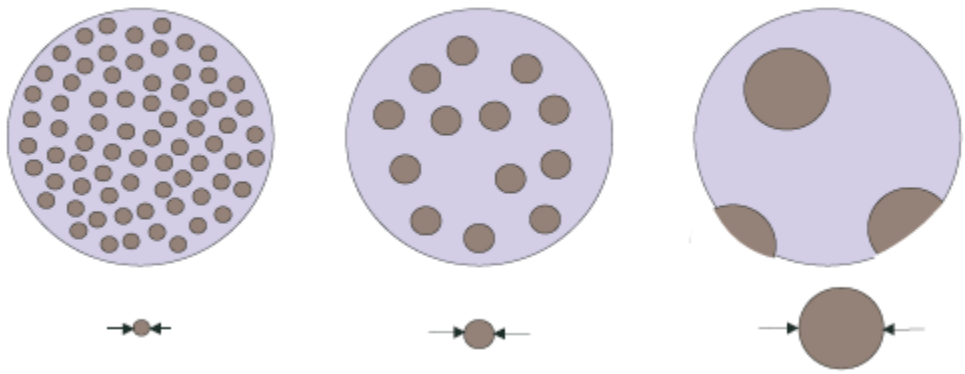

Fig. 2.10 : Surface view of porous membranes of equal porosity ε_s, but differing pore size (Baker, 2004, p.68).

With real membranes a so called tortuosity facor τ is introduced. It reflects the length of the average pore compared to the membrane thickness (Fig. 2.11). Simple cylindrical pores at right angles to the membrane surface have a tortuosity of 1. Usually pores take a more meandering path through the membrane, so typically tortuosities are in the range of 1.5-2.5. Eq. (2.4) modified with tortuosity factor gives:

$$\dot{V} = \frac{\varepsilon_s d^2}{32\eta\tau} \frac{\Delta p}{\Delta x} \qquad (2.5)$$

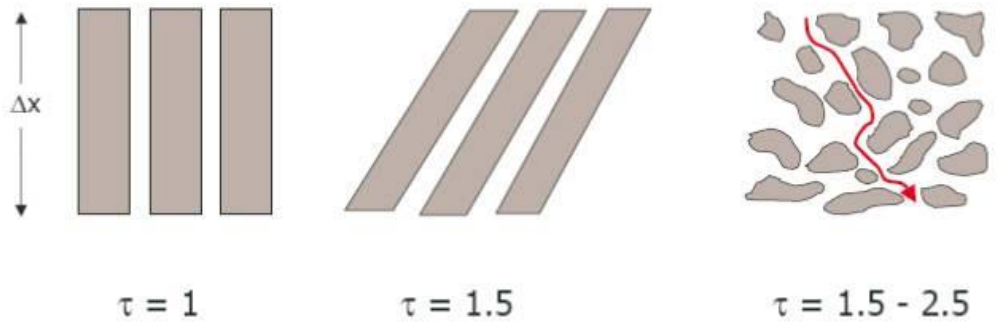

Fig. 2.11 : Cross sections of porous membranes of different tortuosity (Baker, 2004, p. 68)

Model B

In this model the membranes are regarded as a system of closed packed spheres (Fig.2.9b). This structure can be found in organic and inorganic sintered membranes or in phase inversion membranes with nodular top layer structure.

Membranes consisting of closed packed spheres can best be described by the Kozeny-Carman
equation (Eq. 2.6) :

$$\dot{V} = \frac{\varepsilon_v^3}{K\eta S^2 (1-\varepsilon)^2} \frac{\Delta p}{\Delta x} \qquad (2.6)$$

Where ε_v is the volume fraction or volume porosity of the pores, S the internal surface area and K the Kozeny-Carman constant, which depends on the shape of the pores and the tortuosity. For spherical particles and assuming K=5 then Eq. (2.6) can be written as:

$$\dot{V} = \frac{\varepsilon_v^3 d^2}{\eta\,(1-\varepsilon)^2} \frac{\Delta p}{\Delta x} \qquad (2.7)$$

As in model A, Eq. (2.7) relates volume flow to simple structural parameters such as porosity and pore diameter in model B. In both models the flux through a given membrane can be simplified considered as being directly proportional to the applied pressure:

$$\dot{V} = A \cdot \Delta P \qquad (2.8)$$

Where, the so called permeability constant A contains all structural factors.

2.1.2.3 Parameters affecting membrane performances

A pressure driven membrane filtration process (section 2.1.2.2) based on pressure gradient is affected by the following factors:

- Intrinsic resistance of the membrane
- Transmembrane pressure (TMP)
- Hydrodynamic regime at the interface between the membrane and the solution to be filtered.
- Concentration polarisation phenomenon
- Fouling

2.1.2.3.1 Intrinsic resistance of the membrane

Intrinsic resistance of a membrane is the physical resistance opposed by the clean membrane to the filtration of pure water. It is the function of pore dimension, of surface porosity of the membrane, of the ratio between surface and volume of porous surface ($m^2 \cdot m^{-3}$) and of membrane depth (Manigas, 2008). This is denoted by $\frac{1}{A}$ as shown in Eq. (2.8).

2.1.2.3.2 Transmembrane pressure (TMP)

Transmembrane pressure (TMP) is denoted as the pressure difference applied between upstream and downstream of the membrane in order to determine the permeate crossing through the membrane (section 2.1.2.2). TMP is thus defined as

$TMP = P_{feed} - P_{permeate}$

Where,

P_{feed} = pressure on the side of the solution to be filtrated (bar)
$P_{permeate}$ = pressure on the side of the permeate (bar)

For submerged membranes, pressure in the upstream of the membrane is calculated as average hydrostatic charge between upper and lower extremity of the module:

$$P_{feed} = \frac{\rho . g . h_{up} + \rho . g . h_{low}}{2} \qquad (2.9)$$

Where,
ρ = feed density (kg/m^3)
g = acceleration due to gravity (m/s^2)
h_{up} = immersion depth of the upper extreme of the filtering surface (m)
h_{low} = immersion depth of the lower extreme of the filtering surface (m) (Manigas, 2008).

2.1.2.3.3 Hydrodynamic regime

Usually, turbulence obtained by means of increase of feed flow rate can be helpful in decreasing membrane fouling (details on fouling is described in section 2.1.3.2). However, overcoming a certain feed flow rate can cause membrane fouling, because while turbulence cleans away the bigger molecules from the surface of the membrane, the small molecules enter into the pores of the membrane causing its irreversible fouling.

A membrane system can be operated in two ways:

- at constant TMP, with progressive flux decrease, caused by the gradual membrane fouling;
- at constant flux, with progressive increase of TMP, due to the gradual membrane pores blocking.

2.1.2.4 Hydraulic geometry of MBR

Hydraulic geometry of MBR is a complex aspect. So many parameters and geometries are involved in the hydraulic systems of MBR. Microbiology in the reactor is one of them. The microbiological aspect is described in section 2.1.2.4.1 below.

2.1.2.4.1 Microbiological aspects of MBR

Microbiological species of MBR are influenced by several common parameters such as:

- Hydraulic residence time (HRT)
- Mixed liquor suspended solids (MLSS)
- Sludge retention time (SRT)
- Sludge loading (SL) etc.

An overview of these common parameters have been outlined in the following sections.

Hydraulic residence time (HRT)

Hydraulic residence time (HRT) indicates the time as long the feed solution remains in the MBR reactor in hour before it gets processed as permeate by membrane. The formula for HRT is

$$HRT(h) = \frac{Hydraulic volume(L)}{Permeate\ flow(L/h)} \qquad (2.10)$$

From equation (2.10) it is clear that HRT depends on the hydraulic volume of the reactor and the permeate flow. If HRT is very high, it is easier for bacteria to acclimate the reactor conditions but very low HRT affects the conditions inversely.

Mixed liquor suspended solids (MLSS)

Mixed liquor suspended solids (MLSS) is the concentration of suspended solids in mixed liquor, usually expressed in g/L (wateronline, 2011). Mixed liquor is a mixture of raw or settled wastewater and activated sludge contained in an aeration basin in the activated sludge process. The MLSS is used to control the wastewater treatment plant in suspended growth process.

Sludge retention time (SRT)

Sludge retention time (SRT) indicates how frequently the sludge is taken away from MBR reactor. In another way, it means the sludge age. According to (Laera et al, 2007) a significant correlation between SRT and organic loading rate has been observed. This study suggested that the biomass activity is weak-

ly affected by the sludge age. Membrane cleaning requirements also appear to be scarcely dependent on SRT.

Sludge loading (SL)

The sludge loading or feed to microorganism (F/M) ratio is an important design parameter for MBR process. Generally, the MBR process can operate at higher F/M ratios when compared to an activated sludge plant (Robinsion, 2003). It is defined by kg COD/kg MLSS·day.

Microbiological aspects:

In the biochemical stage of wastewater treatment, organic carbon and nutrients are removed from wastewater by microbes. These microbes live and grow enmeshed in Extra-cellular Polymeric Substances (EPS) that bind them into discrete micro-colonies forming three-dimensional aggregated microbial structures called flocs. The ability of microorganisms to form flocs is vital for the activated sludge treatment of wastewater. The floc structure enables not only the adsorption of soluble substrates but also the adsorption of the colloidal matter and macromolecules additionally found in wastewaters (Michael *et al*., 2002, Liwarska-Bizukojc *et al*., 2005). The diversity of microbial community in activated sludge is very large, containing prokaryotes (bacteria), eukaryotes (protozoa, nematodes, rotifers), and viruses. In this complex microsystem, bacteria dominate the microbial population and play a key role in the degradation process (Michael *et al.*, 2002).

MBR technology with biochemical and sludge-separation stage integrated into one step implies a continuous generation of new sludge with the consumption of feed organic materials, while some sludge mass is decayed by endogenous respiration. Endogenous respiration involves consumption of cell-internal substrate, which leads to a loss of activity and slightly reduced biomass. Endogenous respiration implies all forms of biomass loss and energy requirements not associated with growth by considering related respiration under aerobic conditions: decay, maintenance, endogenous respiration, lyses, predation, and death. It can be both aerobic and anoxic, though under anoxic conditions it is a lot slower and especially protozoa are considerably less active under denitrifying conditions (slower predation) (Gujer *et al*., 1999).

Endogenous respiration of a microbial community in MBR can be encouraged by very high sludge age, i.e., high sludge concentration. The energy available to microorganisms is determined by the supply of substrate. By increasing the

Sludge Retention Time (SRT), which increases biomass concentration, it would be theoretically possible to reach a situation where the amount of energy provided equals the maintenance demand. This concept was first introduced. by Pirt (Pirt, S.J., 1965), where maintenance energy is defined as the amount of biochemical energy strictly necessary for sludge endogenous respiration. Microorganisms satisfy their maintenance energy requirements in preference to producing additional biomass. Therefore, under the conditions of decreased nutrient supply, external substrate is used only for the upkeep of bacterial functions, while the amount of bacteria is not changed. In various studies on applications of MBR in wastewater treatment, zero sludge production was established at different F/M ratios, obviously depending on feed compositions which determine the growth of microbial populations (Liu *et al*., 2005; Rosenberger *et al*., 2000; Yoon *et al.*, 2002).

However, there is an optimal biomass concentration (i.e., SRT) for a successful operation of MBR. Biomass retention results in a slow-growing population with high sludge ages, where cell dormancy and death reduce the viability of population (Cicek *et al.*, 2001; Macomber *et al.*, 2005). An example of changes in sludge yield and biomass concentration with sludge age are presented in Fig. 2.12 (HRT- hydraulic retention time, *k*-rate constant for endogenous metabolism, *k*d-rate constant for biomass decay) (Howell *et al*., 2003).

Several explanations are suggested for this phenomenon. Since MBR sludge acts as a non-Newtonian fluid, by increasing the mixed-liquor suspended solids (MLSS) concentration, the viscosity of sludge increases exponentially. This results in mass transfer limitations for both the oxygen and substrate, which increases aeration costs as well as causing extensive membrane fouling (Wei, Y., 2003). On the other side, at lower MLSS concentrations, more specific surface area is available for the uptake of a substrate and enzyme production, and the enzymatic activity is higher. Thus, when operating at low SRT, response of the system in degradation of xenobiotic waste should be faster.

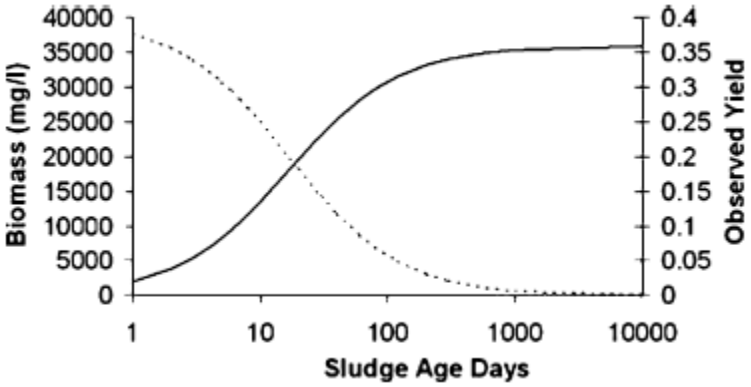

Fig. 2.12 : Net observed yield and biomass concentration as a function of sludge age in a MBR, HRT=2.7 h, Y=0.4, k = 0.07 d^{-1}, kd = 0.06 d^{-1}(Howell et al., 2003).

Moreover, the chances of genetic mutation and adaptation of microorganisms to different organic loadings should be greater (Cicek *et al*., 2001). Horan *et al*., (1990) also noted that at high sludge ages the solubility of substrate becomes rate-limiting.

Ng *et al*., (2005b) studied the performance of MBR at low SRT (0.25–5 days). They indicated that modification of sludge morphology, i.e., proliferation of non-flocculating microorganisms, could have a positive impact on removal performance. In addition, works of Wilen *et al*., (1999) showed that the surface properties and the structure of biological flocs in activated sludge are correlated to the chemical constituents of EPS, and can be significantly influenced by the operating condition. However, some investigations have given completely opposite results. Massé *et al*., (2006) observed a decrease in floc size at higher SRTs. This could be due to lower production of EPS, which is responsible for the formation of flocs or other cell aggregates. Moreover, growth of non-flocculating bacteria is enhanced because they are more exposed to the present substrate than when they are arranged into macro-flocs.

Some authors believe that there should be a minimal rate of sludge wasting in order to keep an optimal range of sludge concentration in MBR (Cicek, *et al*., 2001; Hasar *et al*. 2004; Lubbecke *et al*.,1995; Huang *et al*., 2001). When no sludge is withdrawn from the reactor, accumulation of inorganic compounds can be expected (Rosenberger, S., 2002; Huang, *et al*., 2001; Li *et al*., 2006; Xing *et al*., 2000). Retention and accumulation of non-biodegradable compounds in the bioreactor could lead to microbial inhibition or toxicity, which

limits the alternatives available for excess sludge disposal. Several works have described a possible negative long-term effect of accumulation of recalcitrant compounds on process stability (Muller, E.B., 1995; Knoblock *et al*., 1994; Ross *et al.*, 1992; Zaloum *et al*., 1994). Non-biodegradable solids (solids that are not metabolized under present conditions) are either present in the influent or they are produced in the microbial process. Their forming can also be a result of protozoan activity, which may not degrade the bacterial cell walls fully, leaving behind the inert material. However, inerts are not ultimately inert: it is possible that degradation of inert material occurs by slow-growing bacteria, which will depend on the SRT (Van Loosdrecht *et al*., 1999). Many studies have reported a stable performance of MBR during long operating periods, with a dynamic balance of active biomass and inorganic fraction during long-term operating periods (Muller, E.B., 1995; Xing, CH., 2000; Rosenberger *et al*., 2002).

Taking into account all of the above-mentioned aspects of SRT control in MBR, SRT should be chosen in such a way to avoid both the adverse effects of accumulated non-biodegradable substances resulting from low sludge discharge and also an excessive production of sludge at low sludge ages. High sludge ages are one of the main advantages of MBR, considering that in conventional treatment processes long SRTs are impossible because of bad settling ability of sludge at high concentration and withdrawal of suspended solids with the effluent. Typical values for MLSS concentration in MBR vary from 10 to 25 g $MLSSL^{-1}$, while in CAS they are around 1.5–5 g MLSS L^{-1} (Rosenberger *et al*., 2000; Metcalf *et al*., 1991).

Besides the "prolonged SRT" strategy, sludge decay rate in MBR could be boosted by disintegration of some part of sludge. The most common way for achieving this is sludge lyses. Lyses imply death and the breaking apart of cells, and therefore loss of bacteria. The autochthonous substrate formed contributes to the organic loading and is reused in microbial metabolism. Since the biomass growth on this substrate cannot be distinguished from the growth on the original organic substrate, it is called cryptic growth, and it was first introduced by Ryan *et al*., (1959). Limiting step for cell lyses is the degradation of the cell wall, and in order to accelerate it, physical or chemical treatment can be used (Mason *et al.*, 1987). Canales *et al*., (1994) managed to improve the endogenous metabolism in anaerobic membrane bioreactor (anMBR) by inducing cell death and lyses with a thermal treatment. Biomass was extracted and treated at three different temperatures (50, 70, and 90° C) (Fig. 2.13), while the hydrolysates were recycled to the bioreactor. Thus, improvement of endoge-

nous metabolism was obtained by cryptic growth with very low HRT and SRT (2 and 10 h, respectively).

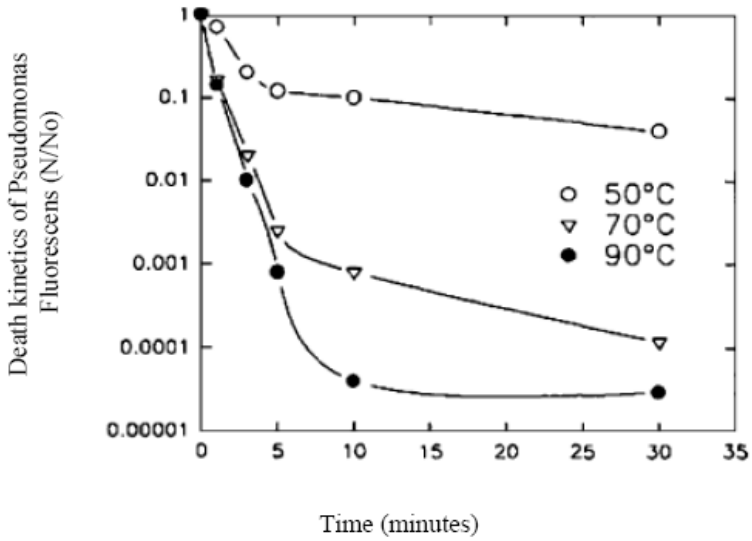

Fig. 2.13 : Death kinetics of P. Fluorescens at different temperatures (Adapted from Canales et al., 1994)

Environmental factors that influence and limit microbial growth are temperature and pH value, i.e., the acidity or alkalinity of the aqueous environment. Temperature has a profound effect not only in governing the rate of the treatment but it also affects bacterial composition. Chiemchaisri *et al*., (1994) investigated performances of MBRs at various temperatures and noted a reduction in the number of strict aerobic bacteria when temperature was lowered, suggesting a limited oxygen transfer, partly due to reduced viscosity of mixed liquor at lower temperatures. The temperature range for optimal performance of MBR was found to be from 15 to 25° C, while the treatment efficiency deteriorated as the temperature decreased to 10° C. As far as pH is concerned, autotrophic metabolism is considered impaired outside the optimal pH range (7.2–8.5) (Marsili-Libelli *et al*., 2002).

How to operate MBR systems efficiently remains a topic of argument because there is a lack of information on the development of microbial community structure in the reactor (Li *et al*., 2006). The characteristics of sludge morphology (dispersed bacteria, lower amount of large filamentous bacteria, floc densification) certainly play an important role in the removal efficiencies, but they

also affect sludge filterability and fouling mechanisms. Under the high organic loading conditions (i.e., low SRT), foaming and sludge bulking may rise.

In particular, the modification of sludge structure induced by membrane separation compared to a settling separation is still unclear. Because MF and UF membrane retain dispersed bacteria as well as colloidal and supra-colloidal material, the biological medium in MBR can be significantly diffeent from those produced in an activated sludge (Gao *et al.*, 2004). It can be assumed that if operated at high sludge ages, bacteria in MBR face conditions of extreme competition for the inflowing substrates. However, microbiology and physiology of MBR are far from being understood (Radjenovíc *et al.*, 2008).

2.1.3 Resistance model

During an actual pressure driven membrane separation process the membrane performance or system performance may change very much with time: the flux decreases over time. Flux decline has a negative influence on the economics of a given membrane operation, and for this reason measures must be taken to reduce this incident (Mulder, 1996).

In MBR technology, flux decline can be caused by several factors, such as fouling (section 2.1.3.2) due to adsorption, gel layer formation, and plugging of the pores etc. All these factors induce additional resistances on the feed side to the transport across the membrane. The extent of these phenomena is strongly dependent on the types of membrane process and feed solution employed.

According to Dracy's Law a relationship between TMP and flux can be developed as shown in Eq. (2.11)

$$J = \frac{TMP}{\mu R_t} \qquad (2.11)$$

Where,

J = Membrane permeate flux (L/m^2.h)
TMP = Transmembrane pressure (mbar)
μ = Dynamic viscosity of permeate (N.s/m^2)
R_t = Total filtration resistance (1/m)

R_t can be expressed as the sum of individual resistances which can be varied based on the number and type of resistances considered (adapted from Jifeng et al., 2008). The expression of R_t can be written as follows:

$$R_t = R_m + R_e + R_i = R_m + R_p + R_c + R_i \qquad (2.12)$$

Where,

R_m = Constant resistance of the clean membrane (1/m)

R_e = Internal fouling resistance which includes R_p (resistance due to concentration polarizsation which can be neglected) and R_c (cake layer resistance) (1/m)

R_i = Resistance due to pore blocking (1/m)

Eq. (2.12) can be termed as resistance in membrane series (RIS) model which is applied to describe membrane fouling mechanisms (Jifeng et al. 2008).

In this section of the thesis works, the RIS model has been adapted according to applied experimental set ups and test media (Section 5.6.13 and section 6.3.13 in this thesis).

2.1.3.1 Membrane resistance

For pressure driven membrane processes, pure water flux can be defined as:

$$J = \frac{\Delta p}{\eta \cdot R_m} \qquad (2.13)$$

Where,

J = pure water flux

Δp = pressure difference (TMP)

η = dynamic viscosity and

R_m = membrane resistance for pure water filtration across the membrane (Fig. 2.14)

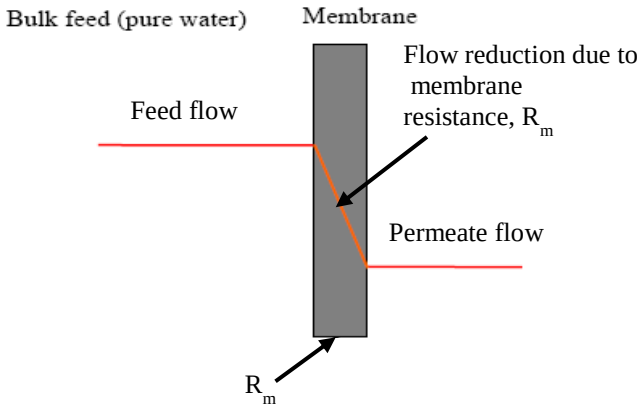

Fig. 2.14 : Membrane resistance (R_m) in pure water flux

R_m can be determined from the experimental data of pure water permeate flux J, under various mean TMPs (section 2.12.2, Eq. 2.8, where $A = \frac{1}{\eta \cdot R_m}$).

2.1.3.2 Membrane fouling

When treating organic solutions (as macromolecule solutions) the solute concentration at the membrane surface can attain a very high value and a maximum concentration, the gel concentration, may be reached. The formation of a gel layer on the membrane surface is often denoted as fouling. The gel concentration depends on the size, shape, chemical structure and degree of solvation but is independent of the bulk concentration.

2.1.3.2.1 General considerations of fouling

A decrease in the permeate flux or increase in TMP during a membrane process is generally understood by the term "fouling". Fouling occurs as a consequence of interactions between the membrane and the mixed liquor, and is one of the principal limitations of the MBR process. There has been done a lot of research on this subject (Chua *et al*., 2002), so it is of interest to describe the fouling in more details. Fouling of membranes in MBRs is a very complex phenomenon with diverse relationships among its causes, and it is very difficult to localize and define membrane fouling clearly. The main causes of membrane fouling are (Radjenovíc *et al*., 2008):

- Adsorption of macromolecular and colloidal matter
- Growth of biofilms on the membrane surface
- Precipitation of inorganic matter
- Aging of the membrane

The formation of a gel or cake layer is one cause for membrane fouling. Gel or cake formation may be caused by a variety of materials including inorganic precipitates such as $CaSO_4$, $Fe(OH)_2$ and other metal hydroxides, organic materials such as proteins, humic acids and other macromolecular materials, and biological components such as micro-organisms and products of their metabolism. The attachment of the substances to the membrane surface may be caused by adsorption due to hydrophobic interactions, van der Waals force attractions or electrostatic forces. The fouling layer itself may be rather porous and thus permeable for aqueous solutions as some inorganic precipitants or highly impermeable as some films of mineral oils or hydrophobic surfactants (Cassano *et al*., 2005, p.94).

2.1.3.2.2 Fouling mechanism

MBRs are normally operated under a constant flux. Since the fouling rate increases roughly and exponentially with the flux, MBR plants are operated at modest fluxes and preferably below the so-called critical flux. The critical flux concept, firstly introduced by Field *et al*., (1995), assumes that in MF/UF processes exists a flux below which a decline of permeability with time does not occur, and above which fouling occurs. In MBR operations, critical flux is normally defined as the highest flux under which a prolonged filtration with constant permeability is possible.

Pollice *et al*., (2005) reviewed the sub-critical fouling phenomenon in MBR. From the reviewed data it is evident that even sub-critical operation inevitably leads to fouling. This fouling is often reported to follow a two-stage fouling pattern (Brookes *et al*., 2004 and Wen *et al*., 2004) which includes slow TMP increase over a long period of time, followed by a rapid increase after some critical time period. In the work of Zhang *et al*., (2006), this pattern is extended with an initial period of conditioning fouling (Radjenovíc et al., 2008).

Membrane fouling is regarded as the most important bottleneck for further development of MBRs. It is the main limitation to faster development of this pro-

cess, particularly when it leads to flux losses that cleaning cannot restore (Howell *et. al*., 2004). In a survey of papers published between 1991 and 2004, more than one third of studies on fundamental aspects of MBRs were related to membrane fouling (Yang *et al*., 2006).

Generally, membrane fouling can be caused by a variety of constituents, among them bacteria, suspended solids, colloids as well as dissolved inorganic and organic compounds (Hilal *et al*., 2004). In MBRs, fouling can be attributed to pore blocking (deposition within the pores) or to cake layer formation on the membrane surface (Jiang *et al*., 2003); (Fig. 2.15). Colloidal and soluble foulants (SMP) can cause pore blocking and irreversible fouling due to their small size.

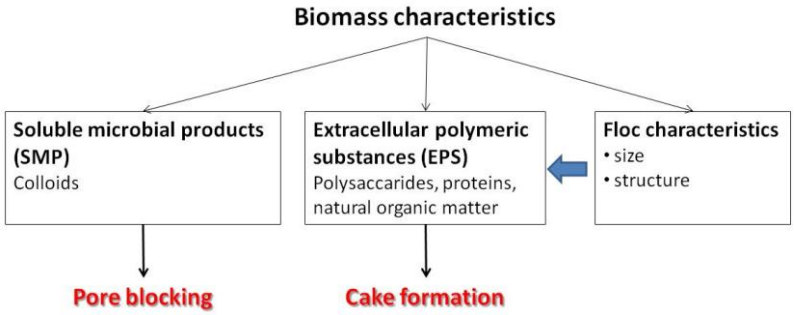

Fig. 2.15 : Biomass characteristics and biofouling

In many publications, membrane fouling in MBRs has been largely attributed to extracellular polymeric substances (EPS) (Drews *et al*. 2006; Rosenberger and Kraume, 2002). EPS consists of polymeric materials secreted by the cell, shed from the cell surface or generated by cell lysis (Bouhabila *et al*., 2001). With its heterogeneous and changing nature, EPS can form a gel matrix in which microbial cells are embedded and can thus create a significant barrier to permeate flow. It has been observed that the supernatant of bio sludge has a 20-30 times higher specific membrane resistance than the sludge suspension itself, which illustrates the high fouling potential of the soluble and colloidal matter in the suspended biomass (Drews *et al*. 2006). In many cases, the accumulation of a filter cake is the principle fouling mechanism. It was reported by Chang and Lee that cake resistance was the major contributor to the resistance of a membrane coupled with an activated sludge system, particularly under low sludge age conditions (Chang and Lee, 1998).

Fouling of polymer membranes is influenced by membrane chemistry and morphology. Currently, typical MBR membrane materials used are modified polyolefins, polysulfone, polyethersulfone, polyvinylidene difluoride (section

2.1.1.5). In these porous membranes, the polymers used have chemical and mechanical stability, but are generally hydrophobic in nature, and as a consequence are highly prone to adsorption of organic foulants like EPS (Choi et al., 2002). With increased tendency to fouling, the MBR filtration performance inevitably decreases with filtration time. Membrane fouling is the most serious problem affecting system performance as it leads to a significant increase in hydraulic resistance, resulting in a decline of permeates flux. Also, an increase of transmembrane pressure (TMP) occurs under constant-flux conditions.

The bacteria responsible for bio-degradation are also affected by accumulated stress-inducing compounds (e.g. additives, oil, etc.), which leads to a further decrease in the overall MBR performance. As a consequence, laborious membrane cleaning or even replacement of several components is required, increasing maintenance and operating costs of the MBR significantly.

According to the literature review (Zhang *et al*., 2006), the fouling in MBR under sub-critical conditions can be divided into three stages as mentioned below:

- Initial conditioning fouling
- Slow fouling
- Sudden TMP jump

Initial conditioning fouling

This is the very early stage of the fouling. According to Ognier *et al*., (2002) and Jiang *et al*., (2005) during this stage, interaction takes place between membrane surface and soluble components of the mixed liquor. This fouling is usually rapid (measured in hours), irreversible by nature, and occurs even for zero flux operation (Zhang *et al*., 2006).

Slow fouling

In this stage membrane surface is gradually covered by biopolymers such as EPS. It changes the properties of the membrane surface and promotes the microbial flocs to be attached on the surface of the membrane. Over the time, complete or partial pore blocking takes place.

Sudden TMP jump

For uneven distribution of air and liquid flow in MBR, inhomogeneous pore blocking occurs in the slow fouling stage. Flux variation also takes place due to occurrence of inhomogeneous fouling, exceeding the critical flux in some areas of the membrane surface. This leads to sudden TMP jump due to operation above the critical flux.

2.1.3.2.3 Factors affecting membrane fouling

Factors affecting fouling can be summarized in three general categories (Cassano *et al*. 2005, p.97):

- Membrane properties;
- Solute properties;
- Operating parameters.

2.1.3.2.3.1 Membrane properties

Hydrophilicity

With aqueous feed streams the ideal membrane should be hydrophilic (water-attracting). If the material is hydrophobic, it will adsorb components that are hydrophobic or amphoteric resulting in fouling. For example, many proteins have hydrophobic regions within their structure that can interact strongly with hydrophobic materials. Unfortunately, many robust polymeric membranes are relatively hydrophobic (water-repelling, but organic- and oil-attracting). One measure of the relative hydrophilicity of a membrane is the contact angle, which is a measure of the wettability of a surface. If a drop of water is placed on a completely hydrophilic material, the water would spread out on the surface, resulting in a zero or low contact angle, which can be measured with a goniometer. A hydrophobic material, on the other hand, would repel the water, causing it to have as little contact with the surface as possible, resulting in a high value of the contact angle (Fig. 2.16).

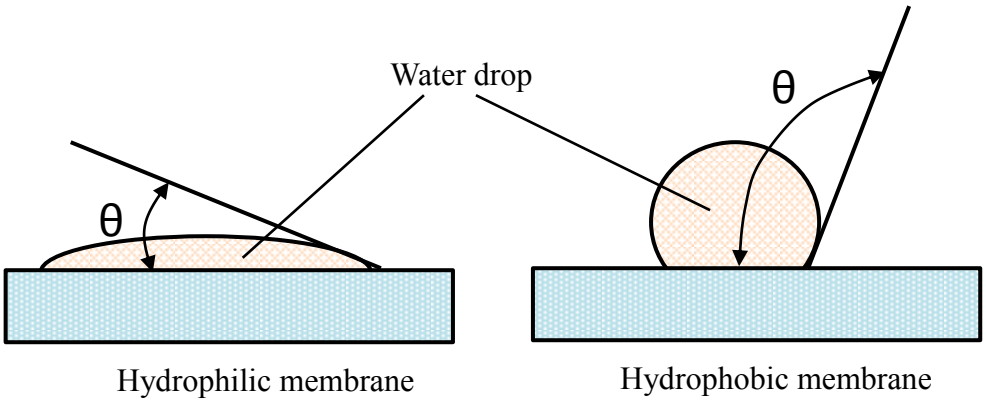

Fig. 2.16 : Contact angle (Cassano et al., 2005, p.98)

Hydrophobic materials would tend to attract oil in an oily wastewater stream, but hydrophilizing the membrane could minimize oil fouling. The well-known hydrophobic materials (PTFE, PP) tend to have high contact angles (>100°) while cellulosics and ceramics and some specially hydrophilized materials have low values (<30°) (Cassano *et al*. 2005, p.97).

Surface topography

An interesting reason why cellulosic membranes foul less compared to other polymeric membranes may be related to the roughness of their surfaces. The surface of cellulosic acetate (CA) membranes appears smooth and uniform; in contrast, polyamide thin-film composite membranes appear to have protuberances on the surface, which could act as hooks for suspended matter in the feed, thus leading to greater fouling. This could explain why polyamide-based membranes tend to foul more than CA membranes, especially with regard to biofouling.

Pore size

There are numerous examples in literature in which larger pore membranes show initially higher flux than tighter membranes; however, during the process, sometimes rapidly, these membranes have lower flux (Fig. 2.17).

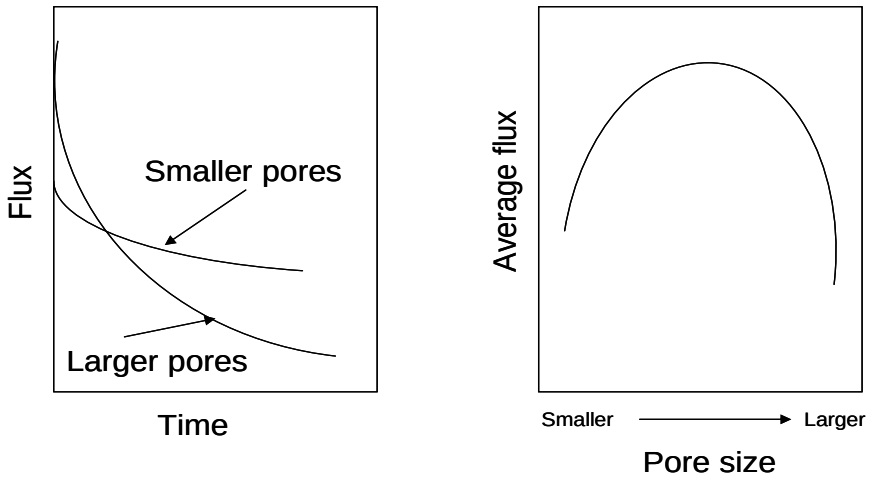

Fig. 2.17 : Effect of membrane pore size on flux (Cassano et al, 2005, p.99)

This phenomenon is especially pronounced in MF applications. If the size of the particle to be separated is of the same order of magnitude as the range of pore sizes being used, some of the smaller particles of the sample could lodge in the pores without necessarily going through them (Fig. 2.18). This physically blockage of the pores will cause a rapid drop in flux in the first few minutes of operation. Many MF membranes have pores much larger than their rating: these are the pores that will get plugged first causing a steep drop in permeation rate. Higher pressures will aggravate the problem by causing a compression of the adsorbed cake and forcing the partially lodged particles to become even more firmly lodged in the pores, making cleaning more difficult. In contrast, if the pores are much smaller than the particles to be separated, the particles will not get caught within the pores but will roll off the surface under the shear forces generated by the flow: in this case the system should be cleaned as soon as possible.

Surface modification

A membrane can be made more hydrophilic and, by implication, less prone to fouling by aqueous feed stream components by introducing a large number of hydrophilic functional groups on its surface, i.e. those capable of binding water or forming hydrogen bonds, such as hydroxyl groups (-OH). Methods include surface coating by adsorption, free radical or radiation grafting of hydrophilic groups and coating with oriented mono layers using Languimir-Blodgett methods. One early technique still in use is simply to soak a membrane in a non-ionic surfactant or water-soluble polymer and then dry it. This is reported par-

ticularly effective with PS and PVDF membranes, although the coating may not last through several cycles of use. Adding sulfonate groups helps minimize fouling by negatively charged foulants.

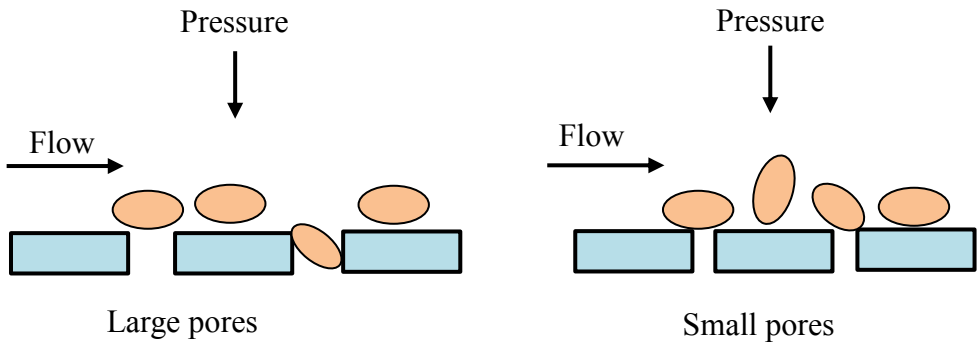

Fig. 2.18 : Mechanism of membrane fouling by particulates, showing the effect of pore size in relation to particle size (Cassano et al, 2005, p.100).

There are several methods of making PS and PES membranes more hydrophilic, most involving blending with hydrophilic polymers (e.g. polyvinylpyrrolidone) or chemical modification of the polymer chain (Cassano *et al*. 2005, p.97).

2.1.3.2.3.2 Solute properties

Proteins

Proteins are a major foulant in MBR membrane processing, considering the multiplicity of functional groups, the charge density within protein molecules, the varying degrees of hydrophobicity and the complex secondary and tertiary structure that allows a protein to interact with other feed components, as well as the membrane itself. All these properties, and thus the nature and extent of fouling, are affected by pH, ionic strength, shear, heat treatment and other environmental factors.

Salts

Mineral salts have a profound influence on the fouling of membranes. They can precipitate on the membrane because of poor solubility or bind to the membrane directly by charge interactions. At a concentration lower than satu-

ration sodium chloride appears to have no effect by itself. In presence of proteins, it appears to increase protein deposition and loss of flux. Sodium chloride in the feed solution reduced fouling by polyphenols. Calcium has been identified as a major cause of fouling in dairy streams, not only due to precipitation in the form of tricalcium phosphate, but also because it`s ionic form could act as a salt bridge between the membrane and proteins, which will lead to faster protein fouling.

pH

In general, flux is lowest at the isoelectric point of the protein and is higher as the pH is moved away from the isoelectric point. Changes in pH affect solubility and conformation of feed components. The solubility of a protein is generally lowest at the isoelectric point; it increases as the pH is adjusted away from the isoelectric point, and this could explain the mentioned phenomenon. However, if there are salts that decrease in solubility and precipitate on the membrane, then flux could decrease at higher pH. The removal of insoluble calcium salts from cheese whey at pH 6.4-7 by filtration or centrifugation improved flux significantly (Cassano et. al, 2005, p.100).

Lipids, fats and oils

The removal of lipids in whey by centrifugation or microfiltration has a beneficial effect on UF flux. With oil-in-water mixtures, it should be remembered that “like attracts like”; if hydrophobic membranes are used, free oils can coat the membrane, resulting in poor flux. Oils have a structure similar to the functional groups of membranes such as PVDF and PS, thus resulting in considerable fouling. Hydrophilic membranes such as the modified PAN membranes have functional groups more like water which gives it excellent hydrophilicity. This preferentially attracts water rather than the oil, resulting in much higher flux.

Antifoams

These are used to suppress foaming in evaporators and fermenters. Many commercial antifoaming agents (e.g. polyoxyethylene, polyglycols, silicone oils, etc.) severely foul hydrophobic membranes. Hydrophilic membranes are fouled less by antifoams.

Humic substances

These are weak acidic electrolytes that are amphiphilic, controlled largely by carboxylic- and phenolic-OH groups. They are micelle-like with molecular weights of 500 and 100,000 and can represent up to 80% of the total organic carbon of natural waters. They become more hydrophobic as pH decreases and, thus, deposit to a greater extent on hydrophobic membranes at lower pH. Other components that have been reported as fouling agent include microbial slime, polyhydroxy aromatics and polysaccharides (Cassano *et al*. 2005, p.97).

2.1.3.2.3.3 Operating parameters

In addition to the complicated interaction of feed components, process parameters such as temperature, flow rate, pressure and feed concentration, as well as overall equipment design, have great influence on membrane fouling.

Temperature

The effect of the temperature on fouling is not too clear. According to the Hagen-Poiseuille model (section 2.1.2.2, model A) on which the pore flow phenomenon is based, increasing temperature should result in higher flux. However, it could also result in a decrease in flux for certain feeds such as cheese whey. At temperatures below 30°C, flux decreases with increasing temperature because of a decrease in solubility of calcium phosphate. However, as temperature is increased further, the beneficial effects (lower viscosity, higher diffusivity) determine a net increase in flux (Fig. 2.19).

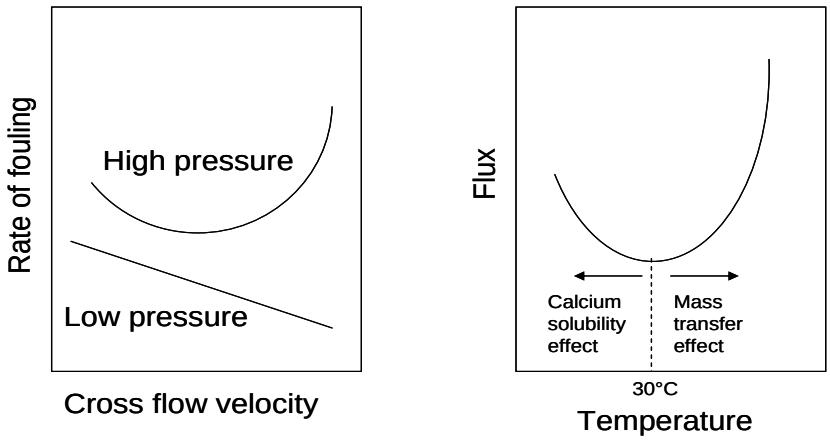

Fig. 2.19 : Fouling of UF membranes by cheese whey (Cassano et al, 2005)

For biological systems high temperatures will result in protein denaturation which will result, other heat damage, in a lowering of the flux.

Flow rate and turbulence

High shear rates generated at the membrane surface tend to shear off deposited materials and thus reduce the hydraulic resistance of the fouling layer in iMBR. However, this may not always happen if the transmembrane pressure is high in relation to the permeation velocity. Tubular modules (sMBR) have flow channels large enough (1.25 - 2.5 cm diameter) to allow most suspended matter to flow easily. Since flow velocity are usually 1-4 m/sec, this results in fairly high Reynolds numbers in the turbulent region, but pumping cost to maintain the high flow velocity is also quite high (sometimes as much as 100 times more energy per unit permeate volume removed than spirals or hollow fibers). At the other extreme are the hollow fiber modules, with inside diameters of 0.5-1.1 mm, which operate in the laminar region but under high shear rates (4000-14,000 sec^{-1}) in sMBR.

Pressure

When transmembrane pressure is in the pre-gel region, flux increases as pressure increases, though usually not linearly for macromolecular feeds. As pressure increases further, the concentration polarization layer reaches a limiting concentration and the flux becomes independent of pressure and becomes mass transfer-controlled. Any pressure increase beyond this point will only bring up the flux momentarily, but as soon as the equilibrium is re-established between the rate of transport of solute to and from the membrane surface, the flux remains essentially unchanged. The situation changes, however, when fouling layers are compressed under the high pressures. Increasing pressure above a critical point may result in a lower flux. With MF and high flux UF membranes, high pressures may cause severe fouling probably due to compaction of the fouling layer. Sometimes it is more important to maintain a low flux rather than low pressures to minimize fouling (Cassano *et al*., 2005, p.102).

2.1.3.2.4 Control of membrane fouling

Completely getting rid of fouling problem in membrane technology is impossible but it can be controlled. The control of fouling and clogging in practice is generally limited to five main strategies (Judd, 2006, p.94):

- Feed pre-treatment,
- Employing appropriate physical or chemical cleaning protocols,
- Reducing the flux,
- Increasing the aeration, and
- Chemically or biochemically modifying the mixed liquor

All of these five strategies are viable for full-scale operating MBRs and are described in the following sections below.

2.1.3.2.4.1 Feed pre-treatment

It is generally recognised that the successful retrofitting of an ASP or SBR with an MBR is contingent on upgrading the pre-treatment and, specifically, the screening. Whilst an MBR can effectively displace primary sedimentation, biotreatment and secondary solid-liquid separation, as well as tertiary effluent polishing, classical screens of around 6 mm rating are normally insufficient for an MBR. Such relatively coarse screens increase the risk of clogging of the membrane module retentate flow channels, especially by hairs in municipal wastewaters, which aggregate and clog both the membrane interstices and aeration ports. Hollow Fiber (HF) membranes have a tendency for aggregates of hair and other debris to collect at the top of the membrane element. Hairs may then become entwined with the filaments and are not significantly removed by backflushing. Flat Sheet (FS) membrane clogging occurs when debris agglomerate at the channel edges and entrance. If the aeration fails to remove these aggregates, sludge accumulates above the blockage, increasing the affected excluded area. Fibres collecting in the aeration system can change the flow pattern and volume of air to the membranes, reducing the degree of scouring. As a result of the decreased scouring, membrane fouling is increased. Aerations are thus normally designed to resist clogging and /or allow periodic flushing with water.

Since HF modules are more susceptible to clogging and the impact is rather more severe, for such modules screens normally rated at between 0.8 and 1.5 mm are usually employed. FS modules are slightly more tolerant of clogging, despite being non-back flushable, and screens of 2-3 mm rating are normally adequate for MBRs of this membrane configuration (Judd, 2006, p.94). The FS module applied in this thesis is back flushable.

2.1.3.2.4.2 Employing appropriate physical or chemical cleaning protocols

To control fouling in membrane technology certain physical and chemical cleaning protocols on process design and operation can be applied. These cleaning protocols have been described in the following sections below.

Physical cleaning

Key general cleaning parameters are duration and frequency, since these determine process downtime. For back flushing, a further key parameter is the back flush flux, generally of 1-3 times the operational flux and determined by the back flush TMP. Less frequent, longer back flushing (600 s filtration/45 s back flushing) has been found to be more efficient than more frequent but shorter back flushing (200s filtration/15 s back flush) (Jiang *et al*., 2005). In another study based on factorial design, back flush frequency (between 8 and 16 min.) was found to have more effect on fouling removal than either aeration intensity (0.3 to 0.9 m^3/h per m^2 membrane area) or back flush duration (25-45s) for an HF iMBR (Schoeberl *et al*., 2005). Hence, although more effective cleaning would generally be expected for more frequent and longer back flushing, the possible permutations need exploring to minimise energy demand. This has been achieved through the design of a generic control system which automatically optimised back flush duration according to the monitored TMP value (Smith *et al.*, 2005). However, increasing back flush flux leads to more loss product and reduces the net flux.

Air can also be used to affect back flushing (Sun *et al*., 2004) or to enhance back flush with water. Up to 400% in the net flux over that attained from continuous operation has been recorded using an air back flush, although in this case 15 minutes of air back flush were required every 15 minutes of filtration (Visvanathan *et al*., 1997). Whilst air back flushing is undoubtedly effective, anecdotal evidence suggested that it can lead to partial drying out of some membranes, which can then produce embrittlement and so problems of membrane integrity.

Membrane relaxation encourages diffusive back transport of foulants away from the membrane surface under a concentration gradient, which is further enhanced by the shear created by air scouring (Chua *et al*., 2002; Hong *et al*., 2002). Detailed study of the TMP behaviour during this type of operation revealed that, although the fouling rate is generally higher than for continuous filtration, membrane relaxation allows filtration to be maintained for longer periods of time before the need for cleaning arises (Ng *et al*., 2005a). Although some authors have reported that this type of operation may not be economically

feasible for operation of large-scale iMBRs. Recent studies assessing maintenance protocols have tended to combine relaxation with back flushing for optimum results (Vallero *et al*., 2005; Zhang *et al*., 2005).

In practice, physical cleaning protocols tend to follow those recommended by the suppliers. Relaxation is typically applied for 1-2 minutes every 8-15 minutes of operation, both for FS and HF systems. The relaxation and back flush time for this thesis work is 1 minute and 0.5 minute respectively for every 10 minute of operation cycle.

For HF systems, back flushing, if employed, is usually applied at fluxes of around 2-3 times the operating flux and usually supplements rather than displaces relaxation. It is likely that operation without back flushing, whilst notionally increasing the risk of slow accumulation of foulants on or within the membrane, conversely largely preserves the biofilm on the membrane which affords a measure of protection. This fouling layer is substantially less permeable and more selective than the membrane itself, and thus can be beneficial to the process provided the total resistance it offers does not become too great (Judd, 2006, p.95).

Chemical cleaning

Chemical cleaning consists mainly of:

- Maintenance cleaning and
- Intensive (or recovery) chemical cleaning

Maintenance cleaning is conducted in situ and is used to maintain membrane permeability and helps reduce the frequency of intensive cleaning. It is performed either with the membrane in situ, a normal "cleaning in place" (CIP), or with the membrane tank drained, sometimes referred to as "cleaning in air" (CIA). Intensive, or recovery, cleaning is either conducted ex situ or in the drained membrane tank to allow the membranes to be soaked in cleaning reagent. Intensive cleaning is generally carried out when further filtration is no longer sustainable because of an elevated TMP. Intensive chemical cleaning methods recommended by suppliers are all based on a combination of hypochlorite for removing organic matter, and organic acid (either citric or oxalic) for removing inorganic scalants (Judd, 2006, p.96).

Maintenance cleaning, usually taking 30-60 minutes for a complete cycle, is normally carried out every 3-7 days at moderate reagent concentrations of 200-

500 mg/L NaOCl for classical aerobic MBRs. Recovery cleaning employs rather higher reagent concentrations of 0.2 - 0.3 wt% NaOCl, coupled with 0.2 - 0.3 wt% citric acid or 0.5 - 1 wt% oxalic acid. Membrane cleaning studies on anaerobic systems have generally indicated that a combination of caustic and acid washes are required to remove organic and inorganic foulants from organic MBR membranes (Choo *et al*., 2000a; Kang *et al*., 2002; Lee *et al*., 2001a). For inorganic membranes, acid washing has been found to be less effective, and this has been attributed to surface charge effects (Kang *et al*., 2002).

2.1.3.2.4.3 Reducing the flux

Reducing the flux always reduces fouling but obviously then impacts directly on capital cost through membrane area demand. There are essentially two modes of operation of an MBR regarding operating flux, which then determine the cleaning requirements and thus net flux (the flux based on through put over a complete cleaning cycle):

- Sustainable permeability operation
- Intermittent operation

Sustainable permeability operation

In this condition stable operation condition (little or negligible increase in TMP at constant flux) is maintained over an extended period of time with only moderate remedial measures (namely relaxation). All immersed FS and all side stream systems are operated in this condition.

Intermittent operation

In this operating condition, the operational flux is above that which can be sustained by the filtration cycle operating conditions and, as a result, intermittent remedial measures are employed. These comprise relaxation supplemented with back flushing and, usually, some kind of maintenance chemical cleaning procedure. All immersed HF systems are operated in this manner (Judd, 2006, p.97).

2.1.3.2.4.4 Increasing aeration intensity

Whilst increasing aeration rate invariably increases the critical flux upto some threshold value, increasing membrane aeration intensity is normally prohibitively expensive. Commercial development of efficient and effective aeration

systems to reduce the specific aeration demand are possibly the most important publications arising in the patent literature (Côté *et al*., 2002; Miyashita *et al*., 2000) and including cyclic aeration (Rabie *et al*., 2003) and jet aeration (Fufang and Jordan 2001, 2002) is highly demandable. The use of uniformly distributed fine air bubbles form 0.5 mm ports has been shown to provide greater uplift and lower resistance compared to a coarse aerator having 2 mm ports at similar aeration rates (Sofia *et al*., 2004). In the same study, a bi-chamber (a riser and down-comer) in an FS MBR has been shown to play a significant role in inducing high cross flow velocities (CFVs). The use of a variable aeration rate to increase the flux during peak loads has been reported for short-term tests (Howell *et al*., 2004). However, a study from Choi and co-workers (Choi *et al*., 2005a) carried out with a sMBR indicated tangential shear (imparted by liquid cross flow) to have no effect on flux decline when pseudo-steady-state is reached (i.e. once the fouling layer governs permeability) (Judd, 2006, p.98).

2.1.3.2.4.5 Chemically or biochemically modifying the mixed liquor

The mixed liquor can be controlled biochemically, through adjustment of the SRT or chemically. From different studies it is shown that the modification of fouling can be attained through addition of chemicals.

Coagulant or flocculant such as ferric chloride and aluminium sulphate (alum) can be applied for membrane fouling amelioration. According to Holbrook *et al*., (2004), addition of alum to reactor of MBRs led to a significant decrease in SMPc concentration, along with an improvement in membrane hydraulic performances. Small biological colloids (size: 0.1 to 2 µm) have been observed to coagulate and formed larger aggregate when alum was added to MBR activated sludge (Lee *et al*., 2001b). Dosing of ferric chloride was found to be more effective than alum but it is more expensive. In a recent example, the ferric dosing was shown to control both irreversible fouling and suspension viscosity (Itonaga *et al*., 2004). Precoating of MBR membranes with ferric hydroxide has also been studied as a means of increasing permeability and improving permeate quality (Zhang *et al*., 2004). In this study (Zhang *et al*., 2004), additional ferric chloride was added to remove non-biodegradable organics which accumulated in the bioreactor.

Addition of adsorbents into biological treatment systems decreases the level of organic compounds. Dosing with powdered activated carbon (PAC) produces biologically activated carbon (BAC) which adsorbs and degrades soluble organics and has been shown to be effective in reducing SMP and EPS levels in a

comparative study of a side stream and immersed hybrid PAC-MBR (Kim and Lee, 2003). Decreased membrane fouling has also been demonstrated in studies of the effects of dosing MBR supernatant at up to 1 g/L PAC (Lesage *et al*., 2005) and dosing activated sludge itself (Li *et al*., 2005a), for which an optimum PAC concentration of 1.2 g/L was recorded. In the latter study, floc size parameters were influenced, resulting in a reduced cake resistance, when PAC was dosed into the bioreactor. Tests have been performed using zeolite (Lee *et al*., 2001c) and aerobic granular sludge, with an average size around 1 mm (Li *et al*., 2005b) to create granular flocs of lower specific resistance. Granular sludge was found to increase membrane permeability by 50% but also lower the permeability recovery from cleaning by 12%, which would be likely to lead to unsustainable operation. Yoon *et al*., (2005) observed that addition of 1 g/L of membrane performance enhancing agent (MPE50) directly to the bioreactor led to the reduction of SMPc from 41 to 21 mg/L. The interaction between the polymer and the soluble organics in general, and SMPc in particular, was identified as being the main mechanism responsible for the performance enhancement (Judd, 2006, p.98).

2.2 Section II : Aerobic Submerged MBR in Textile Wastewater Treatment

2.2.1 Textile Wastewater

Textile industries are one of the biggest users of water and complex chemicals during textile processing at various processing stages. The unused materials from the processes are discharged as wastewater that is high in colour, biochemical oxygen demand (BOD), chemical oxygen demand (COD), pH, temperature, turbidity and toxic chemicals. The direct discharge of this wastewater into the water bodies like lakes, rivers etc. pollutes the water and affects the flora and fauna. Effluent from textile industries contains different types of dyes, which because of high molecular weight and complex structures, shows very low biodegradability (Hsu and Chiang, 1997; Pala and Tokat, 2002; Kim et al., 2004; Gao et al., 2007). Also, the direct discharge of this industrial effluent into sewage networks produces disturbances in biological treatment processes. These effluents produce high concentrations of inorganic salts, acids and bases in biological reactors leading to the increase of treatment costs (Gholami et al., 2001; Babu et al., 2007). Some of the chemicals such as heavy metals either in free form in effluents or adsorbed in the suspended solids are either carcinogenic (Tamburlini et al., 2002; Bayramoglu and Arica, 2007) or may cause harm to children even before birth while others may trigger allergic reactions in some people.

There are more than 100,000 commercially available dyes with over 7×10^5 ton of dye-stuff produced annually (Meyer, 1981; Zollinger 1987). Many dyes are difficult to decolourise due to their complex structure and synthetic origin. There are many structural varieties, such as acidic, basic, disperse, azo, diazo, anthroguinone based and metal complex dyes. Decolourisation of textile dye effluent doesn't occur when treated aerobically by municipal sewerage systems (Willmott et al., 1998).

In addition, there are many structural varieties of dyes that fall into either the cationic, non-ionic or anionic type. Anionic dyes are the direct, acid and reactive dyes (Mishra and Tripathy, 1993). Brightly coloured, water soluble reactive and acid dyes are the most problematic as they tend to pass through conventional treatment systems unaffected (Willmott et al., 1998). Municipal aer-

obic systems, dependent on biological activity, were found to be inefficient in the removal of these dyes (Moran et al., 1997).

Non-ionic dyes refer to disperse dyes because they do not ionise in an aqueous medium. Concern arises, as many dyes are made from known carcinogens such as benzidine and other aromatic compounds (Baughman and Perenich, 1988). Weber and Wolfe (1987) demonstrated that azo- and nitro-compounds are reduced in sediments, and similarly Chung et al. (1978) illustrated their reduction in the intestinal environment, resulting in the formation of toxic amines. Anthroquinone-based dyes are most resistant to degradation due to their fused aromatic ring structure. The ability of some disperse dyes to bioaccumulate has also been demonstrated (Baughman and Perenich, 1988).

Textile wastewater is a complex and highly variable mixture of many polluting substances including dye (Robinson et al., 2001). Dyes are used in different industrial sectors, among which the textile industries is one of the most significant users. The manufacture of several textile products involves the use of numerous different dyes and auxiliary chemicals (e.g. salts) in many different industrial processes that causes the formation of wastewaters with complex and very variable characteristics that makes their treatment particularly difficult. The textile industry is also one of the most water consuming industrial sectors (Correia et al., 1994; Delee et al., 1998; vandevivere et al., 1998; O'Neill et al., 1999). According to Brik et al., (2006), it is illustrated that for each ton of fabric products, 20 – 350 m^3 of water are consumed, which differs from the color and procedure used.

Textile dyeing industry demands large quantities of water which results in large amounts of wastewater streams of complex contaminant matrix from different steps (dyeing, bleaching, printing, soaking and finishing) of textile industry process. The discharged wastewater which has strong colour, high value of chemical oxidation demand (COD) and extremely low biochemical oxygen demand (BOD) to COD ratio may exert a great impact on the environment and therefore the related ecology (Kritikos et al., 2007).

2.2.2 Conventional Methods in Textile Wastewater Treatment

Conventional processes treating textile (dyeing and printing) wastewater include biological, physical and chemical methods such as oxidation, adsorption or coagulation or iron salts (Vlyssides et al., 2000, Tratnyek, et al.,1994, Liu et al. 2001, Sheng et al., 1994).

Virtually all the known physic-chemical and biological techniques have been explored for treatment of extremely recalcitrant textile dye wastewater; none, however has emerged as a panacea (Hai et al., 2007). Residual dyes along with other auxiliary chemical reagents used for textile processing impose massive load on wastewater treatment systems, eventually leading to poor color and COD removal performances. The presence of even trace concentration of dyes in effluent is highly visible and the release of such colored wastewater in the ecosystem is a remarkable source of esthetic pollution eutrophication and perturbations (due to toxicity and persistence) in aquatic life (Robinson et al., 2001).

Traditional methods for dealing with the textile wastewater consists of various combinations of biological, physical and chemical methods (Hamza and Hamoda, 1980; Mckay, 1980; Brower and Reed, 1987; Paprowicz and Slodczyk, 1988). Because of large variability of the composition of textile wastewaters, most of those traditional methods are becoming inadequate.

From different literature reviews it is revealed that a large number of well-structured conventional deocolourisation methods involving physical, chemical and biological processes, as well as some emerging techniques like sonochemical or advanced oxidation processes have been explored. However, there is no single economically and technically viable method to solve this problem and usually two or three methods have to be combined in order to achieve adequate level of colour removal (Kang and Chen, 1997; Robinson et al., 2001). Researches on chemical coagulation/flocculation, is observed as one of the most practised technology. Regardless of the generation of considerable amount of sludge, it is still used in developed and in developing countries. Because the mechanism of coagulant applied to decolourise wastewater is still not absolutely clear, colour removal by coagulation is found in some cases very effective, in some cases however has failed completely (Verma et al., 2011).

Since small amount of dye in textile wastewater gives very bright appearance and stays far below to the discharge limit, making the wastewater treatment difficult, the conventional decolourisation methods have been focused in the following section. Until today plenty of different methods (physical, chemical and biological) have been investigated by various researchers and applied throughout the world. A brief discussion on some of these methods are presented in the following sections.

2.2.2.1 Physical Method

One of the most commonly used physical methods is the ultrafiltration technology. Filtration methods such as ultrafiltration, nanofiltration and reverse osmosis have been used for water reuse and the chemical recovery (Marcucci et al., 2001; Fersi and Dhahbi 2008). In the textile industry, these filtration methods can be used for both filtering and recycling of not only pigment rich wastewaters, but also mercerising and bleaching wastewaters. The specific temperature and chemical composition of the wastewaters determines the type and porosity of the filter to be applied. Further, the utilisation of membrane technology for dye removal from textile wastewaters is very effective as reported by various researchers (Ledakowicz et al., 2001; Ahmad et al., 2002). However the main drawbacks of membrane technology are the high cost, frequent membrane fouling, requirement of different pretreatments depending upon the type of influent wastewaters and production of concentrated dyebath which further needs proper treatment before its safe disposal to the environment (Robinsion et al., 2001; Akbari et al., 2006). For membrane filtration, proper pre-treatment units for removing suspended solids (SS) of the wastewaters are almost mandatory to increase the life time of the membranes. This makes the process more expensive and thereby limit the application of this expensive technology for wastewater treatment.

Another popular method is adsorption technology. Adsorption method for colour removal is based on the affinity of various dyes for adsorbents. It is influenced by physical and chemical factors such as dye adsorbent interactions, surface area of adsorbent, particle size, temperature, pH and contact time (Anjaneyulu et al., 2005; Patel and Vashi, 2010). The main criteria for selection of adsorbents are based on the characteristics like high affinity, capacity of target compound and possibility of adsorbent generation (Karcher et al., 2002). Activated carbon is the most commonly used adsorbent and can be very effective for many dyes (Walker and Weatherly, 1997; Pala and Tokat, 2002). However, efficiency is directly dependent upon the type of carbon material used and wastewater characteristics (Robinson et al., 2001). The limitations of this technology are the eco-friendly disposal of the spent adsorbents, excessive maintenance costs, and pre-treatment of the wastewater to reduce the SS under acceptable range before it is fed into the adsorption column. Because of these reasons, field scale application of adsorption technology is limited not only for colour removal of textile wastewaters but also for other water and wastewater treatment (Verma et al., 2011).

2.2.2.2 Chemical Method

Chemical methods mainly involve use of oxidising agents such as ozone (O_3), hydrogen peroxide (H_2O_2), permanganate (MnO_4^-) and Cl_2 to change the chemical composition of compounds or group of compounds, e.g. dyes (Metcalf and Eddy, 2003). Among these oxidants, ozone is widely used because of its high reactivity with dyes and good removal efficiencies (Alaton et al., 2002). However, it is also reported that ozone is not efficient in decolourising non-soluble disperse and vat dyes which react slowly and take longer reaction time (Marmagne and Coste, 1996; Rajeswari, 2000). The decolourisation efficiency also depends upon the pH. As the pH decreases, ozonation of hydrolysed dyes (Reactive Yellow 84) decreases (Rein, 2001; Konsowa, 2003). It has also been reported that O_3/UV as the more effective method for decolourising of dyes compared to oxidation by UV or ozonation alone. However, Perkowski and Kos, (2003) has reported no significant differences between ozonation and O_3/UV in terms of colour removal. This may be due to the fact that production of hydroxyl radical (HO**.**) during photodecomposition of ozone may improve the degradation of organics. However, most of the UV light gets absorbed by the dyes and hence very small amount of hydroxyl free radical can be produced to decompose the dyes. Therefore, approximately same colour removal efficiencies using O_3 and O_3/UV could be expected. In H_2O_2/UV process, HO**.** radicals are formed when water containing H_2O_2 is exposed to UV light, normally in the range of 200 – 280 nm (Metcalf and Eddy, 2003). The H_2O_2 photolysis occurs as per the reaction shown in Eq. (2.14)

$$H_2O_2 + UV\ (\lambda = 200 - 280\ nm) \rightarrow HO\cdot + HO\cdot \qquad (2.14)$$

This process is widely used in Advanced Oxidation Process (AOP) technology for the decompositon of chromophores present in the dyes (Ferroro, 2000; Kurbus et al., 2002) and consequently relies on complete decolourisation. Fenton reaction is also an example of AOP in which H_2O_2 is added in an acid solution (pH: 2 – 3) containing Fe^{2+} (Eq. 2.15)

$$Fe^{2+} + H_2O_2 \rightarrow Fe^{3+} + HO\cdot + HO^- \qquad (2.15)$$

As compared to ozonation, this method is relatively cheap and also presents high COD reduction and decolouisation efficiencies (Van der Zee, 2002). The main drawback is high sludge generation due to the flocculation of reagents and dye molecules (Robinson et al., 2001; Azbar et al., 2004). Most of the AOP for textile wastewaters are highly expensive and its effectiveness varies

widely with the type of constituents present in the textile wastewaters. Also, from the several reports it is observed that in cases, at certain conditions, these technologies give very attractive results, however, in some other cases; their application has been reported not worthy considering the cost and complexity involved in these technologies.

Coagulation of dye-containing wastewaters has been used for many years as main treatment or pre-treatment due to its low capital cost (Anjaneyulu at al, 2005; Golob et al., 2005). However, the major limitation of this process is the generation of sludge and ineffective decolourisation of some soluble dyes (Anjaneyulu et al., 2005; Hai et al., 2007). Further, the sludge production can be minimised if only a small volume of highly coloured effluent is treated directly after the dyeing bath (Golob et al., 2005). The reasons could be the non-availability of the other chemical additives except hydrolysing and fixing agents in the effluent coming from dyeing bath. The chemical additives that are normally present in the textile wastewaters provide hindrance to the colour removal. If interfering chemical additives are absent in the textile wastewater except colour causing dyes, then less coagulant dosage might be required which in turns will reduce the sludge production (Verma et al., 2011).
The disadvantage of the advanced oxidation process are the high capital cost and operation cost (Green Co., 2013)

The physical and chemical methods discussed in section 2.2.2.1 and 2.2.2.2 can be also combined together such as physico-chemical method and can be applied as pre-treatment, post treatment or main process for textile wastewater treatment worldwide.

2.2.2.3 Biological Method

2.2.2.3.1 Biological Activated Sludge Process

In recent years, textile wastewater is usually treated by the combination of activated sludge process and coagulation-flocculation process. The activated sludge process removes the part of organic compounds degraded by biological microorganisms, and reduces treatment loading for the next process. The arrangement in which the activated sludge process is in front of the coagulation-flocculation process reduces the chemical cost and sludge treatment cost (Green Co., 2013). An overview of a biological activated sludge process is shown in Fig. 2.20.

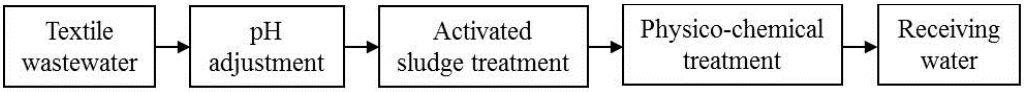

Fig. 2.20: Overview of activated sludge process for textile wastewater treatment (adapted from Green Co. 2013)

In addition, aerobic and anaerobic activated sludge processes are also evaluated as high performance treatments, however, the long retention time and low recalcitrant organics removal performnace reduce their widely utilization in textile wastewater treatment (Green Co., 2013).

The biological activated sludge process alone cannot comply with the dye removal limit of textile wastewater treatment. Recently many researches show the decolourisation of textile wastewater applying micro-organisms. Some of the decolourisation methods applying microbial cultures have been discussed in sections 2.2.2.3.2 through 2.2.2.3.5.

2.2.2.3.2 Decolourisation by white - rot fungi

The dye removal from textile wastewater can be achieved by micro-organisms under specific operation conditions. White-rot fungi are those organisms that are able to degrade lignin, the structural polymer found in woody plants (Barr and Aust, 1994). White-rot fungi are able to degrade dyes using enzymes, such as lignin peroxidases (LiP), manganese dependent peroxidases (MnP). Azo dyes, the largest class of commercially produced dyes, are not readily degraded by micro-organisms but these can be degraded by *P.chrysosporium* (Paszczynski and Crawford, 1995). Other fungi such as *Hirschioporus larincinus Inonotus hispidus, Phlebia tremellosa* and *Coriolus versicolor* have also been shown to decolourise dye-containing effluent (Banat et al., 1996; Kirby, 1999).

Although white-rot fungi have been shown to decolourise dyes in liquid fermentations, enzyme production has also been shown to be unreliable. This is mainly due to the unfamiliar environment of liquid fermentations. The ability to utilise these fungi in their natural environment means that they are more likely to be more effective in solid state fermentation (SSF) (Robinson et al., 2001).

2.2.2.3.3 Decolourisation by mixed bacterial cultures

It was found that mixed bacterial cultures are able to decolourise the diazolinked chromophore of dye molecules in 15 days (Knapp and Newby, 1995). Nigam and Marchant (1995) and Nigam et al. (1996) demonstrated that a mixture of dyes were decolourised by anaerobic bacteria in 24-30 h, using free growing cells or in the form of biofilms on various support materials. Ogawa and Yatome (1990) also demonstrated the use of bacteria for azo dye degradation. These microbial systems have the drawback of requiring a fermentation process, and are therefore unable to cope with larger volumes of textile effluents.

A number of research groups have investigated the ability of bacteria to degrade azo dyes. Under aerobic conditions azo dyes are not readily metabolised although Kulla (1981), reported the ability of *Pseudomonas* strains to aerobically degrade certain azo dyes. However, the intermediates formed by these degradative steps resulted in disruption of metabolic pathways and the dyes were not actually mineralised. Under anaerobic conditions, such as anoxic sediments, many bacteria gratuitously reduce azo dyes reportedly by the activity of unspecific, soluble, cytoplasmic reductases. These enzymes are reported to result in the production of colourless aromatic amines which may be toxic, mutagenic and possibly carcinogenic to animals (Robinson et al., 2001).

2.2.2.3.4 Bio-sorption by microbial biomass

Textile dyes vary greatly in their chemistries, and therefore their interactions with micro-organisms depend on the chemistry of a particular dye and the specific chemistry of the microbial biomass (Polman and Brekenridge, 1996). Depending on the dye and the species of micro-organism used different binding rates and capacities can observed. It can be said that certain dyes have a particular affinity for binding with microbial species (Robinson et al., 2001).

Adsorption by biomass occurs by ion exchange. Hu (1992) demonstrated the ability of bacterial cells to adsorb reactive dyes. Zhou and Zimmerman (1993) used actinomyces as an adsorbent for decolourisation of effluents containing anthroquinone, phalocyanine and azo dyes.

The simplest mechanism of colour removal by whole bacterial cells is that of the adsorption of the dye onto the biomass (Bras et al., 2001). However, this mechanism is similar to many other physical adsorption mechanisms for the removal of colour and is not suitable for long term treatment. This is because,

during adsorption, the dye is concentrated with time, and the dye-adsorbent composition must also be disposed of (Southern et al. 1995).

2.2.2.3.5 Anaerobic textile-dye bioremediation systems

Anaerobic bioremediation allows azo and other water-soluble dyes to be decolourised. This decolourisation involves an oxidation-reduction reaction with hydrogen rather than free molecular oxygen in aerobic systems. Typically, anaerobic breakdown yields methane and hydrogen sulphide (Carliell et al., 1996).

Azo dye acts as an oxidising agent for the reduced flavin nucleotides of the microbial electron chain and is reduced and decolourised concurrently with reoxidation of the reduced flavin nucleotides. In order for this to occur, additional carbon is required for decolourisation to proceed at a vaiable rate. This additional carbon is converted to methane and carbon doxide, releasing electrons. These electrons cascade down the electron transport chain to a final electron acceptor, in this case the azo-reactive dye. The electrons react with the dye reducing the azo bonds, and ultimately causing decolourisation (Carliell et al., 1996).

Anaerobic degradation of textile dyes yields only azo reduction. Mineralisation doesn't occur. It has been shown that azo- and nitro-components are reduced in the sediments and in the intestinal environment, resulting in the regeneration of the parent toxic amines (Banat et al., 1996). Therefore, careful monitoring is required before treated wastewater is released into waterways (Robinson et al., 2001).

2.2.3 MBR in Textile Wastewater Treatment

2.2.3.1 Current Status

With respect to filtration of organic compounds, **Membrane Bioreactors (MBR)** in combination with subsequent **Nanofiltration (NF)** or **Reverse Osmosis (RO) membranes** are well established, state of the art technology preferably in industrial wastewater treatment, for example, textile wastewater treatment (Fig. 2.21).

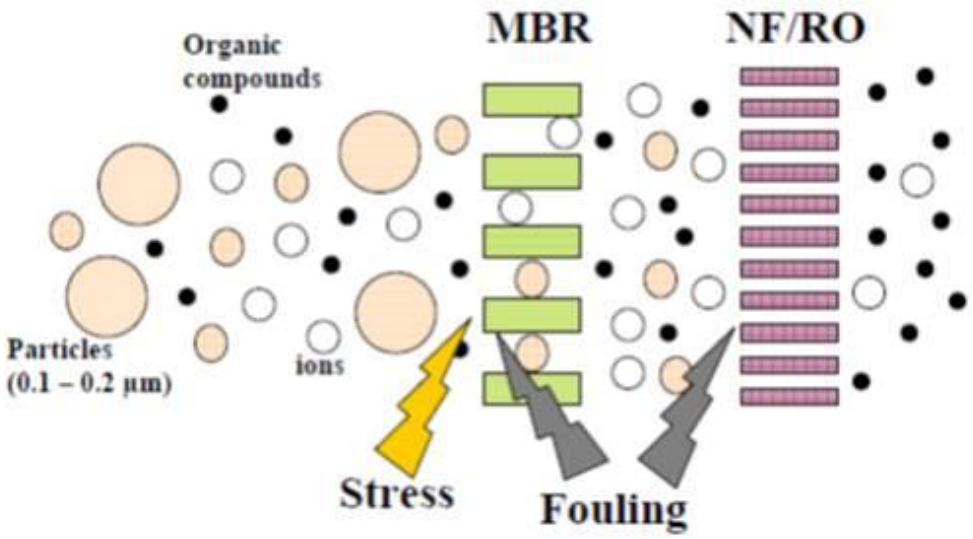

Fig. 2.21 : State of the art of MBR technology

Due to use of MF and "loose" UF membranes (molecular weight cut-off typically > 100 kDa) state-of-the art MBR membranes offer only low rejection of micropollutants with low molecular weight such as textile dyestuff. Dye rejection only takes place by biodegradation. Therefore application of state-of-the art MBR technology for textile wastewater treatment as single- step process is rather limited in this sector and typically requires downstream post-treatment such as e.g. NF/RO or activated carbon treatment.

For textile wastewater treatment especially for dye removal several physical-chemical decolourisation techniques have been reported in the literature such as adsorption, membrane separation, advanced oxidation process etc; none however, has appeared as a panacea due to high cost, low efficiency and limited versatility (Hai et al., 2007). Biodegradation is an environmentally friendly and cost competitive alternative. However, due to persisting nature and type of dyes, it is not easy to remove dye from textile wastewater. To deal with the problems associated with textile effluents, several studies have been directed at the treatment of polluted streams close to the point of source (integrated approach) (Porter, 1997; Minke and Rott, 1997; Minke and Rott, 2001) and at the treatment of the final effluents (end of pipe approach) (Lopez et al. 1999; Rozzi et al., 1997; Marcucci et al., 2001; Braun and Felgener, 1997). From different literature studies it is revealed that the MBR alone is not enough to get com-

plete decolourisation of textile wastewater but a combination of a MBR with subsequent nanofiltration or reverse osmosis system can do the job and it has proved to meet all requirements for reuse. Besides, this technique, MBR associated with other chemical or biological approaches (e.g. hybrid process) shows the viability of the process removing dyes in textile wastewater treatment.

Hai et al., (2011) demonstrated that stable decolourisation along with significant organics (TOC, TN) removal over a prolonged period under extremely high dye-loadings was observed in a bio-augmented aerobic MBR with a Granular Activated Carbon (GAC) packed anaerobic zone. The GAC-packed anaerobic zone played the key role in decolourisation, while the aerobic zone was vital for TOC removal (Hai et al., 2011). But the disposal of the saturated GAC or sludge treatment with saturated GAC remains questionable.

Consequently, Hai et al., (2008) presented that a fungal MBR (MBR associated with white-rot fungi) achieved 93% removal of azo dye (Acid Orange II, 100 mg/L) from synthetic textile wastewater during long-term non-sterile operation at a hydraulic retention time of 1 day. The large scale implementation of such white-rot fungal system, however, has been impeded due to lack of appropriate reactor system that can sustain stable performance under non-sterile environment (Hai et al., 2008).

Spagni et al., (2010) demonstrated that a system comprising an anaerobic bio filter and an anoxic, aerobic MBR is suitable for synthetic textile wastewater treatment. Although aromatic amines are considered easily degradable under aerobic conditions, the results confirm that at least the sulfonated aromatic amines formed under anaerobic conditions from the dye Reactive Orange 16 (RO16) are recalcitrant to biodegradation (Spagni et al., 2010).

Yigit et al., (2009) found that the complex and highly polluted textile wastewaters can be treated much more effectively by MBR processes than conventional activated sludge processes, and the treated wastewaters by MBRs have high potential for reuse in the textile industry (Yigit et al., 2009). Though this MBR system faced the fouling problem after operation of 3 months, the fouling was eliminated by applying chemical backwashing and chemical cleaning procedures.

Feng et al., (2011) reported that the combined Fenton Oxidation and MBR process was efficient in the reduction of TOC and colour of effluent from integrated dyeing wastewater treatment plant (IDWTP), reaching average values about 88.2% and 91.3% respectively. Fenton oxidation accounted for 39.3% while

MBR made up the rest i.e. 48.9% in case of TOC removal. As for the contribution of colour removal, the percentage of oxidation was 69.6% and MBR was 21.7% (Feng et al., 2011). Since Fenton oxidation cannot mineralise the colour completely, some intermediates and by-products are generated and contributed to Fenton sludge which might be the concern of disposal for industrial scale plant.

Zheng and Liu (2006) demonstrated that a laboratory-scale membrane bioreactor (MBR) with a gravity drain was feasible and effective for dyeing and printing wastewater treatment from a wool mill. The COD and colour removal efficiencies were 80.3% and 58.7% respectively (Zhen and Liu, 2006). The efficiencies might not be enough to be complied with discharge limit of many countries worldwide.

You et al., (2010) presented that two stage anaerobic SBR-aerobic MBR and anaerobic MBR with immobilized and suspended bio cells and an integrated membrane photocatalytic reactor (MPR) using slurry UV/TiO_2 shows 99.9% colour (Reactive Black5) removal and 80-95% organic COD and TOC removal efficiency (You et al., 2010).

Huang et al., (2009) has reported that an aerobic MBR applied in printing and dyeing factory at maximum HRT of 22.5h shows the COD removal efficiency as 85-92% where 10-20% was contributed by MBR. Among other parameters, NH_3-N and colour removal efficiencies were 90 - 95% and 60 -75% respectively (Huang et al., 2009). Concerning MBR operational parameters, Schoeberl et al., (2005) demonstrated the effect of suction time, aeration intensity and backflush time in membrane resistance increase treating dye house wastewater with a tubular membrane module (pore size 0. 4µm) immersed in a 60 L aerated activated sludge tank. The maximum and minimum values for suction time were 8 – 16 minutes backflush time 25 – 45 second and aeration intensity 0.3 – 0.9 m^3/m^2.h. Concerning the fouling ability of the three factors, suction time was observed to have the largest effect on resistance increase followed by aeration intensity and back flush time.

2.2.3.2 Future Approach

The future of MBR technology seems to be promising. Since 1990 the numbers of installed membrane bioreactors have grown almost exponentially. There are probably around 3000 plants currently in use worldwide, although a lot of these

are quite small. MBR is a continuous process and it is quite easily controllable. It is rapidly becoming the best available technology (BAT) for wastewater treatment.

MBRs in wastewater reclamation and reuse are effective tools for sustainable industrial development programs. Increasingly stringent environmental legislation and generally enhanced intensity, efficiency, and diversity of treatment technologies have made the reuse of water more viable in many industrial processes. Membrane bioreactors (MBRs) is an essential part of advancing such water sustainability, because they encourage water reuse and open up opportunities for decentralized treatment.

From the description of section 2.2.3.1, it is revealed that the conventional MBR technology alone is not enough in treating textile wastewater to reach the colour removing efficiency needed to comply with the discharge limit in many countries worldwide. To reach the target, high dye removal efficiency of textile wastewater by MBR technology, it needs to be combined with other technology or membrane materials of MBR needs to be modified. Fouling effect of MBR is another factor which is the main obstacles for wider application of MBR technology. Once the membrane is affected by fouling and extensive chemical cleaning can't regain the flux, the membrane needs to be replaced which may account for 30-50% of the operation cost.

Over the past few years, considerable investigations have been performed to understand MBR fouling in detail (Meng et al., 2009) and to tackle it. As outcomes of the researches, membrane modification or new membrane material development has been focused to reduce the high cost of investment for the membrane modules or to enhance and maintain membrane flux in MBR membranes. Membrane modification could be done as follows:

- By improving anti-fouling property of the membranes
- By increasing the hydrophilicity
- By increasing surface smoothness
- By changing pore geometries, etc.

Many researchers have modified and tested membranes applying different techniques but not a single of the modified membranes has been applied on large-scale so far due to some significant drawbacks. Yu et al. (2005a, 2005b, 2008) modified the hollow fibre membrane surface of MBR by NH_3 and CO_2 plasma treatment and showed that the fouling indices of the modified mem-

brane was lower than the unmodified membrane. Although the plasma treatment process has many advantages, such as a very shallow modification depth compared to other surface modification techniques, it still has drawbacks. For example, the chemical reactions of the plasma treatment are rather complex, so the surface chemistry of the modified surface is difficult to understand in detail and thus, currently it is not possible to extend plasma treatment on large-scale (Yu et al, 2007). To overcome the disadvantages of plasma treatment, Yu et at., (2007) applied the surface graft polymerisation method to improve the membrane permeation in MBRs. The performance of the modified membrane was better than the unmodified but resulted in an increase in membrane production cost (Asatekin et al., 2006).

Asatekin et. al. (2006) obtained a novel NF membrane by coating commercial PVDF UF membrane with the amphiphilic graft copolymer PVDF-g-POEM. This material exhibited high fouling resistance for a variety of model biofoulant solutions and a high effluent quality. However, the pure water permeability was much lower than that of UF membranes, currently employed in MBRs (Musolff et al., 2009).

Bae and Tak (2005a, 2005b) prepared TiO_2 embeded polymeric membranes by a self - assembly process and applied to the filtration of MBR sludge. TiO_2 embeded membrane shows less fouling propensity due to higher hydrophilicity compared to virgin membranes and it can be applied in membrane modification for fouling control in MBRs.

To achieve the viable application of MBR, non-fouling or low fouling membranes applied in MBR are very much needed. The non-fouling or low fouling membrane should have much narrower pore size distributions, stronger hydrophilicity and larger porosity than the currently used membranes. In the future, the study on membrane materials in MBRs should still focus on development of anti-fouling membranes or modification of current membranes (Meng et al., 2009).

Choi et. al. brought forward a new idea suggesting the application of **NF membranes in MBR technology** (Choi et. al, 2002). Research on NF MBR is only at its very early stage and it is missing a breakthrough regarding commercialised applications. Choi et. al. refered to high flux NF membranes with high organic matter rejection and low salts rejection are needed. A MBR using a hollow-fiber-type cellulose acetate NF membrane was performed to treat synthetic wastewater (Choi et al., 2005a). Electrolytes were not accumulated in the bioreactor, as its rejection was also low. This enabled the NF MBR to be operated under a low suction pressure and prevented from

inhibition against microorganisms, whose activity might be deteriorated by high salt concentration (Choi et al., 2002). Choi et. al. operated a submerged NF MBR using cellulose acetate membranes for 240 days to examine the performance in the domestic wastewater treatment. However, they noticed a qualitative deterioration of the NF membrane caused by the hydrolysis of cellulose acetate (Choi 2005a).

The new approach of MBR application could be osmotic MBR applying forward osmosis (FO) process. For textile dye removal purpose, MBR might be applied in combination with anaerobic and aerobic MBR process.

Throughout this PhD thesis works, UF membrane for MBR application has been modified applying nano-structured novel coating on it via polymerisable bicontinuous microemulsion (PBM) process. The antifouling effect of the membranes have been tested in short term tests with model foulant humic acid and model textile dye wastewater (MTDW) in ultrafiltration cross-flow testing cells and long term tests with model textile dye wastewater (MTDW) in a lab-scale MBR plant for the duration of 6 months. The overall performances of the modified membranes and their benefits have been discussed in chapter7 within this thesis report.

References

aaflowsystem, www.aaflowsystem.com, accessed on May, 2011

Aggerwasser, Kubota; Info CD "Membrantechnik", www.aggerwasser.de, accessed on May, 2011

Ahmad, A.L., Harris, W.A., SyafiieOoi, B.S. (2002), Removal of dye from wastewater of textile industry using membrane technology. Universiti Teknologi Malaysia Jurnal Teknologi 36 (F), 31 - 44.

Akbari, A., Desclaux, S., Rouch, J.C., Aptel, P., Remigy, J.C. (2006), New UV-photografted nanofiltration membranes for the treatment of colored textile dye effluents. Journal of Membrane Science 286 342 - 350.

Alaton, I.A., Balcioglu, I.A., Bahnemann, D.W. (2002), Advanced oxidation of a reactive dye bath effluent: comparison of O3, H2O2/UV-C and TiO2/UV-A processes. Water Research 36 1143 - 1154.

Anjaneyulu, Y., Chary, N.S., Raj, D.S.S. (2005), Decolourization of industrial effluents available methods and emerging technologies-a review. Reviews in Environmental Science and Biotechnology 4 245 - 273.

Asatekin, A., Menniti, A., Kang, S., Elimelech, M., Morgenroth, E., and Mayes, A.M. (2006), Antifouling nanofiltration membranes for membrane bioreactors from self-assembling graft copolymers, *J. Membr. Sci*. 285, 81-89.

Azbar, N., Yonar, T., Kestioglu, K. (2004), Comparison of various advanced oxidation processes and chemical treatment methods for COD and colour removal from a polyester and acetate fiber dying effluent. Chemosphere 55 35 - 43.

Babu, B.R., Parande, A.K., Raghu, S., Kumar, T.P. (2007), Cotton textile processing: waste generation and effluent treatment. Textile technology. The Journal of Cotton Science 11 141 - 153.

Bae, T. – H., Tak, T. – M. (2005a), Effect of TiO_2 nanoparticles on fouling mitigation of ultrafiltration membranes for activated sludge filtration, journal of membrane science, 249 (1-2). 1-8

Bae, T. – H., Tak, T. – M. (2005b), Preparation of TiO_2 self-assebmled polymeric nanocomposite membranes and examination of their fouling mitigation effects in a membrane bioreactor system, journal of membrane science 266 (1-2), 1-5

Bailey, J., Bemberis, I. and Presti, J. (1971), Phase I Final Report-Shipboard sewage treatment system, General Dynamics Electric Boat Division, November. 1971, NTIS.

Baker, R.W. (2000), Membrane Technology and Applications, Chapter 3, ISBN 0-07-135440-9, McGraw-Hill.

Baker, R. W. (2004), Membrane Technology and Applications, John Wiley & Sons Ltd, second edition.

Banat, I.M., Nigam, P., Singh, D., Marchant, R. (1996), Microbial decolorization of textile-dye containing e.uents: a review. Bioresour. Technol. 58, 217 - 227.

Barr, D.P., Aust, S.D. (1994), Mechanisms white rot fungi use to degrade pollutants. Environ. Sci. Technol. 28, 320 - 328.

Baughman, G.L., Perenich, T.A. (1988), Fate of dyes in aquatic systems: I Solubility and partitioning of some hydrophobic dyes and related compounds. Environ. Toxicol. Chem. 7 183 - 199.

Bayramoglu, G., Arica, M.Y. (2007), Biosorption of benzidine based textile dyes Direct Blue 1 and Direct Red 128 using native and heat-treated biomass of Trametes versicolor. Journal of Hazardous Materials 143 (1 - 2), 135 - 143.

Bemberis, I., Hubbard, P.J. and Leonard, F.B. (1971), Membrane sewage treatment systems-potential for complete wastewater treatment, *American Society of Agricultural Engineers* Winter Meeting, 71-878, 1-28.

Bérubé, P.R., Hall, E.R. and Sutton, P.M. (2006), Parameters governing permeate flux in an anaerobic membrane bioreactor treating low-strength municipal wastewaters: A literature review. *Water Environment Research*, 78(8), 887-896.

Botha, G.R., Sanderson, R.D. and Buckley, C.A. (1992), Brief historical review of membrane development and membrane applications in wastewater treatment in Southern Africa. *Wat. Sci. technol*., 25 (10), 1-4.

Bouhabila, E.H., Aïm, R.B., Buisson, H. (2001), Fouling characterisation in membrane bioreactors, *Separation and Purification Technology* Volumes 22-23, 123-132.

Bras R, Ferra IA, Pinheiro HM, Goncalves IC. (2001), Batch tests for assessing decolourisation of azo dyes by methanogenic and mixed cultures. Journal of Biothechnology 89, 155–62.

Braun, G. and. Felgener, O.W. (1997), Treatment of Wastewaters from Textile Processing, TU-Berlin Schiftenreihe biologische A wasserreinigung, Vol. 9, Berlin.

Brookes, A., Jefferson, B. and Judd, S. (2004), IWA 4th World Water Congress, Marrakech, Marruecos.

Brik, M.; Schoeberl, P.; Chamam, B; Braun, R and Fuchs, W. (2006), Advanced treatment of textile wastewater towards reuse using a membrane bioreactor, Process Biochemistry 41, 1751 - 1757

Brower, G. R. and Reed G. D. (1987), Economic pretreatment for color removal from textile dye wastes. In *Proc. 41st Purdue Ind. Waste Conf.*, Lafayette, Indiana.

Canales, A., Pareilleux, A., Rols, J. L., Goma, G. and Huyard, A. (1994), Decreased Sludge Production Strategy for Domestic Wastewater Treatment, *Wat. Sci. Technol*., 30, 97-106.

Cassano, A, Drioli, E., Figoli, A., Hoinkis, J., Deowan, S.A., Islam, M.A., Huang, R.R. (2005), Membrane Technology for Water Treatment, *Membrane Training Handbook, p.94,* Jiangsu Polytechnic University, China.

Carliell, C.M., Barclay, S.J., Buckley, C.A. (1996), Treatment of exhausted reactive dye bath effluent using anaerobic digestion: laboratory and full scale trials. Water S.A. 22, 225 - 233.

Chang, I.S. and Lee, C.H. (1998), Membrane filtration characteristics in membrane-coupled activated sludge system - the effect of physiological states of activated sludge on membrane fouling. *Desalination* 120(3), 221-233.

Chang, I.S., Lee, C.H. and Ahn, K.H. (1999), Membrane filtration characteristics in membrane-coupled activated sludge system: The effect of floc structure on membrane fouling. *Separation Science and Technology* 34(9), 1743-1758.

Chiemchaisri, C. and Yamamoto, K. (1994), Performance of membrane separation bioreactor at various temperatures for domestic wastewater treatment. J. Memb. Sci., 87, 119-129.

Choi, J.H., Dockko, S., Fukushi, F., and Yamamoto, K. (2002), A novel application of a submerged nanofiltration membrane bioreactor (NF MBR) for wastewater treatment. *Desalination* 146, 413-420.

Choi, J.H., Fukushi, F. and Yamamoto, K. (2005a), Comparison of treatment efficiency of submerged nanofiltration membrane bioreactors using cellulose treated and polyamide membrane, *Wa. Sci. Technol.*, 51 (6/7) 305-312.

Choi, H., Zhang, K., Dionysiou, D.D., Oerther, D.B. and Sorial, G.A. (2005b), Effect of permeate flux and tangential flow on membrane fouling for wastewater treatment. *Desalination*, 178, 219-225.

Chung, K.T., Fulk, G.E., Egan, M. (1978), reduction of azo dyes by intestinal anaerobes, Appl. Environ. Microbiol., 35, 558 - 562

Choo, K.H., Kang, I.J., Yoon, S.H., Park, H., Kim, J.H., Adiya, S. and Lee, C.H. (2000a), Approaches to membrane fouling control in anaerobic membrane bioreactors. *Wat. Sci. Technol.*, 41(10-11), 363-371.

Cicek, N., Macomber, J., Davel, J., Suidan, M. T., Audic, J. and Genestet, P. (2001), Effect of solids retention time on the performance and biological characteristics of a membrane bioreactor. *Wat. Sci. Technol.*, 43 (11), 43-50.

Choo, K.H. and Lee, C.H. (1996), Effect of anaerobic digestion broth composition on membrane permeability. *Wat. Sci. Technol.*, 34(9), 173-179.

Choo, K.H., Kang, I.J., Yoon, S.H., Park, H., Kim, J.H., Adlya, S. and Lee, C.H. (2000b), Approaches to membrane fouling control in anaerobic membrane bioreactor. *Water Res*., 32, 3387-3397

Chua, H.C., Arnot, T.C. and Howell, J.A. (2002), Controlling fouling in membrane bioreactor operated with a variable throughput. *Desalination*, 90, 323-331.

Côté, P. (2002), Inverted air box aerator and aeration method for immersed membrane, US Patent 6,863, 823.

Correia, V.M., Stephenson, T., Judd, S. (1994), Characterisation of textile wastewaters - a review, Environmental Technology 15 917 - 929.

Drews, A., Lee, C.-H., Kraume, M. (2006), Membrane fouling - a review on the role of EPS, *Desalination* Volume 200, Issues 1-3, 186-188

Drioli, E., Figoli, A., Cassano, A, Hoinkis, J., Deowan, S.A., Islam, M.A., Huang, R.R. (2005), Membrane Technology for Water Treatment, *Membrane Training Handbook, p.9*, Jiangsu Polytechnic University, China.

Delee, W., O'Neill, C., Hawkes, F.R., Pinheiro, H.M. (1998), Anaerobic treatment of textile effluent: a review. Journal of Chemical Technology and Biotechnology 73, 323 - 335.

Elmaleh, S. and Abdelmoumni, L. (1997), Cross-flow filtration of an anaerobic methanogenic suspension. *J. Membr. Sci.*, 131(1-2), 261-274.

Field, R.W., Wu, D., Howell, J.A. and Gupta, B.B (1995), Critical flux concept for microfiltration fouling. *J Membr Sci* 100:259-272.

Figoli, A., Drioli, E., Cassano, A, Hoinkis, J., Deowan, S.A., Islam, M.A., Huang, R.R. (2005), Membrane Technology for Water Treatment, *Membrane Training Handbook, A. Figoli, Chapter 4, p.81*, , Jiangsu Polytechnic University, China.

Fraunhofer IGB (1997), press release, August, www-alt.igb.fraunhofer.de, accessed May, 2011

Fufang, Z., and Jordan, J. (2002), Apparatus and method for cleaning membrane filtration modules US Patent 0075504.

Ferroro, F., (2000), Oxidative degradation of dyes and surfactant in the Fenton and photo-Fenton treatment of dye house effluents. Coloration Technology 116 (5 - 6), 148 - 153.

Fersi, C., Dhahbi, M. (2008), Treatment of textile plant effluent by ultrafiltration and/ or nanofiltration for water reuse. Desalination 222, 263 - 271.

Feng, F., Xu, Z., Li, X., You, W. and Zhen, Y. (2010), Advanced treatment of dyeing wastewater towards reuse by the combined Fenton oxidation and membrane bioreactor process, Journal of Environmental Sciences 22(11), 1657 - 1665

Gander, M., Jefferson, B. and Judd, S. (2000), Aerobic MBRs for domestic wastewater treatment: a review with cost considerations. *Separation and Purification Technology* 18(2), 119-130.

Gao, M., Yang, M., Li, H., Yang, Q. and Zhang Y. (2004), Comparison between a submerged membrane bioreactor and a conventional activated sludge system on treating ammonia-bearing inorganic wastewater. *Journal of Biotechnology*, 108, 265 – 269.

Gao, B.Y., Yue, Q.Y., Wang, Y., Zhou, W.Z. (2007), Color removal from dye-containing wastewater by magnesium chloride, Journal of Environmental Management 82 167 - 172.

Gholami, M., Nasseri, S., Fard, M.R.A., Mesdaghinia, A., Vaezi, F., Mahvi, A., Naddaffi, K. (2001), Dye removal from effluents of textile industries by ISO9888 method and membrane technology. Iranian Journal of Public Health 30, 73 - 80.

Ghyoot, W.R. and Verstraete, W.H. (1997), Coupling membrane filtration to anaerobic primary sludge digestion. *Environmental Technology* 18(6), 569-580.

GIA, Global Industrial Analysts Inc., (2013), http://www.prweb.com/releases/membrane_bioreactors/MBR/prweb8973361.htm, accessed on November 22, 2013

Green Co. LTD., (2013), Treatment of textile wastewater treatment using biological activated sludge process combined with coagulation, 2013, Vietnam (accessed on 24.03.2013)

Golob, V., Vinder, A., Simonic, M. (2005), Efficiency of coagulation/flocculation method for treatment of dye bath effluents. Dyes and Pigments 67, 93 - 97.

Gujer, W., Henze M., Mino T. and Van Loosdrecht, M. (1999), Activated sludge model No. 3. *Wat. Sci. Technol.* 39:183-193.

Hai, F.I., Yamamoto, K., Nakajima, F. and Fukushi, K. (2011), Bioaugmented membrane bioreactor (MBR) with a GAC-Packed zone for high rate textile wastewater treatment, water research 45, 2199 - 2206

Hai, F.I., Yamamoto, K., Nakajima, F. and Fukushi, K. (2008), Factors governing performance of continuous fungal reactor during non-sterile operation – The case of a membrane bioreactor treating textile wastewater, Chemosphere 74 810 – 817

Hai, F.I., Yamamoto, K., Fukushi, K. (2007), Hybrid treatment systems for dye wastewater. Crit. Rev. Environ. Sci. Technol. 37, 1–64.

Hamza A. and Hamoda M. F. (*1980),*Multiprocess treatment of textile wastewater. In *Proc. 35th Purdue Ind. Waste Conf.*, Lafayette, Indiana

Harada, H., Momonoi, K., Yamazaki, S. and Takizawa, S. (1994), Application of Anaerobic-UF Membrane Reactor for Treatment of A Waste-Water Containing High-Strength Particulate Organics. *Wat. Sci.Technol.*, 30(12), 307-319.

Hardt, F.W., Clesceri, L.S., Nemerow, N.L. and Washington, D.R. (1970), Solid separation by ultrafiltration for concentrated activated sludge. *J. Wat.Pollut*. Con. Fed., 42, 2135-2148.

Hasar, H., Kinaci, **C.,** Unlu, A., Toğrul, H., Ipek, U. (2004), Rheological properties of
activated sludge in a sMBR, *Biochem Eng. J.*, 20(1): 1-6.

Hilal, N., Kochkodan, V., Al-Khatib, L., Levadna, T. (2004), Surface modified polymeric membranes to reduce (bio) fouling: a microbiological study using E. coli, *Desalination* Volume 167, 293–300.

Holbrook, R.D., Higgins, M.J., Murthy, S.N., Fonseca, A.D., Fleishcher, E.J., Daigger, G.T., Grizzard, T.J., Love, N.G., and Novak, J.T. (2004), Effect of alum addition on the performance of submerged membranes for wastewater treatment. *Water Env. Res*., 76, 2699-2702.

Hong, S.P., Bae, T.H., Tak, T.M., Hong, S and Randball, A. (2002), Fouling control in activated sludge submerged hollow fiber membrane bioreactors. *Desalination*, 143, 219-228.

Horan, N. (1990), Biological Wastewater Treatment Systems: Theory and Operation. Wiley, Chichester.

Howell, J.A. and Nystrom, M. (1993), Fouling Phenomena. in Membranes in bioprocessing : theory and applications in: J. A. Howell, V. Sanchez and R. W. Field. London, Chapman & Hall. First Edition**:** 203-244.

Howell, J.A., Arnot, T.C. and Liu, W. (2003), Membrane bioreactor for treating waste streams. Ann NY Ac Sci 984:411-9.

Howell, J.A., Chua, H.C. and Arnot, T.C. (2004), in situ manipulation of critical flux in a submerged membrane bioreactor using variable aeration rates, and effects of membrane history. *J. Membr. Sci*., 242, 13-19.

Hsu, T.C., Chiang, C.S., (1997), Activated sludge treatment of dispersed dye factory wastewater. Journal of Environmental Science and Health 32, 1921 - 1932.

Hu, T.L., (1992), Sorption of reactive dyes by Aeromonas biomass. Water Sci. Technol. 26, 357 - 366.

Huang, X., Gui, P. and Qian, Y. (2001), Effect of sludge retention time on microbial behaviour in a submerged membrane bioreactor. *Process Biochem*. 36, 1001-1006.

Huang, R.R., Hoinkis, J., Hu, Q. and Koch, F. (2009), Treatment of dyeing wastewater by hollow fiber membrane biological reactor, Journal of desalination and water treatment, 11, 1 - 6

Itonaga, T., Kimura, K. and Watanabe, Y. (2004), Influence of suspension viscosity and colloidal particles on permeability of membrane used in membrane bioreactor (mbr). *Wat. Sci. Technol*., 50, 301-309.

Jifeng, G., Siqing, X., Rongchang, W., (2008), Study on Membrane Fouling of Submerged Membrane Bioreactor in Treating Bathing Wastewater, Journal of Environmental Sciences 20, 1158–1167

Jiang, T. (2007), Characterization and modelling of soluble microbial products in membrane bioreactors, PhD thesis, Ghent University, Belgium, 241-248.

Jiang, T., Kennedy, M.D., Guinzbourg, B.F., Vanrolleghem, P.A. and Schippers, J.C. (2005), Optimising the operation of a mbr pilot plant by quantitative analysis of the membrane fouling mechanism. *Water Sci. Technol*., 51, 19-25.

Jiang, T., Kennedy, M.D., van der Meer, W.G.J., Vanrolleghem, P.A., Schippers, J.C. (2003), The role of blocking and cake filtration in MBR fouling,*Desalination* Volume 157, Issues 1-3, 1, 335-343

Judd, S. (2006), The MBR Book: Principles and Applications of Membrane Bioreactors for Water and Wastewater Treatment, editor, Elsevier.

Kang, S.F., Chen, M.C. (1997), Coagulation of textile secondary effluents with fenton's reagent. Water Science and Technology 36 (12), 215 - 222.

Kang, I.J., Yoon, S.H. and Lee, C.H. (2002), Comparison of the filtration characteristics of organic and inorganic membranes in a membrane-coupled anaerobic bioreactor. *Water Research* 36(7), 1803-1813.

Karcher, S., Kornmuller, A. (2002), Jekel, M., Anion exchange resins for removal of reactive dyes from textile wastewaters. Water Research 36, 4717 - 4724.

Kim, J.S. and Lee, C.H. (2003), Effect of powdered activated carbon on the performance of an aerobic membrane bioreactor: comparison between cross-flow and submerged membrane systems. *Water Env. Res*., 75, 300-307.

Kim, T.H., Park, C., Yang, J., Kim, S., (2004), Comparison of disperse and reactive dye removals by chemical coagulation and fenton oxidation. Journal of Hazardous Materials 112 (1-2), 95 - 103.

Kirby, N. (1999), Bioremediation of textile industry wastewater by white rot fungi. DPhil Thesis, University of Ulster, Coleraine, UK.

Knoblock, MD., Sutton, PM., Mishra, P.N., Gupta, K., Janson, A. (1994), Membrane bioreactor for industrial wastewater treatment : Applicability and selection of optimal systems configuration. *Water Environ Res.* 66:133.

Kritikos D E, Xekoukoulotakis N P, Psillakis E, Mantzavinos D, (2007), Photocatalytic degradation of Reactive Black 5 in aqueous solution: Effect of operating conditions and coupling with ultrasound irradiation. *Water Research*, 41(10): 2236–2246.

Konsowa, A.H. (2003), Decolorization of wastewater containing direct dye by ozonation in a batch bubble column reactor. Desalination 158, 233 - 240.

Kurbus, T., Slokar, Y.M., Marechal, A.M. (2002), The study of the effects of the variables on H2O2/UV decolouration of vinylsulphone dye: Part II. Dyes And Pigments 54, 67 -78.

Knapp, J.S., Newby, P.S. (1995), The microbiological decolorization of an industrial e.uent contain ing a diazo-linked chromophore. Water Res. 7, 1807 - 1809.

Kulla, M.G. (1981), Aerobic bacterial degradation of azo dyes. Microbial degradation of xerobiotics and recalcitrant compounds. In: Leisinger, T., Cook, A.M., Hutter, R., Nuesch, J. (Eds.), FEMS Symposium, 12. Academic Press, London, 387 - 399.

Laeraa, G., Polliceb, A., Saturnob, D., Giordanob, C., Sandullia, R. (2009), Influence of sludge retention time on biomass characteristics and cleaning requirements in a membrane bioreactor for municipal wastewater treatment, *Desalination* 236, 104–110

Ledakowicz, S., Solecka, M., Zylla, R. (2001), Biodegradation, decolourisation and detoxification of textile wastewater enhanced by advanced oxidation processes. Journal of Biotechnology 89, 175 - 184.

Lesage, N., Sperandio, M. and Cabassud, C. (2005), Performances of a hybrid adsorption/submerged membrane biological process for toxic waste removal. *Wat. Sci. Technol*., 51, 173-180.

Lesjean, B., and Huisjeslow, E.H. (2008), Survey of the European MBR market: trends and perspectives, *Desalination* Volume 231, Issues 1-3, 71-81.

Lee, S.M., Jung, J.Y. and Chung, Y.C. (2001a), Novel method for enhancing permeate flux of submerged membrane system in two-phase anaerobic reactor. *Water Research.,* 35, 471-477.

Lee, J., Ahn, W.Y. and Lee, C.H. (2001b), Comparison of the filtration characteristics between attached and suspended growth microorganisms in submerged membrane bioreactor . Water Research 35(10), 2435-2445.

Lee, J.C., Kim, J, S., Kang, I.J., Cho, M.H., Park, P.K. and Lee, C.H. (2001c), Potential and limitations of alum or zeolite addition to improve the performance of a submerged membrane bioreactor. *Water Res*., 35, 2435-2445.

Li H, Yang M, Zhang Y, Yu T and Kamagata, Y. (2006), Nitrification performance and microbial community dynamics in a submerged membrane bioreactor with complete sludge retention. J. Biotechnol., 123, 60-70.

Li, Y.Z., He, Y.L., Liu, Y.H., Yang, S.C. and Zhang, G.J. (2005a), Comparison of the filtration characteristics between biological powdered activated carbon sludge and activated sludge in submerged membrane bioreactors. *Desalination*, 174, 305-314.

Li, X., Gao, F., Hua, Z., Du, G. and Chen, J. (2005b), Treatment of synthetic wastewater by a novel mbr with granular sludge developed for controlling membrane fouling. *Sep. Purif. Technol*., 46, 19-25.

Liu, R. Huang, X., Xi, J. and Qian, Y. (2005), Microbial behavior in a membrane bioreactor with complete sludge retention. *Process Biochem.* 40, 3165-3170

Liu, G., Lei, L.C. and Cen, P.L. (2001), Wet air oxidation of printing and dying wastewater. J. Zhejiang University, 35(1) 37–40.

Liwarska-Bizukojć E. and Bizukojć M. (2005), Digital image analysis to estimate the influence of sodium dodecyl sulphate on activated sludge flocs. Process Biochemistry, 40, 2067-2072.

Lopez, A., Ricco, G., R. Ciannarella, Rozzi, A., Pinto, A.C. Di and Passino, R. (1999), Textile wastewater reuse: Ozonation of membrane concentrated secondary effluent. Water Sci. Tech., 40 99-105.

Lubbecke, S., Vogelpohl, A., Dewjanin, W. (1995), Wastewater treatment in a biological high-performance system with high biomass concentration *Water Research.* 29, 793-802.

Macomber J., Cicek N., Suidan M. T., Jan Davel, Ginestet P. and Audic J.M. (2005), Biological kinetic data evaluation of an activated sludge system coupled with an ultrafiltration membrane. *ASCE Journal of Environmental Engineering*, 131-4, 579-586.

Manigas, L. (2008), Use of membrane bioreactor for the bioremediation of groundwater polluted by chlorinated compounds, PhD thesis, University of Cagliari, Italy.

Marsili-Libelli, S. and Tabani, F. (2002), Accuracy analysis of a respirometer for activated sludge dynamic modelling. *Water Research* 36, 1181-1192.

Marcucci, M., Nosenzo, G., Capannelli, G., Ciabatti, I., Corrieri, D., Ciardelli, G., (2001), Treatment and reuse of textile effluents based on new ultrafiltration and other membrane technologies. Desalination 138, 75 - 82

Marmagne, O., Coste, C. (1996), Colour removal from textile plant effluents. American
Dyestuff Reports 85, 15 - 21.

Mason C. A. and Hamer G. (1987), Cryptic growth in *Klebsiellan pneumoniae. Appl. Microbiol. Biotechnol. 25,* 577-584.

McKay G. (1980), Color removal by adsorption. *Am.Dyestuff Rept.* 69, 38

Metcalf and Eddy, (2003), Wastewater Engineering Treatment and Reuse, fourth ed.McGraw-Hill, New York,

Meng, F., Chae, S.R, Drews, A., Kraume, M. and Shind, H.S. (2009), Recent advances in membrane bioreactors (MBRs): Membrane fouling and membrane material, water research 43, 1489 - 1512

Metcalf and Eddy Inc (1991), Wastewater Engineering; Treatment, Disposal, and
Reuse, 3rd edn. McGraw-Hill Inc, New York.

Meyer, U. (1981), Biodegradation of synthetic organic colorants. Microbial degradation of xenobiotic and recalcitrant compounds. In: Leisinger, T., Cook, A.M., Hunter, R., Nuesch, J. (Eds.), FEMS Symposium 12, Academic Press, London, 371 - 385.

Michael, L.S and Fikret, K. (2002), Bioprocess Engineering: Basic Concepts, 2nd edn. Prentice-Hall International, Upper Saddle River, NJ, USA.

Mishra, G., Tripathy, M. (1993). A critical review of the treatments for decolourization of textile effluent, Colourage 40, 35 – 38

Miyashita, S., Honjyo, K., Kato, O., Watari, K., Takashima, T., Itakura, M., Okzaki, H., Kinoshita, I. and Inoue, N. (2000), gas diffuser for aeration vessel of membrane assembly, US Patent 6,328,886.

Minke, R. and Rott, U. (1997), Innerbetriebliche anaerobe Behandlung organisch hoehbelasteter und stark farbiger Teilstromabw~sser der Textilveredelungsindustrie [in German], in: Preprints, Colloquium Produktionsintegrierte Wasser-/ Abwassertechnik, Naeh_haltige Entwicklung in der Textilveredlung, Bremen.

Minke, R. and Rott, U. (2001), Pmzesswasserrttekgewinnung und Abwasservorbehandlung bei der Garnve edelung [in German], in: Preprints, Colloquium Produktionsintegrierte Wasser-/Abwassertechnik, Nachhaltige Entwickltmg in der Textilveredelung, Bremen.

Moran, C., Hall, M.E. (1997), Howell, R.C., Effects of sewage treatment on textile effluent. J. Soc. Dyers. Colour. 113, 272 - 274.

Mulder, M. (1996), Basic Principles of Membrane Technology, second edition, ISBN 0-7923-4248, Kluwer Academic Publishers.

Muller, E.B., Stouthamer, A.H., van Verseveld, H.W., and Eikelboom, D.H. (1995), Aerobic domestic waster water treatment in a pilot plant with complete sludge retention by cross-flow filtration. *Water. Research*. 29, 1179-1189

Musolff, A., Leschik, S., Möder, M., Strauch, G., Reinstorf, F. and Schirmer, M. (2009), Temporal and spacial patterns of micropollutants in urban receiving water, *Environmental Pollution* 157(11), 3069-3077.

Nigam, P., Armour, G., Banat, I.M., Singh, D., Marchant, R. (1996), Physical removal of textile dyes and solid state fermentation of dyeadsorbed agricultural residues. Bioresour. Technol. 72, 219 - 226.

Nigam, P., Marchant, R. (1995), Selection of the substratum for composing bioflm system of textile decolourizing bacteria. Biotechnol. Lett. 17, 993 - 996.

Ng, H.Y., and Hermanowicz, S.W. (2005a),. Membrane bioreactor operation at short solids retention times:performance and biomass characteristics. Water Research. 39, 981-992.

Ng, C.A., Sun, D., Zhang, J., Chua, H.C., Bing, W., Tay, S. and fane, A. (2005b), Strategies to improve the sustainable operation of membrane bioreactors, *Proceedings of International Desalination Association Conference*, Singapore

Ognier, S., Wisniewski, C. and Grasmick, A. (2002), Membrane fouling during constant flux filtration in membrane bioreactors. Membr. Technol. 147, 6–10.

Ogawa, T., Yatome, C. (1990), Biodegradation of azo dyes in multistage rotating biological contra tor immobilized by assimilating bacteria. Bull. Environ. Contam. Toxicol. 44, 561 - 566.

O'Neill, C., Hawkes, F.R., Hawkes, D.L., Lourenco, N.D., Pinheiro, H.M., Delee, W. (1999). Colour in textile effluents e sources, measurement, discharge consents and simulation: a review. Journal of Chemical Technology and Biotechnology 74, 1009 – 1018

Pala, A., Tokat, E. (2002), Color removal from cotton textile industry wastewater in an activated sludge system with various additives. Water Research 36 (11), 2920 - 2925.

Paprowicz J. and Slodczyk S. (1988) Application of biologically activated sorptive columns for textile wastewater treatment. *Environ. Technol. Lett.* 9, 271.

Paszczynski, A., Crawford, R.C. (1995), Potential for bioremediation of xenobiotic compounds by the white-rot fungus Phanerochaete chrysosporium. Biotechnol. Progr. 11, 368 - 379.

Patel, H., Vashi, R.T. (2010), Treatment of textile wastewater by adsorption and coagulation. E-Journal of Chemistry 7 (4), 1468 - 1476.

Perkowski, J., Kos, L. (2003), Decolouration of model dye house wastewater with advanced oxidation processes. Fibres and Textiles in Eastern Europe 11, 67 - 71.

Pillay, V.L., Townsend, B. and Buckley, C.A. (1994), Improving the Performance of Anaerobic Digesters at Waste-Water Treatment Works - the Coupled Cross-Flow Microfiltration Digester Process. *Wat. Sci. Technol.* 30(12), 329-337.

Pirt, S.J. (1965), The maintenance energy of bacteria in growing cultures. *Proc R Soc Lond B Biol Sci* 163:224.

Pollice A., Brookes A., Jefferson B. and Judd S. (2005), Sub-critical flux fouling in membrane bioreactors - a review of recent literature. *Desalination*, 174 (3), 221-230.

Polman, A., Brekenridge, C.R. (1996), Biomass-mediated binding and recovery of textile dyes from waste effluents. Tex. Chem. Colour.28, 31 - 35.

Porter, J. (1997), Wastewater treatment in the textile industry. In: Treatment of Wastewaters from Textile Processing. TU-Berlin Schiftenreihe biologische Abwasserreinigung, Vol. 9, Berlin.

Rabie, H.R., Côté, P., Sing, M. and Janson, A. (2003), Cyclic aeration system for submerged membrane modules, US Patent 6881,343.

Radjenovic, J., (2008), Membrane Bioreactor (MBR) as an advanced Wastewater Treatment Technology, PhD thesis, *Hdb Env Chem* Vol. 5, Part S/2 : 37-101.

Rajeswari, K.R. (2002), Ozonation treatment of textile dyes wastewater using plasma ozoniser. Ph.D thesis, University Malaysia, Malaysia,.

Rein, M. (2001), Advanced oxidation processes-current status and prospects, proc.
estonian acad. Science Chemistry 50, , 59 - 80.

Robinsion, T. (2003), The MBR for industrial effluent, CIWEM & Aqua Enviro Conference, Wakefield, UK.

Robinson, T., McMullan, G., Marchant, R., Nigam, P. (2001), Remediation of dyes in textile effluent: a critical review on current treatment technologies with a proposed alternative. Bioresource Technology 77 247 - 255.

Rosenberger, S., Krüger, U., Witzig, R., Manz, W., Szewzyk, U., Kraume, M. (2002), Performance of a bioreactor with submerged membranes for aerobic treatment of municipal wastewater. *Water Research*, 36, 413-420.

Rosenberger, S., Witzig, R., Manz, W., Szewzyk, U., Kraume, M. (2000), Operation of different membrane bioreactors: Experimental results and physiological state of the microorganisms. *Wat. Sci. Technol.* 10-11 (41), 269-277.

Rosenberger, S. and Kraume M. (2002), Filterability of activated sludge in membrane bioreactors. *Desalination* 151, 195-200.

Ross, WR., Barnard, JP., Strohwald, N.K.H., Grobler C.J. and Sanetra J (1992), Practical application of the ADUF process to the full-scale treatment of a maize-processing Effluent.*Water Sci Technol* 25, (10), 27-39.

Russotti, G., Goklen, K.E. and Wang, W.K. (2001), Crossflow membrane filtration of fermentation broth. in Membrane Separations in Biotechnology. New York, Marcel Dekker Inc. Second Edition 85.

Ryan, F.J (1959), Bacterial mutation in a stationary phase and the question of cell turnover. *J Gen Microbiol* 21, 530–549.

Rozzi, A. Bianchi, R., Liessens, J., Lopez, A. and Verstraete, W. (1997), Ozone, granular activated carbon and membrane treatment of secondary textile effluents for direct reuse, in: Treatment of Wastewaters from Textile Processing, TU-Berlin Sehiftenreihe biologisehe Abwasserreinigung, Vol. 9, Berlin.

Sainbayar, A., Kim, J.S., Jung, W.J., Lee, Y.S. and Lee, C.H. (2001), Application of surface modified polypropylene membranes to an anaerobic membrane bioreactor. *Environmental Technology* 22(9), 1035-1042.

Schoeberl, P., Brik, M., Bertoni, M., Braun, R. and Fuchs, W. (2005), Optimization of operational parameters for a submerged membrane bioreactor treating dyehouse wastewater. *Sep.Purif. Technol*., 44, 61-68.

Shimizu, Y., Okuno, Y., Uryu, K., Ohtsubo, S and Watanabe, A. (1996), Filtration characteristics of hollow fiber microfiltration membranes used in MBR for domestic wastewater treatment. *Water Research* 30 (10), 2385-2392.

Smith, C.V., Gregorio, D.O. and Talcott, R.M. (1969), The use of ultrafiltration membranes for activated sludge separation, *Proceedings of the 24th Industrial Waste Conference*, Purdue University, Ann Arbor Science, Ann Arbor, USA, 1300-1310

Smith, P.J., Vigneswaran, S., Ngo, H.H., Ben-Aim, R. and Nguyen, H. (2005), Design of a generic control system for optimising back flush durations in a submerged membrane hybrid reactor. *J. Membr. Sci*., 255, 99-106.

Sofia, A., Ng, W.J. and Ong, S.L. (2004), Engineering design approaches for minimum fouling in submerged MBR. *Desalination* 160, 67-74.

Stephenson, T., Judd, S., Jefferson, B. and Brindle, K. (2000), Membrane Bioreactors for Wastewater Treatment, *IWA Publishing*, London, UK.

Sun, Y., Huang, X., Chen, F. and Wen, X. (2004), A dual functional filtration/aeration membrane bioreactor for domestic wastewater treatment, Proceedings of water environment-*Membrane Technology Conference*, Seoul, Korea.

Sheng, H and Peng, C.F. (1994), Treatment of textile wastewater by electrochemical method. Water Res., 28 277–282.

Southern TG. (1995), Technical solutions to the colour problem: a critical review. In: Cooper P, editor. Colour in dyehouse effluent. Bradford: Society of Dyers and Colourists;, p. 75.

Spagni, A., Grilli, S., Casu, S. and Mattioli, D. (2010), Treatment of a simulated textile wastewater containing the azo-dye reactive orange 16 in an anaerobic-biofilm anoxiceaerobic membrane bioreactor, International Biodeterioration & Biodegradation 64, 676 - 681

Tamburlini, G., Ehrenstein, O.V., Bertollini, R. (2002), Children's health and environment: a review of evidence. In: Environmental Issue, 129. WHO/European Environment Agency, WHO, Geneva, 22 - 31.

Tonelli, F.A. and Behmann, H. (1996), Aerated membrane bioreactor process for treating recalcitrant compounds, US Pat. No. 410730.

Tonelli, F.A. and Canning, R.P. (1993), Membrane bioreactor system for treating synthetic metal-working fluids and oil based products, USA Pat. No. 5204001. USEPA (2006a), www.epa.gov/region5/defs/html/ppa.htm.

Tratnyek, P.G., Michael, S.E. and Peter, C. (1994), Photoeffects of textile dye wastewater: Sensitization of single oxy-gen formation, oxidation of phenols and toxicity to bacteria. Environ. Toxicol. Chem., 13 27–33.

TU Freiburg, www.tu-freiburg.de, accessed on May, 2011

Ueda, T. and Hata, K. (1999), Domestic wastewater treatment by a submerged membrane bioreactor with gravitational filtration. *Water Research* 33(12), 2888-2892.

Vallero, M.V.G., lettinga, G. and Lens, P.N.L. (2005), High rate sulfate reduction in a submerged anaerobic membrane bioreactor (SAMBaR) at high salinity. *J. Membr. Sci.*, 253, 217-232.

Van Loosdrecht, M.C.M. and Henze, M. (1999), Maintenance, endogenous respiration, lysis, decay and predation. *Wat. Sci. Technol*., 39, 107-117

Vandevivere, P.C., Bianchi, R., Verstraete, W. (1998), Treatment and reuse of wastewater from the textile wet-processing industry: review of emerging technologies. Journal of Chemical Technology and Biotechnology 72, 289 - 302.

Van der Zee, F.P. (2002), Anaerobic azo dye reduction. PhD Thesis. Wageningen University, Wageningen, The Netherlands.

Verma, Akshaya Kumar, Rajesh Roshan Dash, Pupendu Bunia, (2012), A review on chemical coagulation/flocculation technologies for removal of colour from textile wastewaters, Journal of Environmenal Management, 93, 154-168

Visvanathan, C., Yang, B.S., Muttamara, S. and Mythanukhraw, R. (1997), Application of air backflushing technique in membrane bioreactor. *Wat. Sci. Technol*., 36, 259-266.

Vlyssides, A.G., Papaioannou, D., Loizidoy, M, Karlis, P.K. and Zorpas, A.A. (2000), Testing an electr chemical method for treatment of textile dye wastewater.Waste Management, 20, 569–574.

Walker, G.M., Weatherly, L.R. (1997), Adsorption of acid dyes on to granular activated carbon in fixed beds. Water Research 31, 2093 - 2101

Wateronline, 2011; http://www.wateronline.com/article.mvc/Mixed-Liquor-Suspended-Solids-In-Wastewater-0002, loggen on 23.02.11

Wei Y., Houten R. T. V., Borger A. R., Eikelboom, D. H. and Fan, Y. (2003), Minimization of excess sludge production for biological wastewater treatment. *Water Research*, 37, 4453-4467.

Weber, E., Wolfe, N.L. (1987), Kinetics studies of reduction of aromatic azo compounds in anaerobic sediment/water systems. Environ. Toxicol. Chem. 6, 911 - 920.

Wen, X., Bu, Q. and Huang, X. (2004), *Water Environment-Membrane Technology Conference*, Seoul, Korea.

Wilen, B.M. and Balmer, P. (1999), Effect of dissolved oxygen concentration on the structure, size and size distribution of activated sludge flocs. Doktorsavhandlingar vid Chalmers Tekniska Hogskola 1541, 391–400.

Willmott, N., Guthrie, J., Nelson, G. (1998), The biotechnology approach to colour removal from textile effluent. JSDC 114, 38 - 41.

Xing, C.H., Tardieu, E., Qian, Y. and Wen, W.H. (2000), Ultrafiltration membrane bioreactor for urban wastewater reclamation. J. Membr. Sci. 177, 73–82.

Yamamoto, K., Hiasa, M., Mahmood, T. and Matsuo, T. (1989), Direct Solid-Liquid Separation Using Hollow Fiber Membrane in an Activated-Sludge Aeration Tank. *Wat. Sci. Technol.* 21, 43-54.

Yang, W., Cicek, N., and Ilg, J. (2006), State-of-the-art of membrane bioreactors: Worldwide research and commercial applications in North America, *Journal of Membrane Science*, 270, (1-2), 201-211

Yoon, S.H, Kim, H.S. and Chung, Y.C. (2002), Effect of acidity consumption/ production on the pH of aeration tank during the biodegradation of acetic acid/epichlorohydrin. *Water Research*, 36, 2695–2702.

Yoon, S.H., Collins, J.H., Musale, D., Sundararajan, S., Tsai, S.P., Hallsby, G.A., Kong, J.F., Koppes, J. and Cachia, P. (2005), Effects of flux enhancing polymer on the characteristics of sludge in membrane bioreactor process. *Water Sci. Technol*., 51, 151-157.

Yigit, N.O., Uzal, N., Koseoglu, H., Harman, I., Yukseler, H., Yetis, U., Civelekoglu, G. and Kitis, M. (2009), Treatment of a denim producing textile industry wastewater using pilot-scale membrane bioreactor, Desalination 240, 143 – 150

You, S.J, Damodara, R.A. and Hou S.C. (2010), Degradation of Reactive Black 5 dye using anaerobic/aerobic membrane bioreactor (MBR) and photochemical membrane reactor, Journal of Hazardous Materials 177, 1112 - 1118

Yu, H.-Y., Hu, M.-X., Xu, Z.-K., Wang, J.-L., Wang, S.-Y. (2005a), Surface modification of pol propylene microporous membranes to improve their antifouling property in MBR: NH3 plasma treatment. Separation and Purification Technology 45 (1), 8–15

Yu, H.-Y., Xie, Y.-J., Hu, M.-X., Wang, J.-L., Wang, S.-Y., Xu, Z.-K. (2005b), Surface modification of polypropylene microporous membrane to improve its antifouling property in MBR: CO2 plasma treatment. Journal of Membrane Science 254 (1–2), 219 - 227.

Yu, H.-Y., Liu, L.-Q., Tang, Z.-Q., Yan, M.-G., Gu, J.-S., Wei, X.-W. (2008), Mitigated membrane fouling in an SMBR by surface modification. Journal of Membrane Science 310 (1–2), 409 - 417.

Yu, H.-Y., Xu, Z.-K., Lei, H., Hu, M.-X., Yang, Q. (2007), Photoinduced graft polymerization of acrylamide on polypropylene microporous membranes for the improvement of antifouling characteristics in a submerged membrane-bioreactor. Separation and Purification Technology 53 (1), 119–125.

Zaloum, R., Lessard, S., Mourato, D., and Carriere, J. (1994), Membrane bioreactor treatment of oily wastes from a metal transformation mill. *Wat. Sci. Technol.*, 30, 21–27.

Zhang, Y., Bu, D., Liu, C.G., Luo, X. and Gu, P. (2004), Study on retarding membrane fouling by ferric salts dosing in membrane bioreactors, *Proceedings of Water Environment- Membrane Technology Conference*, Seoul, Korea.

Zhang, J., Chua, H.C., Zhou, J. and Fane, A.G. (2006), Factors affecting the membrane performance in submerged membrane bioreactors. *J Membr Sci*., 284, 54-66.

Zhang, S.T., Qu, Y.B., Liu, Y.H., Yang, F.L., Zhang, X.W., Furukawa, K. and Yamada, Y. (2005), Experimental study of domestic sewage treatment with a metal membrane bioreactor. *Desalination*, 177, 83-93.

Zollinger, H. (2006), Colour Chemistry-Synthesis, Properties of Organic Dyes and Pigments. VC Publishers, New York, 92 - 100.

Zheng, X., and Lui, J. (2006), dyeing and printing wastewater treatment using membrane bioreactor with gravity drain, Desalination, 190, 277 - 286

Zhou, W., Zimmerman, W. (1993), Decolorization of industrial effluents containing reactive dyes by actinomyces. Microbiol. Lett. FEMS 107, 157 - 162.

3. Chapter 3 : Materials and Methods

To fulfil the objectives of this thesis, lot of materials and methods were applied under different operating conditions. This chapter reports on the applied materials and methods those were used in every step of the thesis ranging from membrane preparation until the final experimental results obtained. Some of the important materials and methods including their coefficient of variation (% C_v) (which were calculated using equations described in appendix D) are illustrated very briefly in the following sections of this chapter.

3.1 Materials for membrane preparation

All the chemicals used for preparing microemulsions for PBM membranes were bought from Sigma-Aldrich (Germany) with purity higher than 98% (analytical grade).

3.2 Membrane preparation chamber

For novel/PBM membrane preparation different kinds of chemicals were applied (Section 4.1). Finally a microemulsion was casted on commercial UF PES membrane supplied by Microdyn – Nadir, in a casting chamber. The dimensions of the casting chamber were 40 cm × 40 cm × 42 cm (Fig. 3.1) and it was made of plexyglass incorporated with 4 N_2 gas inlet channels (one from left side, one from right side and two from back side). N_2 gas was needed as inert gas required for polymerisation reaction of novel membrane casting. The chamber was also equipped with temperature sensor, heating plate, power supply for the heating plate, thermo-couple, glass plate, commercial UF PES membrane and casting knife. There was a Flapof the glass chamber for opening or closing the chamber. The experimental set up of the device is shown in Fig. 3.2.

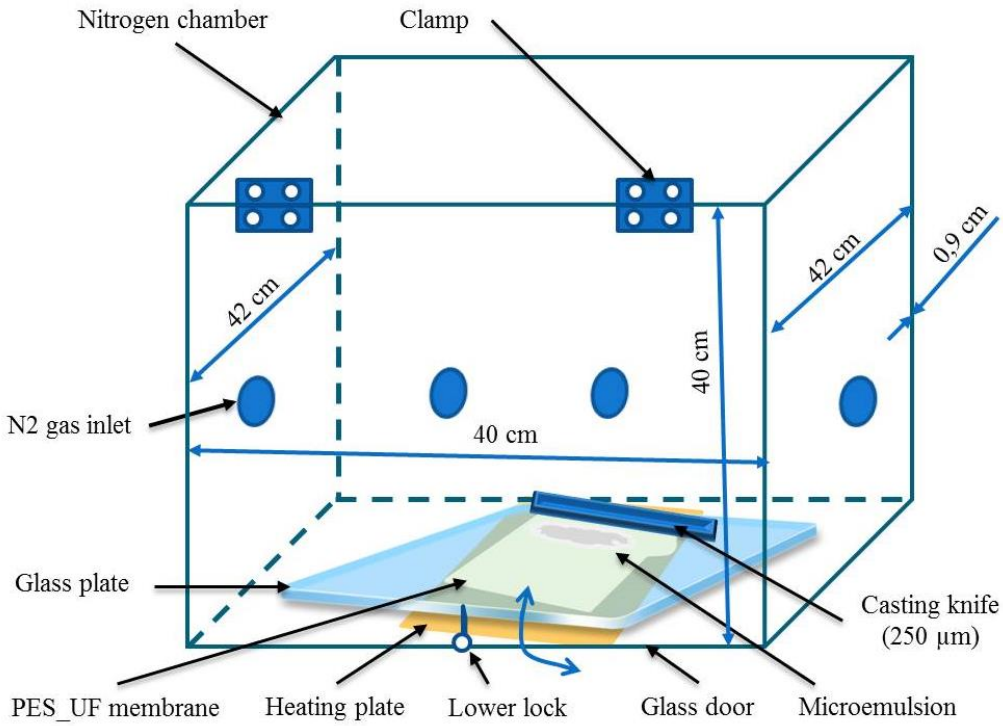

Fig. 3.1 : Schematic diagram of membrane casting chamber saturated with N_2 gas

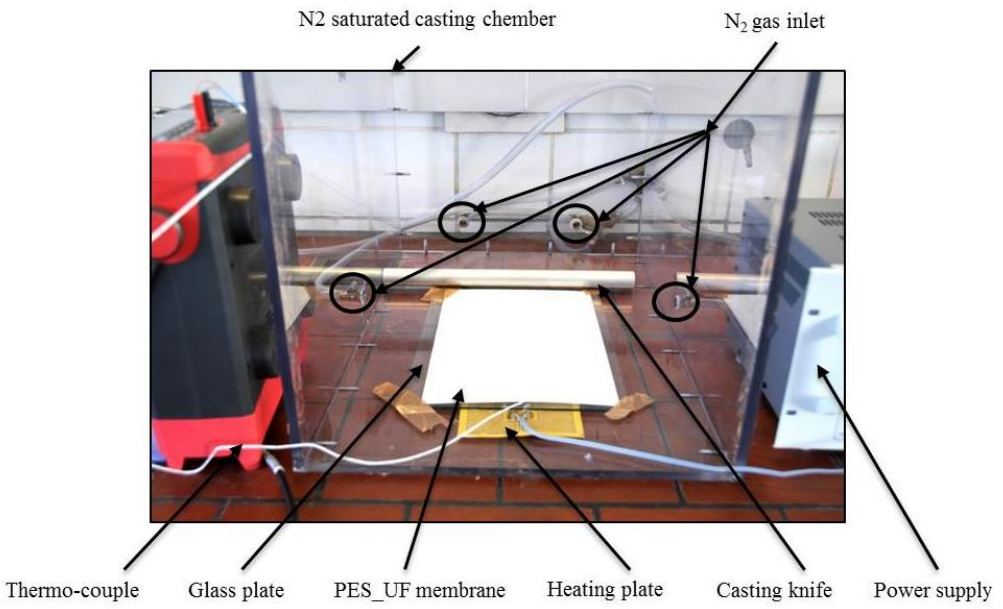

Fig. 3.2 : Experimental set up of membrane casting chamber saturated with N_2 gas

To keep the casting chamber N_2 gas saturated, N_2 gas was supplied for 5 minutes at the rate of 1 bar gas pressure before casting any PBM membrane. The gas flow was indirectly indicated by manually displayed pressure gauge. This display might have ± 5% error. The temperature set for membrane preparation was varied at ± 1 °C due to process variation.

3.3 Instruments/chemicals used for membrane characterisation

The prepared membranes were characterised by membrane surface analysis through scan electronic microscopy (SEM) and atomic force microscopy (AFM), porosity measurement, contact angel measurement, molecular weight cut off (MWCO), water permeabilities in two cross-flow testing cells, salt rejections, dyes rejections and model fouling test. The SEM and AFM analyses were carried out by Dr. Daniel Johnson from Swansea University, England.

Scan Electron Microscopy (SEM)

The SEM applied in this case was Hitachi Field Emission SEM (model S-4800). The resolution of the applied SEM was as follows:

Accelerating voltage 15 kV
Working distance = 4 mm -1.0 nm
Accelerating voltage 1 kV
Working distance = 1.5 mm -2.0 nm

This work was done in collaborating with Swansea University, UK.

Atomic Force Microscopy (AFM)

All AFM measurements were performed with a Multimode AFM with Nanoscope IIIa controller (Veeco, USA) using manufacturer supplied software. Tapping mode measurements in air were performed using TESP (nominal spring constant 20-80 N/m) cantilevers (Bruker AXS). All other measurements were performed using NP-S probes (long thick lever, nominal spring constant 0.12 N/m). Roughness values were obtained from topography scans using the instrument software. The resolution of the most of the images created by AFM instrument was in the form of 512× 512 pixels.This work was done in collaborating with Swansea University, UK.

Porometer

The porosity of the membranes were measured by PMI capillary flow porometer which provided fully automated through-pore analysis including bubble point, pore size distribution, mean flow pore size etc. with accuracy of 0.15% of reading (PMI, porous materials, Inc. USA).

Contact angle meter

The contact angel was determined applying CAM 200 optical contact angle meter (KSV Instrument LTD, Finland). The resolution of the instrument was 800 × 600 pixel.

Gel Permeable Chromatography (GPC)

The molecular weight cut off (MWCO) was determined applying Gel Permeable Chromatography (GPC) from Thermo Scientific (Thermo Fisher Scientific Inc. USA) including column from Labservice, Italy.

Micrometer

The micrometer was used to measure the thickness of PBM coating on top of the PES membrane. The measuring range of the micrometer used in this case was 0 – 25 mm and it was purchased from company Mohr GmbH, Germany. The accuracy of the measurements was ± 5%.

UF cross-flow testing cells

The water permeabilities and fouling tests of the membranes were performed applying manually controlled ultrafiltration (UF) cross-flow testing cell (Fig.3.3) and auto-controlled ultrafiltration (UF) cross-flow testing cell (Fig. 3.5).

The manually controlled ultrafiltration cross-flow testing cell is a laboratory membrane test unit (Fig.3.3 and Fig. 3.4) manufactured by company OSMO Membrane System GmbH (Germany), which was used to test different types of membranes. The main parts of this unit consist of feed tank (1), feed channel (2), feed pump (3), feed pressure gauge (4), cross-flow membrane cell (5), permeate channel (6), cross-flow pressure gauge (7), cross-flow display (8), drain valve (9), inlet pressure control valve (10), cross-flow pressure valve (11) and cooling device (12). The system was cooled by jackted tank. All data from this experiment were collected manually. This is a short term (for several

hours) experimental set up.

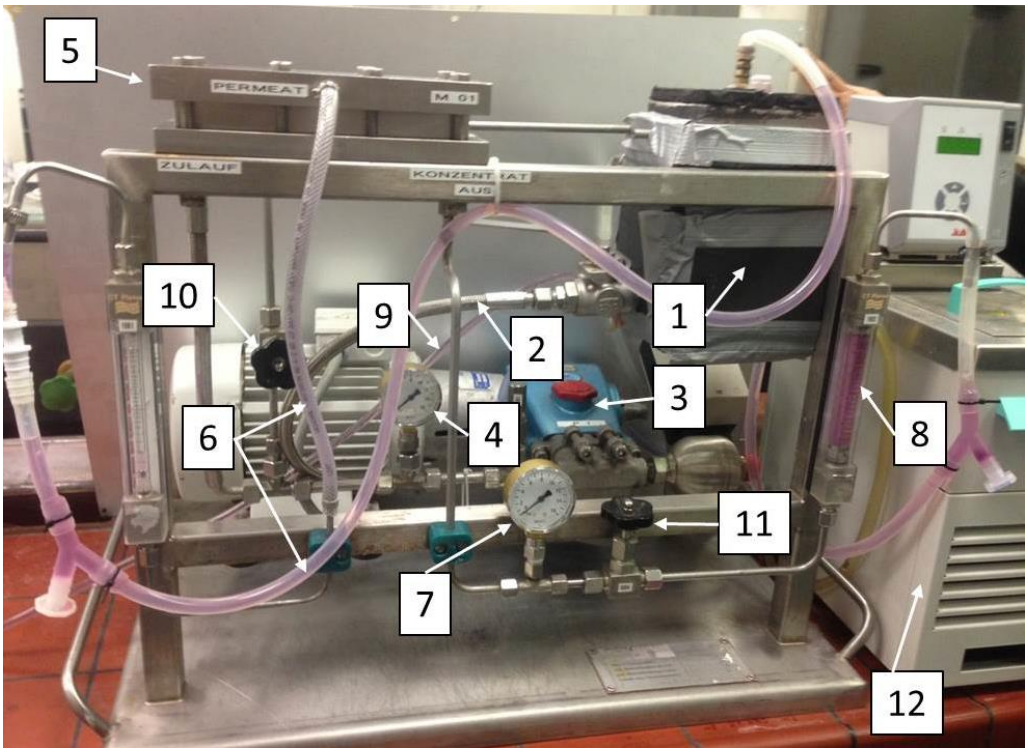

1: Feed tank, 2: Feed channel, 3: Feed pump, 4: Feed pressure gauge, 5: Cross-flow membrane cell, 6: Permeate channel, 7: cross-flow pressure gauge, 8: Cross-flow display, 9: drain valve, 10: Inlet pressure control valve, 11: Cross-flow pressure valve, 12: Cooling device

Fig 3.3. Experimental set up of manually controlled UF cross-flow testing cell

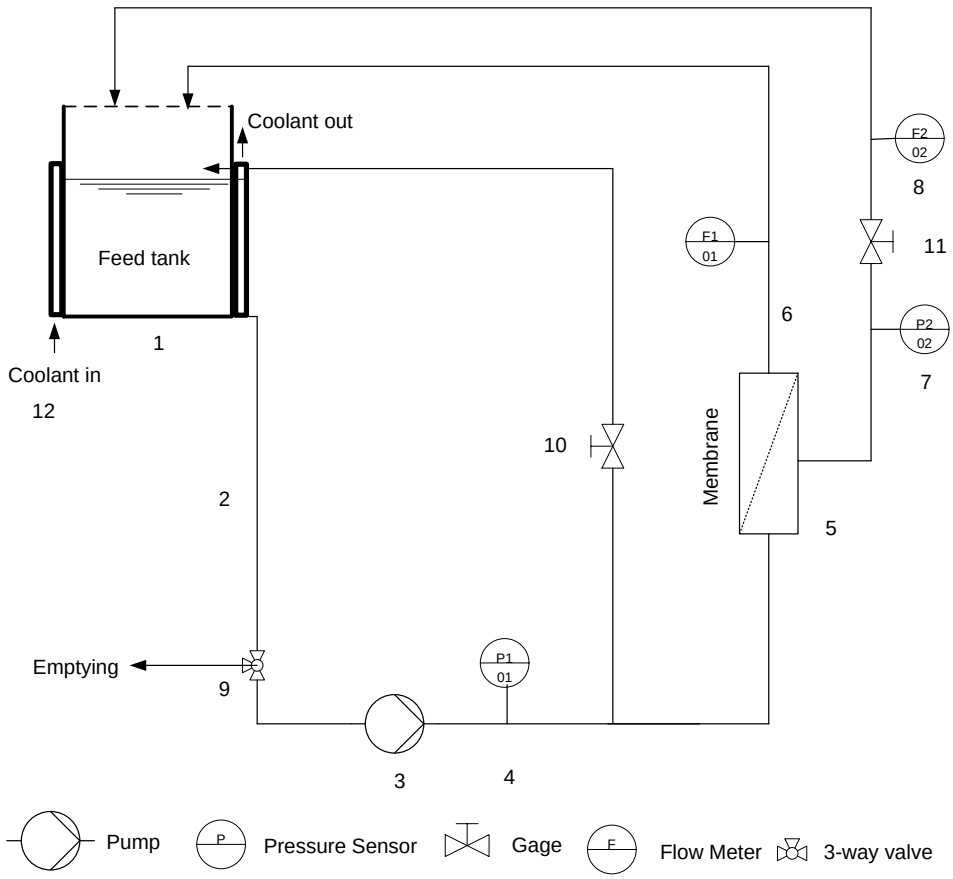

Fig 3.4. Schematic diagram of manually-controlled UF cross-flow testing cell

The pressure was set by the manually controlled valves (10, 11) and it was displayed on the pressure gauges (4, 7). The pressures in the range of 1 – 5 bar were selected as operating pressures to test the membranes. The temperature was set by cooling device (12) connected with a double walled heat exchanger. The temperature of 20°C ±2°C was set as the working temperature for all the experiments carried out. For the experiments, the feed solution was fed into the feed tank (1) which has the capacity of 2 L. The membrane was placed in the membrane cross-flow cell (5). The dimensions of the membrane used in this case were 20 cm × 4 cm covering 80 cm^2 of active membrane surface area. The feed solution from the feed tank was pumped into the membrane module and through the membrane at desired pressure. The permeate and concentrate coming out of the membrane module were recirculated back to the feed tank. The flux of the solution was measured by hand. After the testing, the solution in the feed tank was emptied by opening the discharge valve (9). Since there

was no vibration controller, the indicators of the pressure gauges were vibrating significantly showing pressure measurement error of around ± 10%.

The auto-controlled ultrafiltration (UF) cross-flow testing cell (Fig.3.5 and Fig. 3.6) was purchased from company SIMA-tec GmbH (Germany), which was used to test different types of membranes. This testing unit was equipped with heat-exchanger/temperature controller (2) and LabVIEW program based computerised data acquisition system. To abate the vibration of the unit, it was equipped with damping system (9) by filling vibration controller with N_2 gas at 16 bar pressure. The experiments with this unit were carried out continuously for longer time (from some hours to several days).

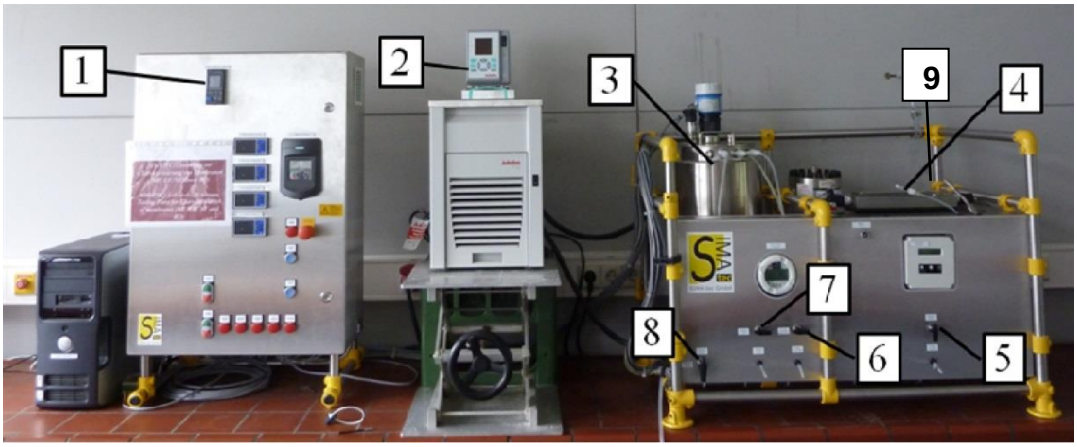

1: Pressure control, 2: Temperature control, 3: Feed tank, 4: Membrane module, 5: Permeate sampling valve, 6: Concentrate sampling valve, 7: Feed sampling valve, 8: drain valve

Fig 3.5. Experimental set up of auto-controlled UF cross-flow testing cell

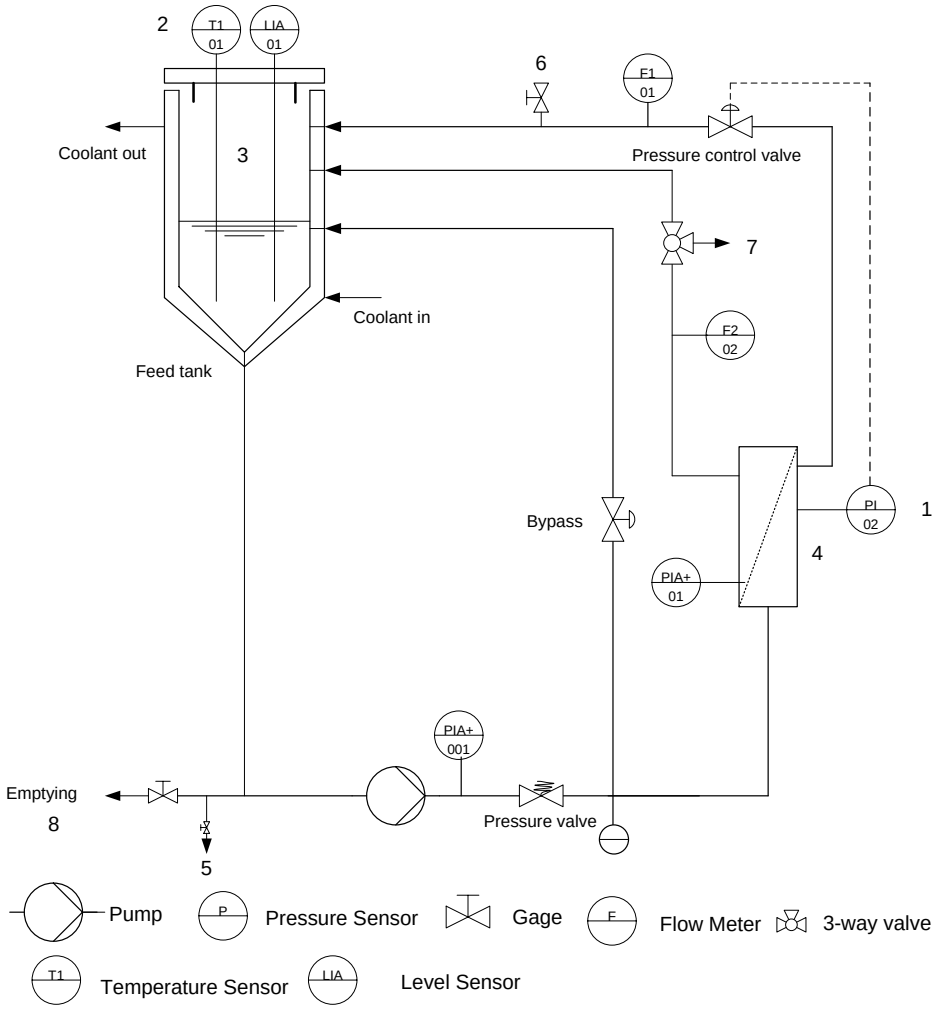

Fig. 3.6. Schematic diagram of auto-controlled UF cross-flow cell

The pressure was set by the pressure controller (1). The pressures 0.5 bar, 1 bar and 2 bar were selected as operating pressures to test the membranes. The temperature was set by the temperature controller (2). The temperature of 20°C ± 2°C was set as the working temperature for the experiments carried out. For the experiments, the feed solution was fed into the feed tank (3) which has the capacity of 5 L. The membrane was placed in the membrane module (4). The dimensions of the active membrane used in this case were 21.4 cm × 4 cm covering 85.6 cm^2 of active membrane surface area. The feed solution from the feed tank was pumped into the membrane module and through the membrane at defined pressure. The permeate and concentrate coming out of the membrane module were recirculated back to the feed tank. The flux of the

solution was measured and recorded by integrated LabVIEW program. During the experiment, it was also possible to collect the permeate, the concentration and the feed samples by opening the valves (5), (6) and (7) respectively. After the experiment was finished, the solution in the feed tank was emptied by opening the drain valve (8). The applied pressure indicator showed ± 2% and temperature indicator had ±1 % accuracy. The error of the flux recorded by LabVIEW program has been assumed as ± 2% since it varied with applied pressure.

For fouling test humic acid (HA) was applied since many fundamental studies of the fouling phenomena have been done by using the readily analyzed humic acid as a model foulant (Sutzkover-Gutman et al., 2010). In addition, humic acid represents foulants in biological sludge system.

For dye rejection tests, feed solution was prepared using two commercial dyes called Remazol Brilliant Blue R (denoted briefly as Blue in this thesis) and Acid Red 4 (denoted briefly as Red in this thesis) and additional chemicals such as NaCl, Na_2CO_3/$NaHCO_3$, Glucose and detergent (Albatex DBC) at various concentrations (section 5.3.1). The error occurred from the weighting balances for dyes were ± 4% and for the rest of the chemicals were 0.12%. The different quantity of the chemicals might have contributed to the variation of accuracies.

3.4 Membrane bioreactor (MBR)

The MBR reactor was designed by Wladimir Korejba (Korejba, 2010) based on commercially available plastic tank and it was adapted to the experimental needs. The experimental set up and schematic diagram of the MBR reactor accompanied with its accessories are shown in Fig.3.7 and Fig. 3.8 respectively.

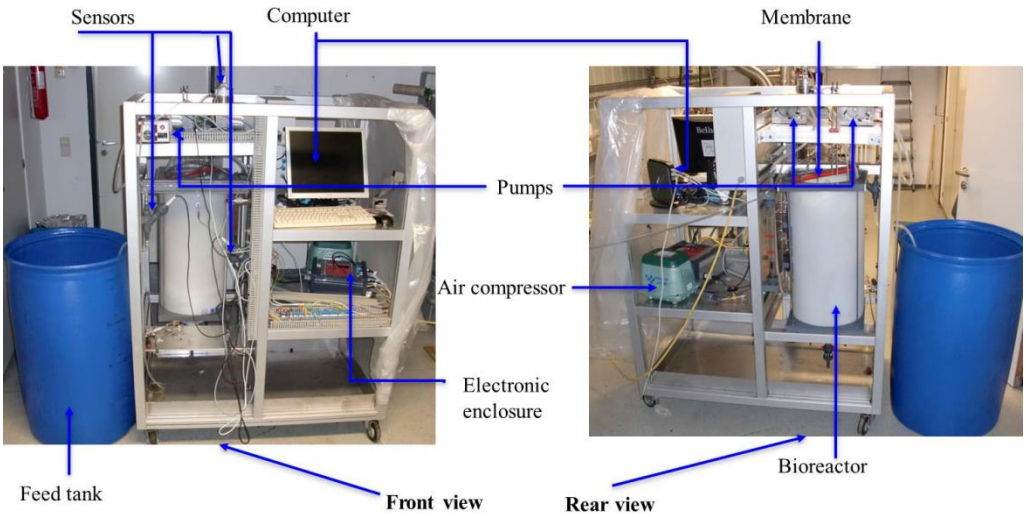

Fig. 3.7 : Experimental set up of membrane bioreactor

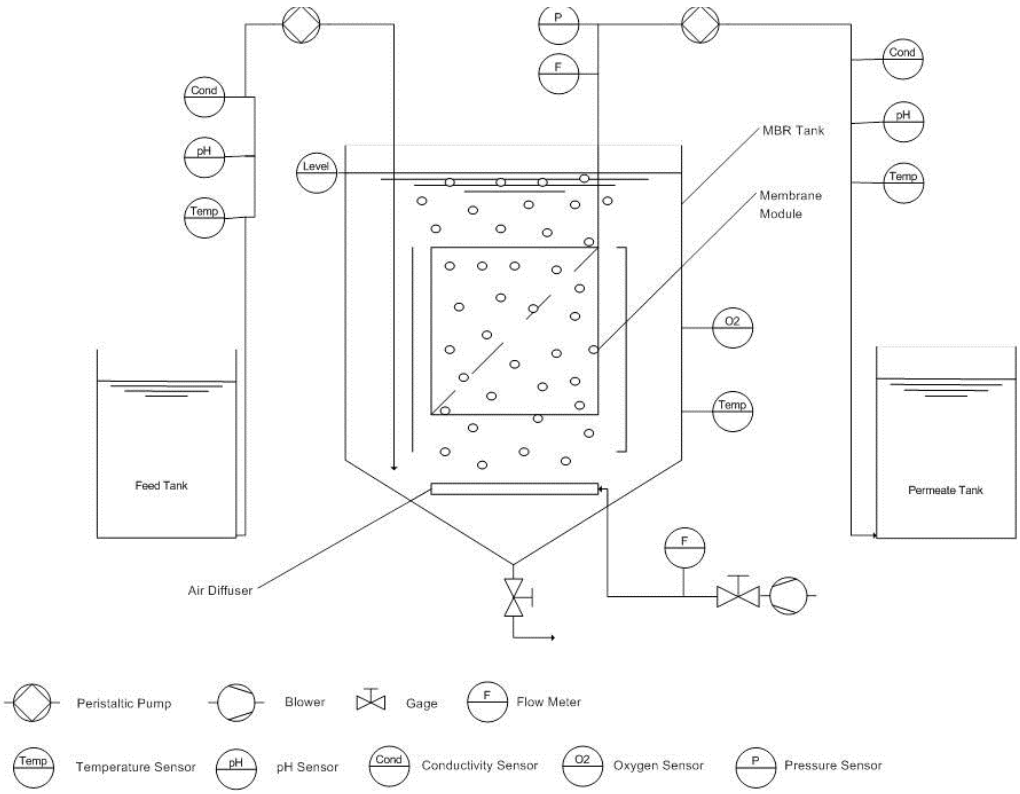

Fig. 3.8 : Schematic diagram of membrane bioreactor

The total volume of the reactor (tank) is around 60 L where hydraulic volume (where MBR module is submerged) was around 57 L. The MBR reactor consists of membrane module, air compressor, level sensor, differential pressure sensor, feed pump, permeate pump, foam pump, foam sensor, flow sensor, pH sensor, temperature sensor, conductivity sensor and air flow meter. The errors of the measurements from different sensors applied in MBR process were as like as the errors of the corresponding /measuring devices/applied sensors.

Selecting the MBR reactor size as shown in Fig. 3.9, the flat sheet membrane module (UF PES membrane, pore size: 0.040 µm, dimensions: 25cm × 25cm) from company Microdyn-Nadir, Germany (Microdyn – Nadir, 2013) was installed inside the reactor. The module consists of 3 flat sheets membrane each of having 0.11 m^2 of area giving total area of 0.33 m^2. The membrane module was equipped with mechanical aerator at the bottom of the module and permeate suction channel in the middle of the module cassette. Air was supplied by a compressor. To avoid any movement of the module, it was fixed with the head of the MBR reactor with the help of module holder. It was taken care that the module was always submerged in the hydraulic volume ensured by level sensor. The permeate suction channel of the module was connected to a differential pressure sensor to measure the transmembrane pressure (TMP) which was created by a vacuum pump to produce permeate flow. Feed was supplied by a feed pump. A foam sensor was incorporated at the top of the reactor to abate excess foam. Some other sensors were installed to ascertain pH, conductivity, temperature of feed and permeate. All the process parameters were monitored and data were acquired by LabVIEW program controlled computer system.

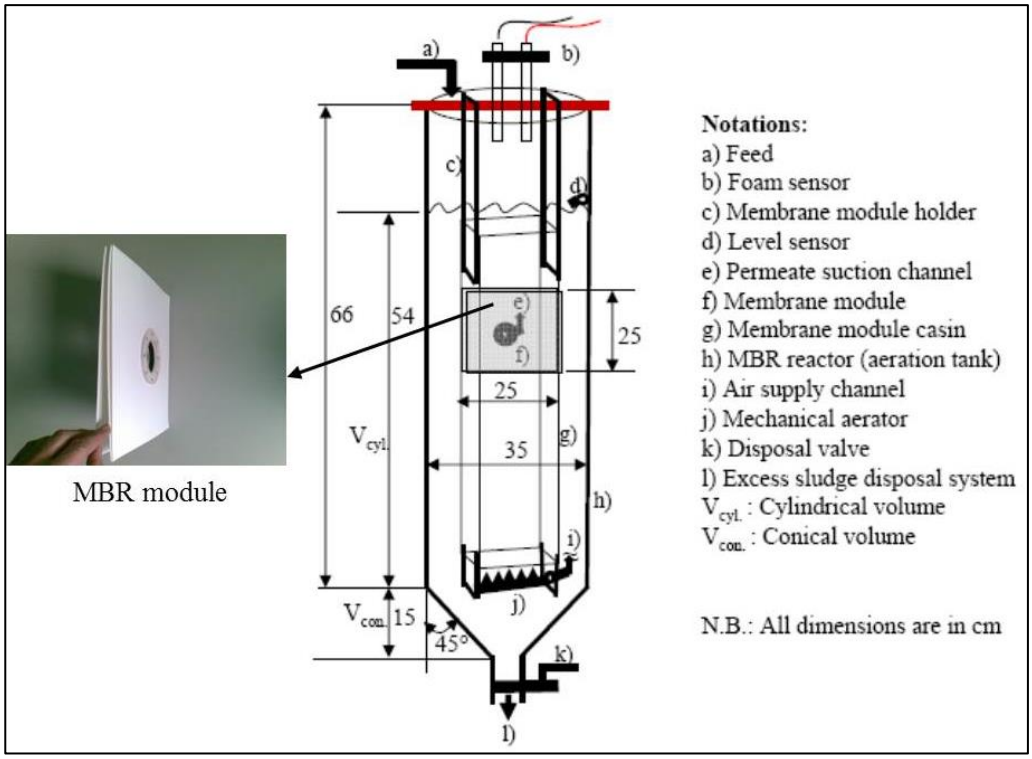

Fig. 3.9 Schematic of MBR reactor with module

3.5 Model foulant humic acid (HA)

A variety of constituents in water can lead to membrane fouling, including dissolved inorganic or organic compounds, colloids, bacteria and suspended solids. Biofouling is largely attributable to accumulated extracellular materials, rather than individual bacterial cells or microbial flocs. These extracellular materials, including soluble microbial products (SMP) and extracellular polymeric substances (EPS), consist mainly of polysaccharides, proteins, and natural organic matter (NOM) (Asatekin et al., 2006).

Natural organic matter (NOM) contained in natural water is one of the main foulants present in surface water and wastewater. The main components of NOM are humic substances which are the macromolecular mixtures of humic acids, fulvic acid, and humin (Srisurichan et al. 2005). Many fundamental studies of the fouling phenomena have been done by using the readily analyzed humic acid as a model foulant (Sutzkover-Gutman et al. 2010).

Humic acid (HA) has been considered to be one of the most significant model foulants to represent NOM in the surface water and waste water. HA exists ubiquitously in the aquatic environment in activated sludge and is considered as a degradation product of lignin, carbohydrates, proteins, etc. (Nystrom et al. 1996). HA is a heterogeneous mixture having both aromatic and aliphatic components with three main functional groups, namely carboxylic acids (COOH), phenolic alcohols (OH), and methoxy carbonyls (C=O) (Wie et al., 1999). The removal of humic acid from aqueous solutions has been investigated by a number of researchers.

The HA applied in this thesis experiments were bought from Alfa Aesar GmbH & Co KG (Germany) in crystalline powder form. The formula of the used HA was $C_9H_9NO_6$ having molecular weight of 227 (Chemical book, 2013). The possible errors might have occurred from the humic acid measuring analytical balance (KERN 770 from company KERN and Sohn GmbH, Germany) which contributed to small variation of humic acid concentration in the feed solution. The error of the measuring balance was ± 4.0%.

3.6 Preparation of model textile dye wastewater (MTDW)

Model textile dye wastewater (MTDW) was prepared based on collected information from different publications (Idil et. al., 2002, Mustafa et. al., 2008 and Bahadur et. al., 2009). To determine the quality of wastewater, Chemical Oxygen Demand (COD) is referred as one of the key parameters. The COD values of original textile wastewater vary from industry to industry based on used processes. For preparing MTDW for this thesis works, chemical compositions were selected in such a way that the COD value remains in the range of around 2450 mg/L which is close to most of the selected literature studies. The compositions of the MTDW is summarised in Table 5.1.

Between two textile dyes, Acid Red 4 was not easily dissolvable. To prepare 100 L of MTDW, 4 L of DI water was taken and 5. g of Acid Red 4 was added. This mixture was kept agitating with magnetic agitator at 150 rotation/minutes with temperature of 80°C for 1/2 hour. When the red dye was fully dissolved, the rest of the chemicals mentioned in Table 3.1 were added according to the required calculated amount and agitation was kept continued until the rest of the chemicals fully dissolved. This 4 L parent chemical solution was added

with 96 L DI water so that the total volume becomes 100 L and the quality of MTDW remains constant. The MTDW prepared in this way was used as feed solution for entire tests. It is worth to mention that Na_2CO_3 was used in the composition to keep pH 10.0 ± 0.5 of MTDW and for pH 7.5 ± 0.5 of the feed solution, $NaHCO_3$ was the choice.

Table 3.1 : Composition of model textile dye wastewater (MTDW)

No.	Dyestuffs & chemicals	Concentration (mg/L)	References
1	Remazol Brilliant Blue R	50	
2	Acid Red 4	50	
3	NaCl	2500	Idil et. al., 2002
4	Na_2CO_3/$NaHCO_3$	1000	Mustafa et. al., 2008
5	Glucose	2000	Mustafa et. al., 2008
6	Albatex DBC (Detergent)	50	Bahadur et. al., 2009
7	NH_4Cl	300	

3.7 Textile dyes in MTDW

Reactive dyes have been identified as the most problematic compounds in textile dye effluents (Caliell et al., 1996, 1994). Reactive dye is a class of highly coloured organic substances, primarily utilised for tinting textiles. These kinds of dyes bind to their substrates by a chemical reaction that forms a covalent bond between the molecule of dye and that of the fibre (Palacios, 2009). To prepare the model textile dye wastewater (MTDW) applied in this thesis, two different dyes named as Acid Red4 (termed as red in this thesis) and Remazol Brilliant Blue R (termed as blue in this thesis) were selected (Fig. 3.10 and Fig. 3.11). Molecular weights (MW) of red and blue are 380.4 g/mol and 626.5 g/mol respectively.

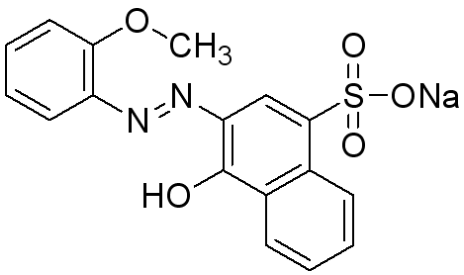

Fig. 3.10 : structure of Acid Red4, formula: $C_{17}H_{13}N_2NaO_5S$

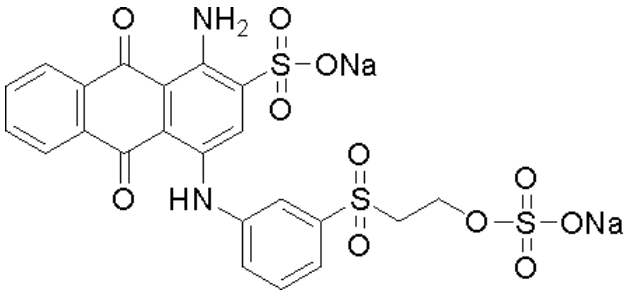

Fig. 3.11 : Structure of Remazol Brilliant Blue R, $C_{22}H_{16}N_2Na_2O_{11}S_3$

With respect to chemical structure acid red is an azo dye whereas blue is an anthraquinone dye.

Azo dye

Azo dye is the largest class of dye used in textile industry. Azo dyes are often used in the colouring process of several textiles and leather products. Some azo dyes contain chemical groups that bind metal ions. Often, the metal ion also unites with the fibre, improving the resistance of the dye to washing and also this bond between the dye and the ion can produce important changes in shade (Palacios, 2009, p.7).

There are high levels of azo dyes in the environment and it is quite difficult to breakdown this azo bonds (R – N = N – R) (Fig. 3.12). They are very stable in acidic and alkaline conditions and resistant to high temperatures and light. In spite of this, they might be degraded with bacteria under anaerobic and aerobic conditions (Seesuriayachan et al. 2007).

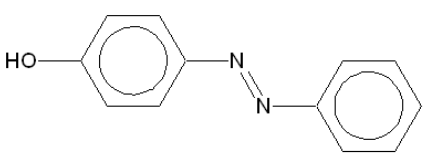

*Fig. 3.12 : General structure of an azo dye (*Palacios, 2009, p. 7)

Various bacteria strains reduce azo dyes under anaerobic conditions. The most generally accepted hypothesis for this phenomenon is that many bacteria strains possess rather unspecific cytoplasmic enzymes, which act as "azo-reductases" and under anaerobic conditions transfer electrons via soluble flavins to the azo dyes (Walker, 1970).

Anthraquinone dye

Anthraquinone dye (Fig. 3.13), constitute the second largest group of textile dyes after azo dyes and are used extensively in the textile industry due to their variety of colour shades and easy of application

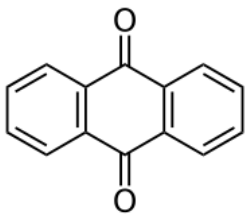

*Fig. 3.13 : General structure of an anthraquinone dye (*Palacios, 2009, p. 8)

Anthraquinone acid dyes contain sulfonic acid groups that render them soluble in water water (Britannica, 2013).

In general, red and blue dyes are actually anionic dyes with sulfonic groups (-SO_3-). The blue dye has two sulfonic groups whereas the red dye has only one sulfonic group meaning the blue dye could be more repelled than the red dye by negative charged membrane surfaces (charge exclusion). The purity of red and blue dyes was more than 98% and the red and blue dye were bought from company BOC Sciences (USA) and Chemos (Germany) respectively. The red and blue dyes applied in this thesis were measured by weight balance with accuracy of ±4.0%.

3.8 DI water and auxiliary chemicals for model textile dye wastewater (MTDW)

The water used for the experiments was purified by ion exchanger from company R.R. Hanovsky (Germany) with electrical conductivity in the range of 1 –

5 µS/cm. The auxiliary chemicals of MTDW such as NaCl (analytical grade), Na_2CO_3 (analytical grade), $NaHCO_3$ (analytical grade), NH_4Cl (analytical grade) and Glucose were purchased from company Merck Milipore (Germany) and Albatex DBC was from company Huntsman (UK).

3.9 MBR samples analyzers

MBR samples were analysed to determine the performance of the biological treatment. Among the significant chemical and biological parameters are: chemical oxygen demand (COD), biological oxygen demand (BOD), total organic carbon (TOC), dye contents (red and blue), mixed liquor suspended solids (MLSS), N-balance (Total-N, NH_4-N, NO_3-N), dissolved oxygen (DO) concentration, drying residue (DR), Chloride (Cl^-) concentration, pH and temperature and electrical conductivity were analysed applying corresponding analyzers/measuring instruments.

3.9.1 COD

All COD were analysed with COD cell tests (Method 1.14541) from Merck KGaA (Germany). The measuring range of this method was 25 - 1500 mg/L of COD. According to the COD product brochure the coefficient of variation (% standard deviation) is supposed to be ± 0.68%. The coefficient of variation of some of the selected samples (experimentally) was ± 1.02%. This gap of accuracy might have occurred due to applied different COD measuring levels.

3.9.2 BOD

All BOD values were analysed by manometric BOD_5 measuring device (Model: OxiTop®IS6) from WTW GmbH, (Germany). The coefficient of variation (C_v) of the analysed samples were ± 13 %.

3.9.3 TOC

At the beginning of the experiments until day 190, the TOC values were analysed by Euroglas TOC 1200 analyzer from Thermo Fisher Scientific Inc., Waltham, USA. The sample was delivered to high temperature (1000°C) furnace and the organic compounds of the sample oxidized into carbon dioxide. The accuracy, in terms of coefficient of variation of this instrument was 1.67% considering the measuring range of 30 – 50 mg/L. After day 190, the TOC values were analysed by total organic carbon analyser (Model: TOC-L CPH/CPN)

from Shimadzu (Japan). This instrument was equipped with a catalyst and its measuring range was 5 – 100 mg/L. The working principle of both of the instruments was similar.

Total organic carbon (TOC) test was performed by modern combustion catalytic oxidation method. It was measured with organic carbon analyzer (Shimadzu TOC L_{CHP}, Shimadzu Corporation, Japan). The combustion catalytic oxidation method achieves total combustion of samples by heating them to 680°C in an oxygen-rich environment inside TC (Total Carbon) combustion tubes filled with a platinum catalyst. The carbon dioxide generated by oxidation was detected using an infrared gas analyzer (NDIR) (Shimadzu, 2013) (Fig. 3.14).

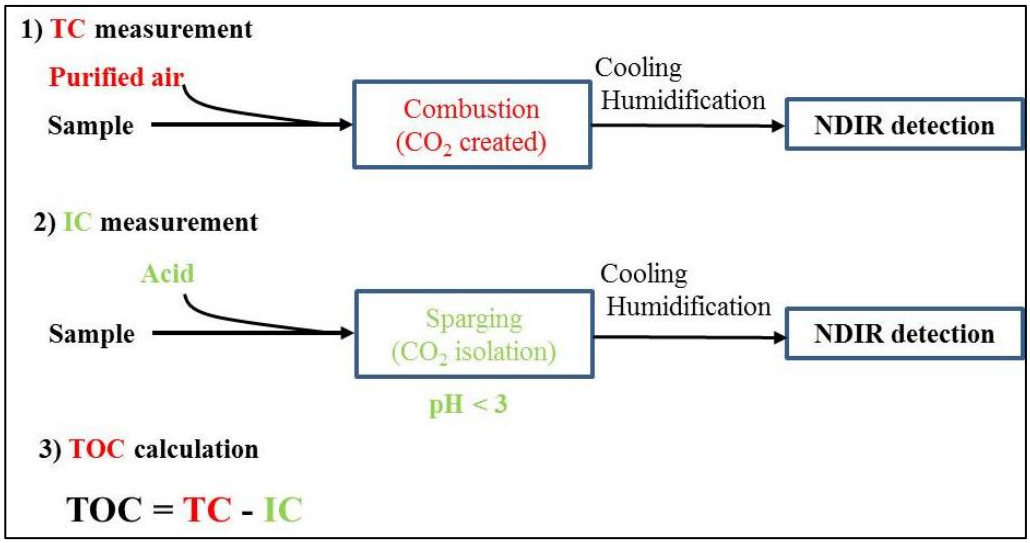

Fig. 3.14 : TOC analyzing process (Shimadzu, 2013)

With this method the sample was delivered to the combustion furnace which was supplied with purified air. There, it undergoes combustion through heating to 680°C with a platinum catalyst. Then, it is decomposed and is converted to carbon dioxide. The carbon dioxide generated is cooled and dehumidified, and then detected by the NDIR. The concentration of TC (Total Carbon) in the sample is obtained through comparison with a calibration curve formula. Furthermore, by subjecting the oxidized sample to the sparging process, the IC (Inorganic Carbon) in the sample is converted to carbon dioxide, and the IC concentration is obtained by detecting this with the NDIR. The TOC concentration is then calculated by subtracting the IC concentration from the obtained TC concentration (Shimadzu.eu, 2013). The C_v (accuracy) of the measurements with this TOC analyser was ± 1.27%.

3.9.4 Red and Blue dyes

The concentration of the dyes, Remazol Brilliant Blue R and Acid Red 4 denoted as "Blue" and "Red" respectively in the feed and permeate were analysed by spectrophotometer (Model: UV-1800) from Shimadzu (Japan).

In order to obtain the absorption spectra, the solution of each dye was taken in a 3 ml cuvette and scanned by the spectrophotometer in within the range 200-700 nm wavelength and the absorbance spectrums were recorded. At first, the absorbance of individual dye i.e. red and blue were measured by spectrophotometer. From the absorbance spectrum the specific wavelength of maximum absorbance for both dyes were found.

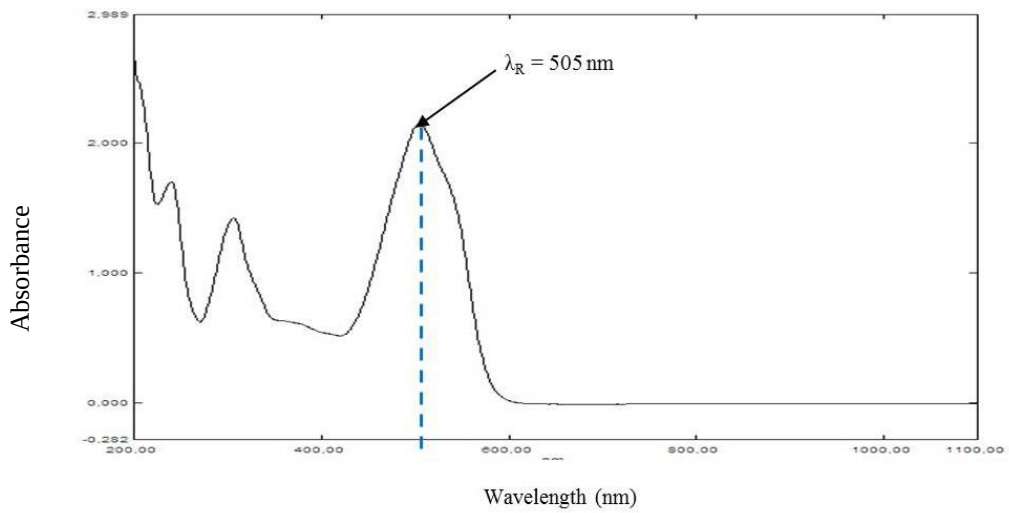

Fig. 3.15 : Absorption spectrum of the Acid Red 4 dye solution (50mg/L)

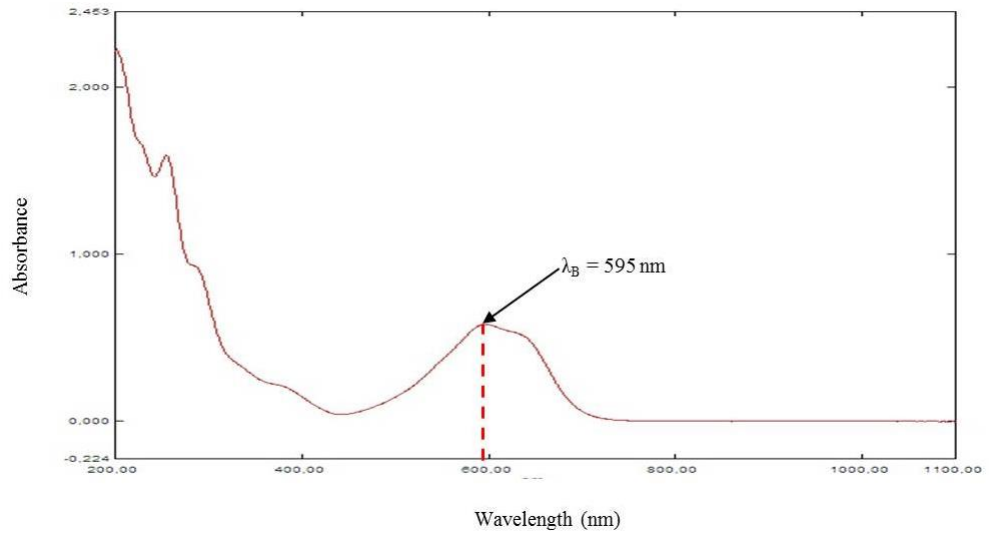

Fig. 3.16 : Absorption spectrum of the Remazol Brilliant Blue R (50 mg/L)

It was noticed that, red and blue dyes showed maximum absorbance at wavelength of 505 nm and 595 nm respectively. The absorbance spectrum of red and blue dye solutions are shown in Fig.3.15 and Fig. 3.16. respectively. Similarly, the absorbance of mixed solutions of these two dyes were also measured as shown in Fig. 3.17. The objective of analysing mixed red and blue curves was to measure both dyes with one scan.

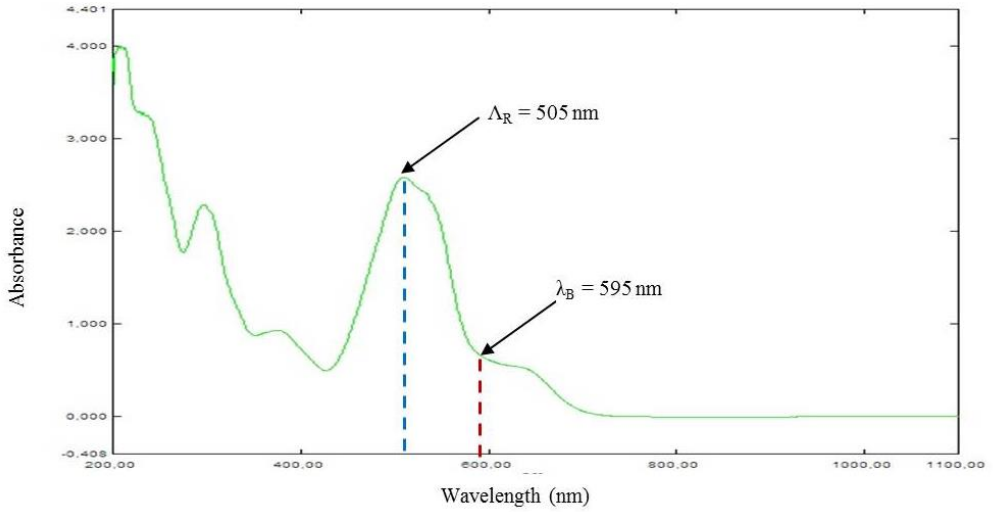

Fig. 3.17 : Absorption spectrum of Red and Blue mixed dye solution (50% of each solution)

Calibration procedure

It should be noted that the mixed dye solution had always a volume of 3 ml. To keep the volume of mixed solution constant, specific amount of each dye solution was poured into the cuvette. The amount of each dye solution varied from 0.25 ml to 2.75 ml but the mixture of these two dyes solution was always 3 ml in the cuvette. The different amount of each dye solution of Red and Blue used in the experiment to fill the 3 ml cuvette are listed below in Table 3.2.

Table 3.2 : Amount of each dye solution in the mixed solution

Remazol Brilliant Blue R (ml)	Acid Red4 (ml)	Mixed Red and Blue solution (ml)
0.25	2.75	3
0.50	2.50	3
0.75	2.25	3
1.0	2.0	3
1.25	1.75	3
1.50	1.50	3
1.75	1.25	3
2.0	1.0	3
2.25	0.75	3
2.50	0.50	3
2.75	0.25	3

A blank solution was used as reference, which contained no dye compounds but contained all auxiliary chemicals, in order to measure the absorbance of dyes in the solution. It is worth mentioning that, distilled water or only pure solvent could not be used here as reference solution. Because all dye solution used in this experiment contained some auxiliary chemicals (section 5.3.1).

Data analysis

At lower concentration, the absorbance is directly proportional to the concentration of the light absorbing species in the sample. By following the Beer-Lambert law (Beer's law in brief), it is possible to calculate the concentration of any species from their absorbance property. Beer's law can be expressed as shown in Eq. (3.1).

$$A = \epsilon \, b \, c \qquad (3.1)$$

Where,
A = Absorbance (Absorbance was measured by spectrophotometer applied in this thesis).
ϵ = Molar absorptivity constant (L/cm. mg)
b = Path length or cuvette width (cm)
c = Concentration (mg/L) in this case

The molar absorptivity is the characteristics of a substance that tells how much light is absorbed at a particular wavelength.

Calculation of molar absorptivity, ϵ:

Every species in solution show their maximum absorbance or absorptivity at a specific wavelength. By knowing the maximum absorbance value at highest peak, the molar absorptivity, ϵ can be calculated for both of the dyes by using Beer's law. The concentrations of both dye solutions were known. From the Fig.3.14, it is found that at 505 nm wavelength of Red shows highest peak and the absorbance value at that peak is 2.1. So, by using Eq. (3.1) the absorptivity of the red dye solution can be calculated.

When there is more than one absorbing species in a solution, the spectrophotometer sees the sum of the absorbance from all species. A spectrophotometer cannot distinguish the individual absorbance which arises from different molecules. However, if the different species have different absorptivities at different wavelengths and if the spectra of the pure components are known, it is possible to mathematically disassemble the spectrum of the mixture into those of its components (Harries, 2000).

Individual dye concentration in mixed solution:

The most important fact that permits to analyze mixtures is that at each wavelength the absorbance of a solution containing dye Remazol Brilliant Blue R (denoted as Blue in this case) and dye Acid Red 4 (denoted as Red in this case) is the sum of the absorbances of each dye as shown by Eq. (3.2).

$$A = \epsilon_R \, \mathrm{b} \, [\mathrm{Red}] + \epsilon_R \, \mathrm{b} \, [\mathrm{Blue}] \qquad (3.2)$$

It is considered that the individual spectra of these components do not overlap very much. The blue dye has maximum absorbance at wavelength 595 nm and the maximum absorbance of red dye falls at wavelength of 505 nm. The absorbance at any wavelength is the sum of absorbances of each component at

that wavelength. For the absorbance at wavelength 595 nm (λ_1) and 505 nm (λ_2), it can be written as

$$A_B = \epsilon_{R_1} \text{ b [Red]} + \epsilon_{B_1} \text{b [Blue]} \quad (3.3)$$

$$A_R = \epsilon_{R_2} \text{b [Red]} + \epsilon_{B_2} \text{b [Blue]} \quad (3.4)$$

Where the ε values apply to each species at each wavelength. The absorptivities of the two dyes at each wavelength were measured in separate experiments. By solving Eq. (3.3) and Eq. (3.4), the following two equations can be written for calculating the two unknowns [Blue] and [Red].

$$[\text{Blue}] = \frac{\begin{vmatrix} A_{\text{Blue}} & \epsilon_{\text{Red1}}\, b \\ A_{\text{Red}} & \epsilon_{\text{Red2}}\, b \end{vmatrix}}{\begin{vmatrix} \epsilon_{\text{Blue1}}\, b & \epsilon_{\text{Red1}}\, b \\ \epsilon_{\text{Blue2}}\, b & \epsilon_{\text{Red2}}\, b \end{vmatrix}} \quad (3.5)$$

$$[\text{Red}] = \frac{\begin{vmatrix} \epsilon_{\text{Blue1}}\, b & A_{\text{Blue}} \\ \epsilon_{\text{Blue2}}\, b & A_{\text{Red}} \end{vmatrix}}{\begin{vmatrix} \epsilon_{\text{Blue1}}\, b & \epsilon_{\text{Red1}}\, b \\ \epsilon_{\text{Blue2}}\, b & \epsilon_{\text{Red2}}\, b \end{vmatrix}} \quad (3.6)$$

Where,

[Blue] = Concentration of blue, mg/L
[Red] = Concentration of red, mg/L
A_{Blue} = Absorbance for Remazol Brilliant Blue R,
A_{Red} = Absorbance for Acid Red 4
ε_{Red1} = Absorptivity of red at 595 nm wavelength, L/cm.mg
ε_{Red2} = Absorptivity of red at 505 nm wavelength, L/cm.mg
ε_{Blue1} = Absorptivity of blue at 595 nm wavelength, L/cm.mg
ε_{Blue2} = Absorptivity of blue at 505 nm wavelength, L/cm.mg
b = Cell length, cm

In summary, for determining dye concentrations, firstly the absorbances at wavelengths of 505 nm and 595 nm were measured followed by absorptivity calculations using Eq. (3.1). Then, the concentrations of blue and red dyes were determined using Eq. (3.5) and Eq. (3.6) respectively where absorbance values of Red and Blue played an important role and where absorbance values were measured by spectrophotometer applied. The measurement accuracy of red and blue dyes were ± 4.08% and ±1.8% respectively.

3.9.5 MBR reactor COD and reactor dyes

For analysing COD and dyes (red and blue) in the reactor, the collected sample from the MBR reactor was sonicated for 10 minutes. Then, it was filtered by microfiltration membrane (PS MF membrane 150 kDa from Microdyn-Nadir, Germany) applying vacuum pressure close to the similar TMP value applied in MBR experiment. Most of the time, the maximum volume of filtrate was around 4 ml and it was diluted to 3 times equal to 12 ml adding DI water since at least 12 ml sample was needed for COD and dye analysis. 3 ml of this volume was used for COD analysis and the rest of 9 ml was used for analysis of dye concentrations following the analysing method described above. The dilution factor might have influence in accuracy of the analyses. The accuracy of the measurements were ± 1.02%, ± 4.08% and ±1.8% for reactor COD, reactor red dye and reactor blue dye respectively.

3.9.6 MLSS

MLSS values were analysed by classical analysing process at drying temperature of 103 °C – 105 °C.
The equipment used in this case were:

- Dessicator
- Dyring oven (operating temperature 103 – 105°C)
- Analytical scale
- Graduated porcelain crucible
- Beaker

For each measurement, 40 ml sample from MBR reactor/permeate were taken in ceramic crucible. The filled ceramic crucible was stored in a drying oven for 24 h. After 24 h of drying, the crucible was taken away from the oven and kept in a dessicator at ambient temperature (20 ± 2°C) for half an hour. Subsequently, the sample was weighted and MLSS was calculated following Eq. (3.7).

$$\text{MLSS} = \left\{\left(\frac{C_1 - D_1}{40}\right) - \left(\frac{C_2 - D_2}{40}\right)\right\} * 1000\ g/L \qquad (3.7)$$

Where,
C1 = weight of ceramic crucible + dried residue of reactor sample, g
D1 = weight of empty ceramic crucible used for reactor sample, g
C2 = weight of ceramic crucible + dried residue of permeate sample, g

D2 = weight of empty ceramic crucible used for permeate sample, g

The C_v value of the analysis was ± 3.4% which might have occurred from weighing the samples by the applied analytical balance.

3.9.7 N-Balance

The N-balance consists of Total-N, NH_4-N and NO_3-N.

Total-N

At the beginning of the experiment until day 190, the Total-N analyses were conducted with cell tests (Model: 1.00613) from Merck KGaA (Germany). The measuring range of this method was 0.5 – 15 mg/L. According to the product brochure the C_v was ± 1.5% but in this experiment it was found as ± 4.24%. After day190 onward, the Total-N was determined by TOC-L CHP/CPN analyser (Shimadzu, Japan) along with TOC since it was cheaper and simpler. The accuracy of the results obtained were comparable to that of cell tests.

NH_4-N

All NH_4-N analyses were conducted with cell tests (Method: 1.14558) from Merch KGaA (Germany). The measuring range of this method was 0.2 – 8 mg/L. The product brochure indicates the C_v as ± 1.0% but it was found as ± 6.85% experimentally in this thesis which could have occurred from fluctuating NH_4-N values in the samples. The fewer number of samples (Number of samples: 5) used in this case compared to the sample numbers of product brochure (Number of samples: 39) might have also created this variation of accuracy.

NO_3-N

All NO_3-N analyses were conducted with cell tests (Method: 1.14542) from Merck KGaA (Germany). The measuring range of this method was 0.5 – 18 mg/L. The product brochure indicates C_v as ±1.5% but experimentally it was found as ± 7.9% which might have occurred from very low concentration of NO_3-N values in the samples. The fewer number of samples (Number of samples used: 5) used in this case compared to the sample numbers of product brochure (Number of samples used: 27) might have created this variation of accuracy too.

3.9.8 Dissolved Oxygen (DO)

The DO concentrations were determined with an oxygen sensor (Model: Oxi 340i meter and CellOX® 325 O_2 electrode) from WTW GmbH (Germany). The C_v of the method according to the product brochure was ± 0.5% but experimentally it was found as ± 3.2% considering 10 number of samples.

Oxygen uptake rate (OUR)

Oxgen uptake rate (OUR) was calculated as described below:

Firstly , roughly 100 ml sample from MBR reactor was taken and DO of this sample was measured. After that the sample was kept on stirring for 10 minutes in an ambient temperature without extra oxygen supply. After 10 minutes, DO of this sample was measured and OUR was calculated in mg/Lmin.

3.9.9 Drying Residue (DR)

DR values were analysed with classical analysing process at operating temperature of 103 – 105° C. The analysing procedure was similar to MLSS but sample volume and sampling location was different.
The equipment used in this case were:

- Dessicator
- Dyring oven (operating temperature 103 – 105°C)
- Analytical scale
- Graduated porcelain cruvible
- Beaker

For each measurement, 20 ml sample from feed/permeate were taken in ceramic crucible. The filled ceramic crucible was stored in a drying oven for 24 h. After 24 h of drying, the crucible was taken out of the oven and kept in a dessicator at ambient temperature (20 ± 2°C) for half an hour. Subsequently, the sample was weighted and drying residue DR was calculated following Eq. (3.8).

$$\mathrm{DR} = \left(\frac{C - D}{20}\right) * 1000\ g/L \qquad (3.8)$$

Where,
C = weight of ceramic crucible + dried residue, g

D = weight of empty ceramic crucible, g

The C_v value of the analysis was found as ± 3.0% which might have occurred due to weighing of the samples.

3.9.10 Chloride (Cl^-)

The concentrations of chloride (Cl^-) were determined by titration method (Model: 716 DMS Titrino) from Metrohm (USA). The C_v of the instrument experimentally found as 1.49% with measuring rang up to 100 mg/L of Cl^-.

3.9.11 pH and Temperature

All values of pH and temperature were measured with a pH meter (Model: pH 323 meter and Sentix® 41-3 electrode) integrated with temperature sensor from company WTW GmbH (Germany). The C_v of the method for pH and temperature according to the product brochure were ± 0.01 pH (for temperature range : -10°C – 35°C) and ± 0.1 K (for temperature range : 15°C – 35°C) respectively. Experimentally, the C_v for pH and temperature measurements were ± 0.5 pH and ±1.08% respectively.

3.9.12 Electrical Conductivity

All conductivity measurements were performed with a conductivity meter (Model: Cond 315i meter) from WTW GmbH (Germany). The measuring range of the instrument was 0.00 – 19.99 mS/cm. The C_v of the product brochure was ± 0.5% and experimentally it was found as ± 2.4%.

References

Asatekin, A., Menniti, A., Kang, S., Elimelech, M., Morgenroth, E., Mayes, A. M. (2006), Antifouling nanofiltration membranes for membrane bioreactors from self-assembling graft *copolymers.* Journal of Membrane Science 285, 81–89.

Bahadır K. Körbahti, Abdurrahman Tanyolac, Continuous electrochemical treatment of simulated industrial textile wastewater from industrial components in a tubular reactor, J. Hazard. Mater 170 (2009) 771–778.

Britannica, 2013, http://www.britannica.com/eb/article-9007791/antrhaquinone-dye, accessed on November 20, 2013

Chemical book, (2013), http://www.chemicalbook.com/ProductChemicalPropertiesCB9368635_EN.htm, accessed on 23.09.2013

Carliell, C.M., Barclay, S.J, Naidoo, N., Buckely, C.A., Mulholland, D.A, Senior, E., 1994. Anaerobic decolourisation of reactive dyes in conventional sewage treatment processes. Water S.A. 20, 341 – 345

Carliell, C.M., Barclay, S.J., Buckley, C.A., 1996. Treatment of exhausted reactive dye bath effluent using anaerobic digestion: laboratory and full scale trials. Water S.A. 22, 225 - 233

Harris , Daniel C. (2000), Quantitative Chemical Analysis, 5th ed. ISBN 0-7167-2881-8, USA

Idil Arslan Alaton, Isil Akmehmet Balcioglu, Detlef W. Bahnemann, Advanced oxidation of a reactive dyebath effluent:comparison of O_3, H_2O_2/UV-A processes, water research 36 (2002) 1143-1154.

Korejba, W. (2010), Aufbau und Inbetriebnahme eines Labor-Membranbioreaktors mit automatischer Datenerfassung und Steuerung, Master Thesis, Sensor Ssystems Technology, Karlsruhe University of Applied Sciences, Germany

Microdyn – Nadir, 2013, http://www.microdyn-nadir.com/en/Products/BIOCEL%C2%AE/, accessed on November 22, 2013

Mustafa Isik, Delia Teresa Sponza, (2008), Anaerobic/ aerobic treatment of a simulated textile wastewater, separation and purification technology 60, 64-72.

Nanotech (2013), http://www.creating-nanotech.com/en/product.php?p_sn=24, acceesed on 26.09.2013

Nystrom, M., Ruohomaki, K., Kaipia, L. (1996), Humic acid as a fouling agent in filtration, *Desalination*, 106, 79-87

Palacios, S. (2009), Decolourization of azo and anthraquinone dyes by mean of microorganisms growing on wood chips, thesis, school of technology and design, department of bioenergy, Vaxjo, University, Sweden

PMI, porous materials, Inc, USA, http://www.pmiapp.com/contact/index.html, accessed on 18.06.2013

Seesuriyachan, P., Takenaka, S., Kuntiya, A., Klayraung, S., Murakami, S., Aoki, K. (2007), Metabolism of azo dyes by lactobacillus casei TISTR 1500 and effecs of various factors on decolorization, water research, 41 (2007), 985 - 992

Shimadzu, 2013, http://www.shimadzu.com/an/toc/lab/toc-l4.html, accessed on 24.09.13

Srisurichan, S., Jiraratananon, R., Fane, A.G. (2005), Humic acid fouling in the membrane distillation process *Desalination,* 174 (2005) 63-72

Sutzkover-Gutman, I., Hasson, D., R. Semiat, (2010), Humic substances fouling in ultrafiltration processes *Desalination*, 261 (2010) 218–231

Walker, R. (1970), The metabolism of azo compounds; a review of the literature, Food Cosmet Toxicol, 8 (6) 659 -676

Wei, Y. and Zydney, A.L. (1999), Humic Acid Fouling During Microfiltration, *J. Membr. Sci.*, 157 (1999) 1-12

4. Chapter 4 : Novel Membrane Preparation and Characterisation

The ultrafiltration (UF) PES membrane is widely applied in the field of food, beverage, dairy, biotechnology, effluent treatment and medical applications. In this thesis, the application of UF PES membrane from company Microdyn Nadir (Germany) and novel coated UF PES membrane, named as PBM membrane, in textile effluent treatment via MBR process were focused. Typically, UF PES membranes are prepared by phase-inversion process in which a homogeneous polymer solution is converted to porous polymer framework through the exchange of a solvent with a coagulant which is a strong non-solvent, resulting in the formation of a thin skin layer and a porous asymmetric substructure (Wijmans, 1985). The UF PES membrane used in this case was composed of permanently, hydrophilic polyether sulfone (PES) supported by polyethylene terephthalate (PET) with a pore size of about 0.04 µm (150 kDa) in active side of the membrane.

As it is reported in different literatures, many researchers have prepared new type/novel membrane in many ways (Section 1.2, p.2; section 2.2.3.2. p.41) to have higher performance in different applications compared to its basis. In addition, Ruckenstein et al (1989, 1992a, 1992b, 1993, 1994, 1995) has developed new approaches for preparation of hydrophobic-hydrophilic composite membranes via concentrated emulsion-polymerisation.

The novel membranes in this thesis were prepared by making a novel coating on top of UF PES membrane applying the process of polymerisable bicontinuous microemulsion (PBM), a protocol developed by ITM-CNR, Italy (Figoli, 2001). The preparation process consists of monomer, co-surfactant, water and surfactant followed by cross-linker and redox initiator. The target of this new approach was to prepare a novel coated membrane with increased hydrophilicity and lower fouling propensity. The classical characterisations of the prepared membranes were performed following the modern techniques (SEM, AFM, contact angle measurement etc.). In this thesis work, commercial UF PES membrane and novel coated UF PES membrane have been referred as PES membrane and PBM membrane respectively.

4.1 Preparation of novel membrane

The membrane preparation was performed through polymerisable bicontinuous microemulsion and it was polymerised with redox initiator in a N_2 saturated temperature controlled casting chamber.

4.1.1 Microemulsions

A microemulsion is a thermodynamically stable dispersion consisting of two immiscible liquids (generally oil and water) stabilized by a surfactant. For the formation of a microemulsion generally a co-surfactant, usually represented by an alcohol of an intermediate chain length e.g. hexanol, is required (Figoli, 2001). The co-surfactant along with a surfactant reduces the interfacial tension significantly. The microemulsions form spontaneously, optically transparent, thermodynamically stable and have smaller droplet size and lower interfacial energy.

There are three types of microemulsions, namely oil-in water microemulsion (O/W), water-in oil (W/O) and bicontinuous microemulsion. The former two types of microemulsions possess droplet-like microstructures, while the latter consists of bicontinuous structures. The numerous numbers of microstructures in each type can be used as micro-reactors for polymerization to obtain ultrafine latex particles or bicontinuous polymeric materials (Gan et al. 1997).

Over the past decades, much research has been devoted to microemulsions as reaction media (Kumar and Mittal, 1999; Holmberg, 2003) and their industrial applications are steadily increasing (The microemulsion book, 1999 and Mialocq, 1987), e.g. polymerization (Gupta, 1992; Candau, 1992), enzymatic (Holmberg, 1994) and oxidation (Minero, 1988; Aubry, 1997). The microstructures of W/O and O/W microemulsions have been widely studied and they have been successfully used for preparing nanoparticles of polymers as well as inorganic compounds by polymerizing the microemulsions (Candau, 1992; Kandori, 1988; Chew et al. 1990, Arriagada and Osseo-Asre, 1995). Bicontinuous microemulsion generates a network of interconnected channels of water and oil (MMA in this case) stabilized with surfactant and facilitated with co-surfactant. After polymerisation the oil phase provides the property of a membrane structure and the water phase defines the pore of the membrane. The pores might be derived from the interconnected water-filled spaces (modified from Gan et al. 1997). By changing the core compositions (%) of bicontinuous microemulsion, the membrane structure can be adjusted.

4.1.2 Phase diagram

Based upon the compositions, various types of microemulsions can be formed and to find the optimal microemulsion composition range, the microemulsion can be investigated in terms of phase diagram (Mehta and Kaur, 2011) as shown in Fig.4.1.

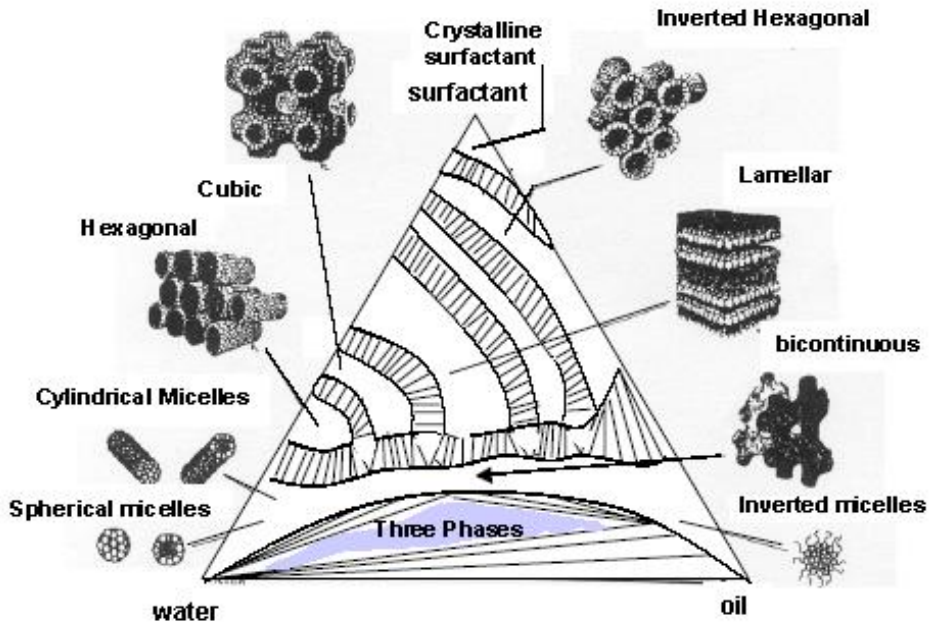

Fig. 4.1 : Schematic Gibbs triangle displaying self-assembled structures forming in microemulsions stabilised by a strong amphiphile close to its balanced state (Daoud and Williams, 1995)

The phase diagrams are helpful in various ways, like knowing the extent of solubilisation, presence of multiphase etc., corresponding to any particular composition chosen. The microemulsion region is usually characterized by constructing ternary-phase diagrams. Three components are the basic requirements to form a microemulsion: an oil phase, an aqueous phase and a surfactant. If a co-surfactant is used, it may sometimes be represented at a fixed ratio to surfactant as a single component, and treated as a single "pseudo-component". The relative amounts of these three components can be represented in a ternary phase diagram. Gibbs phase diagrams can be used to show the influence of changes in the volume fractions of the different phases on the phase behaviour of the system. The three components composing the system are each found at an apex of the triangle, where their corresponding volume

fraction is 100%. Moving away from that corner reduces the volume fraction of that specific component and increases the volume fraction of one or both of the two other components. Each point within the triangle represents a possible composition of a mixture of the three components of pseudo-components, which may consist (ideally, according to the Gibbs' phase rule) of one, two or three phases. These points combine to form regions with boundaries between them, which represent the "phase behaviour" of the system at constant temperature and pressure (Malik et al., 2012).

4.1.3 Membrane preparation protocol

The polymerisable bicontinuous microemulsion is a microemulsion of a thermodynamically stable, interconnected channels of oil phase and aqueous phase. The chemicals used for preparing polymerisable bicontinuous microemulsion (PBM) are shown in Fig. 4.2.

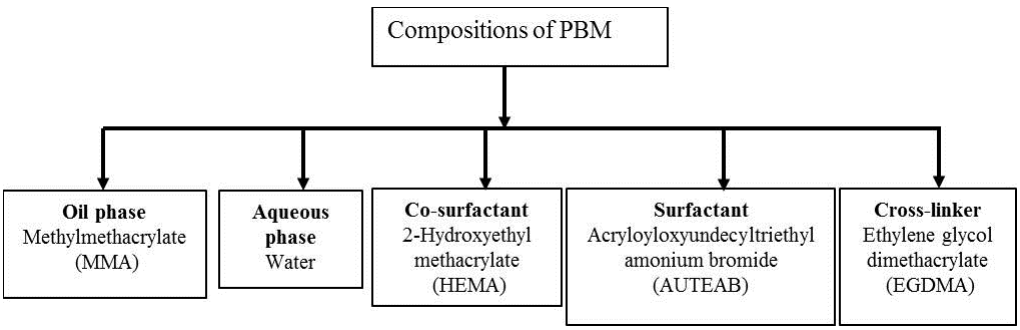

Fig 4.2 : Chemicals used for preparing PBM membrane

The function of the chemicals used for microemulsion preparation are described briefly in the following sections:

Methyl methacrylate (MMA)

The molecular formula and molecular weight (MW) of MMA are $C_5H_8O_2$ (Fig. 4.3) and 100.12 g/mol respectively.

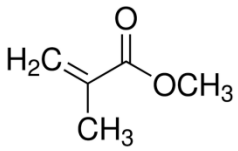

Fig. 4.3 : Structure of MMA (Sigma Aldrich, 2013)

Methyl methacrylate (MMA) was used as monomer constituting the oil phase of the microemulsion.

2-Hydroxylethyl methacrylate (HEMA)

The molecular formula and molecular weight (MW) of HEMA are $C_6H_{10}O_3$ (Fig. 4.4) and 130.14 g/mol respectively.

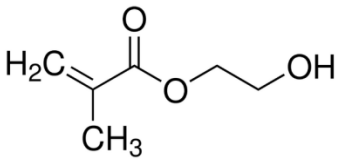

Fig. 4.4 : Structure of HEMA (Sigma Aldrich, 2013)

According to Leung and Shah (1987), it has been found that short chain alcohols can be added to the microemulsions so as to lower the rigidity of the interfacial film. In this study, HEMA which possesses the same characteristics as these alcohols was incorporated into the system to serve the same purpose. By addition of HEMA, the interpenetration between the surface films of two adjacent droplets can be increased, thus increasing the coalescence rates, which might favour the formation of bicontinuous microemulsions (Abillon, et al. 1988). Furthermore, 2-Hydroxylethyl methacrylate (HEMA) used as co-surfactant contributing to tailor the pore size.

Water

Water was used as the aqueous phase of the microemulsion. At lower content the microemulsion consists of very small water droplets dispersed in oil (W/O), while at higher water content the situation is reversed and the system consists of oil droplets dispersed in water (O/W). Between these two phases exists an intermediate situation; the bicontinuous microemulsion (Fig. 4.1) (Adapted from Malik et al. 2013).

Cationic surfactant AUTEAB

The surfactant molecules are amphiphilic in character, i.e., they possess hydrophilic and hydrophobic regions in their molecules. They have a long hydrocarbon tail and a relatively small ionic or polar head group. Amphililes can be ionic (cationic, anionic), zwitterionic, or nonionic depending on the nature of their head groups (Malik et al. 2013). The surfactants are used to reduce the surface tension of two immiscible liquids (e.g. oil and water). For membrane preparation in this case, cationic surfactant acryloyloxyundecyltriethyl ammonium bromide (AUTEAB) (Fig. 4.5) was used as surfactants to lower the surface tension of the microemulsion facilitating the wetting of surfaces and the miscibility among different liquids.

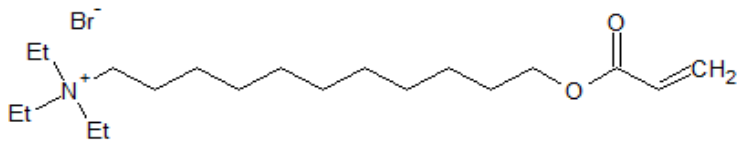

Fig. 4.5 : Structure of AUTEAB (Galiano, et al. 2012)

AUTEAB is a polymerisable surfactant. It has a double bond which can be chemically bound to the polymer chain. AUTEAB was synthesized by ITM-CNR, Italy (Galiano, 2013).

Ethylene glycol dimethacrylate (EGDMA)

The molecular formula and molecular weight (MW) of EGDMA are $C_{10}H_{14}O_4$ (Fig. 4.6) and 198.22 g/mol respectively.

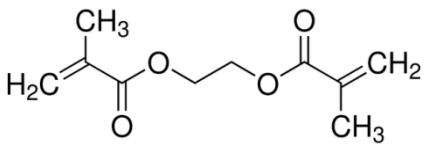

Fig. 4.6 : Structure of EGDMA (Sigma Aldrich, 2013)

Ethylene glycol dimethacrylate (EGDMA) was added as a cross-linker.

Besides these chemicals, as redox initiator, ammonium persulfate (APS)/ *N,N,N´N´*- tetramethylethylene diamine (TMEDA), was chosen because the polymerization could be carried out at relatively low temperature, so as to minimize the occurrence of phase separation as well as evaporation of monomers. In addition, this particular redox system has been found to give a rapid polymerization rate (Chieng et al. 1996).

4.1.4 Preparation of novel membrane

For novel membrane preparation a protocol was developed by ITM-CNR, Italy. The different steps of the preparation process are shown Fig. 4.7.

Microemulsion was prepared in a double necked round bottom volumetric flask by mixing monomer MMA and co-surfactant HEMA. Then water was added to the system followed by the surfactant AUTEAB. The solution was then mechanically stirred and when a clear and transparent solution was obtained, the cross-linker EGDMA was added. Once a clear microemulsion was obtained, redox initiators (Ammonium persulfate, APS: at the rate of 0.3% of used water and *N,N,N´N´*- tetramethylethylene diamine TMEDA: 1 drop per 1 g of microemulsion (where 1 drop represented 13.5 µl of TMEDA) according to the concentrations reported in literature, were added to the system.

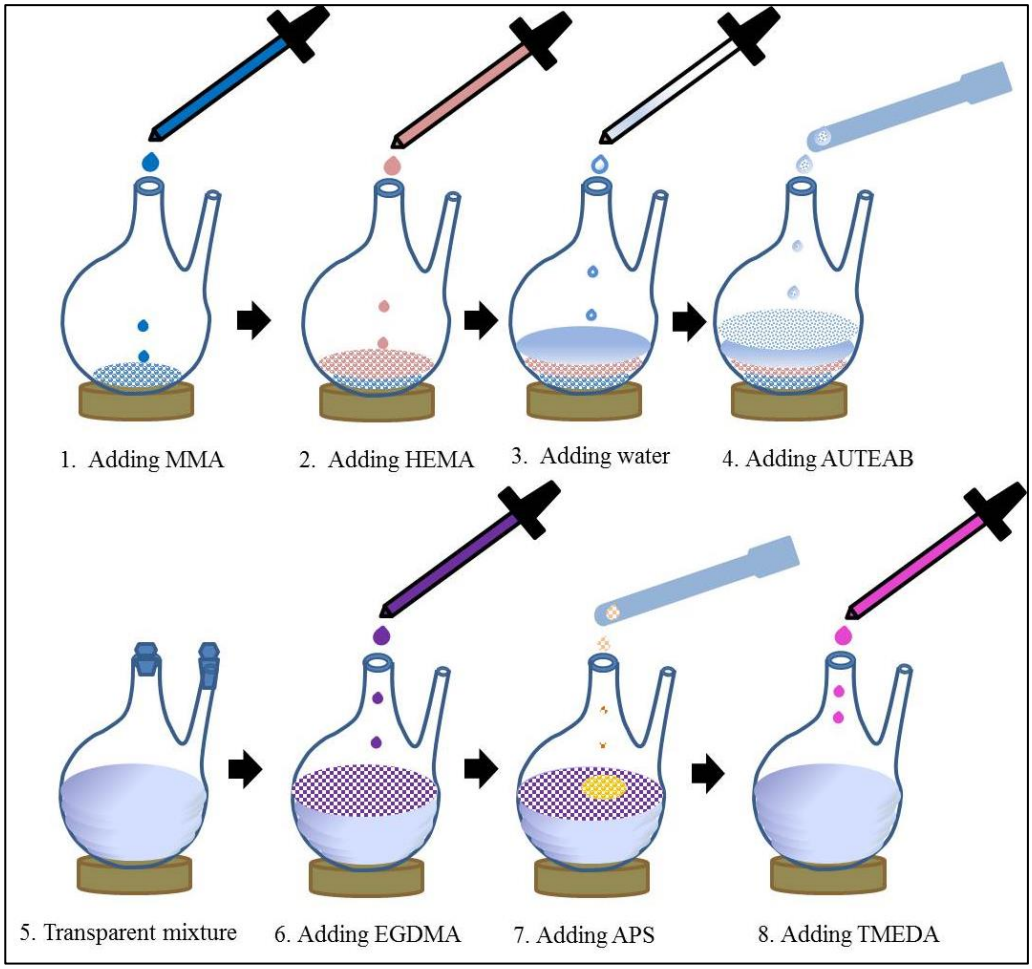

Fig 4.7 : Microemulsion preparation steps

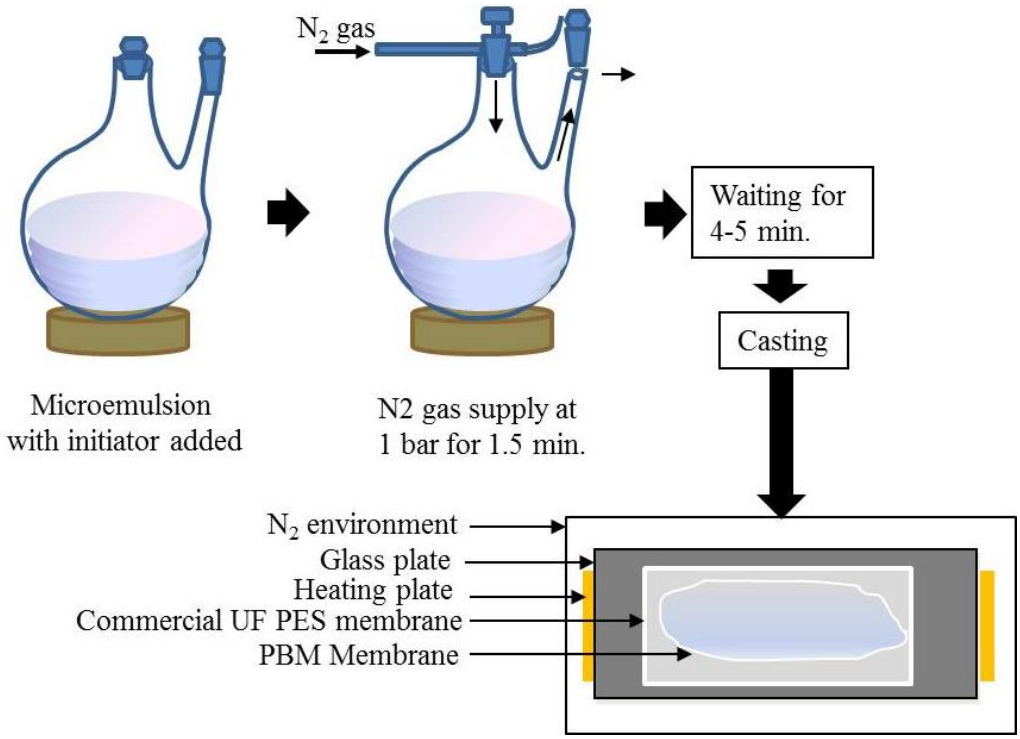

Fig 4.8 : Casting of microemulsion for PBM membrane preparation

The microemulsion was then purged with nitrogen gas at 1 bar pressure for about 1.5 minutes, at 20°C and left for 4-5 minutes as reaction time (Fig 4.8). Then the microemulsion was cast on commercially available membrane (UF PES membrane) from company Microdyn-Nadir (MN), Germany in an inert gas N_2 saturated casting chamber (Section 3.2, Fig.3.1 & Fig. 3.2). The casing knife used in this case was 250 µm. N_2 saturated environment was needed to exclude any contact with air or oxygen since they interfere the polymerisation process. The temperature of the casting chamber was also kept constant at 20 ± 1 °C during the polymerisation and over 24h. After polymerisation, the novel coating was clearly visible on membrane surface and its thickness was measured by micrometer which was in the range of 1 – 10 µm.

4.1.5 Prepared membranes at optimized conditions

Following the membrane preparation protocol several PBM coated membranes were prepared and tested. Based on the tested results, the membrane preparation process was optimised by Galiano (2013). The optimal conditions found for making the PBM membrane were as follows:

- MMA : 21wt%
- HEMA : 10 wt%
- Water : 41wt%
- AUTEAB : 26 wt%
- EGDMA : 3 wt%
- APS : 0.3% of used water
- TMEDA : 1 drop per 1 g of microemulsion (1 drop represents 13.5 µL of TMEDA)
- Temperature : 20 ± 1 °C
- N_2 gas flow : supplied at 1 bar for 1.5 minute.

These optimal conditions were conducted in preparing several numbers of membranes casting on A4 size to study reproducibility and characterisation tests. It was demonstrated that the membrane preparation process was reproducible. Then, The optimized process was used to prepare big size membrane sheets with dimensions of 30 cm×30 cm and a novel MBR module was formulated with dimensions of 25 cm × 25 cm following a lamination process as shown in Fig. 4.9 with the active support of company Microdyn-Nadir (Germany). The membrane module including 3 envelops produced in this way covered active membrane surface are of 0.33 m^2.

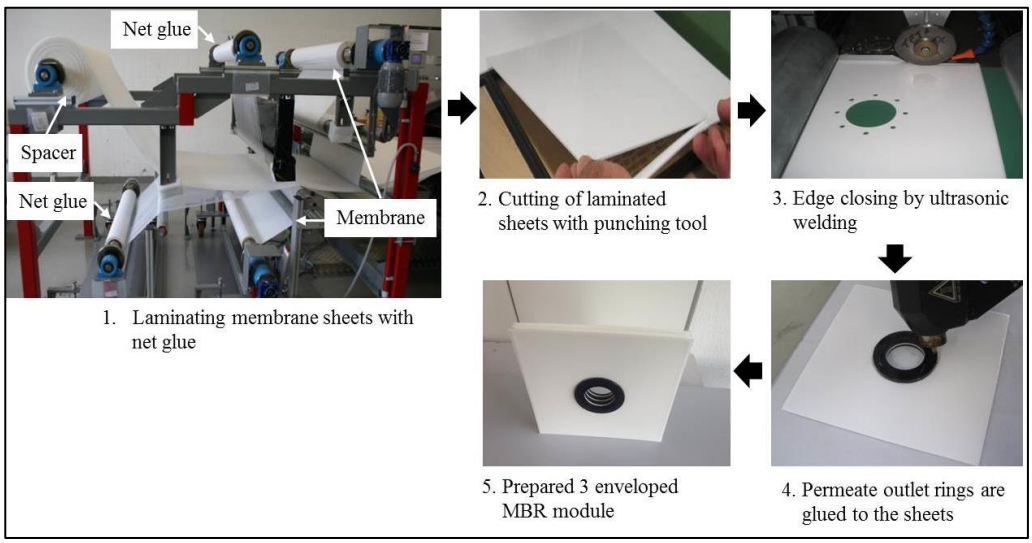

Fig 4.9 : Lamination process of MBR modules

The melting point of the net glue used in between the membrane sheets along with spacer was 135 °C. Finally, the novel MBR module was tested in a submerged MBR process for about 6 months (Chapter 6).

4.2 Characterisation of novel membrane

To define the performance of the prepared novel membranes some characterisations like surface characteristics, pore geometry, contact angle, water permeability, salt rejections, textile dye rejections and fouling behaviour were done.

4.2.1 Surface characteristics

Membrane surface characteristics were determined by scanning electron microscopy (SEM) (Model: S-4800) and surface smoothness were determined by atomic force microscopy (AFM) (Model : AFM with Nanoscope IIIa controller) (Section 3.3) by Dr. Daniel Johnson from Swansea University, UK.

SEM produces images of a sample by scanning it with a focused beam of electrons. The electrons interact with atoms in the sample, producing various signals that can be detected and that contain information about the samples surface topography and composition. The electron beam is generally scanned in a raster scan pattern, and the beam's position is combined with the detected signal to produce an image. SEM can achieve resolution better than 1 nanometer (McMullan, 2006). In AFM, the probe interacts directly with the surface, probing the repulsive and attractive forces which exist between the probe and the sample surface to produce a high resolution three dimensional topographic image of the surface (Johnson, et al., 2009).

Hundreds of SEM and AFM images were taken from different PBM coated membranes prepared at different operation conditions. The SEM and AFM images of novel membrane (denoted as PBM in this thesis) which were prepared at optimal conditions are depicted in Fig. 4.12 through Fig. 4.13. As reference, SEM and AFM images of the commercial UF PES membrane (denoted as PES in this thesis) are also presented in Fig. 4.10 through Fig. 4.11.

Fig. 4.10 a) and Fig. 4.10 b) represents the surface and cross sectional view of PES membrane respectively while Fig. 4.11 a) and Fig. 4.11 b) demonstrates the surface smoothness of UF PES membrane in 2D and 3D format respective-

ly. The dark sports of the Fig. 4.11 depict the valley of the surface while the lighter spots demonstrate the peak of the surface.

Similarly, Fig. 4.12 a) and Fig. 4.12 b) represents the surface and cross sectional view of the PBM membrane respectively while Fig. 4.13 a) and Fig. 4.13 b) depicts the surface smoothness of this membrane in 2D and 3D format. Fig. 4.12 a) shows the typical structure of PBM membrane where white trips indicate the polymerised membranes and the dark strips represent the water channel. Fig. 4.12 b) shows the PBM layer thickness in the range of 1.5 – 3 µm on top of PES membrane. Under the same data scale (50 nm) of investigation, AFM images of the PBM membrane (Fig. 4.13) seemed to be smoother than that of PES membrane (Fig. 4.11) which was expected and it was also confirmed by roughness measurements (Fig. 4.14).

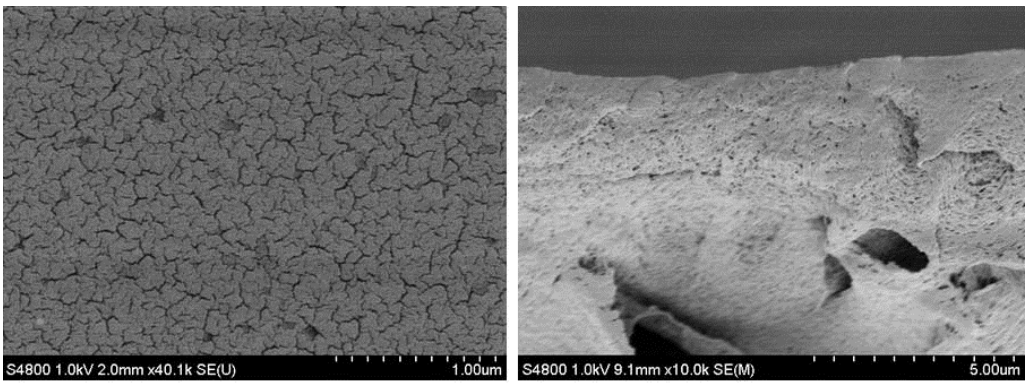

a) Surface *b) Cross section*

Fig 4.10 : SEM images of PES membrane

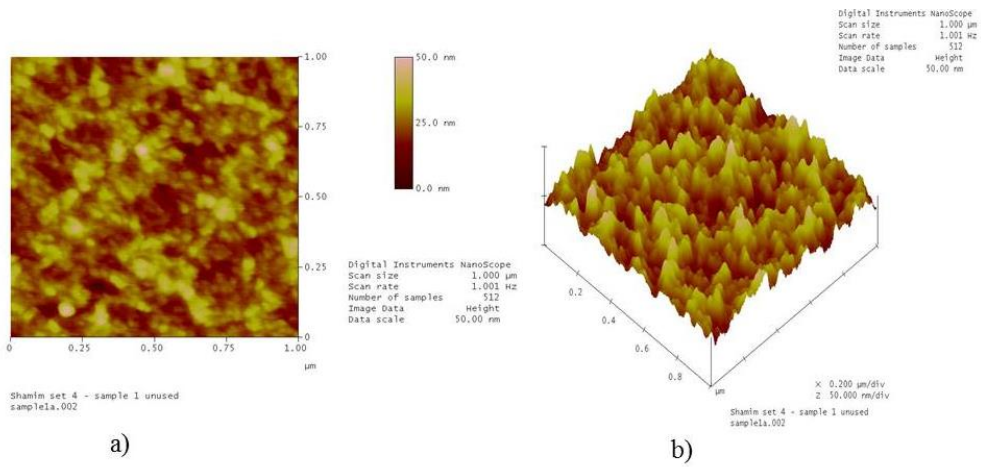

Fig. 4.11 : AFM images of PES membrane – a) 2D b) 3D

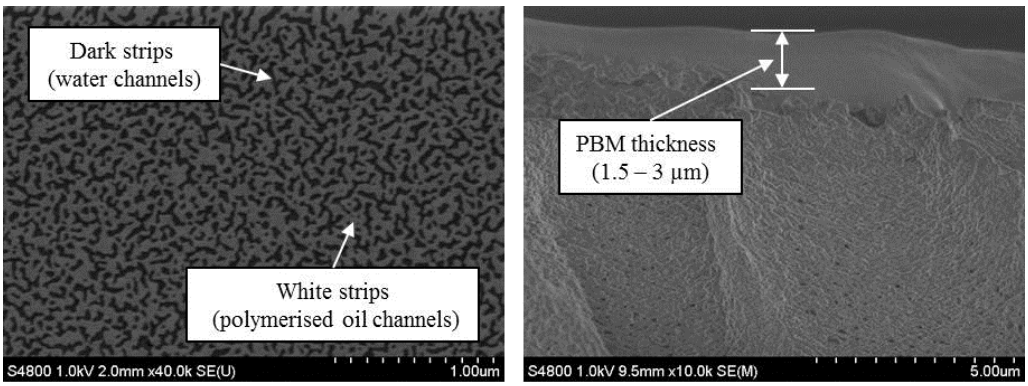

a) Surface *b) Cross section*

Fig. 12 : SEM images of PBM membrane

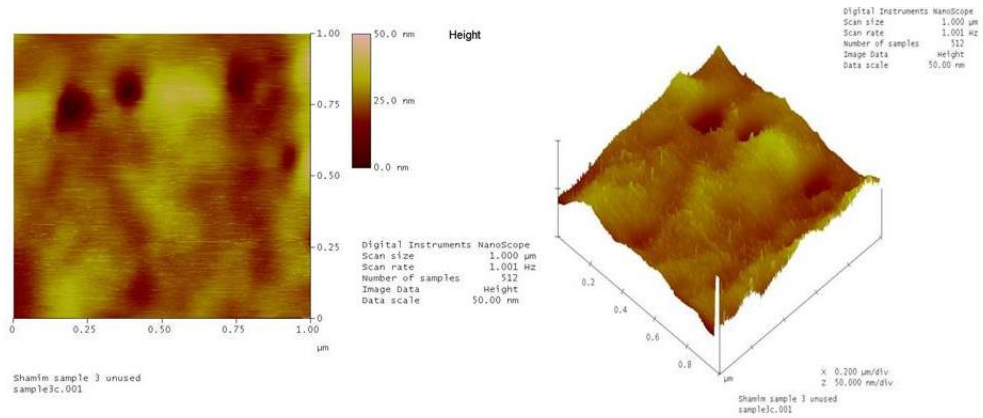

a) b)

Fig. 4.13 : AFM images of PBM membrane – a) 2D b) 3D

From Root Mean Squared (RMS) roughness values, it is also evident that PBM layer has contributed to reduced RMS values of PBM membrane significantly compared to PES membrane (Fig. 4.14).

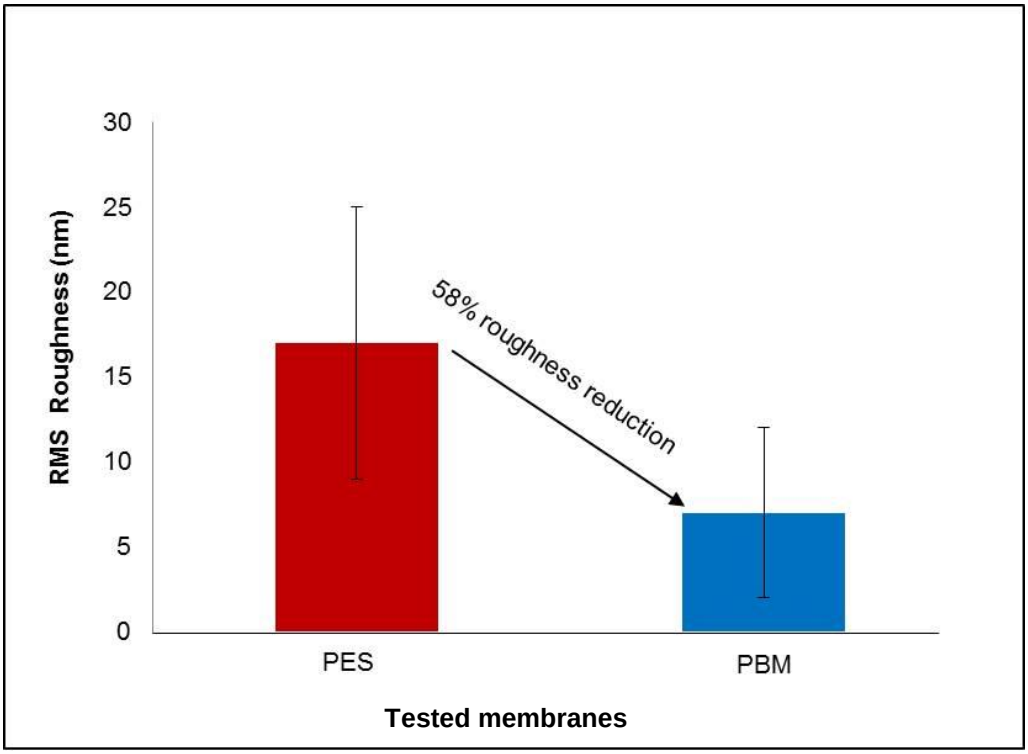

Fig. 4.14 : RMS roughness values (nm) in 5 µm scan

4.2.2 Pore geometry

The pore size distribution of both PES and PBM membranes were done by perporometry. The pore size distribution of PBM membrane reduced to 25% due to the presence of PBM coating on the top active layer of PES membrane. The pore size reduced from a value of 0.1 µm for PES membrane to 0.075 µm for PBM membrane (Fig. 4.15).

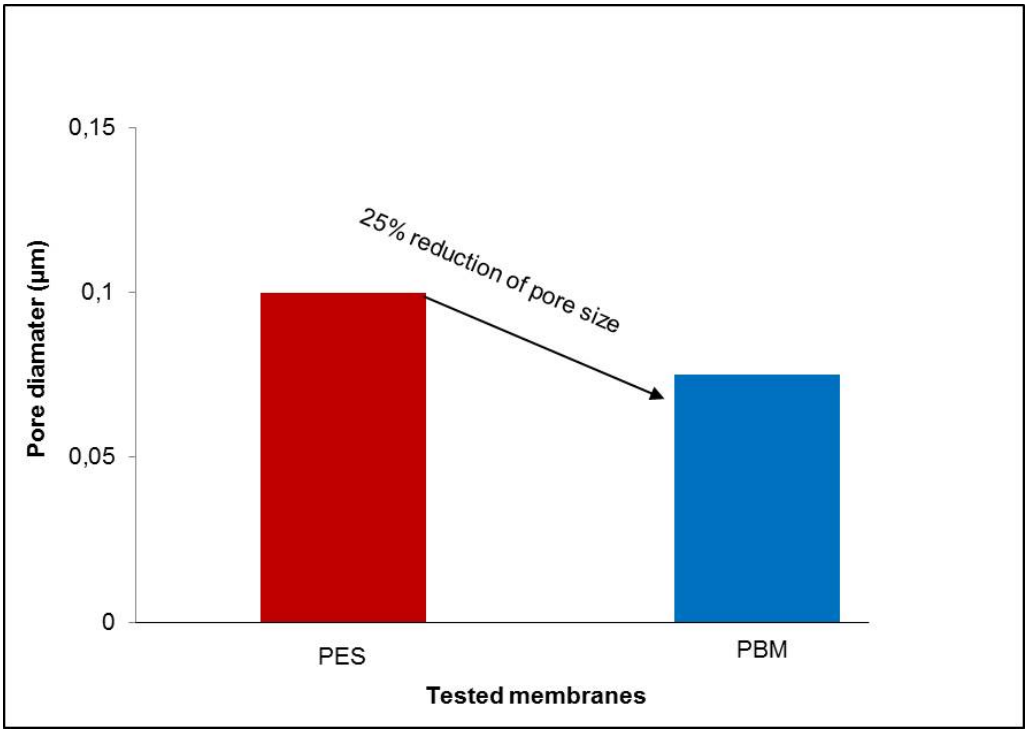

Fig. 4.15 : Pore size of PES and PBM membranes

4.2.3 Contact angle

The contact angle measurements were performed by CAM 200 optical contact angle meter (Section 3.3). From contact angle measurement experiment, it was confirmed that the PES membrane presented a contact angle of around 68° where PBM membrane showed contact angle of around 47° (Fig.4.16). This means around 31% reduction of contact angle has been achieved by PBM membrane which indicates more hydrophilicity of the PBM membrane. A higher degree of hydrophilicity could result in better performances in terms of water permeability and anti-fouling activities.

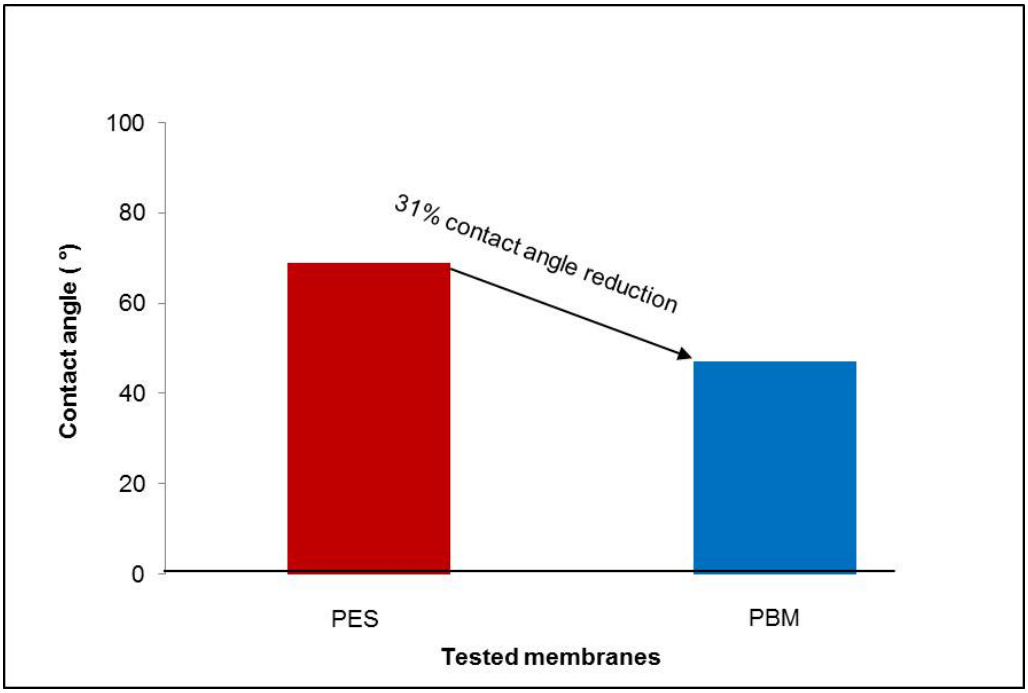

Fig. 4.16 : Contact angle of PES and PBM membrane

4.2.4 Molecular weight cut off (MWCO)

Feed solution for MWCO measurement

Molecular weight cut off (MWCO) of the membranes were measured applying gel permeable chromatography (GPC) (Section 3.3). The phosphate buffer solution of 3 litre for this experiment was prepared using NaH_2PO_4 and NaCl at concentration of 2.76 g/L and 11.68 g/L respectively. Three different types of dextran (9-11 kDa, 70 kDa and 480 kDa) at concentration of each 1.66 g/L were mixed in 2L of phosphate buffer for membrane filtration experiment. The permeates of this filtration experiment were used to analysis MWCO by GPC. The DI water used for all of the experiments was ultrapure water.

Experimental conditions of membrane filtration

The permeates used for MWCO measurements were supposed to be collected under following filtration conditions:
Required flux: < 40 $L/m^2.h$ or

Cross flow velocity: 2 or 3 m/s

The flux of the applied experiment was 42 L/m^2.h performing at 100 mbar TMP. The active membrane surface area of the applied membrane cell was 0.00125 m^2.

After collecting the permeates from the filtration experiment with PES and PBM membranes, these were delivered to GPC which included an auto sampling system. At the end of the experiment, the generated data were analysed which demonstrated the MWCO of PES and PBM membranes as 277 kDa and 99 kDa respectively (Fig. 4.17).

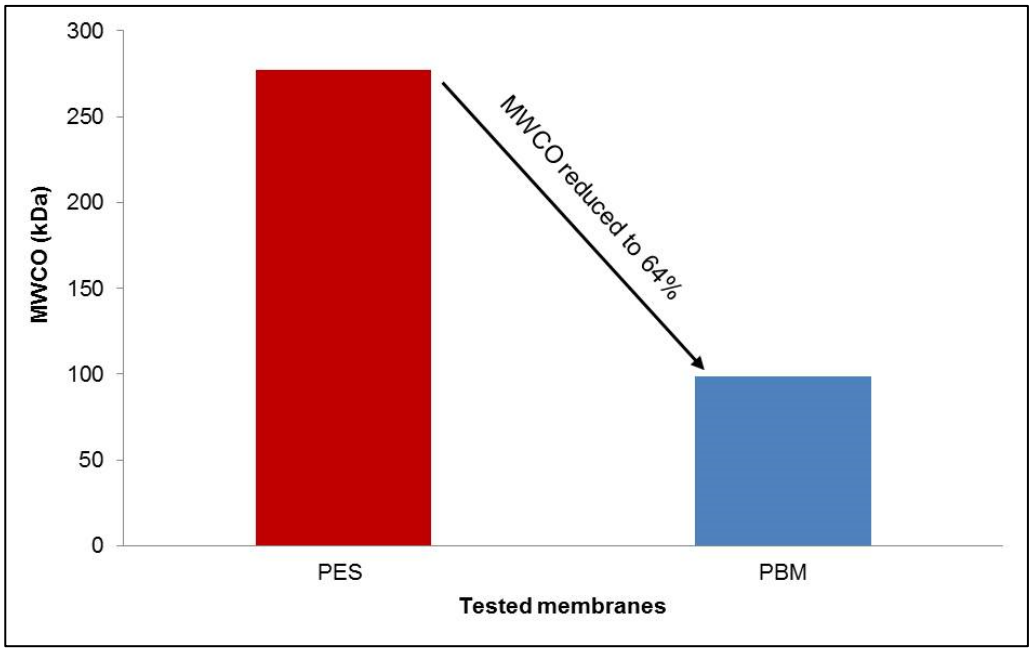

Fig. 4.17 : MWCO of PBM membrane compared to PES membrane

The results indicate that molecular weight cut off of PES membrane is very high (277 kDa) compared to its commercial value (150 kDa). The filtration experiment might have contributed to this variation. The molecular weight cut off of PBM membrane was found as 99 kDa. Considering the obtained results, PBM membrane shows 64% of MWCO reduction compared to its parents PES membrane. This shows that the MWCO of the PBM membrane reduced significantly which might contribute to higher rejection for big molecular sized compounds. Further tests for determining MWCO of both membranes need to be done.

4.2.5 Standard salt rejection test

$MgSO_4$ is widely used as model salts for standard salt rejection test of nanofiltration (NF) membranes. Since the target novel membrane (PBM) was supposed to be classified as close to NF membrane to achieve compromised water permeability and organic compounds rejections, $MgSO_4$ was chosen as model salt for standard salt rejection test. For standard salt rejection test of the novel membrane, the following standard test conditions were applied:

Applied salt: $MgSO_4$
Concentration of salt: 2,000 ppm
Temperature: 25 ± 1°C
Applied pressure (TMP): 0.5 ± 0.02 bar
Test run time: 1 h

Generally, applied pressure for standard salt rejection of NF membrane is close to 5 bar. Since the target application of the novel membrane is MBR, where the applied pressure is very low (vacuum pressure), significantly low pressure around 0.5 bar has been selected for this standard test. The model salt ($MgSO_4$) rejection by the commercial PES membrane was negligible since the entire salt passed through the membrane easily (Fig. 4.18). Because the molecular weight cut off (MWCO) of commercial PES membrane is 150 kDa and the molecular weight of used $MgSO_4$ is 120 Da (120.366 g/mol). The $MgSO_4$ salt rejection with PBM membrane is also negligible since the molecular weight cut off of the PBM membrane was found as 99 kDa (Fig. 4.17) which is much higher than the molecular weight of the used salt. Charge exclusion also may play a major role in obtaining such results.

The PBM membranes prepared only at optimum conditions were applied in different MBR experiments to have higher antifouling effect and other benefits.

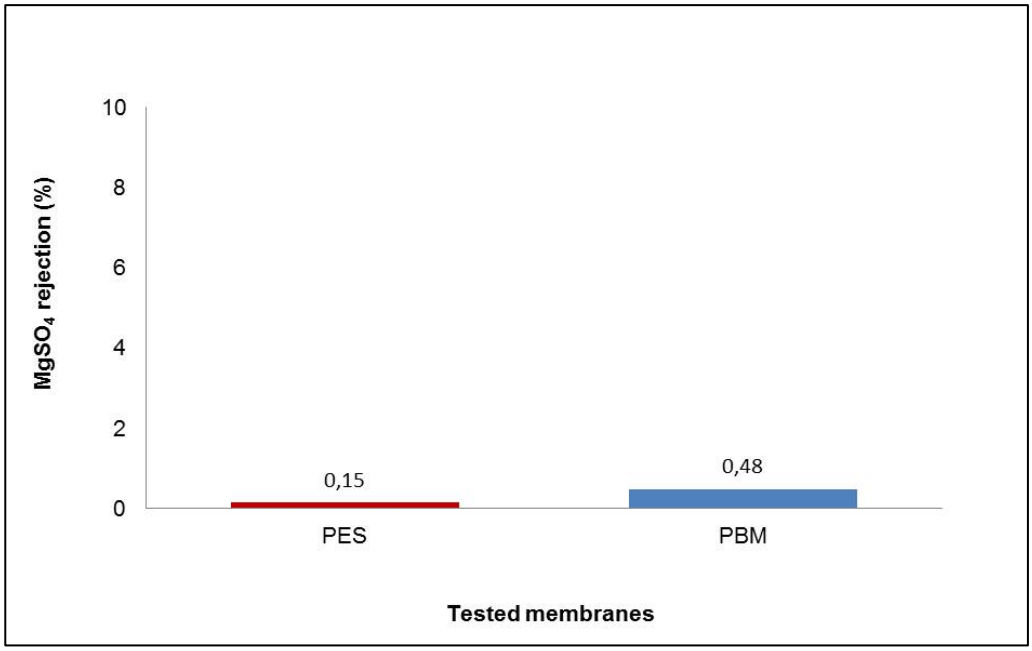

Fig. 4.18 : Standard salt ($MgSO_4$) rejection of commercial PES and PBM membranes

4.2.6 Water permeability test

Water permeability tests were carried out with PES and PBM membranes applying auto-controlled UF cross flow testing cell (Section 3.3, Fig. 3.5). Test conditions were as follows:

Test media : DI water
Conductivity : 60 µS/cm
pH : 6.5-7
Temperature : 20 ± 2°C
TMP : 0.5±0.02 bar
Operation time : 24h
Active surface area of the used membrane : 86 cm^2

The obtained results are shown in Fig. 4.19. The results show that the water permeability of PES and PBM membrane are 630 L/m^2.h.bar and 200 L/m^2.h.bar respectively. The novel coating of PBM membrane on top of PES membrane might have caused the reduction of water permeability compared to PES membrane.

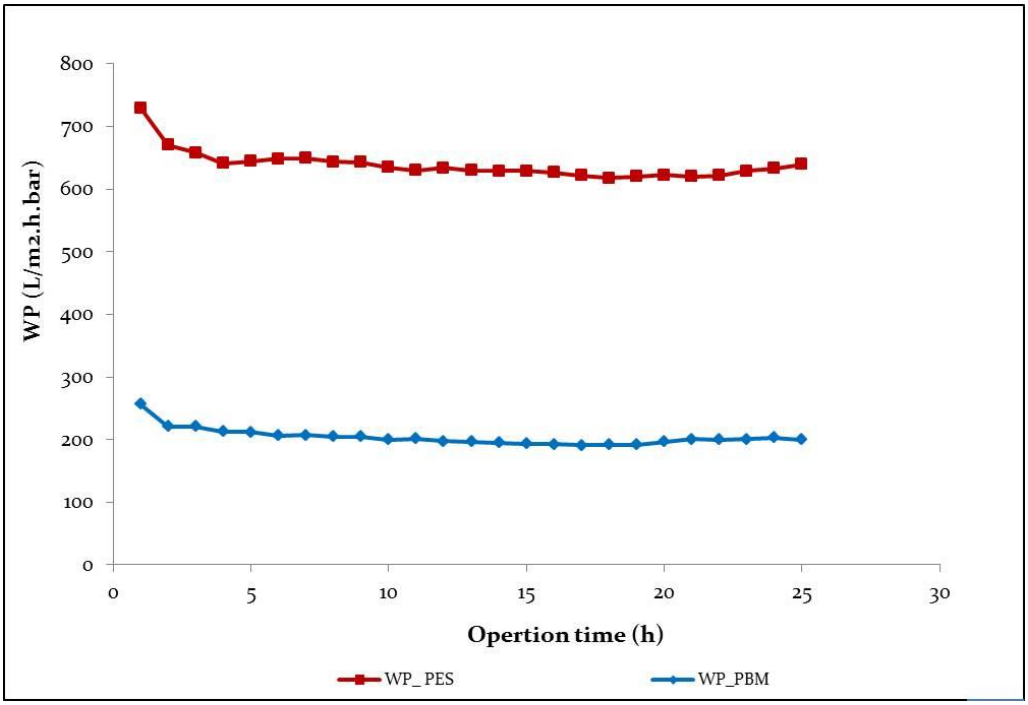

Fig. 4.19 : Water permeability of PES and PBM membranes

4.2.7 Model fouling test

4.2.7.1 Model foulant rejection

To test the fouling propensity of the membrane, humic acid (HA) was used as model foulant in this thesis work applying auto-controlled UF cross testing cell (Section 3.3, Fig. 3.5). The applied test conditions were as follows:

Test media : Humic acid dissolved in DI water
Concentration : 100 mg/L
Conductivity of feed solution : 60 µS/cm
pH : 6.5-7
Temperature : 20 ± 2°C
TMP : 0.5±0.02 bar
Operation time : 24h
Active surface area of the used membrane : 86 cm^2

The experiment performed with model foultant humic acid showed that water permeability (WP) with PES membrane reduced to 80% where the reduction of WP with PBM membrane is only 44% (Fig. 4.20). The results indicate that PES membrane is highly prone to fouling substances.

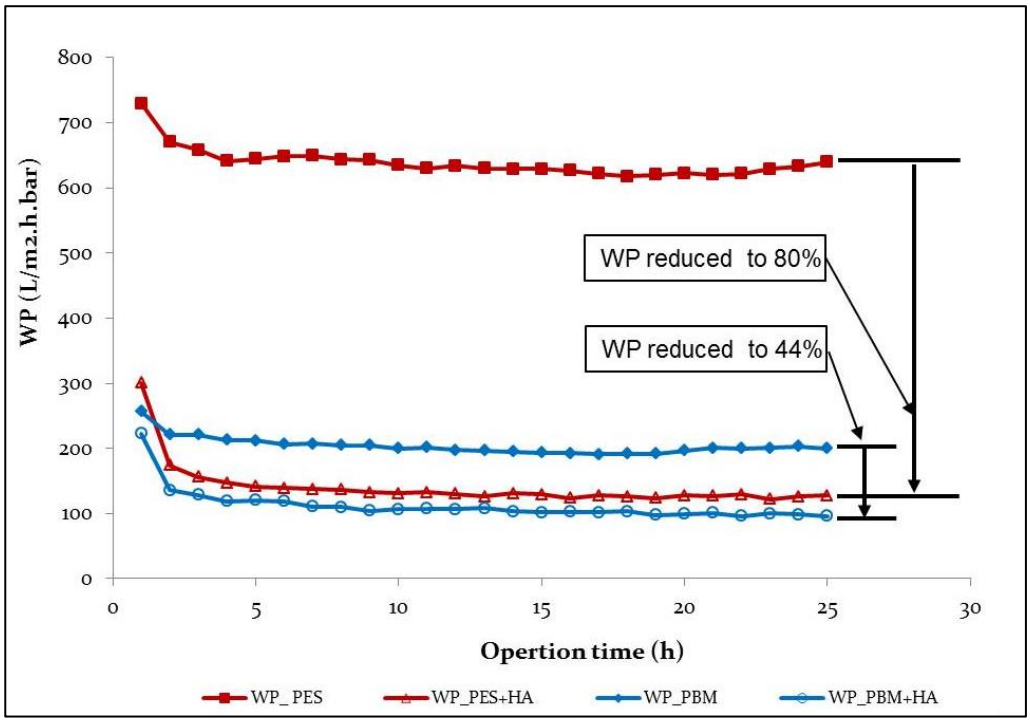

Fig. 4.20 : Water permeability reuduction with model foulant

After 24 h of the test run, samples from feed and permeate were collected and analysed by TOC analyser (Section 3.9.3) using the Eq. 4.1

$$rejection\ [\%] = \frac{C_0 - C}{C_0} \times 100 \qquad (4.1)$$

where C_0 and C are TOC values of feed and permeate, respectively.

The result demonstrates that the HA rejections by PES and PBM membranes are 90% and 95% respectively. This indicates that PBM membrane is denser than the PES membranes due to novel coating on it.

4.2.7.2 Reversible and irreversible fouling

The test carried out in section 4.2.7.1 indicates the fouling behaviour of the membranes besides model foulant rejections. Fig 4.21 indicates that the WP of PES membrane is around 630 L/m^2.h.bar with DI water but this value reduces to around 130 L/m^2.h.bar after treating with humic acid for 24h. This demonstrates that high WP reduction with PES membrane has been obtained.

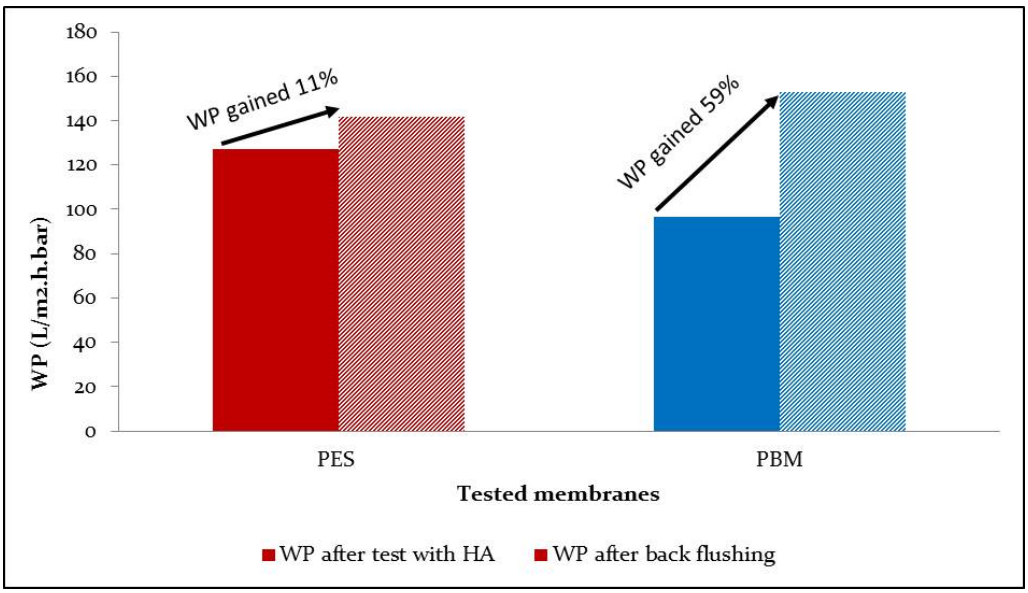

Fig. 4.21 : Fouling behaviour of PES and PBM membranes

Comparing these results with the PBM membrane, it was noticed that WP reduction with humic acid was 44% only (reduced to 112 L/m^2.h.bar from 203 L/m^2.h.bar in average). After 24 h of the test, the HA was replaced by DI water as test media and it was running for 3 h replacing fresh DI water in each hour and the WP regain was calculated using the following Eq. (4.2)

$$WP\ gained = \frac{WPf - WPi}{WPi} \times 100 \qquad (2)$$

Where,
WP_f = Final water permeability after 3rd cleanings with DI water
WP_i = Initial water permeability after 24h test run with HA

WP gained after 3rd cleaning with PBM membrane was 59% where PES membrane had only 11%. Hence WP gain indicates the fouling reversibility mean-

ing removing HA with DI water from its surface. If it is assumed that 80% WP loss of PES membrane is caused by total fouling (reversible and irreversible), the contribution of reversible fouling is only 11% and the rest (69%) represents to irreversible category. Considering the similar hypothesis, PBM membrane encounters with almost 60% reversible fouling because of its high gain of WP after 3rd cleanings with DI water where the rest (40%) falls into irreversible catagory. This is the indication of high antifouling effect of the PBM membrane. The physical appearance for both of the membranes after 3rd cleanings also indicates the different affinity of model foulant to the membrane surfaces (Fig. 4.22).

Fig. 4.22, indicates that HA has less affinity to PBM membrane compared to PES membrane. The higher smoothness of the membrane surface (Fig. 4.13 and Fig. 4.14) and higher hydrophilicity (Section 4.2.3) might have caused this profound characteristic of the PBM membrane. This argument was also validated by investigation of SEM and AFM images as shown in Fig. 4.23 and Fig. 4.24. Fig. 4.23 and Fig. 4.24 show that the model foulant layer thickness on PBM membrane is around 25% and 15% lower than that of PES membrane respectively though the measurements were done at various area of the same membrane.

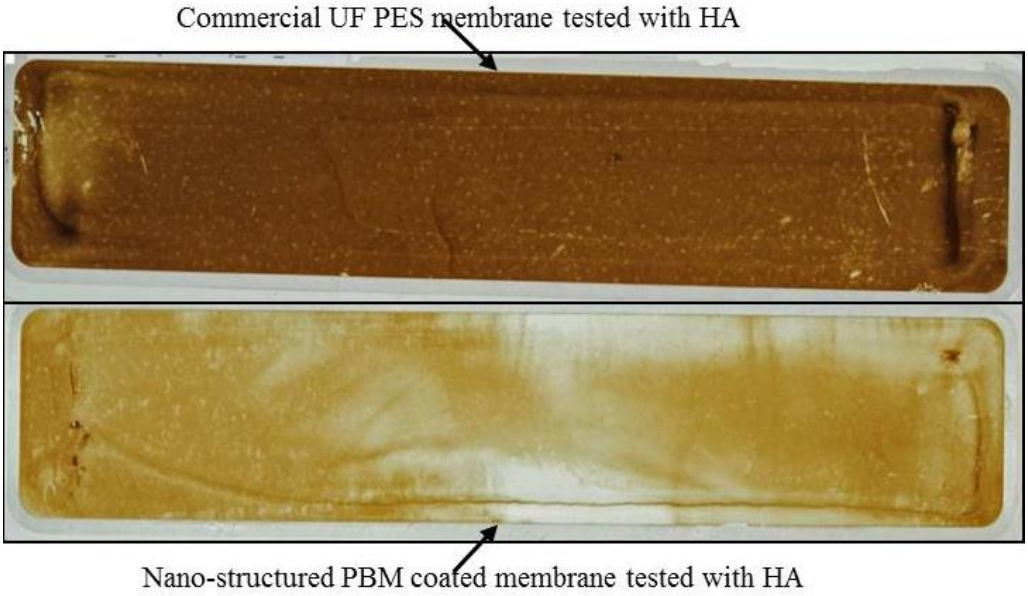

Fig. 4.22 : Affinity of HA to membrane surfaces

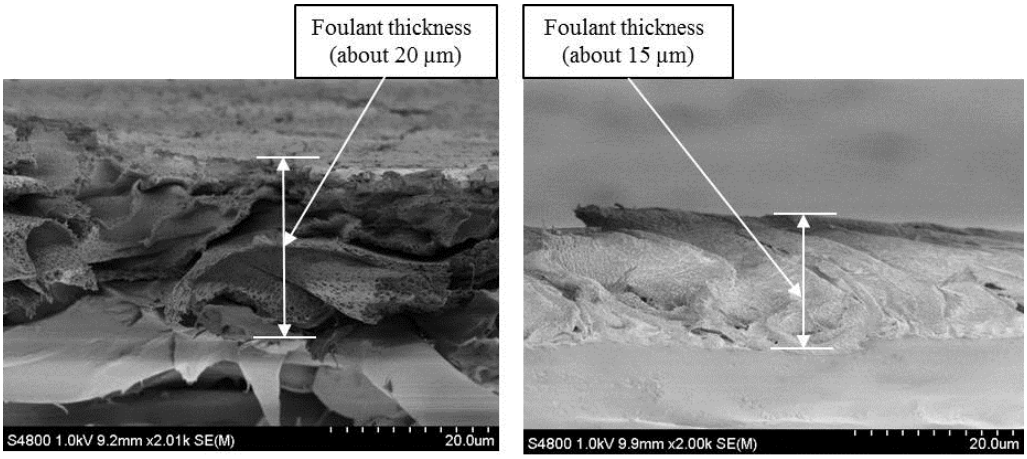

a) Fouled PES membrane *b) Fouled PBM membrane*

Fig. 4.23 : Cross-section of the fouled membranes with model foulant humic acid

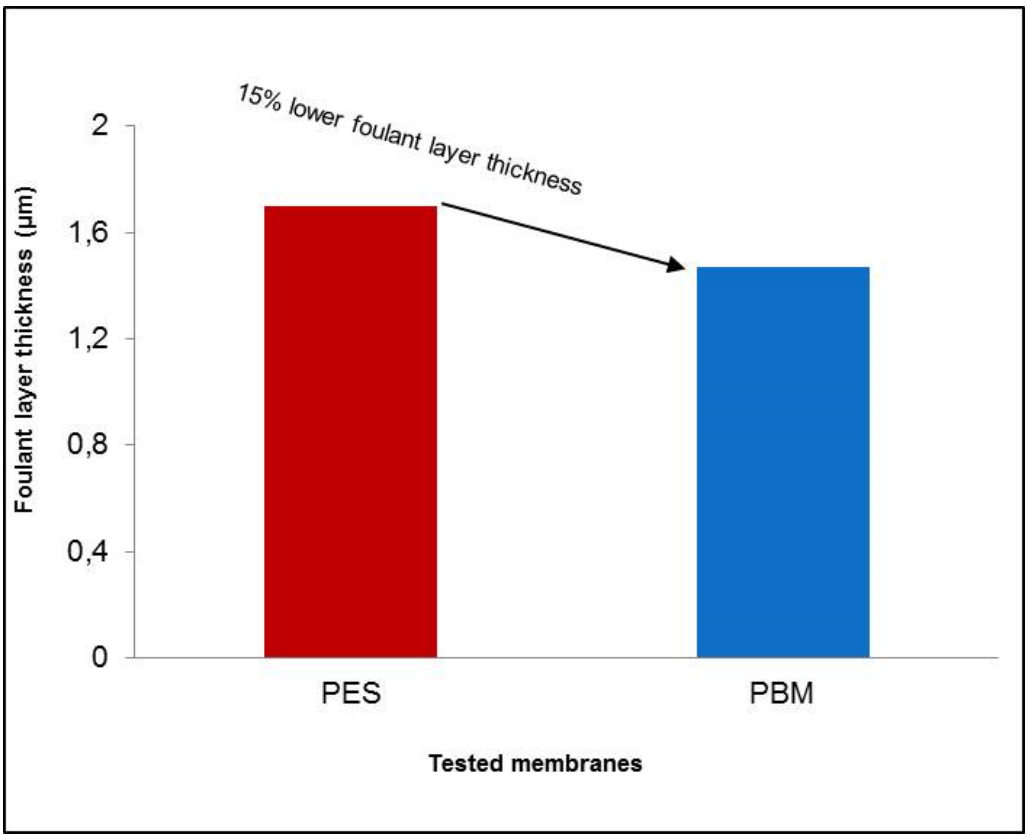

Fig. 4.24 : HA layer thickness on the fouled membranes

4.2.8 Model textile dye rejection test

To perform model textile dye rejection test, model textile dye wastewater (MTDW) including two reactive dyes, Remazol Brilliant Blue R (referred as Blue in this case) and Acid Red 4 (referred as Red in this case), was developed based on literature study (Section 5.3.1). The experiment was carried out with PES and PBM membranes applying a manually controlled UF cross- flow testing cell (Section 3.3, Fig. 3.3). Test conditions were as follows:

Test media : MTDW
pH : 7.5 ± 0.5
Temperature : 22 ± 2°C
TMP : 3.0±0.50 bar
CFV : 1 L/min.
Operation time : 1 h
Active surface area of the applied membrane: 80 cm^2

Compared to the PES membrane, the PBM membrane shows bit higher Blue rejection but the Red rejection remains the same. The Blue and Red rejections of PBM membrane are 52% and 25% respectively where PES membrane shows 45% Blue rejection. This indicates that the Blue rejection by PBM membrane is 7% points higher than the commercial PES membrane but the rejection of Red remains the same like commercial one (Fig. 4.25).

This is also the indication that the pore size of the PBM membrane has been reduced but not enough to reject the materials with low molecular weight cut off like Red (MWCO of Acid Red4:380 KDa).

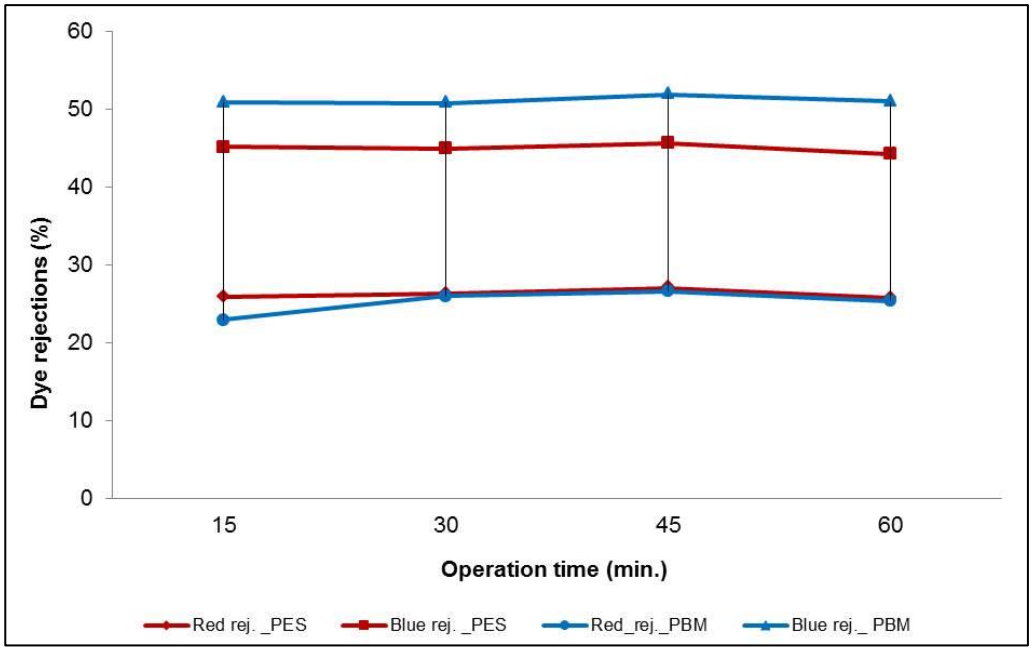

Fig. 4.25 : Textile dye rejections by PES and PBM membranes

4.2.9 Antimicrobial test

PBM membrane shows high antimicrobial properties. Antimicrobial test of the PBM membrane was done by Prof. Sacide Alsoy Altinkaya from Izmir Institute of Technology (IZTECH), Turkey. For antibacterial activity tests, 60 CFU *E.coli* were seeded on the membranes and these membranes were imprinted on Mueller-Hinton agar plates for 24h incubation at 37 $^{\circ}$C. After the 24 h incubation period had elapsed, number of CFU present on membrane surfaces was counted.

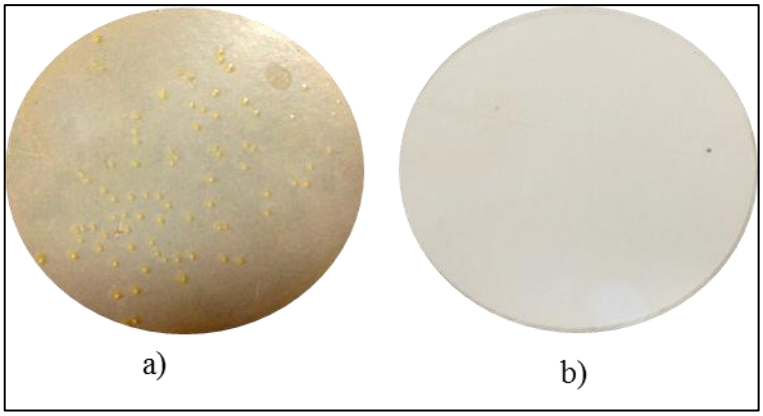

Fig. 4.26 : a) PES membrane showing no antibacterial activity;
b) PBM membrane showing high antimicrobial activity

After the test, the following results were obtained:

- Average number of CFU growth on the surface of commercial UF PES membane was 77
- No bacterial growth was observed on the surface of nano-structured PBM membrane (Fig. 4.26)

4.2.10 Lamination of PBM membranes for MBR applications

The ultimate target of the PBM membranes in this thesis was to be applied for MBR experiments (Chapter 6). According to the requirements of the MBR experimental set up, the PBM membranes was needed to transfer into a MBR module (Section 5.1). The MBR module was prepared through a lamination process at 135°C for 5 minutes supported by MBR module supplier company Microdyn Nadir (Fig. 4.9). After the lamination process the water permeability of the laminated PBM membranes slightly increased compared to non-laminated PBM membranes. After investigation of SEM cross sectional images of laminated PBM membrane, it was noticed that the PBM layer seemed to be bit reduced (Fig. 4.28 b). This effect might have contributed to increased water permeability since reduced thickness might have lower resistance to water permeability. Similarly, the SEM surface images showed that the dark strips (water channels) of the laminated PBM membrane still exist but it became lighter (Fig. 4.27 b).

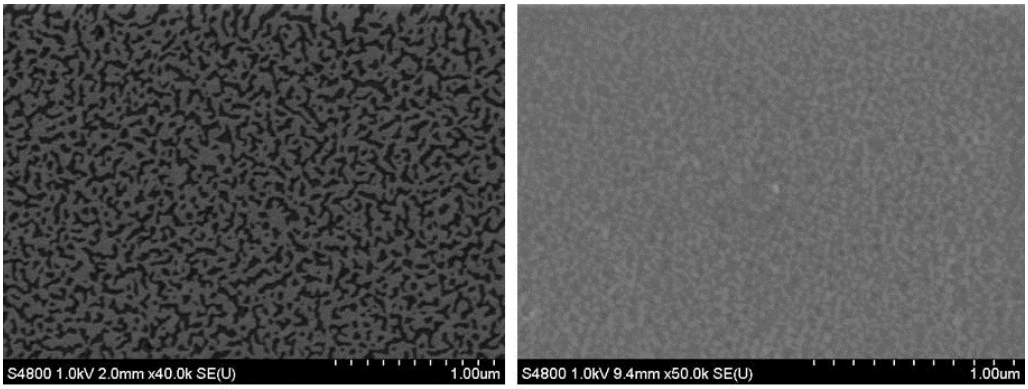

a) Before lamination *b) After lamination*

Fig. 4.27 : SEM images (surface) of lamination effects

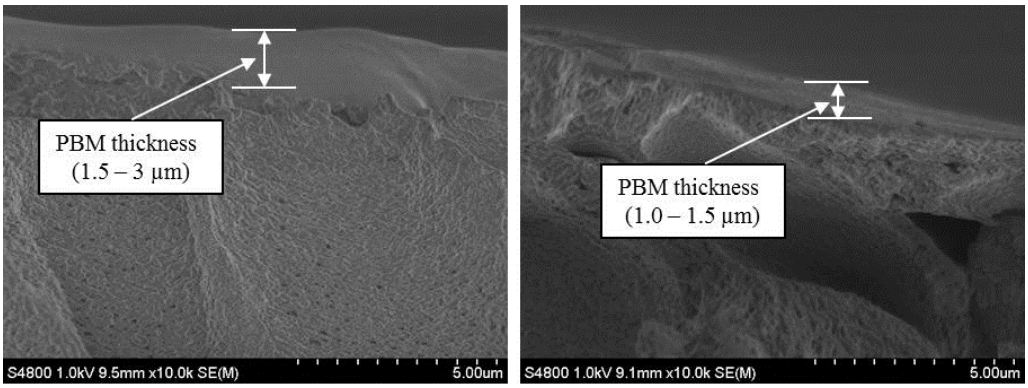

a) Before lamination *b) After lamination*

Fig. 4.28 : SEM images (cross section) of lamination effects

This investigation summarises that the PBM coating is very stable even at high temperature (135°C) and it can be applied in harsh environment like MBR experiments.

References

Abillon, O., Bink, B.P., Otero, C., Langevin, D. and Ober, R. (1988), J. Phys. Chem., 92, 4411

Arriagada, F.J., Osseo-Asare, K. (1995), Synthesis of Nanosize Silica in Aerosol OT Reverse Microemulsions, J. Colloid Interface Sci., 170, 8- 17

Aubry, J.M., Bouttemy, S. (1997), J. Am. Chem. Soc. 119, 5286

Candau, F. (1992), In Polymerization in Organic Media; Paleos, C.M., Gordon & Breach: Philadelphia, 215 - 282

Chew, C.H., Gan, L.M., and Shah, D.O. (1990), The Effect of Alkanes on the Formation of Ultrafine Silver Bromide Particles in Ionic W/O Microemulsions, Journal of Dispersion Science and Technology, 11 (6), 593 - 609

Chieng, T.H., Gan, L.M., Teo, W.K. amd Pey, K.L. (1996), Porous polymeric membranes by bicontinuous microemulsion polymerization: effect of anionic and cationic surfactants, polymer vol.37, 26, 5917-5925

Chow, P Y and Gan, L M. (2005), Microemulsion Polymerizations and reactions, Adv Polym Sci 175, 257-298

Daoud. M and Williams, C.E., (Eds.); Soft Matter Physics, Springer-Verlag Berlin, Germany, 1999]. L.M. Gan, T.D. Li, C.H. Chew, Langmuir (1995) 11, 3316-3320

Figoli, A. (2001), Synthesis of nanostructured mixed matrix membrane for facilitated gas separation, Dissertation of PhD thesis, ISBN 90-365-1673-0

Galiano, F., (2013), Preparation and characterisation of polymerisable bicontinuous microemulsion membranes for water treatment application, on going PhD thesis, Department of Chemistry, University of Calabria, Italy

Gan, L.M., Liu, J., Poon, L.P., Chew, C.H., Gan, L.H. (1997), Microporous polymeric composites from bicontinuous microemulsion polymerization using a polymerizable nonionic surfactant, Polymer, 38 (21), 5339 - 5345

Gupta, B., Singh, H. (1992), Polymerization of Monomers in Microemulsion Systems, Polym. Plast. Technol. Engg., 31, 635

Holmberg, K. (1994), Organic and biorganic reactions in microemulsions, Adv. Colloid Interface Sci., 51, 137 - 174

Holmberg, K. (2003) Organic reactions in microemulsions, Curr. Opin. Colloid Interface Sci., 8, 187 - 196

Johnson, D., Hilal, N. and Bowen, W.R. (2009), Chapter1 of the book: ATOMIC FORCE MICROSCOPY IN PROCESS ENGINEERING // INTRODUCTION TO AFM FOR IMPROVED PROCESSES AND PRODUCTS// ISBN-13:978-1-85617-517-3

Kandori, K., Kon-no, K., Kitahara, A. (1988) Preparation of $BaCO_3$, Particles in Ionic W/O microemulsions, Journal of Dispersion Science and Technology, 9:1, 61 - 73

Kumar, K. and Mittal, K. (1999) Handbook of Microemulsions Science and Technology, Dekker, New York

Leung, R. and Shah, D.O. (1987), J. Colloid Interface Sci., 120, 330

Malik, M. A., Wani, M. Y., Hashim M. A. (2012), Microemulsion method: A novel route to synthesize organic and inorganic nanomaterials, Arabian Journal of Chemistry (2012), 5, 397 - 417

The Microemulsion book (1999), Industrial Applications of Microemulsions, in Surfactant Science Series, Vol. 66, Dekker, New York

McMullan, D. (2006), Scanning electron micropoy, 1928 – 1965, Scanning 17(3): 175. Doi:10.1002/sca.4950170309, http://en.wikipedia.org/wiki/Scanning_electron_microscope, accessed on September, 2013

Mehta, S.K. and Kaur, G. (2011), Microemulsions: Thermodynamic and Dynamic Properties
http://www.intechopen.com/books/thermodynamics/microemulsions-thermodynamic-and-dynamic-properties

Mialocq, J. – C. 81987)J. Chem. Phys., 84, 1083

Minero, C., Pramauro, E., Pelizetti, E (1988), Langmuir 4, 101.

Ruckenstein, E. (1989), Emulsion pathways to composite polymeric membranes for separation processes, Colloid, Polym. Sci. 267, 792 - 979

Ruckenstein, E., Sun, F. (1992a), A New Concentrated Emulsion Polymerization Pathway, J. Appl. Polym. Sci., 1992, Vol. 46, pp. 1271 – 1277

Ruckenstein, E., Chen, H.H. (1992b), Composite Membranes Prepared by Concentrated Emulsion Polymerization and Their Use for Pervaporation Separation of Water-Acetic Acid Mixtures, J. Membrane Sci., 66, 205

Ruckenstein, E and Sun, F. (1993), Optimization of the Mechanical Properties of Polymeric Composite Membranes Prepared via Emulsion Pathways, J. Membrane Sci., 81, 191

Ruckenstein, E., Li H. (1994), Toughened Polystyrene Composites by the Concentrated Emulsion Pathway, J. Appl. Polym. Sci., 1994, Vol. 52, pp. 1949 – 1958

Ruckenstein, E. and Sun, F. (1995), Hydrophobic-Hydrophilic Composite Membranes fort he Pervaporation of Benzene-Ethanol Mixtures, J. Membrane Sci., 103, 271

Sigma Aldrich (2013), http://www.sigmaaldrich.com/catalog/product/aldrich/m55909?lang=de&region=DE, accessed on 16.10.2013

Sripriya, R., Muthu Raja, K., Santhosh, G., Chandrasekaran, M., Noel, M. (2007), The effect of structure of oil phase, surfactant and co-surfactant on the physicochemical and electrochemical properties of bicontinuous microemulsion, Journal of Colloid and Interface Science 314, 712–717

Sun, F., Ruckenstein, E. (1995), Sorption and pervaporation of benzene-cyclohexane mixtures through composite membranes prepared via concentrated emulsion polymerization, J. Membrane Sci., 99, 273

Wijmans, J.G., Kant, J., Mulder, M.H.V. and Smolders, C.A. (1985), phase sepration phenomena in solutions of polysulfone in mixtures of a sovent and a nonsolvent: relationship with membrane formation, Polymer, 26 (10), pp. 1539 – 1545, ISSN 0032 - 3861

William, B. Jr. (2002), Methacrylic Acid and Derivatives, Ullmann's Encyclopedia of Industrial Chemistry, Wiley-VCH, Weinheim

5. Chapter 5 : Membrane Bioreactor (MBR) Applying Commercial Membranes

5.1 Formulation of membrane bioreactor (MBR)

A detailed description of the experimental set up of MBR is given in section 3.4. The commercial membrane used in this MBR module is denoted as **"PES"** or "**Com1**" membrane.The MBR reactor applied in this experiment is defined as "PES MBR reactor".

5.2 Start –up of the System and functionality test

The MBR module was incorporated in an experimental set up as shown in section 3.4, Fig. 3.9. All the wiring and tubing for acquiring process parameters were well connected. For data acquisition and process automization LabVIEW program controlled computer system was connected with the MBR system. After checking all connections and power supply the system was run with DI water and the functionalities of each instrument were checked. Firstly, the MBR plant was started with DI water for 90 minutes. All the equipment and instruments were checked if they were functioning properly. After the first trial, the plant was tested with tap water of Karlsruhe, Germany for almost 90 minutes and functionality of the plant was checked in the similar way. During these test run all the sensors incorporated in the system were calibrated. The results of the DI water test and tap water tests are shown in Fig. 5.1 and Fig.5.2 respectively.

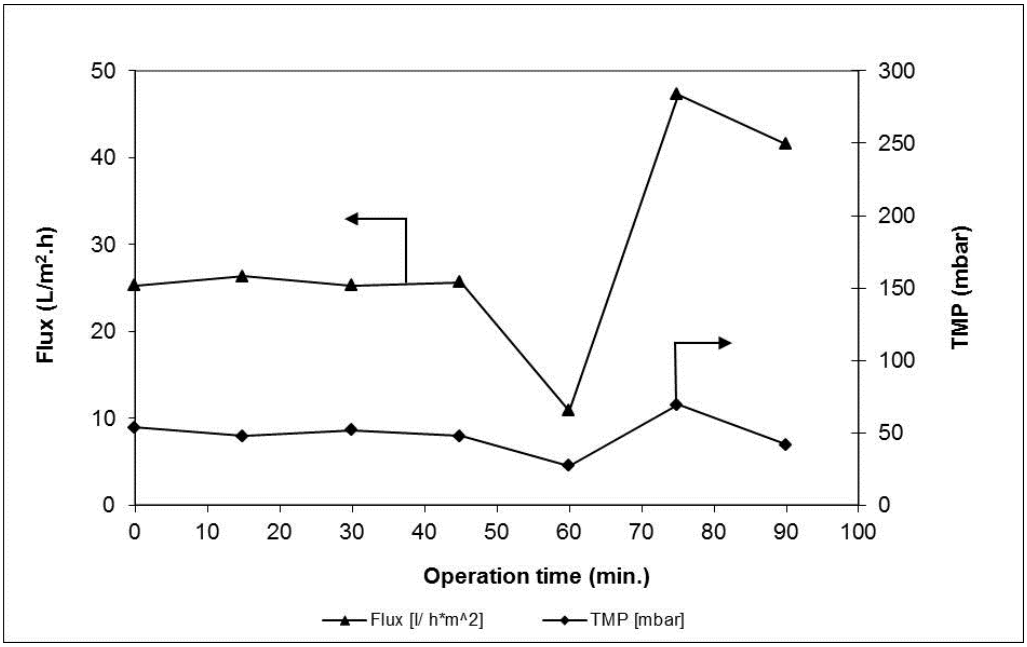

Fig. 5.1: Start up results of PES MBR with DI water (pH: 6.5 ± 0.5, Temp.: 20 ± 2°C, Cond.: 100 ± 5 µS/cm)

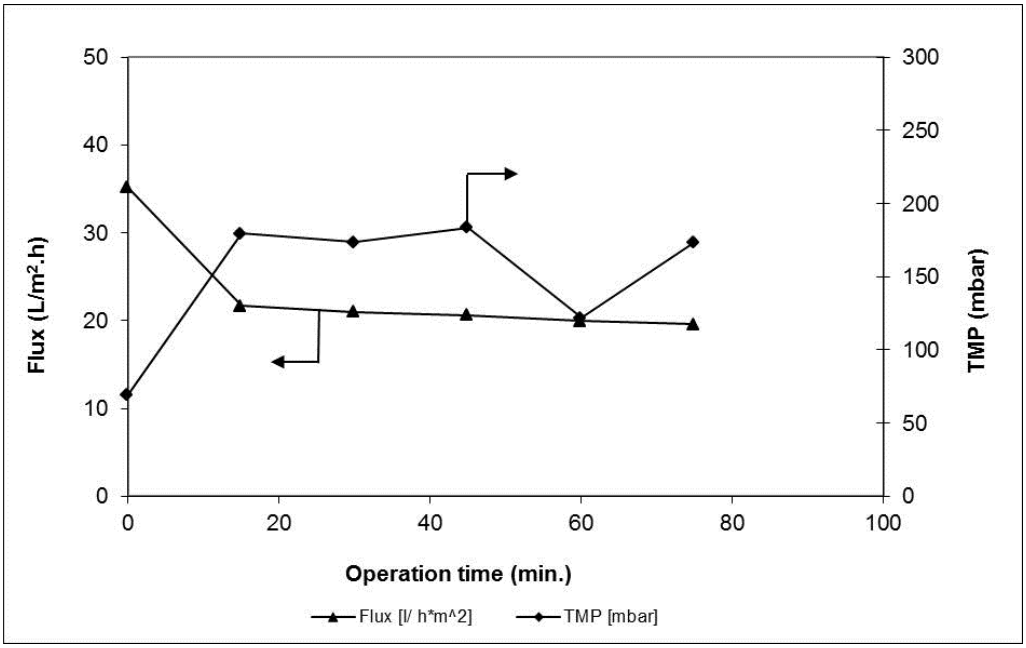

Fig. 5.2: Start up results of PES MBR with tap water (pH: 7 ± 0.5, Temp.: 20 ± 2°C, Cond.: 460 ± 5 µS/cm)

From Fig. 5.1 and Fig. 5.2, it is noticed that the fluxes of the start-up experiments were 25 L/m^2 h with DI water and 20 L/m^2 h with tap water with 50 and 100 mbar of TMPs respectively. The flux with DI water was fluctuating with TMP at the end of the experiment but it can be neglected since it stabilised after a while (not shown). Design pure water flux of this membrane is supposed to be 15 - 25 L/m^2 h with the operating TMP range of 40-400 mbar provided by the membrane company (Microdyn-Nadir, 2010). So, the start-up results were in line with the expected results.

5.3 Selection of test media

Textile wastewater, especially dyes in it, is considered as significant sources of environmental pollution. There are lots of conventional technologies available for textile wastewater treatment but none of them are feasible in commercial scale to remove dyes completely from textile wastewater (Section 2.2). As test media, this thesis focuses on textile dye wastewater with the aim of pursuing two purposes. Firstly, testing the membranes with one of the most critical industrial wastewater and secondly, finding the efficiency of the membrane systems in dye removing from textile wastewater.

Since the quality of textile wastewater changes due to employed coloring matters, dyestuffs, accompanying chemicals and processes from season to season and time to time, the model textile dye wastewater (MTDW) was focused and developed based on literature studies to have constant wastewater quality (Section 3.6). This MTDW was applied as test media for the entire experiments carried out throughout this thesis works.

5.3.1 Characterisation of model textile dye wastewater (MTDW)

After preparing the feed solution following the protocol described in section 3.6, it was analysed to characterise its compositions analytically. After COD analysis, it was noticed its value was close to its theoretical values which indicates the accuracy of the analysis as well. Other process parameters like BOD, pH, chloride conc., Total N (TN) and conductivity were also analysed as reported in Table 5.1.

Table 5.1 : Characteristics of model textile dye wastewater (MTDW)

Parameters	Unit	Calculated values	Measured values
pH			7.5 ± 0.5
			10.0 ± 0.5
Temperature	°C		20 ± 2
COD	mg/L	2506	2450 ± 25
TOC	mg/L	863.29	967 ± 13
BOD_5	mg/L		750 ± 90
Chloride	mg/L	1717	1756 ± 25
Total - N	mg/L	5.9	5.1± 0.25
		84.4	85.4± 3.5
Conductivity	mS/cm		6.6 ±0.15

Table 5.1, indicates that the calculated values (which were applicable) and measured values of the process parameters are closer except some deviations. These deviations might have occurred from the measuring instruments/devices.

As reported in different literature (Hach Lange, 2013), for aerobic wastewater treatment to have optimal nutrient conditions, the C:N:P ratio should be in the range between 100:10:1 and 100:5:1 where C, N and P represent COD, Total N and Phosphorous respectively. Since the MTDW used in this work doesn't contain any P, the COD/N ratio covers the range of 10:1 to 20:1. At the beginning of the experiment, the COD/N ratio was very high (415:1) due to reduced concentration of Total - N (5.9 mg/L) contributed by Red and Blue dyes. In order to achieve to the closer range of expected COD/N ratio, Total - N was increased to 84.4 by adding NH_4Cl (Section 3.6, Table 3.1). This approach made the COD/N ratio of the MTDW as 30:1.

5.4 Selection of the optimum operation conditions

In order to ensure the optimum conditions of the MBR process, some process parameters like transmembrane pressure (TMP), pH, temperature, aeration rate,

hydraulic residence time (HRT), Mixed liquor suspended solids (MLSS), conductivity etc. should be well maintained. These process parameters are discussed and their suitable ranges have been selected in sections 5.4.1 through 5.4.8.

5.4.1 Transmembrane Pressure (TMP)

Transmembrane pressure (TMP) is the driving force for the filtration of the MBR process. For good process functionality the transmembrane pressure should be in the range of 30 mbar to 300 mbar according to the recommendation of the PES MBR module supplier. This pressure was created by a vacuum pump. The maximum limit of the transmembrane pressure depends on the membrane applied along with nature of the membrane module developed by different companies. Generally transmembrane pressure for submerged aerobic MBR more than 500 mbar is not recommended by different MBR companies. The maximum limit of applying TMP for this thesis works were 350 mbar recommended by the MBR module manufacturer company Microdyn – Nadir (Germany) and above this limit, it is considered that the membrane is severely fouled.

5.4.2 pH

Normally the pH of textile dye wastewater is very high (pH 10- pH 11) and it is therefore critical for the microorganism of the sewage treatment plant. Therefore, usually prior to biological treatment processes, the pH value of the industrial wastewater has to be reduced to neutral value in order to improve the biodegradation of the organic compounds by microorganism. In this experiment, two pH values (pH 7.5 ± 0.5 and pH 10.5 ± 0.5) were applied by adapting the chemical compositions of MTDW.

5.4.3 Temperature

Temperature has two effects on MBR process. First effect is on the microorganisms. The favourable temperature for micro-organisms is in the range of 15°C to 30°C. In this range specific micro-organisms can grow effectively and enlarge their community which is expected for better functionality of the process. Second effect is related to the membrane. The temperature being applied to the membrane shouldn't go typically beyond 50°C. Beyond this range it may damage the membrane. The temperature range may differ according to the ap-

plied membrane materials (Lin et. al., 2009). Generally, the typical temperature of the ambient is around 20°C and many industrial scales MBR plants are operated at this temperature. Therefore, the temperature of the experiments for this study was kept 20 ± 2 °C.

5.4.4 Aeration rate

In MBR process, the function of the aeration is twofold. Firstly, aeration creates the cross flow on the surface of the membrane submerged in MBR reactor. This action assists the filterability of the membrane and also keeps the activated sludge away from deposition on the surface of the membrane. That means, it cleans the membrane indirectly. Secondly, aeration supplies oxygen for microorganisms in the reactor. From literature studies it is known that the suitable range of dissolved oxygen for MBR process is in the range of 2 - 4 mg/L (Judd, 2006) which is contributed by suitable aeration rate. For industrial scale application, the recommended aeration rate of MBR module manufacturing company Microdyn – Nadir for the MLSS range of 5 – 12 g/L was 0.5 m^3/m^2_M h. The range of aeration rate for the experiments in this thesis works were from 0.50.±0.05 to 1.0 ± 0.1 m^3/h which shows the aeration rate of 1.5 ± 0.15 and 3 ± 0.3 m^3/m^2_M h where "m^2_M" indicates the membrane area of 0.33 m^2 used in the experiments.

5.4.5 Hydraulic residence time (HRT)

Hydraulic residence time (HRT) indicates the average length of time that the feed solution remains in the MBR reactor before it gets drained as permeate. The calculation of HRT is shown in Eq. (5.1).

$$HRT = \frac{Hydraulic\ volume\ (L) of\ the\ MBR\ reactor}{Permeate\ flow\ (L/h)} \qquad (5.1)$$

From Eq. (5.1), it is clear that HRT depends on the hydraulic volume of the reactor and the permeate flow. In this experiment, the hydraulic volume was 57 L. The HRT of the MBR system depends on the membrane module and type of wastewater applied for treatment. For MBR process, the higher is the flow rate, the lower is the HRT. Since the higher permeate flow could not be kept constant with the experimental set up used in this thesis works due to the limitation

of the membrane module, the HRT was kept in the range of 50-60 h for the whole experiment.

5.4.6 Mixed liquor suspended solids (MLSS)

MLSS indicates the concentration of suspended solids in the MBR reactor. This is the combination of microorganisms and non-biodegradable suspended substances. MLSS plays an important role in degrading organic compounds in wastewater. According to Krampe (2003) and Gunder (2001) the well-accepted MLSS value for MBR process is 8-12 g/L. For this work the MLSS value was kept in the range 8-10 g/L.

5.4.7 Electrical conductivity

Conductivity indicates the amount of total salts in the solutions. Since the membranes used in MBR process are micro to ultrafiltration, normally salts can't be rejected by these membranes. Some part of multivalent ions can be rejected when tighter ultrafiltration membranes are applied. In this MBR trial, the conductivity of the permeate and the feed were more or less the same and it was around 6.6 mS/cm.

5.4.8 Critical flux (CF)

According to Field et al. (1995), the critical flux hypothesis for microfiltration is that on start-up there exists a flux below which a decline of flux with time does not occur, above it fouling is observed. This concept was applied in this thesis with UF PES MBR module following flux step-method. The critical flux of the applied MBR module was around 6.5 L/m^2.h (section 5.6.12). The operating flux of the system was around 3 L/m^2.h which was much lower than the CF.

5.5 Continuous operation of the experiments

After the functionality tests with DI water and Karlsruhe tap water, the MBR system was running continuously with prepared MTDW based on selected suitable operation conditions (Section 5.4) controlled by LabVIEW program

based computer control system. The biological sludge for these trials was brought from a MBR operated commercial company Textilservice Klingelmeyer, Darmstadt, Germany. The MBR unit was running in the following mode of operation (Table 5.2) for 304 days in different operational phases (Table 5.4).

Table 5.2 : Operation mode of MBR system

Mood of operation	Time (min.)
Suction mode	8.5
1st relaxation	0.5
Back flushing mode	0.5
2nd relaxation	0.5

5.5.1 Sampling procedure

Most of the samples were taken every 2nd day and some were taken once in a week as shown in Table 5.3 and these were analysed according to the analysing method as mentioned in section 3.9.

Table 5.3 : Sampling frequency of the MBR experiment

Parameter	Influent and permeate	MBR reactor
Temperature	Continuous	-
pH	Continuous	-
DO	--	Every 2nd day
Conductivity	Continuous	-
COD	Every 2nd day	Once a weak
Colour (red and blue)	Every 2nd day	Once a weak
TMP	Continuous	-
TOC	Every 2nd day	-
Oxygen consumption	Every 2nd day	-
MLSS	Once a weak	Once a weak
Drying residue	Once a weak	-
HRT	Continuous	-
Cl^-	Every 2nd day	-
Flux	Continuous	-

5.6 Results

The results of the experiments carried out under the operation conditions described in section 5.4 are presented in the following sections. Following the operation conditions, the experiments were conducted for 304 days at 8 different phases as shown in Table 5.4.

Table 5.4 : Applied experimental phases

Note	Designation	Duration	Process conditions (continuous)
P1	Phase1	day1 - day36	Acclimation, MTDW with red dye only, pH:7.5 ± 0.5
P2	Phase2	day36 - day46	MTDW with red and blue dyes, pH: 7.5 ± 0.5
P3	Phase3	day46 - day96	Addition of detergent (DBC) to MTDW
P4	Phase4	day96 - day143	New membrane module with varied HRT
P5	Phase5	day143 - day208	Changed to pH : 10.0 ± 0.5 by addition of Na_2CO_3
P6	Phase6	day208 - day256	Addition of NH4Cl to MTDW to have COD/N ratio : 30:1
P7	Phase7	day256 - day278	New MBR module
P8	Phase8	day278 - day304	Replacing Na_2CO_3 by $NaHCO_3$ to obtain pH: 7.5 ± 0.5 in MTDW

5.6.1 Water production

5.6.1.1 Flux and TMP

Flux is considered as the product of any membrane operation system with applied TMP. Fig. 5.1 indicates the flux and TMP of the entire experiments of **P1** through **P8**.

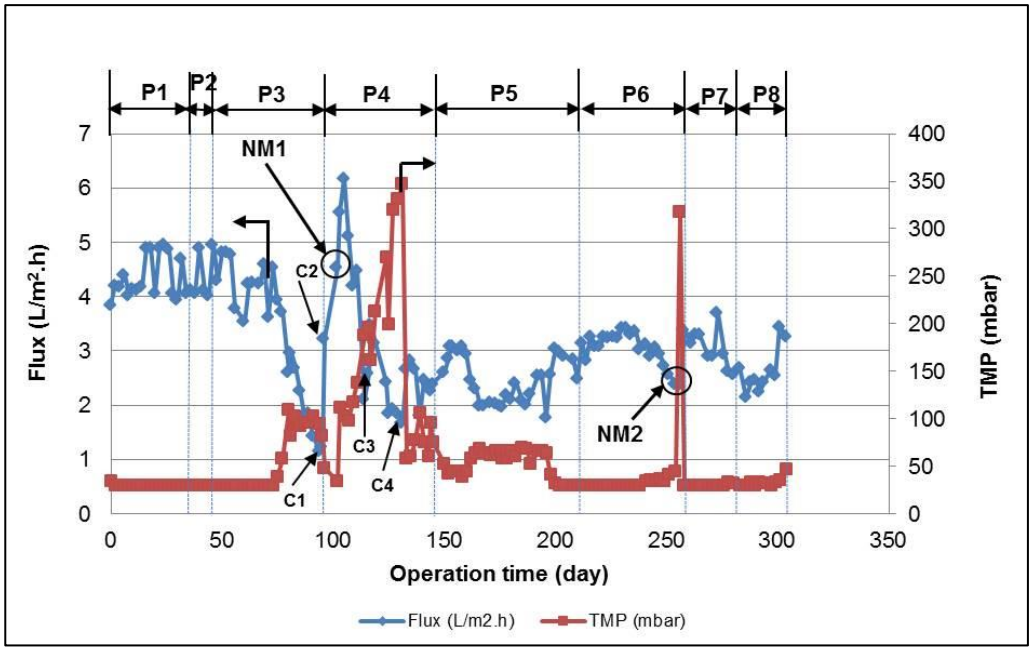

Fig. 5.1 : Flux and TMP of the experiment

N.B.:
C1 : cleaning1 at day95
C2 : cleaning2 at day96
C3 : cleaning3 at day116
C4 : cleaning4 at day131
NM1 : new module1 installed at day102
NM2 : new module2 installed at day 256

At the beginning of the experiment flux was fluctuating as 4 to 5 L/m^2.h with operating TMP of around 30 mbar until **P3**. At the end of P3, membranemodule showedd fouling problem at reduced flux of around 1 L/m^2.h with increased TMP of around 100 mbar. To gain flux, the membrane module was cleaned firstly with DI water and then 1% H_2O_2 for 1 hour at day 96 and reinstalled. But the problem was not solved and it produced turbid permeate after 2nd time cleaning. So, the module was replaced by a new one at day 102 in **P4** and started with HRT of 25 h to check if it is possible to achieve lower HRT operation. At this HRT, flux fell down very quickly with increased TMP. Considerable regain of flux was not possible even after performing 2 times cleaning at day 116 and day131 respectively. So, the membrane module was allowed to keep HRT of 64h and onward at the end of **P4** until **P8.** At the end of **P6**, membrane was replaced by a new one at day256 due to fouling problem.

In summary, the experiments carried out from **P1** to **P8** showed flux of around 3 L/m^2.h with around 60 mbar of TMP and the membrane module was changed 2 times during the whole operation time.

The flux value obtained from this experiment is close to that of Zheng and Liu (2006) where they found the flux of 6 ± 2.5 L/m^2.h at 12.7 kPa with a PVDF hollow fiber MF (0.22 µm) MBR system with a gravity drain treating dyeing and printing wastewater from a wool mill. Similarly, Yigit et al. (2009) obtained a flux of 20 L/m^2.h at TMP of 0.14 – 0.56 bar in a submerged hollow fiber UF (0.04 µm) MBR module (ZW® - 10) treating denim producing textile wastewater in a no extra sludge removal operation system. Huang et al. (2009) also obtained a flux of 2 -8 L/m^2.h at TMP of 0.05 – 0.1 bar with a submerged hollow fiber MF (0.2 µm) MBR module treating dyeing wastewater.

5.6.1.2 Water permeability

The permeate flux presented in Fig. 5.1 can be divided by the respective applied TMP which is termed as permeability in L/m^2.h.bar. The permeability of the whole experimental period is shown in Fig. 5.2. The average permeability of the experiment was around 80 L/m^2.h.bar with several cleanings and 2 times membrane module replacement.

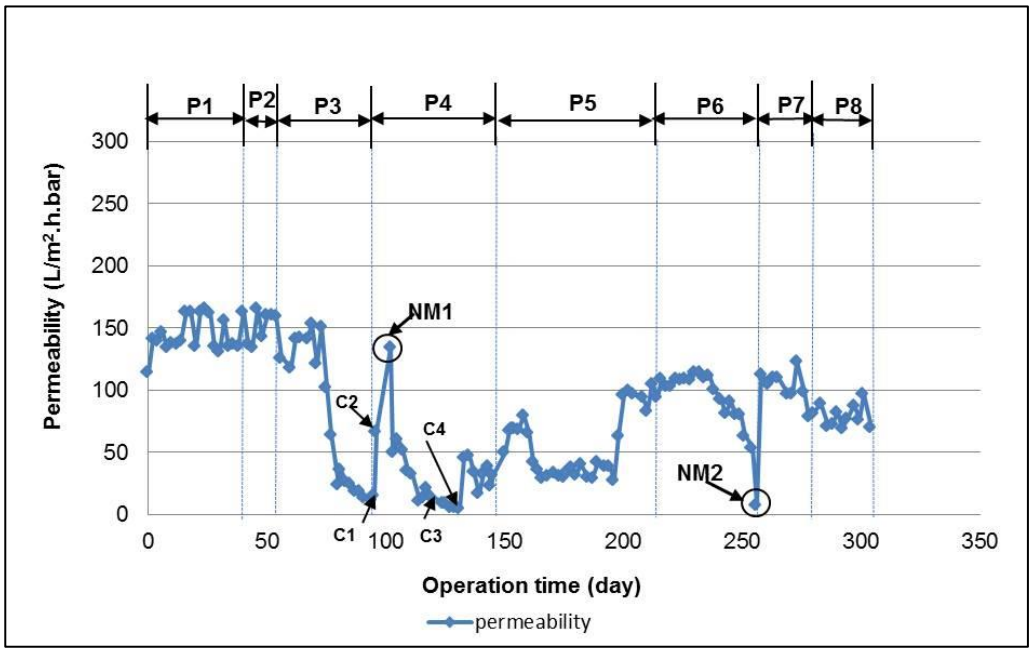

Fig. 5.2 : Water permeability of PES MBR the experiment

The water permeability obtained from this experiment is in line with the water permeabilities reported in different literatures as mentioned in section 5.6.1.1.

5.6.2 Hydraulic Residence Time (HRT)

Fig. 5.3 represents the HRT of the carried out experiments. HRT was fluctuating from 40h to 100h with average value of around 60h. This means, MTDW remained in the MBR reactor for 60h (2 days) before it turned into permeate. This HRT is high compared to the HRT reported in different literature e.g HRT of the experiment carried out by Huang et al. (2009) was in the range of 10 h to 22.5h. This high HRT occurred due to limitation of permeate flow as described in section 5.6.1.1.

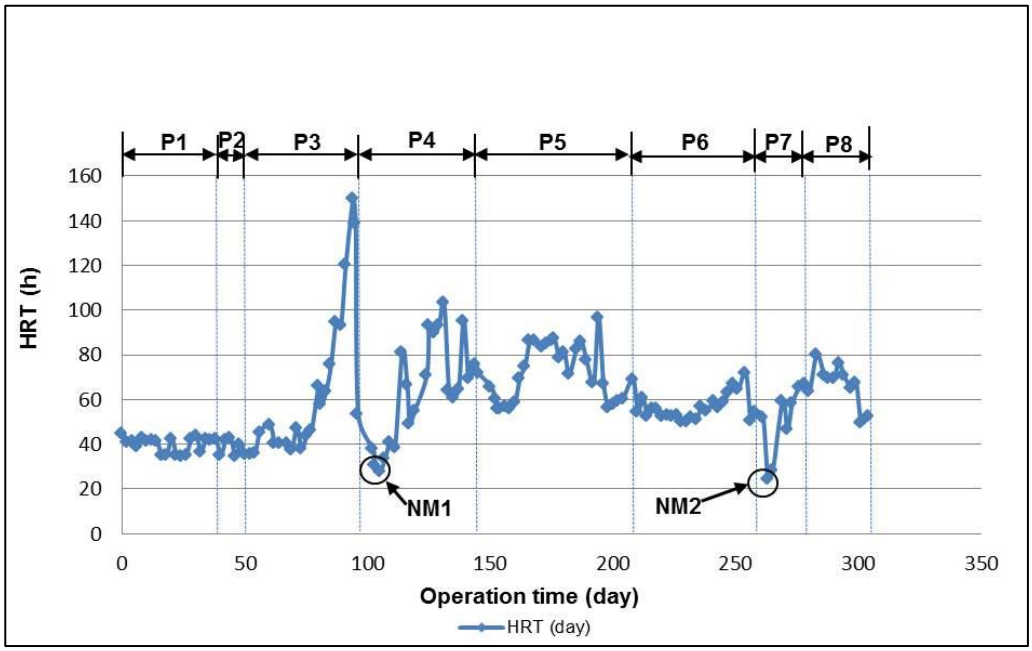

Fig. 5.3 : HRT of the PES MBR experiment

According to Viero et al. (2008), the analysis of HRT in MBR technology is needed to ensure that the system is being operated under steady-state conditions. The average range of HRT (70h-80h) except some fluctuations (in day94, day103 and day263) indicates the system was running roughly at steady-state conditions.

5.6.3 COD and TOC

5.6.3.1 Permeate COD and COD removal efficiency

Fig. 5.4 represents the COD removal efficiency for the whole duration of the experiments. In **P1** (phase1), COD removal efficiency shows low values (around 70%). This was the beginning phase of the experiment with MTDW using red dye only. In this case, the use of MTDW with one dye (Red) was focused so that it might not be stressful for microorganisms since the dye components are the lowest in biodegradability (Palacios, 2009) and they can gradually acclimate the system. At the end of **P1**, COD removal efficiency increased indicating the micro-organisms have been adapted. Consequently, blue dye was added in **P2** (phase2) at pH 7.5 ± 0.5 and it was performing well. Detergent (DBC) was added in **P3** (phase3) to have complete composition of MTDW and this might be stressful for microorganisms since the performance was fluctuating. Because the detergent was not readily biodegradable as it is mention to the safety data sheet of the product. **P4** (phase4) with new MBR module was performing good with around 90% COD removal efficiency. This indicates that microorganisms were fully adapted to the final compositions of MTDW. **P5** (Phase5) was performed at high pH (pH 10.0 ± 0.5) to investigate the system performance at higher pH and it was noticed that they were performing well with around 90% COD removal efficiency. From the performance of **P5**, it is revealed that the pH variation from pH 7.5 ± 0.5 to pH 10.0 ± 0.5 has no effect in COD removal efficiency. All the experiments carried out from **P1** to **P5**, didn't show any nitrification occurred. It was assumed that it might be happened due to very low N-contents (around 5 mg/L) in the applied MTDW. To increase the nutrient content, 300 mg/L of NH_4Cl was added in MTDW in **P6** which gives the COD/N ratio of around 30:1 (Section 3.6). Nutrient was added to check the improvement of the system. At high N-content in **P6**, COD removal efficiency was nearly 90% but still no nitrification was noticed (Section 5.6.5). It summarises that nutrient enrichment had no effect on COD and TOC removal efficiency. In **P7** (phasse7), membrane faced blocking problem and its performance was fluctuating. **P8** (phase8) brings the pH value to the neutral level (pH 7.5 ± 0.5) and smooth performance with 91% COD removal efficiency was noticed.

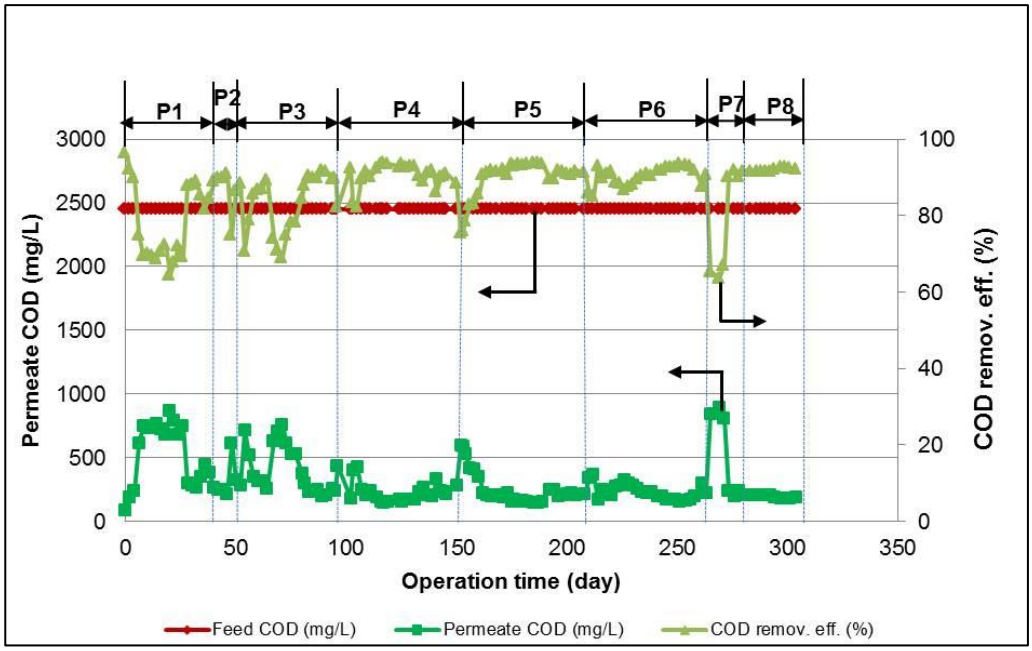

Fig. 5.4 : COD removal efficiency

5.6.3.2 Effect of HRT on COD removal efficiency

The effect of HRT on COD removal efficiency is shown in Fig. 5.5. It shows that the fluctuations of COD removal efficiencies were not highly correspondent to the fluctuation of HRT. This result summarises that there is no influence of HRT on COD removal efficiency. The similar results were obtained by Viero et al. (2008) treating synthetic wastewater by MBR applications operated at HRT in the range of 6h to 14h.

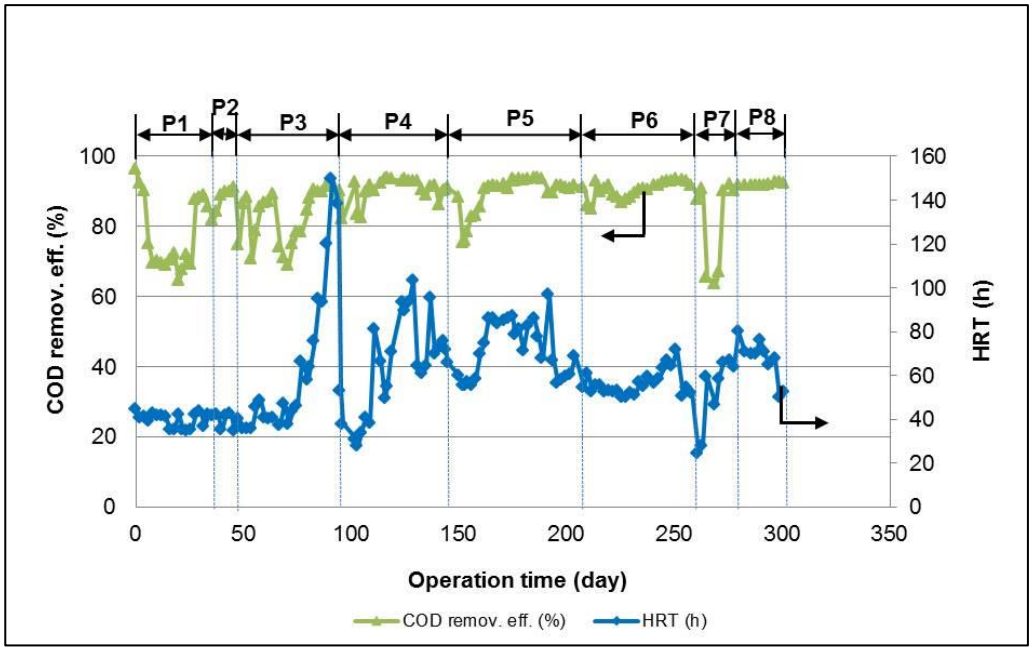

Fig. 5.5 : Effect of HRT on COD removal efficiency

5.6.3.3 COD and TOC relation

COD is a collective value of an oxidizable component (oxygen consumption) where TOC is a collective value of any organic carbon components. COD and TOC can be theoretically calculated by stoichiometry as shown in Table 5.1. The COD value of the wastewater should be correlated with TOC value. Therefore, both COD and TOC parameters are related to the organic load. The COD value is widely used for determining the strength of organic pollution of any wastewater. However, COD can't reflect the degree of wastewater precisely due to the impacts of types and concentration of oxidants, reaction temperature and time, etc. On the other hand, TOC can reflect the strength of organic pollution correctly. TOC measurement has many advantages such as it takes short for measurement, gives fast and accurate results, high reliability and stability. Theoretically, there should be a correlation between COD and TOC. Generally, TOC is considered as 1/4 to 1/3 of COD values based on theoretical calculation. Based on theoretical calculation, the TOC and COD values are 863.29 mg/L and 2506 mg/L respectively as shown in Table 5.1. This indicates that the TOC value is 1/3 of COD value which is in line with expected values.

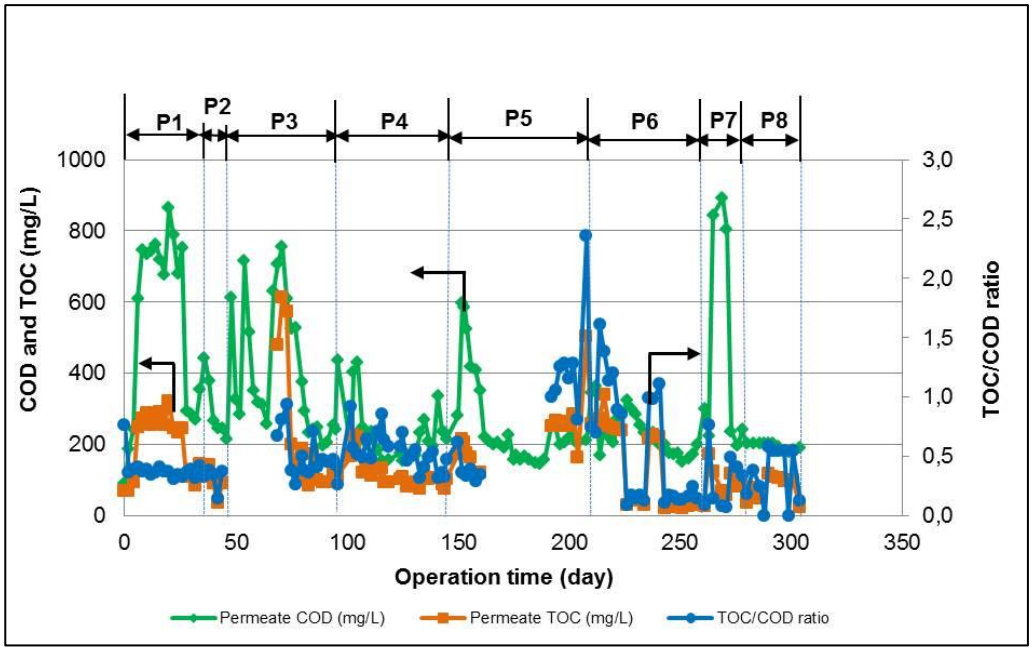

Fig. 5.6 : Relation between COD and TOC

Fig. 5.6 represents the permeate COD and TOC values where the TOC/COD ratio is 0.5 in average. The TOC values in **P1** (phase1) through **P8** (phase8) are highly responsive to those of COD values except at the end of **P5**. The permeate TOC at the end of **P5** could be recommended to repeat the analysis but it was not possible since the collected samples were thrown away mistakenly. Some other samples in **P3** and **P5** were also missing due to misuse of the samples. In general, The TOC values seemed to be responsive to that of COD values.

5.6.3.4 COD and TOC removal efficiency

The average COD and TOC removal efficiencies are 87% and 84% respectively as it is shown in Fig. 5.7 and they are highly correlated in different operation phases except **P6** (phase6) where NH_4Cl was added to achieve sufficient nutrient contents in the MBR system. It is worth to mention here that some of the TOC values were missing due to misused of the samples. Nevertheless, the result shows the high accuracy of the analysis in most of phases except bit fluctuations.

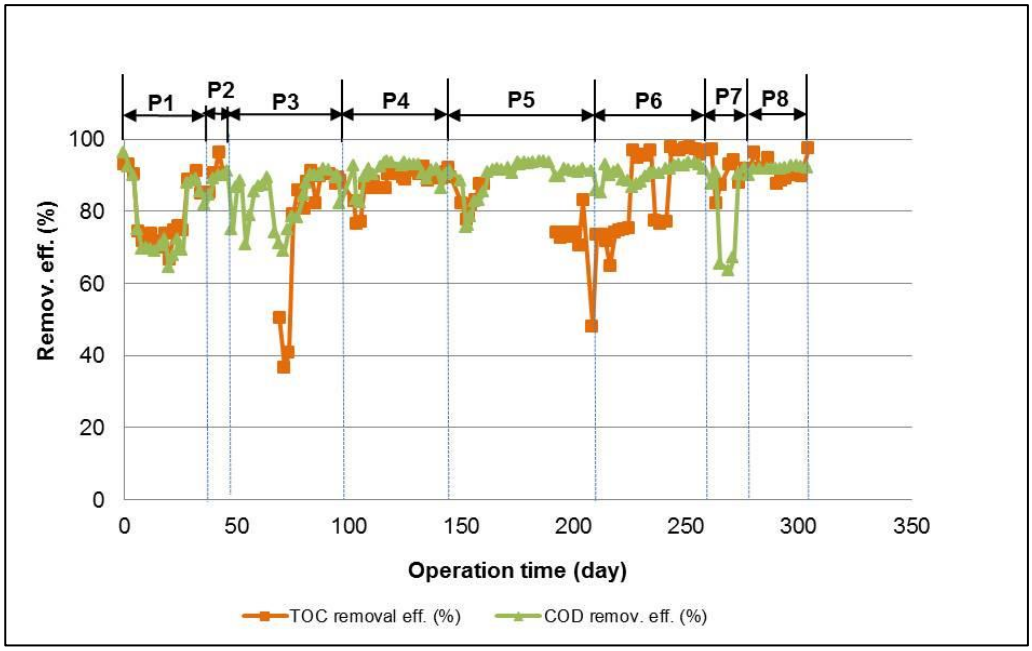

Fig.5.7 : Comparison of COD and TOC removal efficiency

5.6.3.5 Permeate COD and reactor COD

This approach was initiated to check if the organic components (low biodegradable dyes) were accumulated or degraded in the reactor. At the beginning of the experiment, the samples were not possible to be analysed due to unavailability of the analysing device.

The analysis of reactor samples were done by applying sonication process to release potentially adsorbed matter and physical filtration process (Section 3.9.5) and these values were compared with permeate COD values. In sonication process, the biological materials were disrupted or deactivated by applying ultrasound which results in the release of cellular contents from the inside the cells. According to the biological process, the COD removal efficiency of MBR process depends mainly on degradation and adsorption. The degradation occurs due to biological metabolism, where the organic substances are degraded to inorganic substances or smaller size organics. On the other hand, in adsorption process, the organic or inorganic substances are adsorbed by the microorganisms onto their surface or inside themselves without being degraded

Among different phases (Table 5.4), the results of the last 216 days are presented in Fig.5.8. Basically, the COD values of permeate and reactor are supposed to be closer if they are not accumulated in the reactor because biologically they are more or less the same except two different physical separation processes (MBR membrane separation and sonication membrane separation).

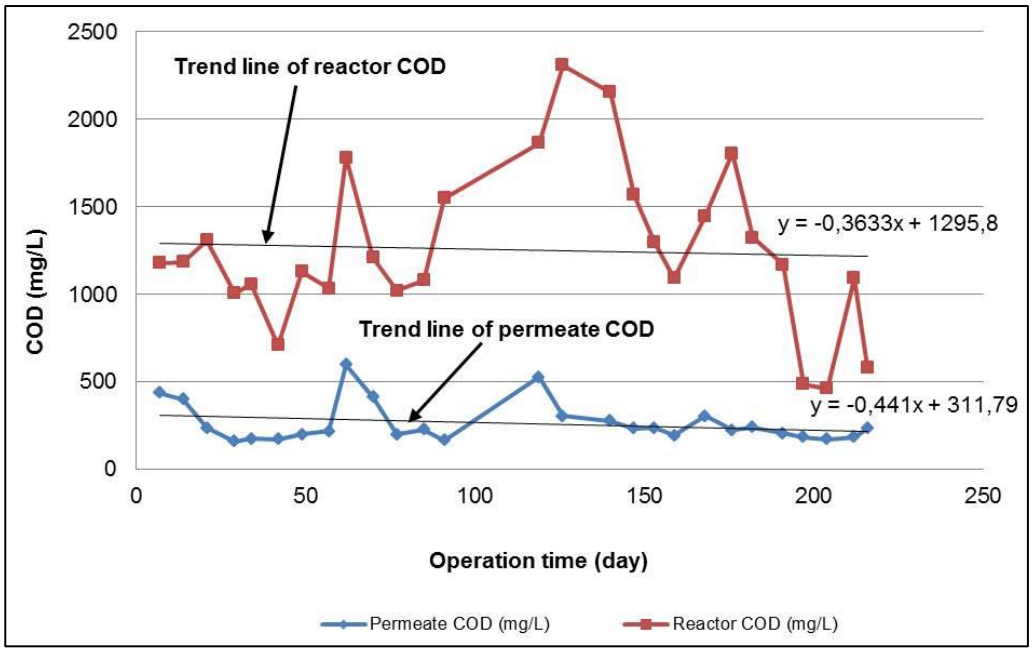

Fig. 5.8 : Comparison of permeate and reactor COD

Reactor COD as shown in Fig.5.8 is higher than the permeate COD but it is tending to be closer at the ending phase. The difference between trend lines of reactor COD and permeate COD is the same. This is the indication of no COD accumulation meaning good degradation for the further approach.

5.6.4 Dye removal efficiency

5.6.4.1 Dyes in permeate

The main mechanisms of dye removal in MBR system are mainly due to biodegradation and adsorption onto biomass (Yigit et al., 2009). Biodegradation seemed to play a minor role in colour removal efficiency as reported by Feng et

al. (2010). This suggests that the dye removal efficiency might occur due to adsorption of dye molecules on biomass. Since the applied dyes (Red and Blue) in this thesis were low biodegradable, the dye rejections might have occurred due to combination of membrane rejection and biodegradation. Membrane rejection might have contributed 20% – 25% dye rejections whereas 10% to 15% dye rejections might have done by biodegradation.

Fig. 5.9, represents red and blue dye removal efficiencies in **P1** through **P8**. Red and blue removal efficiencies are 40% and 30% respectively with lot of fluctuations in different phases. Molecular weights of red and blue dyes are 380.4 and 626.5 respectively (Section 3.7). Since the membrane used in the MBR module was ultrafiltration (Section 3.4) with MWCO of 150 kDa, all red and blue dyes are supposed to pass through the membrane resulting in no rejection. But Fig. 5.9 shows different scenario. There could be three reasons; **firstly**, the applied dyes are negatively charged and the MBR module is also negatively charged. So, there could be charge exclusion mechanism which might have resulted in dye rejections. **Secondly**, the dyes might have been adsorbed on the surface of the membrane and in the reactor sludge. **Thirdly**, the dye rejections might be happened due to partial biodegradation. The higher red dye rejection might be happened due to higher biological degradation of red dye than blue. It can be speculated that the red dye which contains azo bond (-N=N-) is highly prone to digestion with the presence of microorganisms and it might had been decolorized due to decomposition.

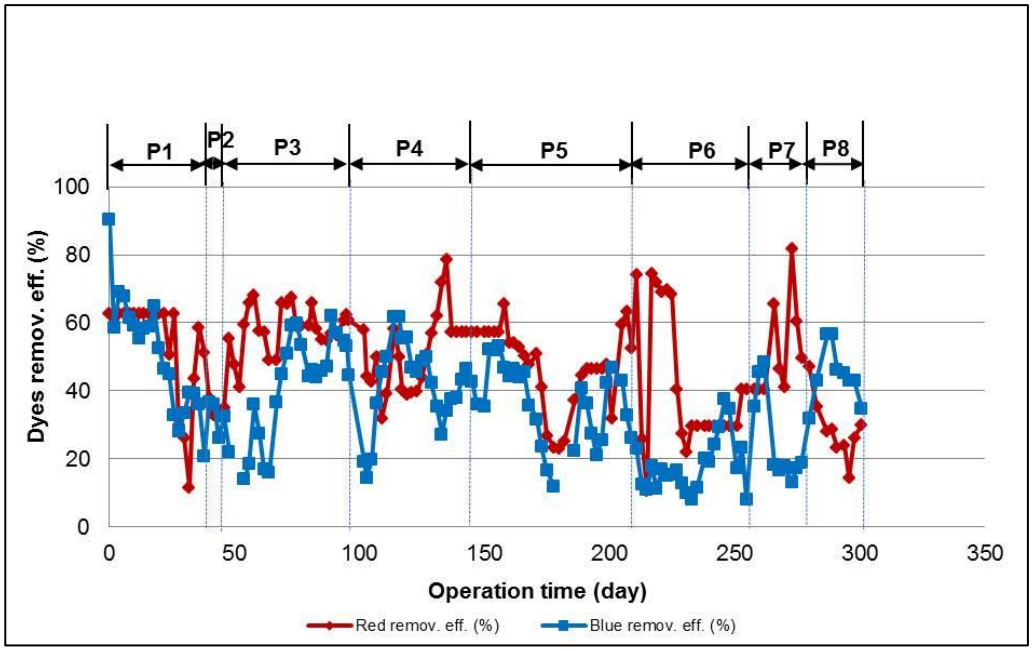

Fig. 5.9 : Red and blue dye removal efficiencies

5.6.4.2 Dyes in reactor

This approach was initiated to check the potential accumulation of in the MBR reactor.

The analysis of reactor dyes were done by applying sonication and physical filtration process (Section 3.9.5) and these values were compared with concentration of dyes in permeate. At the beginning of the experiment, the samples were not possible to analysis due to unavailability of the analysing device. Among different phases (Table 5.4), the results of the last 216 days are presented in Fig.5.13. Basically, the dyes of permeate and reactor are supposed to be closer if they are not accumulated in the reactor because biologically they are more or less the same except two different physical separation processes. Reactor dyes (red and blue) as shown in Fig.5.10 are lower than the permeate dyes which is opposite to the expected values. This might be happened due to the sonication process (Section 3.9.5) especially the dilution factor, applied to analysis the concentration of dyes in reactor samples. However, the results indicate that there is no general trend of dyes accumulation in the reactor.

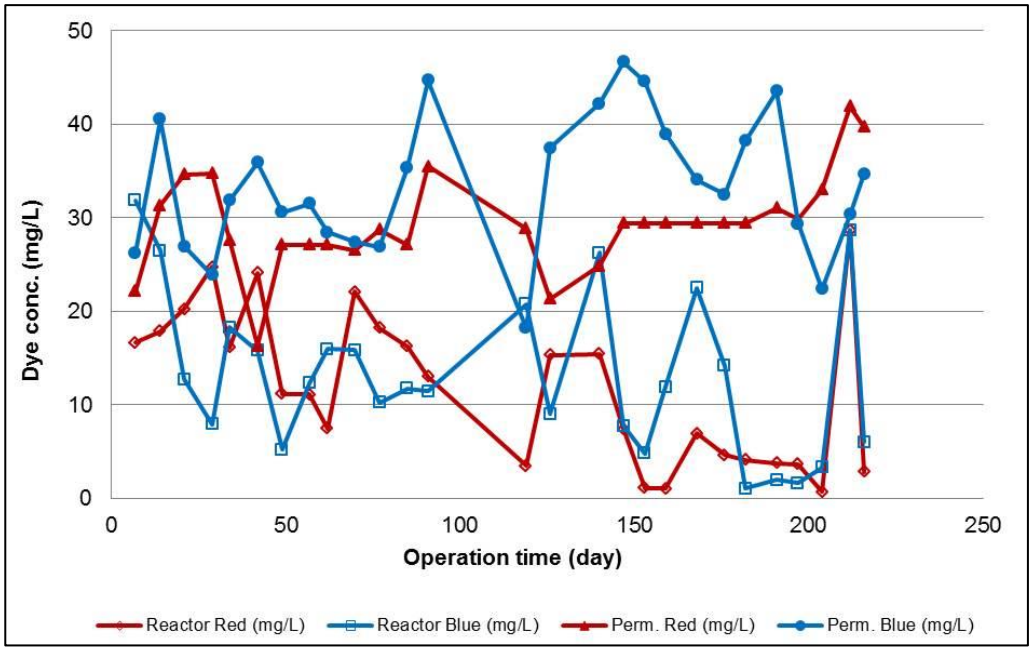

Fig.5.10 : Comparison of permeate and reactor dyes

5.6.5 N-Balance

Sources of Total-N

To obtain the nitrogen (N) balance, the nitrogen content in permeate in terms of Total-N, NH_4^+-N, NO_3^-N were analysed. The main sources of nitrogen (N) were red and blue dyes and NH_4Cl used in MTDW (Section 5.3.1). The molecular formula of blue is $C_{22}H_{16}N_2Na_2O_{11}S_3$ with the molecular weight of 626.5 g/mol and the molecular formula of red is $C_{17}H_{13}N_2NaO_5S$ with the molecular weight of 380.4 g/mol. The concentrations of both dyes in the feed were 50 mg/L. The calculated amount of total-N concentration in MTDW is shown in Table 5.5.

Table 5.5 shows that the theoretical concentration of Total – N is 84.4 mg/L whereas the measured value is 85.4 ± 3.5 mg/L indicating both of the values are closer (Table 5.1).

Table 5.5 : Theoretical concentration of Total - N source in MTDW

Nitrogen (N) source	Individual nitrogen (N)	Total - N conc. in

	conc. (mg/L)	feed (mg/L)
Remazol Brilliant Blue R	(14*2*50)/626.5 = 2.2	(2.2+3.7+78.5) = 84.4
Acid Red4	(14*2*50)/380.4) = 3.7	
NH_4Cl	(14*300)/53.5 = 78.5	

Nitrification and denitrification

According to Judd, S. (2006), the removal of total nitrogen by biochemical degradation demands that oxidation of ammonia to nitrate takes place under aerobic conditions and that nitrate reduction to nitrogen gas takes place under anoxic conditions. Both the processes demand that specific micro-organisms prevail.

The biological generation of nitrate from ammonium (NH_4^+) under aerobic conditions (nitrification), takes place in two distinct stages (Judd, 2006) (Eq. 5.2 through Eq. 5.4):

$$2\,NH_4^+ + 3\,O_2 \rightarrow 2\,NO_2^- + 2H_2O\ (ammonia \rightarrow nitrite) \quad (5.2)$$

$$2\,NO_2^- + O_2 \rightarrow 2\,NO_3^-\ (Nitrite \rightarrow nitrate) \quad (5.3)$$

Overall:

$$NH_4^+ + 2\,O_2 \rightarrow NO_3^- + 2H^- + H_2O\ (Nitrification) \quad (5.4)$$

Since the second step proceeds at a much faster rate than the first, nitrite doesn't accumulate in most bioreactors. Denitrification takes place under anoxic conditions when oxidant of organic carbon takes place using the nitrate ions (NO_3^-), generating molecular nitrogen (N_2) as the primary end product (Judd, 2006).

$$C_{10}H_{19}O_3N + 10\,NO_3^- \rightarrow 5N_2 + 10CO_2 + 3H_2O\ (Denitrification) \quad (5.5)$$

Where, $C_{10}H_{19}O_3N$ represents wastewater.

Fig. 5.11 represents N-compounds in **P1** through **P8.** The Total-N contents in feed (MTDW) in **P1** through **P5** were very low and the Total-N contents in permeate also shows the corresponding low values. Total-N contents in MTDW were increased from **P6** until **P8** in the feed by adding NH_4Cl at day

208. In these phases, Total-N in permeate were less than that of feed. This gap might have been created due to nitrogen (N) accumulation in the biological sludge during conversion to NO_3-N. The calculated Total-N (summing up NO_3–N and NH_4–N) (termed as Total-N_perm.calc.) in permeate are little bit lower than that of the experimental Total-N (termed as Total-N_perm.expt.) in permeate until phase7 (Fig. 5.11). This gap might have occurred from N-contents in dyes as reported in Fig. 5.12. In **P8**, experimental Total-N in permeate (Total-N_perm.expt.) is higher than the Total-N in feed which shouldn't occur logically. It can be speculated that the accumulated Total-N in the previous phases could be released in **P8**.

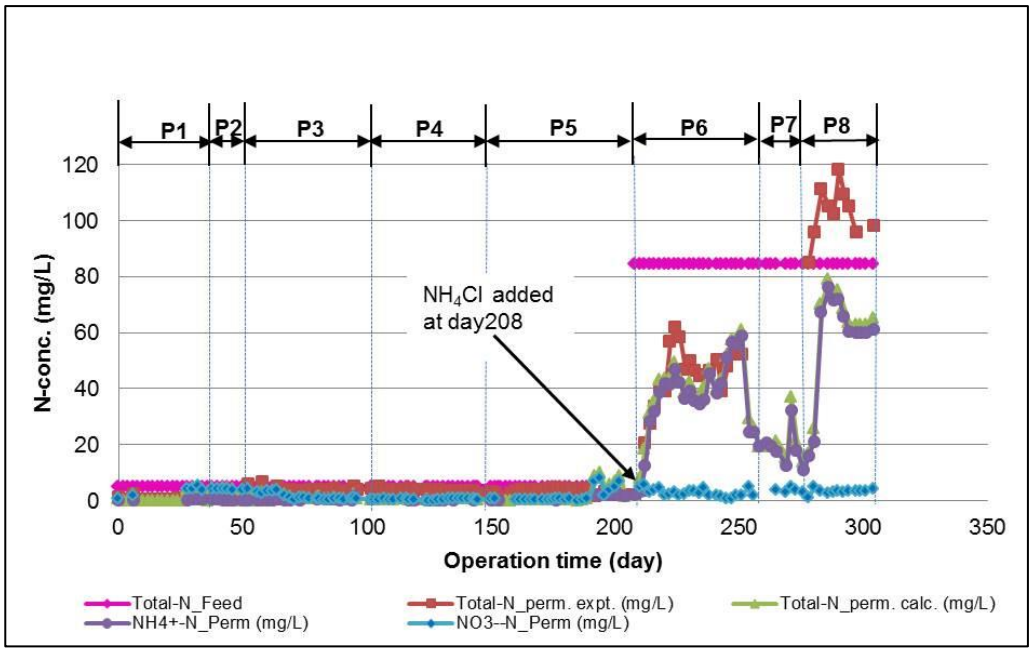

Fig. 5.11 : N- Balance

Difference between experimental and calculated TN

Fig. 5.11 shows that there is a gap between experimental TN (Total-N_perm.expt) and calculated TN (Total-N_perm.calc.) in the permeate. The difference of TN concentration (termed as Diff._N) might have occurred from the analysis error or from other form of nitrogen source. The Diff._N (mg/L) was calculated using Eq. (5.6).

$$Diff._N = Total.N_{perm}.expt. - Total.N_{perm}.calc \quad (5.6)$$

$$Total.N_{perm}.calc = NO_3^- - N + NH_4^- - N + Dye - N \qquad (5.7a)$$

The total nitrogen (TN) in dyes (termed as Dye_N) in mg/L can be calculated using Eq. (5.8) as follows:

$$Dye\_N = \frac{14 * 2\frac{g}{mol} * perm.blue\ conc.\frac{mg}{L}}{626.5\ \frac{g}{mol}} + \frac{14 * 2\frac{g}{mol} perm.red\ conc.\frac{mg}{L}}{380.4\ \frac{g}{mol}} \qquad (5.7b)$$

The obtained Diff._N from P1 through P8 are shown in Fig.5.12. In most of the cases, the Diff._N is almost equal to baseline (zero line) except some differences (negative/positive values) in **P3** and **P4**. The negative values of Diff._N indicate that the calculated TN (generating from NH_4-N, NO_3-N and Dye_N) is higher than experimental TN. This might be occurred from the measurement errors of NH_4-N, NO_3-N and Dye_N. On the other hand, the positive values of Diff._N might be occurred from unidentified nitrogen source like NO_2–N which was not detected and these could be generated due to the applied process variations or change of microbial activities in MBR reactor.

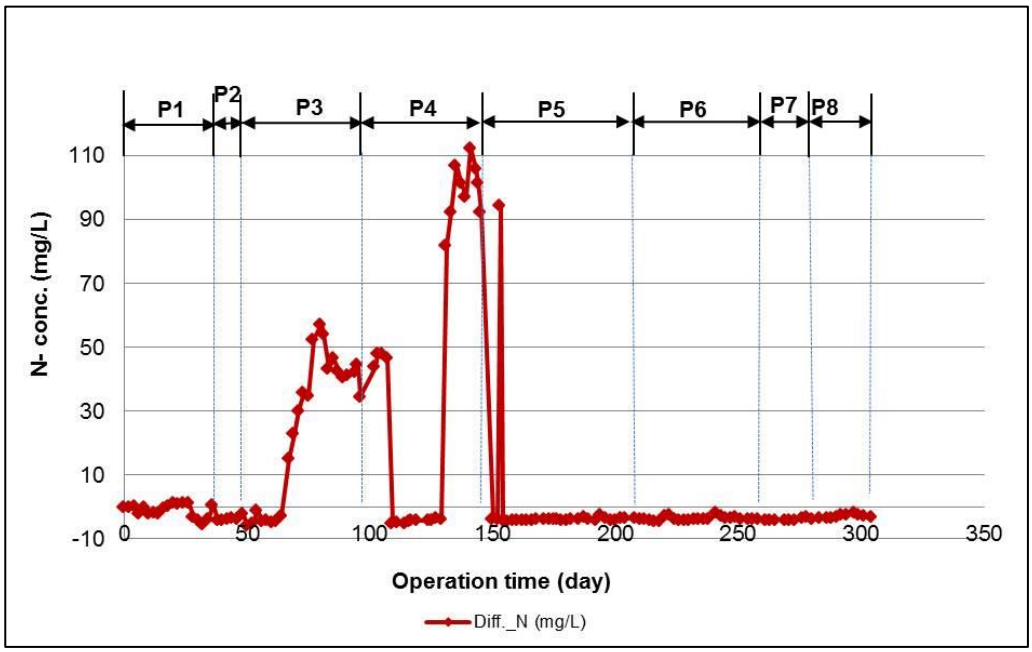

Fig.5.12 : Total – N uptake or release

5.6.6 O_2 concentration and consumption

5.6.6.1 Aeration rate vs dissolved oxygen (DO)

Aeration in MBR is required mainly for maintaining the cross flow velocity for scouring purpose and dissolved oxygen (DO) supply for microorganism for respiratory (food) system. For MBR DO is normally considered as a key design parameter. According to Drews and Kraume (2005), the rate of fouling was 5 times higher in the low DO MBR. The oxygen is most commonly transferred to the biomass by bubbling air or in some cases pure oxygen into the system by diffusers. In this thesis, oxygen transferred into the reactor was done with the help of an air-bubble diffuser.

The oxygen transfer efficiency from gas phase to liquid phase is theoretically described by Eq. (5.8) (Francisco et al. 2011)

$$\frac{dc}{dt} = K_{La} * (Cs - C) \quad (5.8)$$

Where,

K_{La} = Mass transfer coefficient
C_s = Saturated oxygen concentration
C = Instant oxygen concentration

The mass transfer coefficient K_{La} in the reactor is affected by many factors such as temperature, salinity, viscosity, bubble size etc. The effect of temperature on the mass transfer was correlated by Eq. (5.9) (Francisco et al. 2011)

$$K_{La\,(T)} = K_{La\,(20°C)}\,\varphi(T - 20) \quad (5.9)$$

Where,

T = Temperatue (°C), a constant

φ = Typical constant, the values in the range of 1.015 to 1.040 with 1.024 being the ASCE standard (Iranpour et al. 2000).

The alpha factor (α), the ratio of oxygen mass transfer coefficient (K_{La}) between processed water to clean water as shown in Eq. (5.10) is an important

factor for the design of any aeration device in a wastewater treatment plant. It accounts for the effect of process water characteristics on the oxygen transfer coefficient and the K_{La} of clean water is considered as a reference (Henkel et al. 2009).

$$\alpha = \frac{K_{La}\ of\ biomass}{K_{La}\ of clean\ water} \tag{5.10}$$

Many researches had been performed on α factor and a correlation between α factor and MLSS has been formulated as shown in Fig.5.13

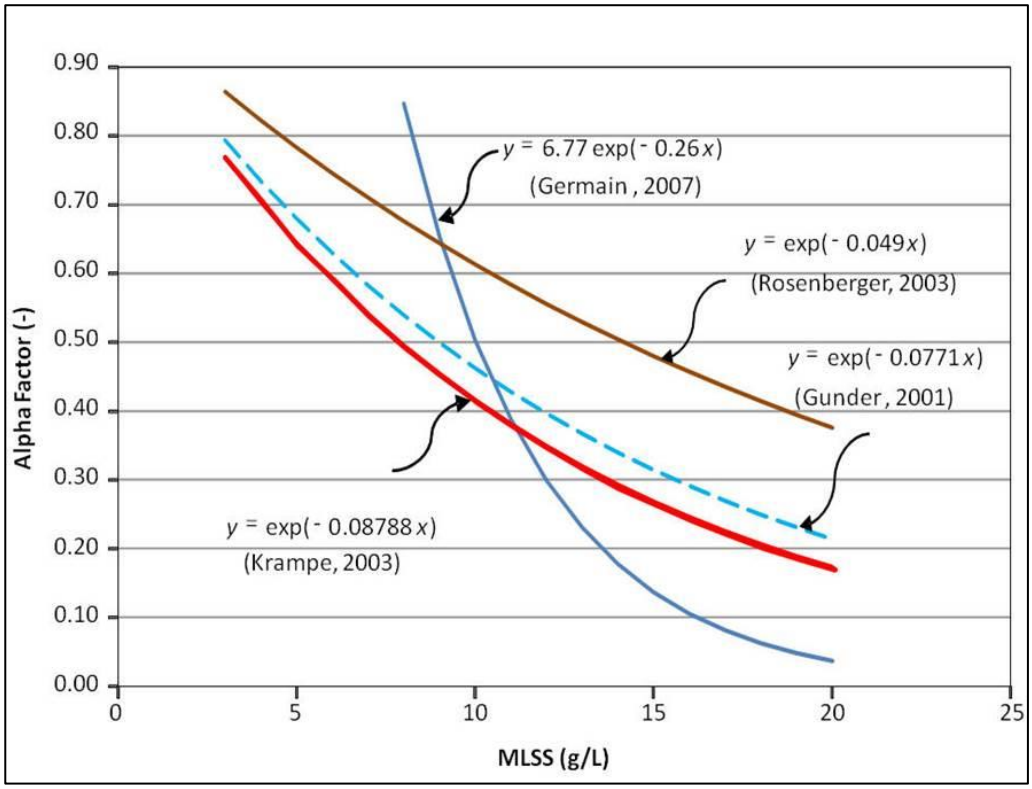

Fig.5.13 : Alpha factor and MLSS correlation (Online MBR info, 2013)

Due to the viscosity of the biomass led by the increase of MLSS, the α factor decreases exponentially. Among various researches (Fig. 5.13), the curve of Gunder (2001) and the curve of Krampe (2003) were accepted as a norm by most of other researchers. These correlations also set a limit to the development of MBR technology: most MBR installations work at the MLSS level of 8 – 12 g/L, while with a higher MLSS value, the oxygen transport efficiency

becomes too low to supply the biological degradation. On the other hand, generally, the exact correlation between MLSS and α factor varies in different MBRs, due to the different biomass compositions, concentration as well as the target pollutant. However, the exponential relationship is widely accepted.

The recommended DO for MBR is 2 – 4 mg/L (Judd, 2006) which may differ according to the applied processes. In this study, the aeration rate supplied in MBR reactor for all phases was 1.0 m^3/h with fluctuations due to varied accuracy of the control valve used for air supply and the corresponding dissolved oxygen (DO) were also fluctuating in the range of 1 to 6 mg/L (Fig. 5.14). This suggests that the DO obtained from the aeration is higher than the requirements.

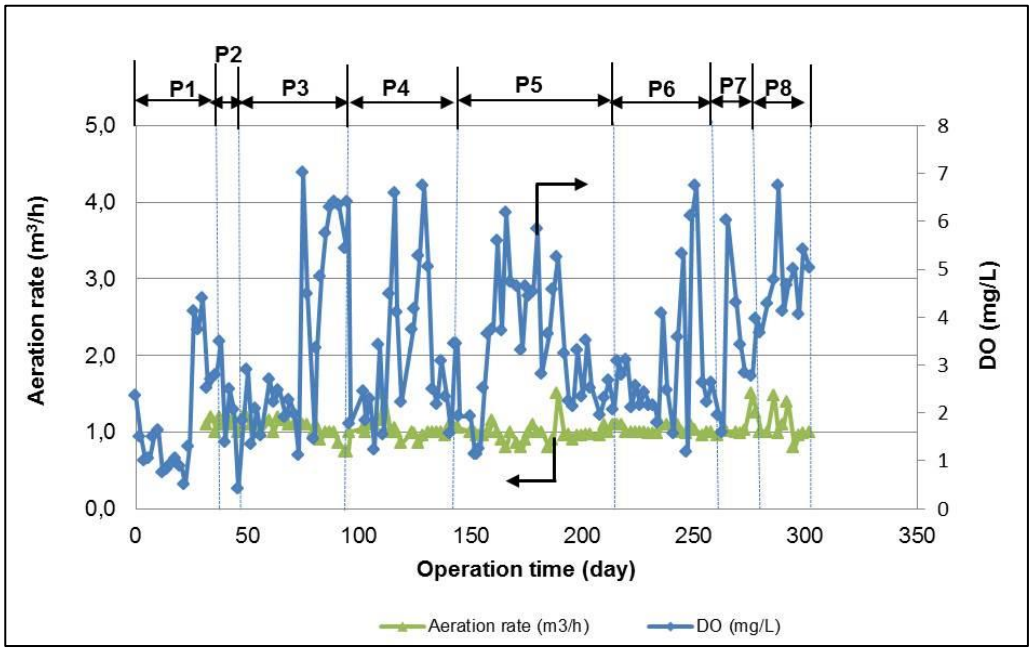

Fig. 5.14 : Effect of aeration rate and dissolved oxygen

5.6.6.2 Oxygen upate rate (OUR) vs dissolved oxygen (DO)

The oxygen uptake rate (OUR) is a parameter used to evaluate the rate at which metabolic processes take place in activated sludge treatment processes with sludge in suspension. The uses of the OUR test are to :

- Estimate the values of kinetic and stoichiometric parameters;
- Obtain data required to set up a mass balance of organic – and /or nitrogenous material;
- Evaluate the sludge activity in terms of the maximum and endogenous material;
- Determine the degree of sludge stabilisation after aerobic digestion

(Wastewater hand book, 2013)

The OUR in MBR reactor is highly responsive to DO (Fig. 5.15). This indicates that the microorganisms in the MBR reactor are very active and consume most of the available DO in the reactor. The corresponding COD removal efficiencies of the respective phases are also high (Fig.5.4). According to wastewater hand book (2013), in most activated sludge processes, the OUR will be in the order of 30 to 100 mg O^2/L.h for low and high rate systems respectively. The Fig. 5.15 shows the average value of OUR is 0.23 mg/L.min. which is equal to around 14 mg O^2/L.h. This result indicates that the OUR in this thesis is half of the lower range of OUR value reported by literature (Wastewater hand book, 2013) but the performance in terms of COD removal efficiency was high (Fig. 5.4)..

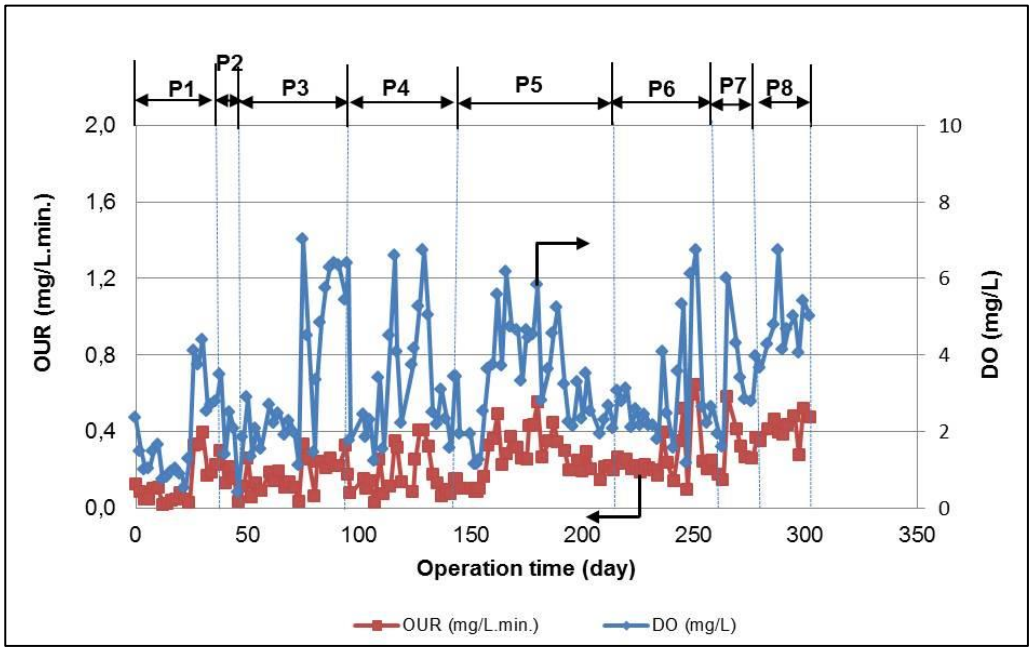

Fig. 5.15 : Effect of DO and O2 consumption

5.6.7 MLSS

5.6.7.1 MLSS in operation phases

Most of MBR units operate at mixed liquor suspended solids (MLSS) in the range of 8 to 12 g/L (Section 5.6.6.1, Fig. 5.13) and occasionally even higher (Van Nieuwenhuijzen et al., 2008; Visvanathan et al., 2000; Yang et al., 2006) reaching 20 to 35 g/L since membrane filtration is capable, in principle, to achieve effective solids-liquid separation. The consequence of such high MLSS is that the biomass (sludge) no longer behaves like a Newtonian fluid. Instead, it exhibits much higher viscosity that is also a function of solids, concentration, sludge characteristics, and applied shear stress (Trussell et a., 2007).

The range of MLSS in different operation phases in this sections were 10 to 12 g/L with little down grading values at the end of **P3** and **P8** (Fig. 5.16).

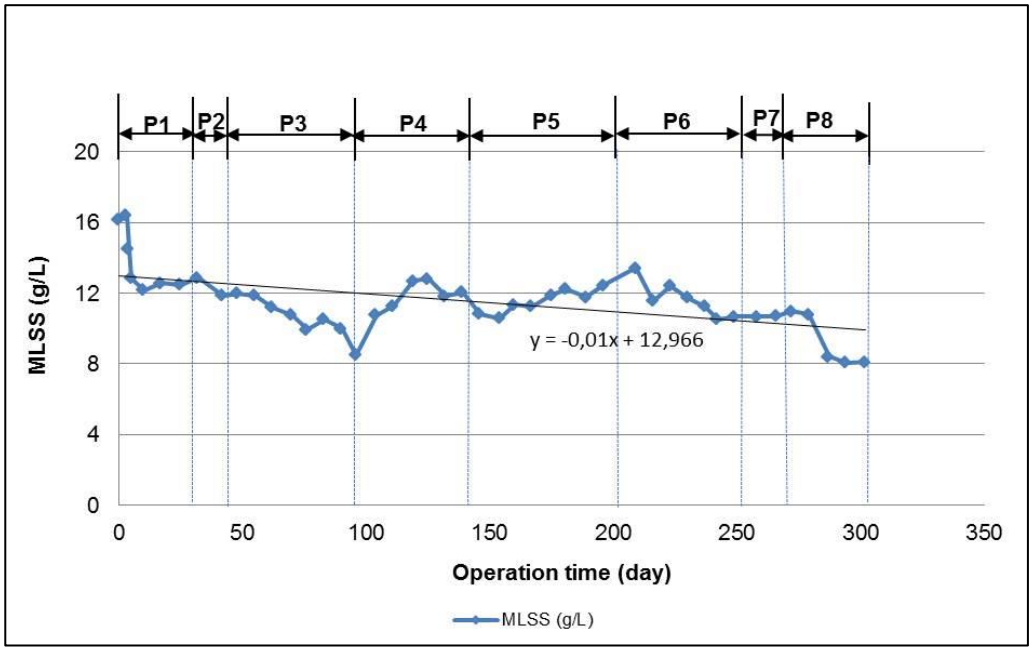

Fig. 5.16 : MLSS in different operation phases

These happened due to loss of reactor sludge through excess foaming. This suggests that the MLSS applied in this section of the thesis works is in line with the MLSS values reported in literatures. The trend line shows bit down-

grading values suggesting decrease of MLSS though no sludge was extracted except samplings. This concludes that the sludge age was extremely high.

5.6.7.2 Effect of MLSS on COD removal efficiency

Generally higher MLSS values contribute to higher COD removal efficiency. Because in higher MLSS value, quantity of microorganisms are expected to be high who can perform better degradation meaning higher COD removal rate from the reactor. But in this section, MLSS values show irresponsive to COD removal efficiency (Fig. 5.17). The extremely decreased value of COD removal efficiency in day 266 and day 272 occurred due to feed sample digestion (rotten) but not affected by MLSS.

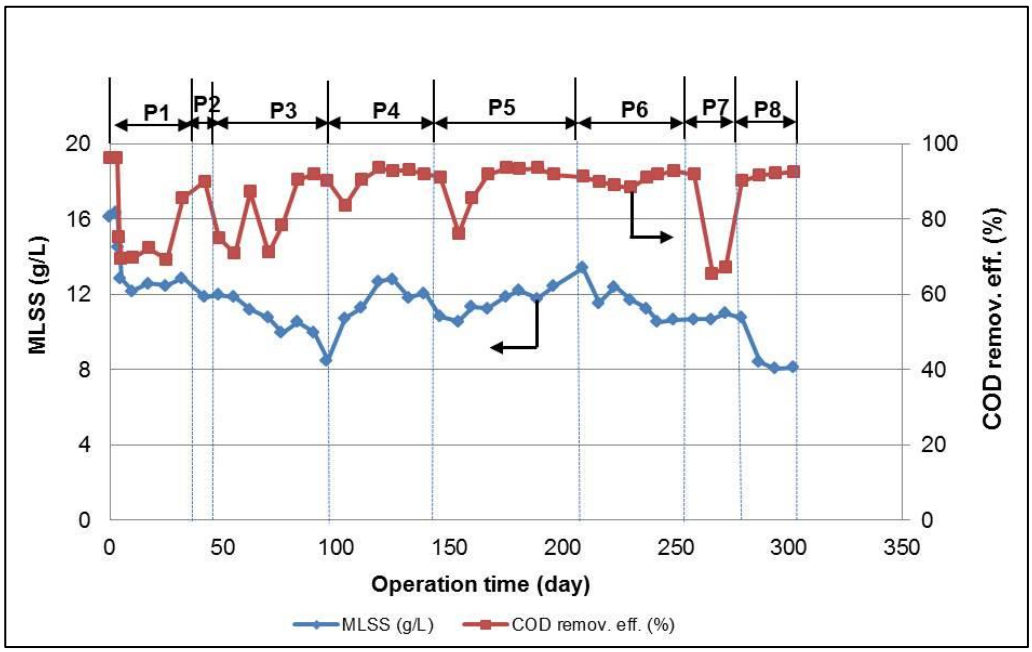

Fig. 5.17 : MLSS in COD removal efficiency

5.6.8 F/M ratio

Food to microorganism (F/M) ratio is one of the most fundamental control parameters for the activated sludge process. This is the relationship between load

of COD (bacterial "food") entering to the tank and the "mass of bacteria" in the tank.

The F/M ratio of the experiments carried out in **P1** through **P8** is around 0.1 Kg COD/Kg MLSS.d as shown in Fig. 5.18. It represents that the F/M ratio has very little effect in COD removal efficiency. The F/M ratio increased for a short time in day102 which happed due to comparative low HRT (25h) and in day265 due to feed decomposed (rotten). However, the value of F/M ratio applied in this section was close to the F/M ratio applied by Wu et al. (2013) in a full scale MBR operation treating TFT-LCD (Thin-film transistor liquid crystal display) wastewater with high strength of organic nitrogen where they found expected performance with increased nitrification at F/M ratio in the range of 0.1 to 0.3 COD/Kg MLSS.d. But almost no nitrification was observed at F/M ratio of 0.1 COD/Kg MLSS.d. in this PhD works as it is described in section 5.6.5. Further investigation for poor nitrification needs to be done.

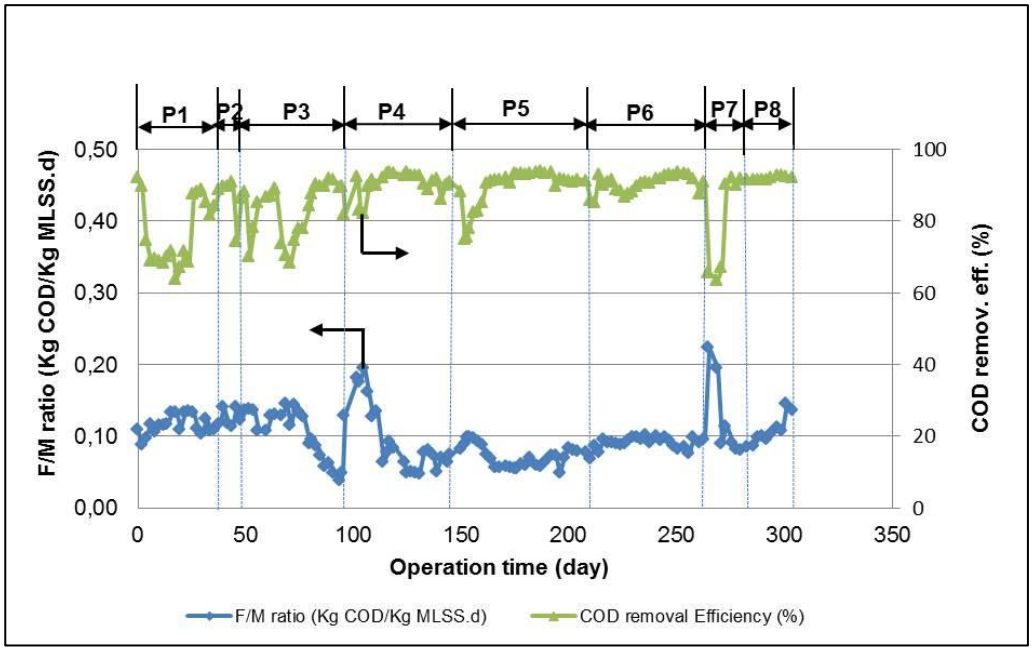

Fig. 5.18 : F/M ratio on COD removal efficiency

5.6.9 Chloride concentration and conductivity

The analysis of Chloride (Cl^-) concentrations were performed to check that permeate contains the same concentration of Cl^- as in MTDW. Because, theo-

retically Cl^- of MTDW should pass through the applied UF membrane to permeate due to membrane classification (Section 3.4). The accumulation of Cl^- in MBR reactor is not expected since it might create toxicity to the microorganisms in the reactor. The Cl^- concentration in permeate in **P1** through **P8** are in the range of 1700 to 1800 mg/L (Fig. 5.19) which are close to the concentration of Cl^- (1517 mg/L – 1756 mg/L) in MTDW. This means there is almost no accumulation of Cl^- in the MBR reactor.

Cl^- content represents the salt concentration which can be determined by conductivity measurement. Fig. 5.19 shows that the conductivity measurement is highly responsive to the Cl^- content. The addition of NH^4Cl from **P6** (phase6) lifted the Cl^- concentration in MTDW. Therefore, Cl^- also increased from **P6** until **P8** (phase8) which was confirmed by the conductivity measurements as shown in Fig. 5.19.

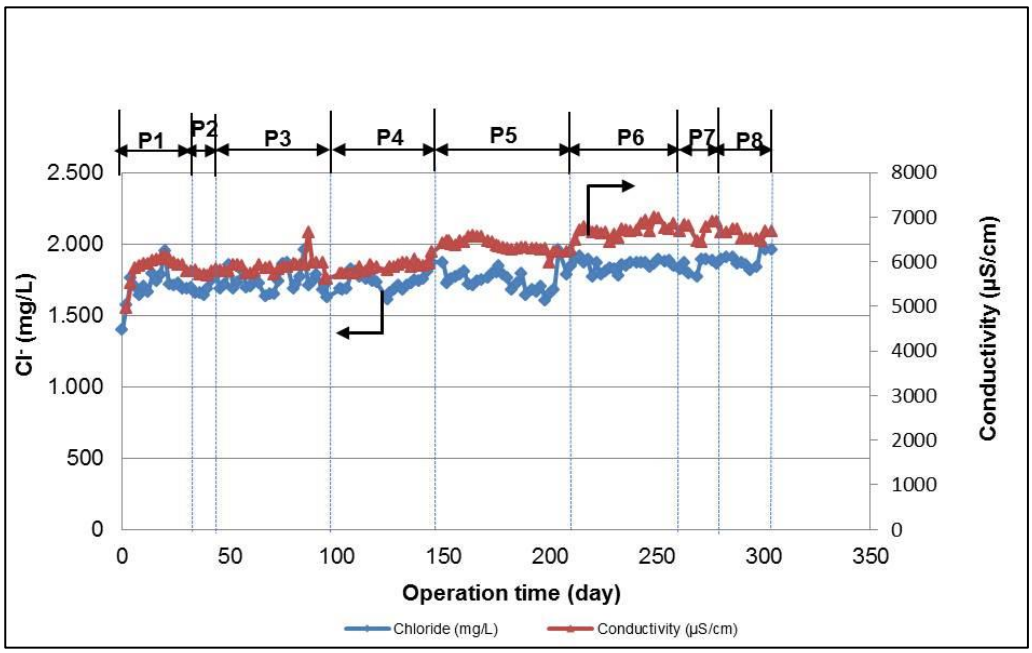

Fig. 5.19 : Cl^- concentration in permeate

5.6.10 Drying residue (DR) and Conductivity

Drying residue (DR) is the indicator of the amount of dissolved solid substances in permeates. The dissolved substances include Na^+, CO_3^{2-}, HCO_3^-, Cl^-

(salts), undegraded glucose, organic degradation products etc. The Fig. 5.20 showed that, the DR in the permeate kept almost constant during the entire experimental period. From the composition of the feed, DR can be calculated as shown in Eq. (5.11).

$$NaCl\ \left(2.5\frac{g}{L}\right) + \frac{NaCO3}{NaHCO3}\ \left(1.0\frac{g}{L}\right) \rightarrow DR\ \left(3.5\frac{g}{L}\right) \qquad (5.11)$$

The NaCl and $NaHCO_3^-$ in the feed were not biodegradable but highly soluble, and they can pass through the membrane pores as it was confirmed by salt rejection test (Section 4.2.5). Therefore, the same concentration of these contents could be expected in the permeate. The lowest level of drying residue in the permeate was around 3.5 g/L. Due to the biodegradability of the other contents in the feed, the difference of drying residue between the feed and permeate could be considered that those contents were partially degraded or adsorbed by the biomass.

Salt accumulation in the MBR reactor creates toxicity to the microorganisms which may hinder the regular activity of the biomass. The measurement of conductivity indicates if any salt accumulation is taking place or not. Fig. 5.20 indicates that permeate conductivity is roughly in the range of 5.5 to 6.5 mS/cm which is in line with the conductivity of MTDW (Table 5.1). This means no salt accumulation in the reactor took place.

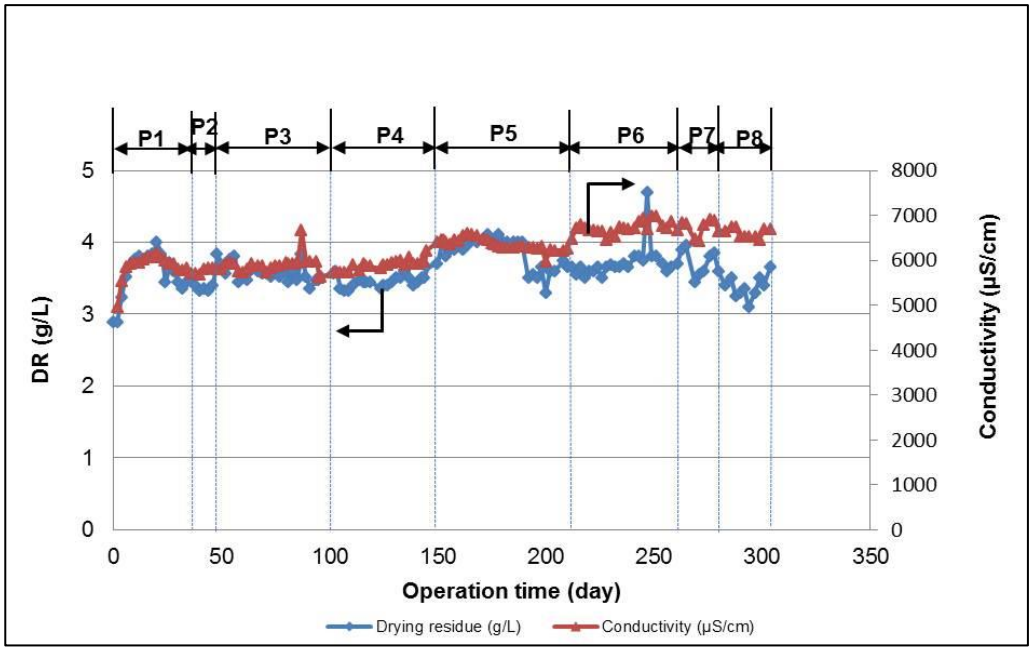

Fig. 5.20 : Permeate DR and conductivity

NH_4Cl was added at concentration of 300 mg/L in **P6** until **P8** which slightly increased the conductivity due to increased salt contents and DR increase was also expected but it was constant as shown in Fig. 5.20.

5.6.11 pH and temperature

pH sensor in permeate was used to detect the pH and temperature simultaneously. The Fig. 5.21, indicates permeate pH in the range of pH 7.5 to pH 8. These pH ranges have been achieved due to biological activities of microorganisms though feed pH values in **P5** through **P7** were high (pH10 ± 0.5). This indicates that pH 10 instead of pH7 didn't significantly change permeate pH.
The applied experimental temperature was 20 ± 2 °C except a little increased values in **P5** and **P6** due to summer time temperature rise of the experimental room but it had no significant effect in the results obtained.

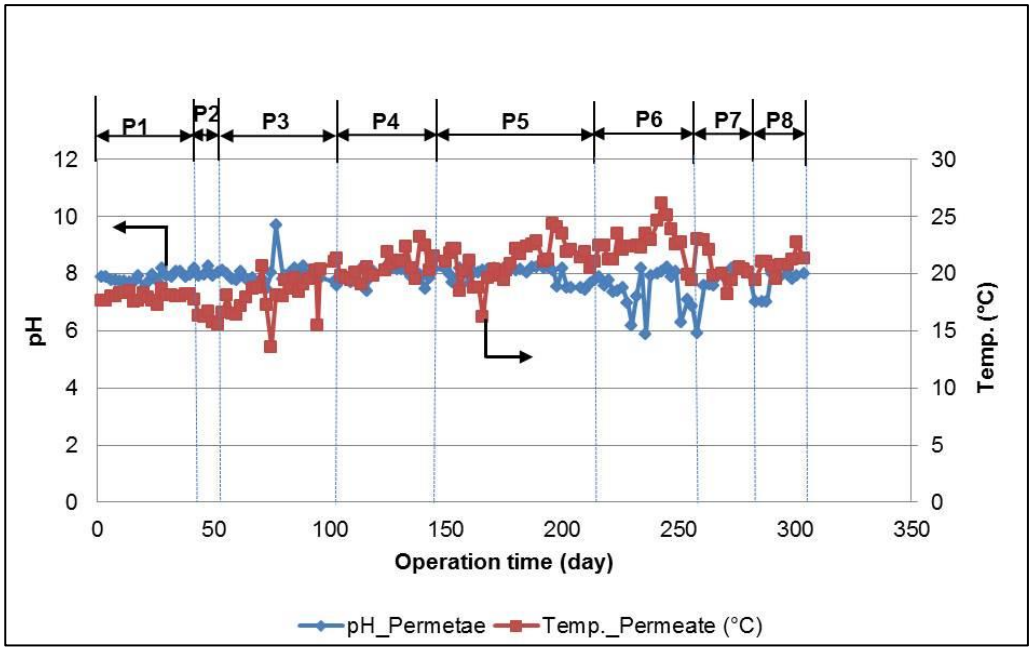

Fig. 5.21 : pH and temperature of permeate

5.6.12 Critical flux

According to Clech et al. (2003) no single and precise agreed protocol exists for critical flux measurement. A common practice is to incrementally increase the flux for fixed duration for each increment, giving a stable TMP at low flux but an ever-increasing rate of TMP increase at fluxes beyond critical flux (Bouhabila, 1998, Chen, 1997, Defrance, 1999a, Defrance, 1999b) . This method is preferred over the TMP-step method since it provides better control of the flow of material deposition on the membrane surface, as the convective flow of solute towards the membrane is constant during the run (Defrance, 1999a).

According to Bouhabila (1998), by plotting flux against TMP, it is possible to observe the transition between constant and non-constant permeability at the onset of fouling. The flux at this transition has been termed "Secondary critical flux". This approach was followed in this PhD works to determine critical flux.

For determining critical flux, the power of the suction pump (in terms of applied voltage) was increased step wise (Table 5.6) to have step wise flux increase with corresponding TMP. The experiment was carried out for 100

minutes with PES MBR module operated with activated sludge feeding MTDW. The maximum limit of TMP for the applied membrane module was 350 mbar recommended by the supplier (Microdyn-Nadir, Germany. The membrane was considered as fouled at above the TMP of 350 mbar.

Table 5.6 : Determination of critical flux in PES MBR module

Time interval (min.)	Applied voltage (V)	Flux (L/m^2.h)	TMP (mbar)
10	0.08	2.44	40.53
20	0.16	4.00	71.78
30	0.24	4.51	104
40	0.32	5.27	151.9
50	0.4	6.55	201.7
60	0.48	6.73	247.6
70	0.56	5.91	289.6
80	0.64	5.00	377.4
90	0.72	4.55	463.4
100	0.8	4.05	513.5

The critical flux of the applied PES MBR module is shown in Fig.5.22.

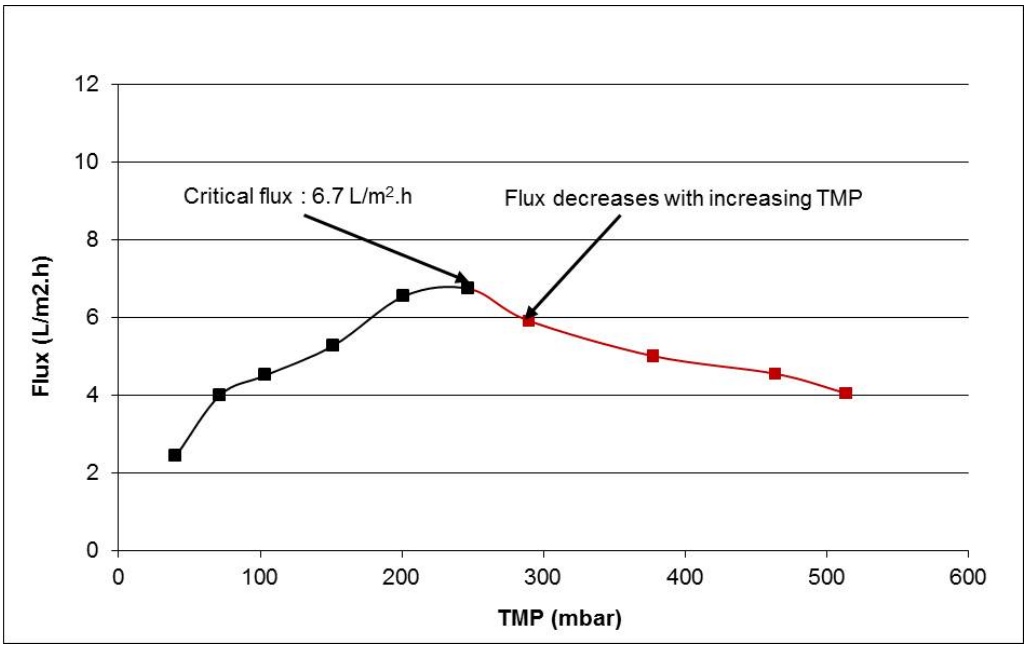

Fig. 5.22 : Critical flux of PES membrane

Fig. 5.22 shows the maximum flux 6.7 L/m^2.h at TMP of 247 mbar. After that the flux declined with increased TMP which is the indication of severe fouling. So, the critical flux of the membrane is 6.7 L/m^2.h.

5.6.13 Membrane resistance model

According to Dracy's Law a relationship between TMP and flux can be developed as shown in Eq. (5.12) (Section 2.1.3).

$$J = \frac{TMP}{\mu R_t} \tag{5.12}$$

Where,

J = Membrane permeate flux (L/m^2.h)
TMP = Transmembrane pressure (mbar)
μ = Dynamic viscosity of permeate (N.s/m^2)
R_t = Total filtration resistance (1/m)

R_t can be expressed as the sum of individual resistances which can be varied based on the number and type of resistances considered (adapted from Jifeng et al., 2008). For this thesis, the expression of R_t was different based on the test media and experimental set up. R_t for model foulant humic acid, model textile dye wastewater and MBR sludge were defined as R_f, R_dye and R_mbr respectively and these are shown in Eq. (5.13) through Eq. (5.15).

$$Rt\_f = R_m + R_{ha} \tag{5.13}$$

$$Rt\_dye = R_m + R_{mtdw} \tag{5.14}$$

$$Rt_{mbr} = R_m + R_{sludge} \tag{5.15}$$

Where,

R_m = Constant resistance of the clean membrane (1/m)
R_{ha} = Fouling resistance due to humic acid (1/m)
R_{mtdw} = Fouling resistance due to MTDW (1/m)
R_{sludge} = Fouling resistance due to MBR sludge deposited on membrane surface (1/m)

Eq. (5.13) can be termed as resistance in membrane series (RIS) model which is applied to describe membrane fouling mechanisms (Jifeng et al. 2008).

In this section of the thesis works, the RIS model has been adapted according to applied experimental set ups and test media. The membrane resistances in different experimental set ups with varied test media have been calculated in the following sections.

a) Resistances in "UF_auto" set up with model foulant humic acid (HA)

Prior to MBR applications, the commercial UF PES membrane was tested with model foulant humic acid (HA) to check the fouling behaviour of the membrane. The experimental set up used in this experiment was an auto-controlled UF cross-flow testing cell (Section 3.3, Fig. 3.5), termed as "UF-auto" in this section. Before starting the experiment with humic acid, the pure resistance of the membrane with DI water was determined. The TMP of the experiment was 500 mbar and the obtained flux was 319.80 $L/m^2.h$ with DI water. Considering dynamic viscosity of the water as $1.002*10^{-3}$ at 20°C (Raymond, 1996), R_m was calculated using Eq. (5.12) to $0.56*10^{12}$ 1/m. In this calculation, dynamic viscosity of water was assumed to be equal to that of permeate.

Similarly, the fouling test was carried out with humic acid applying UF auto set up and membrane resistance was calculated using Eq. (5.13). In this case, flux of the experiment was 63.67 $L/m^2.h$ with TMP of 500 mbar. Using the same viscosity value, the calculated membrane resistance (denoted as R_{ha}) was $2.26*10^{12}$ 1/m. In summary, pure membrane resistance contributes to around 20% to its total resistance where the rest of the 80% is contributed by humic acid.

b) Resistances in "UF_manu" set up with MTDW

The commercial PES membrane was also tested with model textile dyes to check the affinity of dyes to the membrane surface. The experimental set up used in this experiment was a manually -controlled UF cross-flow testing cell (Section 3.3, Fig. 3.3), termed as "UF-manu" in this section. The TMP of the experiment was 1500 mbar and the obtained flux was 528.17 $L/m^2.h$ with DI water. Considering dynamic viscosity of the water as $1.002*10^{-3}$ at 20°C (Raymond, 1996), R_m was calculated using Eq. (5.12) to $1.02*10^{12}$ 1/m.

Similarly, the test was carried out with MTDW and membrane resistance was calculated using Eq. (5.14). In this case, flux of the experiment was 231.92 $L/m^2.h$ with TMP of 1500 mbar. Using the same viscosity value, the calculated membrane resistance (denoted as R_{mtdw}) was $2.32*10^{12}$ 1/m. In summary, membrane resistance contributes to around 30% to its total resistance where the rest of the 70% was contributed by MTDW.

c) Resistances in MBR experiment with biological sludge

In MBR experiment, firstly the test was carried out with DI water before the trial with biological sludge (Section 5.2). The TMP of the experiment was 50 mbar and the obtained flux was around 25 $L/m^2.h$ with DI water (Fig.5.1). Considering the same dynamic viscosity of the water as $1.002*10^{-3}$, R_m was calculated using Eq. (5.12) to $0.72*10^{12}$ 1/m.

After that the experiment was carried out in MBR set up for almost 300 days starting from **P1** until **P8** (Section 5.6).

In this case, the average flux of the entire experiment was 2.8 $L/m^2.h$ with average TMP of 82.16 mbar. Using the same viscosity value, the calculated membrane resistance (denoted as R_{sludge}) using Eq. (5.15) was $10.54*10^{12}$ 1/m. In summary, membrane resistance contributes to around 7% to its total resistance where the rest of the 93% was contributed by biological sludge.

The summary of different resistances in different experiments is presented in Fig. 5.23 and Fig. 5.24. From Fig. 5.23, it is clear that the resistances with humic acid, MTDW and MBR have been increased significantly compared to their pure membrane resistances. This means that these kinds of media significantly contribute to membrane fouling. Fig. 5.24 indicates that percentage resistances of MBR bio sludge, humic acid and MTDW in their respective experiments are 93%, 80% and 70% respectively and these values compared to their pure membrane resistances are very high.

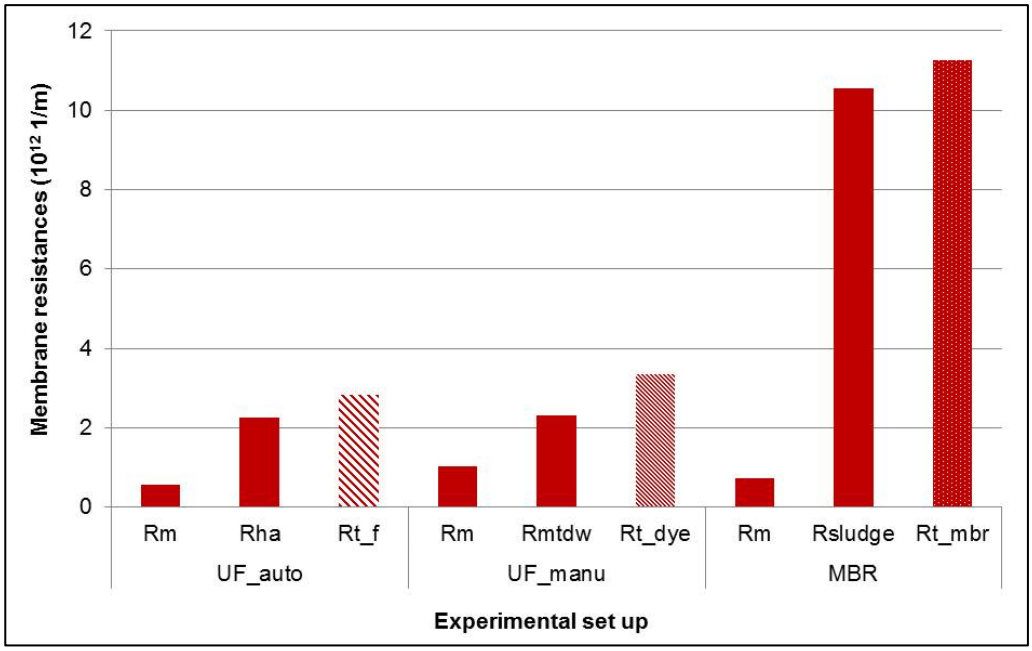

Fig. 5.23 : Numerical values of membrane resistances

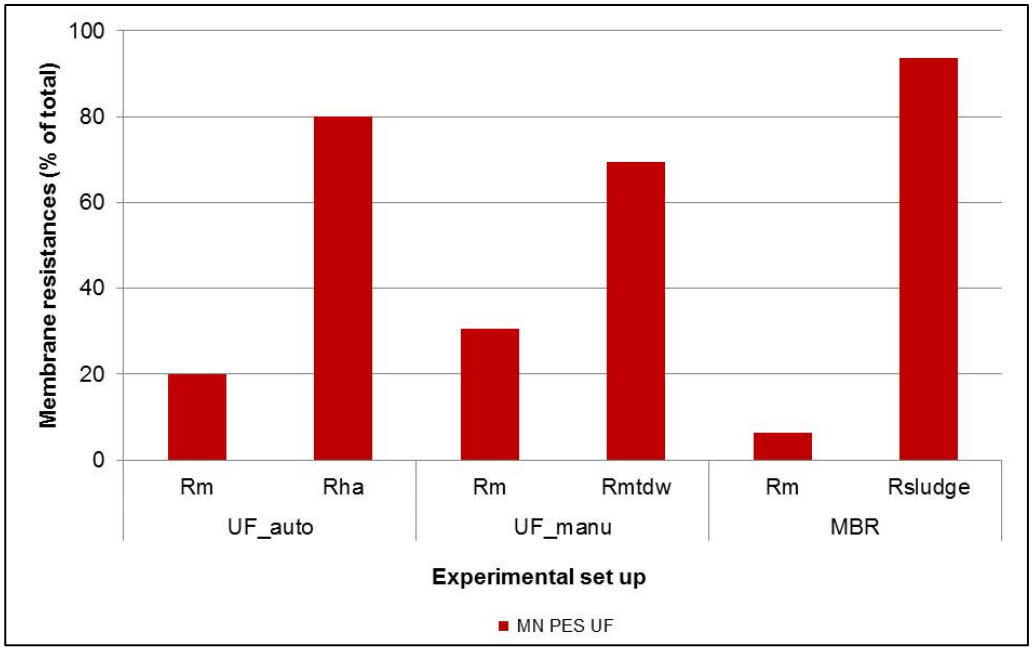

Fig. 5.24 : Individual contribution of membrane resistances

References

Bahadır K. Körbahti, Abdurrahman Tanyolac, (2009), Continuous electrochemical treatment of simulated industrial textile wastewater from industrial components in a tubular reactor, J. Hazard. Mater 170, 771–778.

Bouhabila, E.H., Aim, B. R., Buisson, H. (1998), Microfiltration of activated sludge using submerged membrane with air bubbling application to wastewater treatment, Desalination 118 (1998) 315 - 322

Brik, M., Schoeberl, P., Chamam, B., Braun, R. Fuchs, W., (2006): Advanced treatment of textile wastewater towards reuse using a membrane bioreactor, Process Biochem, 41 (8), 1751 – 1757, ISSN 0032 – 9592

Chen, V., Fane, A.G., Madaeni, S.S., Wenten, I.G., (1997), Particel deposition during membrane filtration of colloids transition between concentration polarization and cake formation, J. Membr. Sci. 125 (1997) 109 - 122

Clech, P.L., Jefferson, B., Chang, I.S., Judd, S.J. (2003) Critical flux determination by the flux-step method in a submerged membrane bioreactor, Journal of Membrane Science 227 (2003) 81 - 93

Defrance, L., Jaffrin, M.Y. (1999a) comparision between filtrations at fixed transmembrane pressure and fixed permeate flux: application to membrane bioreactor used for wastewater treatment, J. Membr. Sci. 152 (1999a) 203 - 210

Defrance, L., Jaffrin, M.Y. (1999b) Reversibility of fouling formed in activated sludge filtration, J. Membr. Sci. 157 (1999b) 73 - 84

Drews, A., Kraume, M. (2005), Process improvement by application of membrane bioreactors, Trans. IChemE A3, Chem, Eng. Res. Des. 83, 276 - 284

Feng, F., Xu, Z., Li, X., You, W., Zhen, Y. (2010), Advanced treatment of dyeing wastewater towards reuse by the combined Fenton oxidation and membrane bioreactor process, Journal of Environmental Sciences, 22 (11), 1657 - 1665

Field, R.W., Wu, D. Howell, J.A., Gupta, B.B. (1995) Critical flux concept for microfiltration fouling, J. Membr. Sci. 100 (1995) 259 - 272

Francisco A. Rodríguez, Patricia Reboleiro-Rivas, Francisco Osorio, María V. Martínez-Toledo, Ernesto Hontoria, José M. Poyatos (2011), Influence of mixed liquid suspended solids and hydraulic retention time on oxygen transfer efficiency and viscosity in a submerged membrane bioreactor using pure oxygen to supply aerobic conditions, Biochemical Engineering Journal 60, 135 - 141

Gunder, B. (2001). "The Membrane Coupled-Activated Sludge Process in Municipal

Wastewater Treatment." Technomic Publishing Company Inc., Lancaster, USA

Hach Lange, 2013, http://www.hachlange.ma, accessed on November 23, 2013

Henke, J., Lemac, M., Wagner, M., Cornel, P. (2009), Oxygen transfer in membrane bioreactors treating synthetic greywater, Water Res. 43, 1711 - 1719

Huang, R.R., Hoinkis, J., Hu, Q., Koch, F. (2009), Treatment of dyeing wastewater by hollow fiber membrane biological reactor, J. Desalination and Water Treatment, 11, 1 - 6

Idil A., A., Isil, A., B., Bahnemann, D.W., (2002), Advanced oxidation of a reactive dyebath effluent:comparison of O_3, H_2O_2/UV-A processes, water research 36, 1143-1154.

Iranpour, R, Magallanes, A., Zermeno, M., Varsh, V. Brishamchi, A., Stenstrom, M. (2000), Assesment of aeration basin performance efficiency: sampling methods and tank coverage, Water Res. 34 (12), 3137 - 3152

Isik, M., Sponza, D. T., (2008), Anaerobic/ aerobic treatment of a simulated textile wastewater, separation and purification technology 60, 64-72.

Judd, S. (2006), The MBR Book: Principles and Applications of Membrane Bioreactors in Water and Wastewater Treatment, editor, Elsevier

Jifeng, G., Siqing, X., Rongchang, W. (2008), Study on Membrane Fouling of Submerged Membrane Bioreactor in Treating Bathing Wastewater, Journal of Environmental Sciences 20, 1158–1167

Krampe, J., and Krauth, K. (2003), Oxygen transfer into activated sludge with high

MLSS concentrations. Water Science and Technology 47**,** 297-303.

Lin, S.H., Peng, C.F. (1996), Continuous treatment of textile wastewater by combined coagulation, electrochemical oxidation and activated sludge, Water Res. 30, 587–592.

Microdyn-Nadir GmbH (2010). MBR operating manual, Wiesbaden, Germany, www.microdyn-nadir.de.

Noor Sabrina Ahmad Mutamim, Zainura Zainon Noor, Mohd Ariffin Abu Hassan, Gustaf Olsson, (2012), Application of membrane bioreactor technology in treating high strength industrial wastewater: a performance review, Desalination 305, 1–11

Online MBR info (2013), http://onlinembr.info/MBR%20Design/MLSS%20and%20viscosity.htm , accessed on 27.10.2013

Palacios, S. (2009), Decolourization of azo and anthraquinone dyes by mean of microorganisms growing on wood chips, thesis, school of technology and design, department of bioenergy, Vaxjo, University, Sweden

Raymond A. Serway (1996), Physics for Scientists & Engineers (4th ed.). Saunders College Publishing. ISBN 0-03-005932-1

Trussell, R.R., Merlo, R.P., Hermanowicz, S.W. (2007), Influence of mixed liquor properties and aeration intensity on membrane fouling in a submerged membrane bioreactor at high mixed liquor suspended solids concentration, Water Research, 41 (5), 947 - 958

Van Nieuwenhuijzen, A.F., Evenblij, H., Uijterlinde, C.A. (2008), Review on the state of science on membrnae bioreactors for municipal wastewater treatment, Water Science and Technology, 57(7), 979 - 986

Viero, A.F., Sant' Anna Jr., G. L. (2008), Is hydraulic retentime an essential parameter for MBR performance?, Journal of Hazardous Materials 150, 185 – 186

Visvanathan, C., Ben Aim, R., Parameshwaran, K. (2000), Membrane separation bioreactors for wastewater treatment, Critical Review in Environmental Science and Technology, 30 (1), 1 - 48

Yang, W.B., Cickek, N., and Ilg, J. (2006), State-of-the –art of membrane bioreactors: Worldwide research and commercial applications in North America, Journal of Membrane Science, 270 (1-2), 201 - 211

Yigit, N.O., Uzal, N., Koseoglu, H., Harman, I., Yukseler, H., Yetis, U., Civelekoglu, G., Kitis, M. (2009), Treatment of a denim producing textile industry wastewater using pilot-scale membrane bioreactor, Desalination 240, 143 - 150

Zheng, X. and Liu, J. (2006), Dyeing an printing wastewater treatment using a membrane bioreactor with a gravity drain, Desalination, 190, 277 – 286

Wastewater handbook (2013)
http://www.wastewaterhandbook.com/webpg/th_organics_34OUR.htm#3_4_1, accessed on November 24, 2013

6. Chapter 6 : Membrane Bioreactor (MBR) Applying Novel Membrane

6.1 Experiment part

In this section, experiments were carried out using the same MBR set up as described in section 5.1 but the commercial PES module was replaced by novel MBR module that was prepared by coating the polymerisable bicontinuous microemulsion (PBM) on commercial PES membranes (Chapter 4) and the biological sludge conditions of the reactor kept the same as for the commercial module. The MBR module applied in this experiment is denoted as "PBM MBR module: PBM in short". Before applying this PBM MBR module with biological sludge, the functionality tests were done with DI water. The test result of PBM MBR module with DI water is shown in Fig. 6.1 below.

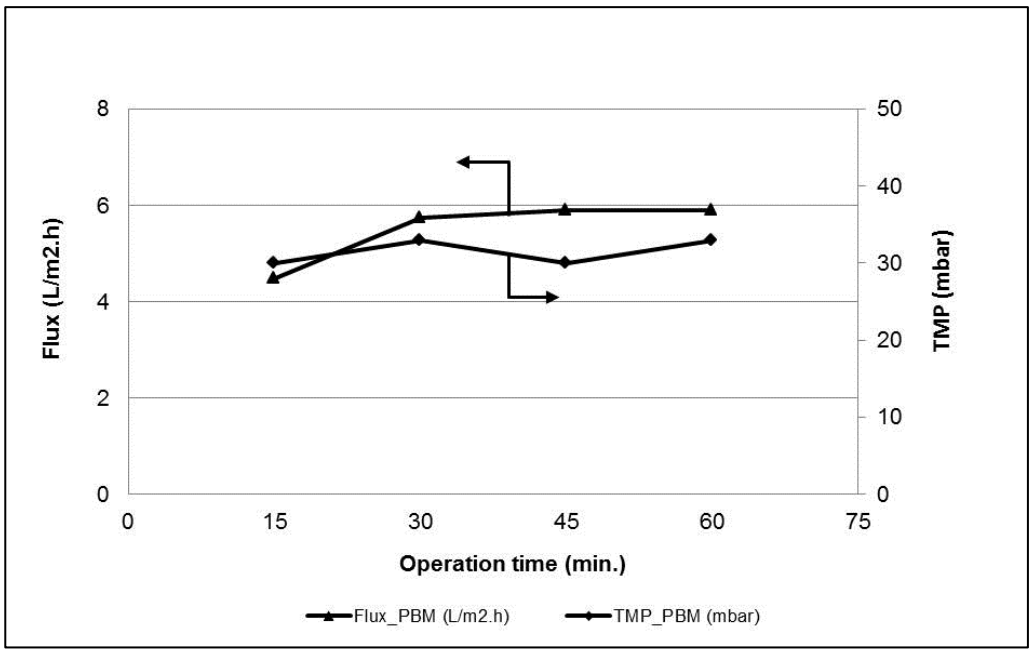

Fig.6.1: Start up results of PBM MBR module with DI water (Temp.: 20 ± 2°C, pH: 6.5 ± 0.5, cond.: 10 µS/cm)

Fig. 6.1 shows that the flux is close to 6 L/m^2.h with TMP of around 30 mbar which results in water permeability to around 200 L/m^2.h.bar. The water permeability of this PBM MBR module is similar to that of PBM membrane tested in section 4.2.6. To compare this water permeability value to that of commer-

cial PES MBR module it can be mentioned that PES MBR module shows the flux of 25 L/m^2.h with 50 mbar TMP resulting in 500 L/m^2.h.bar water permeability. This indicates that the water permeability of PBM MBR module is half or above the half of the commercial PES MBR module due to novel coating on the PBM module.

6.2 Operation conditions

The similar operating conditions as described in section 5.4 were also applied for the experiments carried out in this chapter. The applied operating conditions are summarised in Table 6.1.

Table 6.1 : Applied operating conditions

Parameter	Unit	Operating range
TMP	mbar	30 – 300
Critical flux	L/m^2.h	3.27
Operating flux	L/m^2.h	1.5
pH		7.5 ± 0.5
Temperature	°C	20 ± 2
Aeration rate	m^3/h	0.5 ± 0.05 – 1.0 ± 0.1
HRT	h	80 - 200
MLSS	g/L	6.5 – 8.5
Conductivity	mS/cm	6.6 ± 0.01

Sampling procedure

The sampling procedure used for this experiment was the same as the procedure described in section 5.5.1.

6.3 Results

The results of the experiments carried out under the operation conditions mentioned in section 6.2 are presented in the following sections. Following the operation conditions, the experiments were carried out for 183 days at 3 different conditions as shown in Table 6.2. The different conditions were applied to check the effect of the performance and the conditions were termed as **T1** (Trial1), **T2** (Trial2) and **T3** (Trial3) for better representation. Although the HRT of the PBM module is high (80 – 110 h) compared to the HRT (10 – 22 h) reported in different literature e.g. Huang et al. (2009), it is defined as normal in this section for experimental purpose.

Table 6.2 : Applied experimental trials

Notation	Designation	Duration	Process conditions (continuous)
T1	Trial1	day1 – day123	Continuation with normal HRT (80-110h); normal aeration rate (1.0 ± 0.10 m^3/h)
T2	Trial2	Day123 – day154	Increased HRT (167-203 h); normal aeration rate (1.0 ± 0.10 m^3/h)
T3	Trial3	Day154 – day183	normal HRT (80-110 h); reduced aeration rate (0.5 ± 0.05 m^3/h)

6.3.1 Water production

6.3.1.1 Flux and TMP

Fig. 6.2 indicates the flux & TMP of the entire experiments from **T1** (Trial1) to **T3** (Trial3). The flux in **T1** was around 2 L/m^2.h with TMP of around 50 mbar at the beginning of the experiment but the values were fluctuating at the end. The TMP jumped at day 102 with corresponding flux increase. The reason of this jump was not clear. It might be happened due to faulty behaviour of the suction pump. The flux reduced significantly in **T2** with reduced TMP. At the end of the experiment, it was noticed after opening the module that 2 out of 3 membrane sheets of MBR module got clogged (probably mechanical blocking) which might have reduced the active area of the membrane and consequently the flux declined. The flux improved a bit in **T3** (Trial3) but the TMP was significantly high. The reduced aeration intensity in **T3** might have caused weaker scouring effect on the membrane surface favouring fouling generation which might lead the TMP jump with expected flux production.

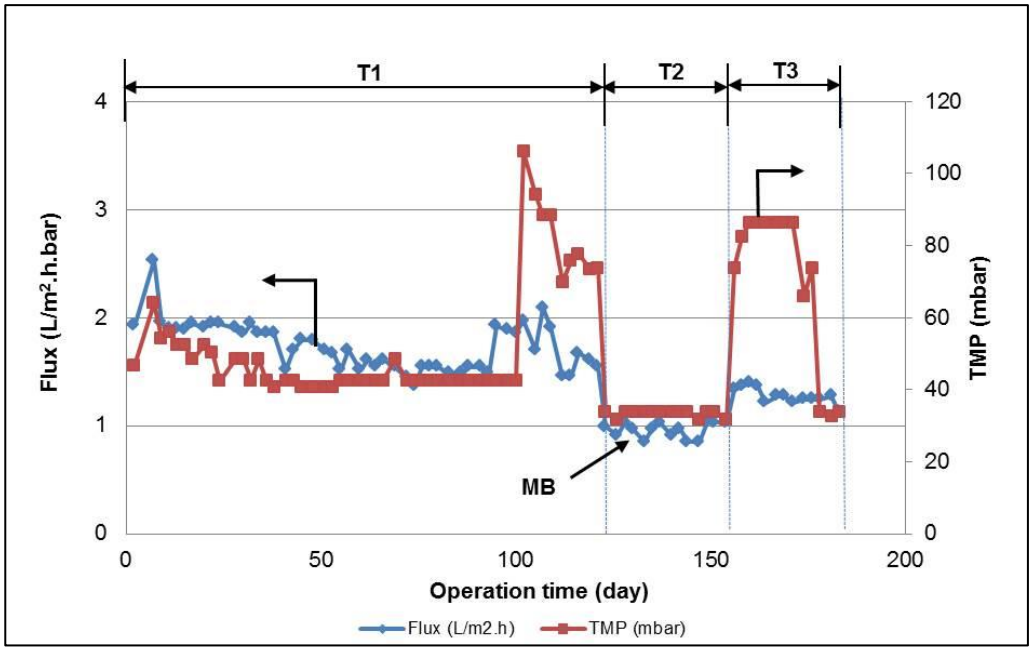

Fig. 6.2 : Flux and TMP of the experiment

N.B.:
MB : Mechanically blocked (probably)

6.3.1.2 Water permeability

The permeability of the whole experimental period is shown in Fig. 6.3. At the beginning of the experiment in **T1** (Trial1), the permeability was around 40 L/m^2.h.bar but it dropped significantly at the end of **T1.** The aeration intensity closed to this region (day 88 – day 98) was fluctuating with downgrading values. Since aeration intensity plays an important role (Section 6.3.6.1, T3), it might occurred due to variation of the aeration rate. It was assumed that the mechanical blocking of two membrane sheets (Section 6.3.1.1) might have caused this result. The permeability improved a bit in **T2** (Trial2) assuming that the blocking might have reduced due to constant aeration rate. The permeability declined to below 20 L/m^2.h.bar in **T3** (Trial3) due to high TMP jump at reduced aeration rate. The membrane surface might have covered with biological sludge due to less scouring effect resulting from reduced aeration intensity. At the end of **T3** there was a sudden TMP jump. The MTDW used as feed was decomposed and partial anaerobic condition might have occurred at this stage which could have caused this jump.

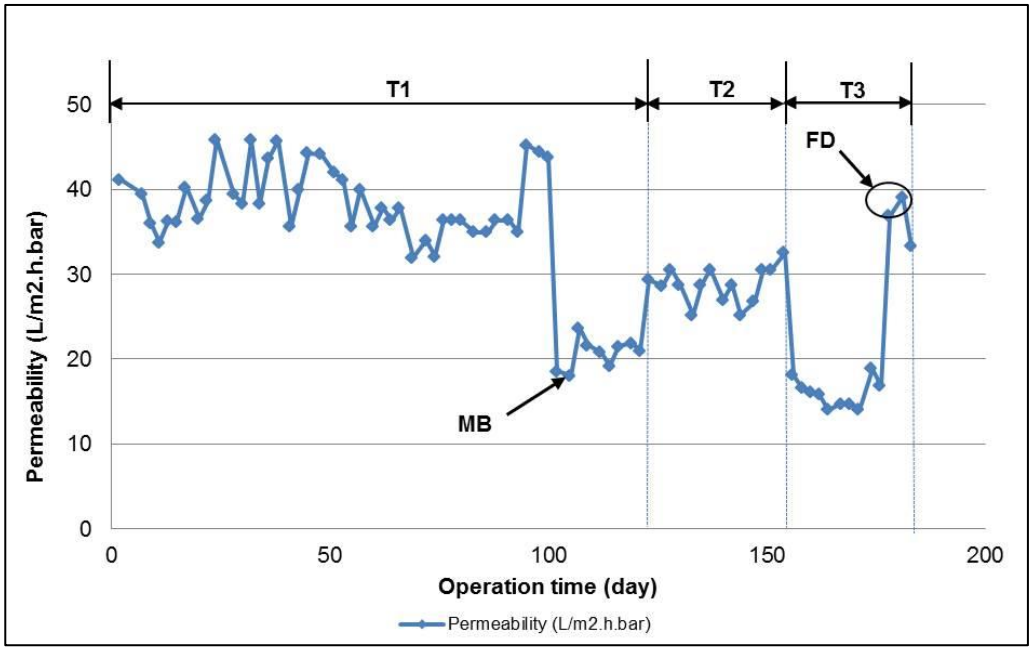

Fig. 6.3 : Water permeability of the PBM MBR experiment

N.B.:
MB : Mechanically blocked (probably)
FD : Feed decomposed (rotten)

6.3.2 Hydraulic Residence Time (HRT)

Fig. 6.4, represents the hydraulic residence time (HRT) of the experiments of **T1** (Trial1) to **T3** (Trial3). HRT values were different at different trials starting from 80 h to around 200 h. with average range of 100 h – 110 h except some high HRT area (day108-day137) which was increased intentionally to observe the effect of nitrification. This indicates that MTDW remained in this PBM MBR reactor for longer time compared to PES MBR reactor. As reported by Viero et al. (2008), the HRT in MBR technology indicates if the system is being operated under steady-state conditions meaning if the system is running smoothly, without significant fluctuation of HRT. The experiment in **T1** and **T3** are in line with this argument but **T2** was fluctuating due to process variation which was done intentionally to see the effect of process variations. This suggests that this experiment could be run at steady-state conditions.

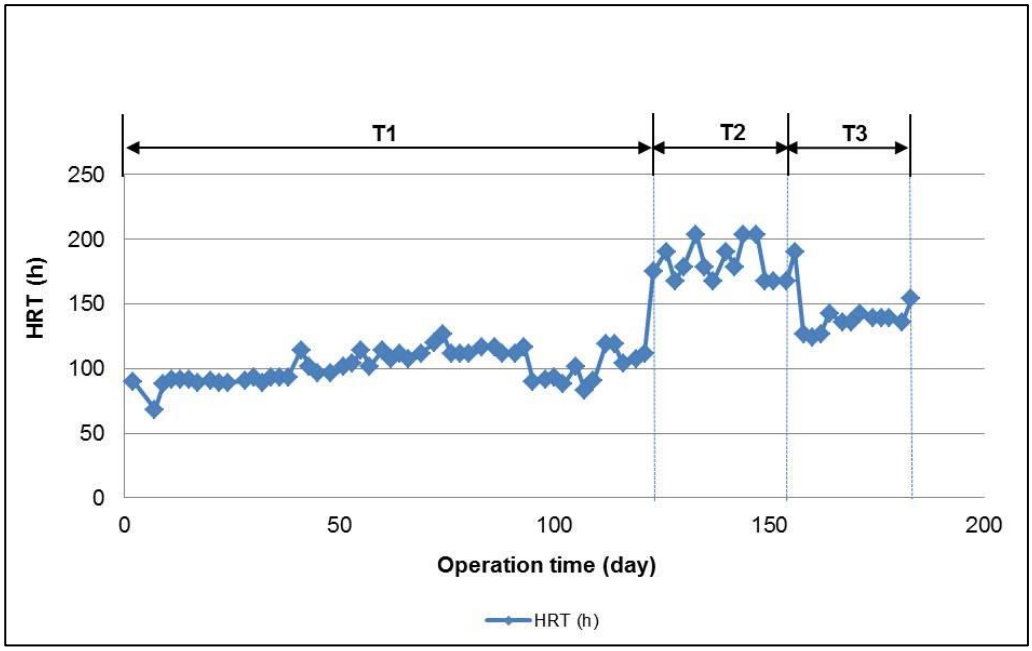

Fig. 6.4 : HRT of the PBM MBR experiment

6.3.3 COD and TOC

6.3.3.1 Permeate COD and COD removal efficiency

Fig. 6.5 represents the COD removal efficiency for the whole duration of the experiments. With all experimental trials (**T1**-**T3**), the COD removal efficiency was in the range of 95%-96% with high degree of stability. This means that variation of operating process conditions like increasing HRT or decreasing aeration intensity had no effect on COD removal efficiency. It was expected that at high HRT especially at HRT of 200h in **T2** (Trial2), there could be higher COD removal efficiency (more than 96%) since MTDW remained in the reactor for longer time which could better degraded by microorganisms. Similarly, at reduced aeration rate in **T3** (Trial3), it was speculated that micro-organism could face the short fall of oxygen availability in the reactor which could result in poor COD removal efficiency. But in both of the cases (**T2** and **T3**), COD removal efficiency were not affected by the changes of the process conditions. This indicates that PBM MBR process is a robust process and it might be due to the modified membranes applied in the process. The feed COD

values from day 102 to day 112 were bit lower than the usual values. This happened due to analysis error.

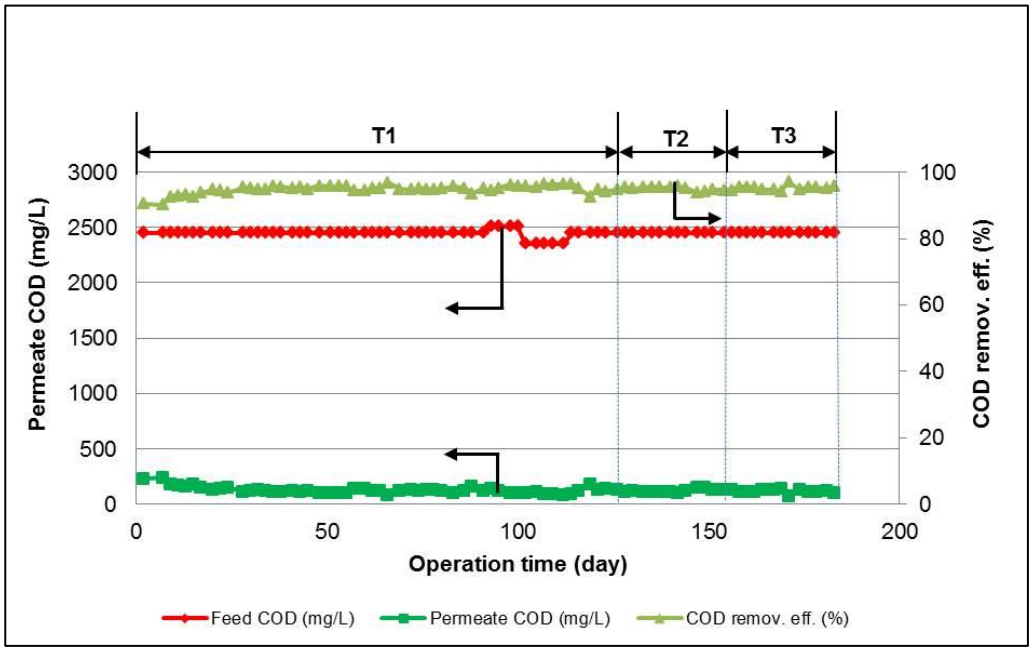

Fig. 6.5 : COD removal efficiency

6.3.3.2 Effect of HRT on COD removal efficiency

The effect of HRT on COD removal efficiency is shown in Fig. 6.6. This result summarises that there is no influence of HRT on COD removal efficiency. This result is in line the results obtained by Viero et al. (2008) treating synthetic municipal wastewater with hollow fibre MBR module at HRT in the range of 2 h to 5 h.

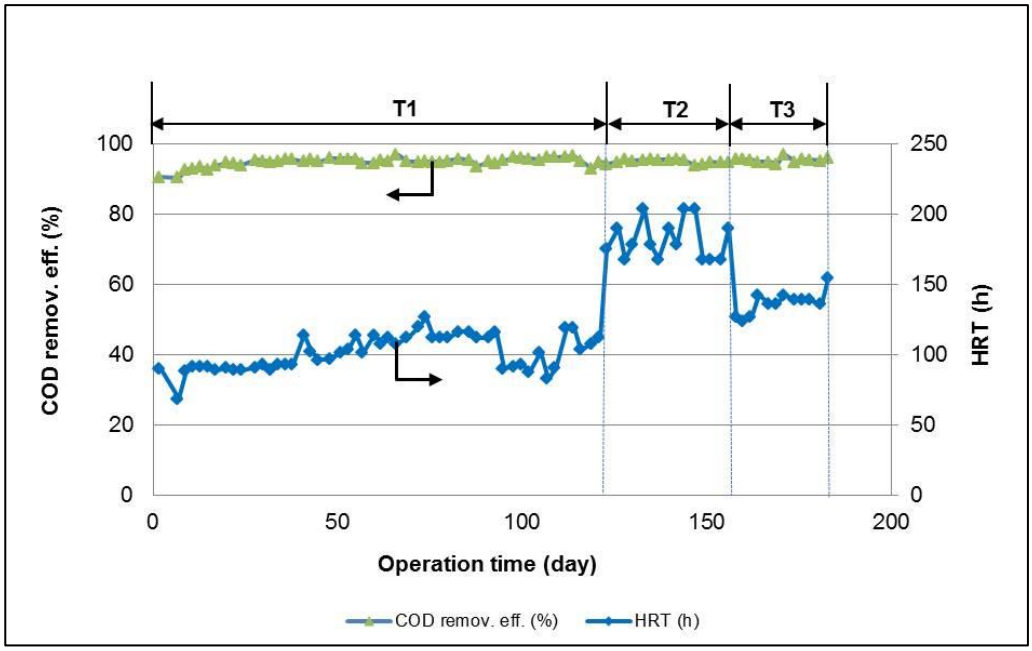

Fig. 6.6 : Effect of HRT on COD removal efficiency

6.3.3.3 COD and TOC relation

Generally the COD value of the wastewater should be correlated with TOC value since both of them are chemical parameters. Therefore, both COD and TOC parameters are related to the organic load. Though the COD value is widely used for determining the strength of organic load but it can't reflect the degree of wastewater precisely due to the impacts of types and concentration of oxidants, reaction temperature and time, etc. On the other hand, TOC does this job precisely with high reliability. Theoretically, TOC is considered as ¼ - 1/3 of COD values.

Fig. 6.7 represents the permeate COD and TOC values where the TOC/COD ratio is 0.23 in average. The TOC values in **T1** (Trial1) through **T3** (Trial3) are responsive to those of COD values (neglecting the small variations of permeate COD) except some fluctuations in **T2** (Trial2) and **T3** (Trial3). The COD values at the beginning of **T1** were high. This might be happened due to application of PBM MBR module which was a new situation to microorganisms and it was acclimated gradually. TOC values were less fluctuating compared to COD values. Some TOC values were missing from day38 to day62 in **T1** (Trial) due

to samples disposed mistakenly. The good correlation of COD and TOC indicates the robustness of obtained process parameters.

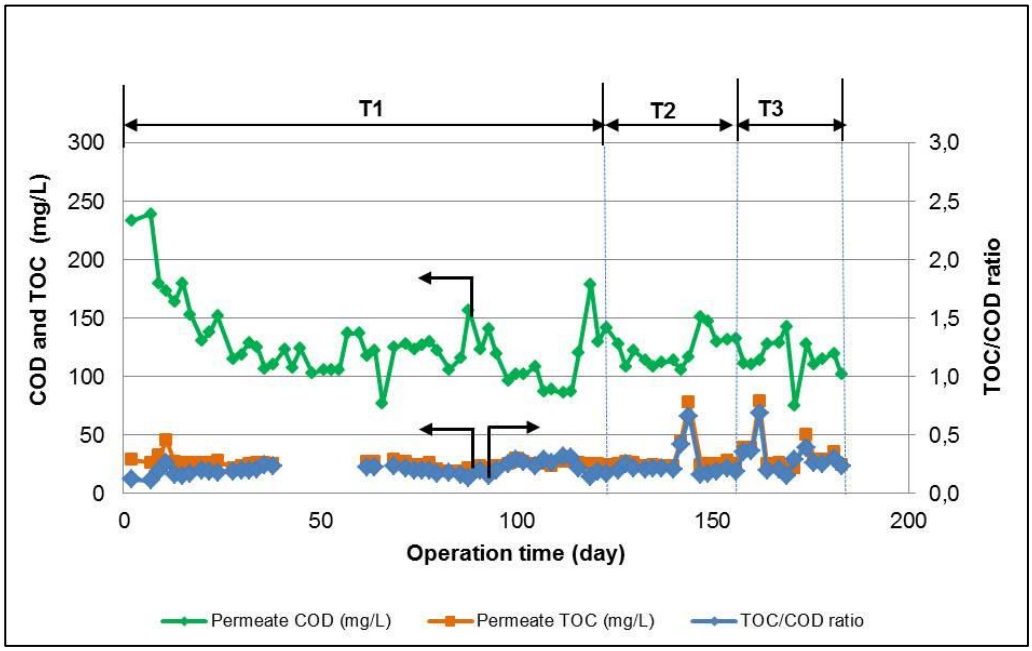

Fig. 6.7 : Relation between COD and TOC

6.3.3.4 TOC removal efficiency

As described in section 6.3.3.3, the TOC result represents more reliability than that of COD in terms of organic load contents. The reflection of this kind of reliability was also noticed in this section. Fig. 6.8 shows that the maximum COD and TOC removal efficiencies are 96% and 98% respectively presenting TOC removal efficiency is lightly higher than COD removal efficiency and they are highly correlated in different operation trials (**T1** through **T3**). It is worth to mention here that some of the TOC values were missing due to misused of the samples in **T1**. Nevertheless, the result shows the high accuracy of the analyses.

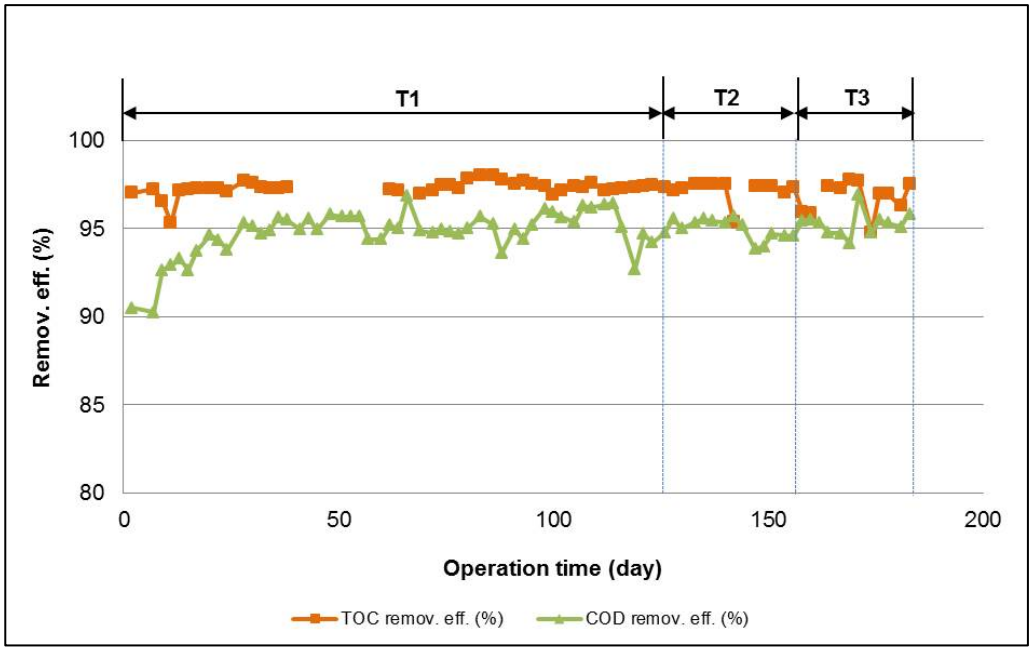

Fig. 6.8 : Comparison of COD and TOC removal efficiency

6.3.3.5 Permeate COD and reactor COD

The analysis of reactor COD were done (Section 3.9.5) and these values were compared with permeate COD values. The rector COD were analysed to check if the organic compounds were accumulated in the reactor. The results of the whole trial periods of **T1** to **T3** (Table 6.2) are presented in Fig. 6.9. Basically, the COD values of permeate and reactor are supposed to be closer if they are not accumulated in the reactor because biologically they are more or less the same except two different physical separation processes. Reactor COD values as shown in Fig.6.9 are generally higher than the permeate COD values showing fluctuations. The occurring fluctuations and the gap between permeate COD and reactor COD, which are not so high, might be due to the processes applied to determine them. The special observation is that the reactor COD values were not increasing over the trial periods indicating no trend of COD accumulation in the MBR reactor and representing a good degradation process.

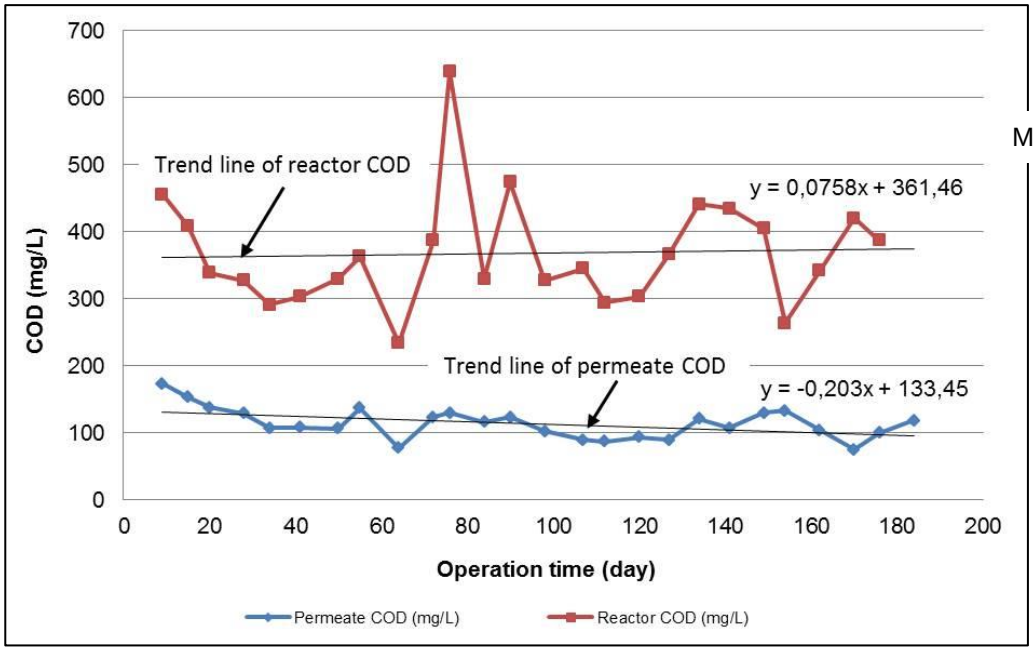

Fig. 6.9 : Comparison of permeate and reactor COD

6.3.4 Dye removal efficiency

6.3.4.1 Dyes in permeate

Fig. 6.10 represents red and blue dye removal efficiencies of **T1** to **T3**. Red and blue removal efficiencies are roughly 40% with higher fluctuations and 60% with reduced fluctuations respectively in different trials. Between these two dyes, Blue is slightly higher biodegradable than Red. This also might have contributed these results. Since the membrane used in the MBR module was PES ultrafiltration modified by novel coating (Chapter 4) which reduced its pore size blue dye removal efficiency was supposed to be higher than red due to their reduced molecular weight cut off (Section 4.2.4). Fig. 6.10 represents the similar results as expected.

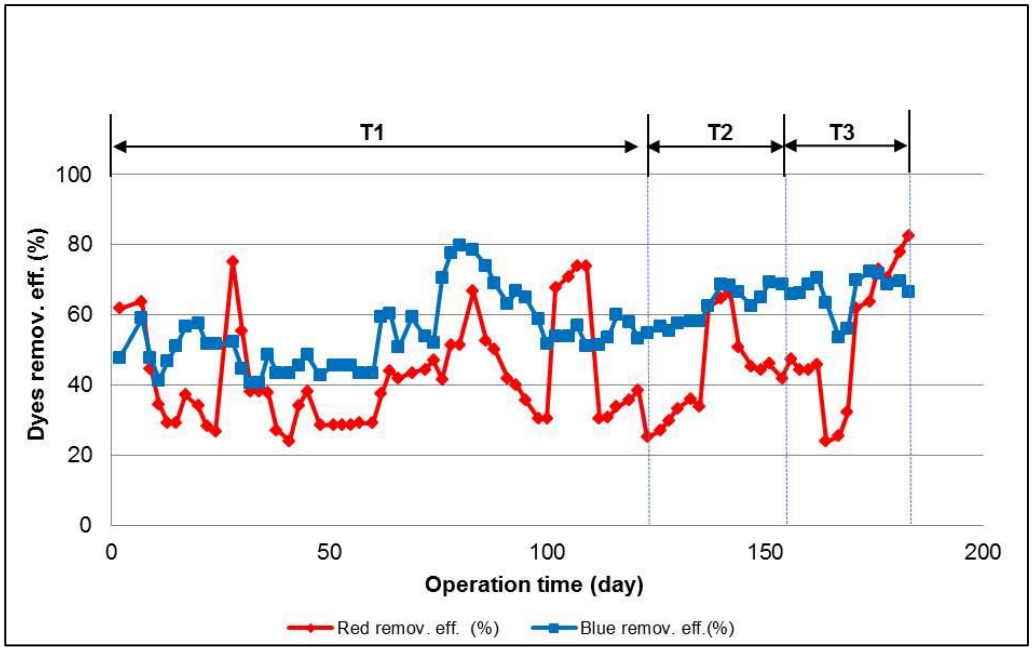

Fig. 6.10 : Red and blue dye removal efficiencies

6.3.4.2 Reactor dyes

The analysis of reactor dyes were done (Section 3.9.5) and these values were compared with concentration of permeate dyes. These were done to check if the dyes were accumulated in the reactor. The results of the whole periods of **T1** to **T3** (Table 6.2) are presented in Fig. 6.11. Basically, the dyes (red and blue) of permeate and reactor are supposed to be closer if they are not accumulated in the reactor because biologically they are more or less the same except two different physical separation processes. Reactor dyes (red and blue) as shown in Fig.6.11 are lower than the permeate dyes with some fluctuations. The occurring gap between permeate dyes and reactor dyes might have occurred due to applied sonication process. It was assumed that after sonication, the dyes adsorbed on the sludge will be released. Since dyes in permeate are lower than those of reactor, the dyes might have not released from the sludge. Further investigation on this work is needed.

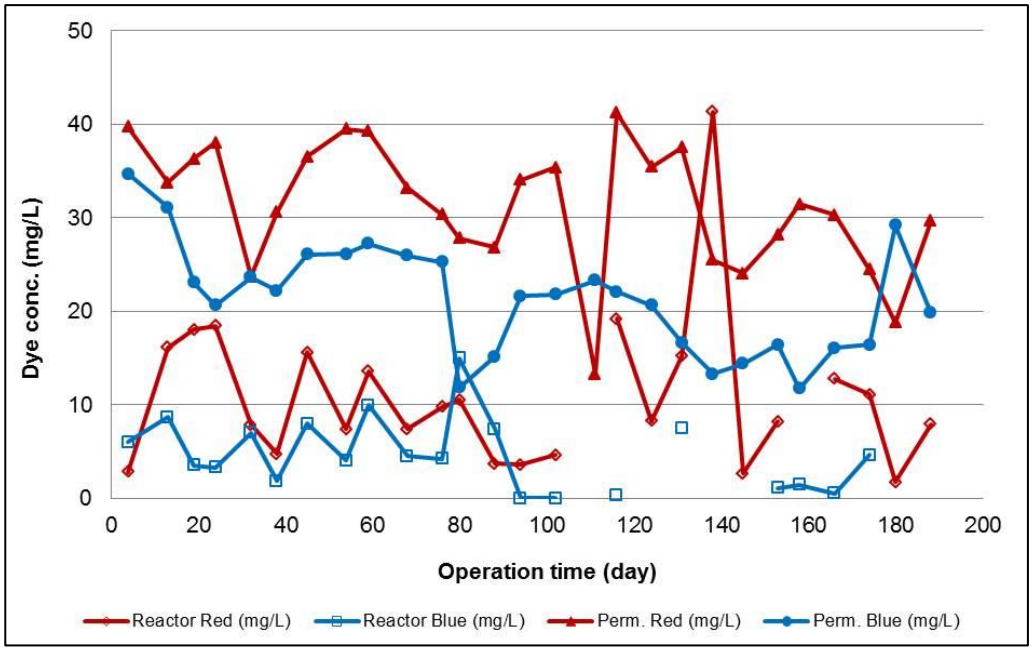

Fig. 6.11 : Comparison of permeate and reactor dyes

6.3.5 N-Balance

Sources of Total-N

The main source of nitrogen (N) in MTDW (Section 3.6) were dyestuffs (red and blue) and NH_4Cl where red, blue and NH_4Cl contributed (calculated theoretically) to nitrogen (N) amount of 2.2 mg/L, 3.7 mg/L and 78.5 mg/L respectively summing up total N (TN) in feed as 84.4 mg/L (Section 5.6.5). In this case, NH_4Cl was added as N-source to reach nutrient enriched feed for the experiment.

Nitrification and denitrification

Generally in wastewater treatment, the removal of total nitrogen by biochemical degradation takes place by oxidation of ammonia to nitrate under aerobic conditions and conversion of nitrate to nitrogen gas under anoxic conditions. Both of the processes demand that specific micro-organisms prevail. The biological generation of nitrate from ammonium (NH_4^+) under aerobic conditions (nitrification), takes place in two distinct stages and denitrification takes place

under anoxic conditions when oxidant of organic carbon takes place using the nitrate ions (NO_3^-), generating molecular nitrogen (N_2) as the primary end product as described in section 5.6.5 (Judd, 2006) (Section 5.6.5). Since this PhD works focused on aerobic MBR, no denitrification was considered.

Fig. 6.12 represents N-balance from **T1** to **T3**. Theoretically, the Total-N in the permeate supposed to be equal to that of feed. It was noticed that at the beginning of T1, the Total-N in the permeate (Total-N_perm.expt.) were higher than that of feed which doesn't support the logic. It can be assumed that some of the Total-N in the permeate might have released which were accumulated in the previous phase. The Total-N in the permeate from the middle of **T1** until end of **T3** were close to the Total-N of feed which is the good indication of steady state condition. The calculated Total-N (summing up NO_3^--N and NH_4^+-N) in permeate (Total-N_perm.calc.) were bit lower than the experimental Total-N in permeate. This gap might have been created due to nitrogen (N) accumulation in the biological sludge during conversion to NO_3^--N or NH_4^+-N or nitrogen (N) conversion in other form like NO^{2-}-N which was not detected.

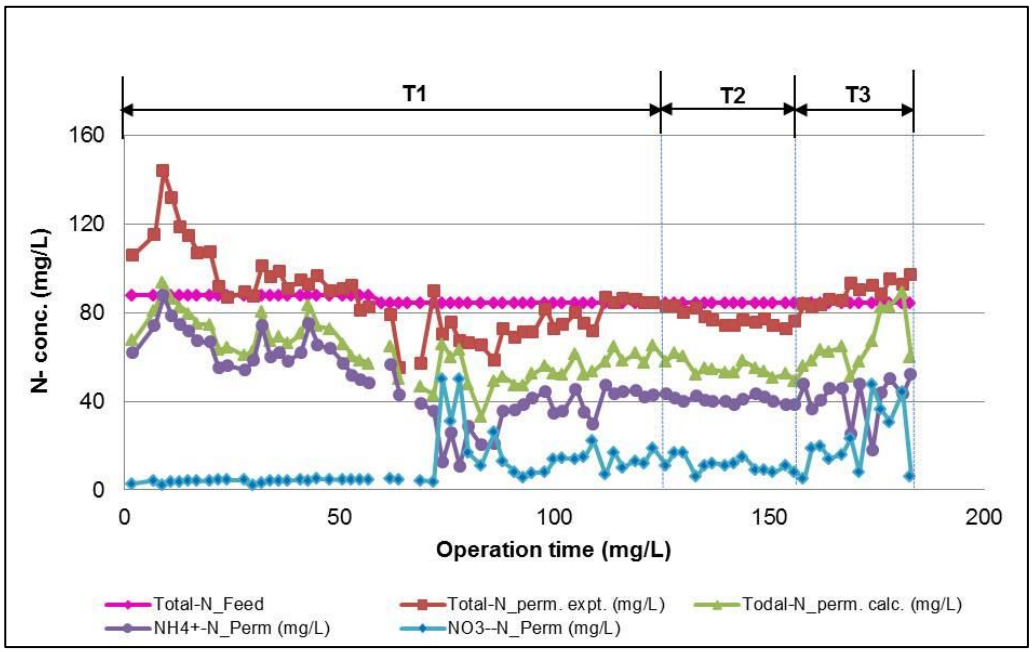

Fig. 6.12 : N- compounds

Fig. 6.12 indicates conversion of feed NH_4^+ to 55% of NH_4^+–N and 15% of NO_3^-–N in permeate and the rest of the total-N in permeate was undetected. This indicates very low nitrification especially for MBR application.

Difference between experimental TN and calculated TN

The difference between experimental TN (Total-N_perm.expt) measured by spectrophotometer from Shimadzu (Section 3.9.7) and the calculated TN (Total-N_perm.calc.) generated from addition of NH_4^+-N, NO_3^-N and Dye-N (Eq. 5.7a and Eq. 5.7b) were shown in Fig. 6.13. It shows positive values of nitrogen from **T1** until **T3** calculated using Eq. (5.7a) and Eq. (5.7b) (Section 5.6.5).

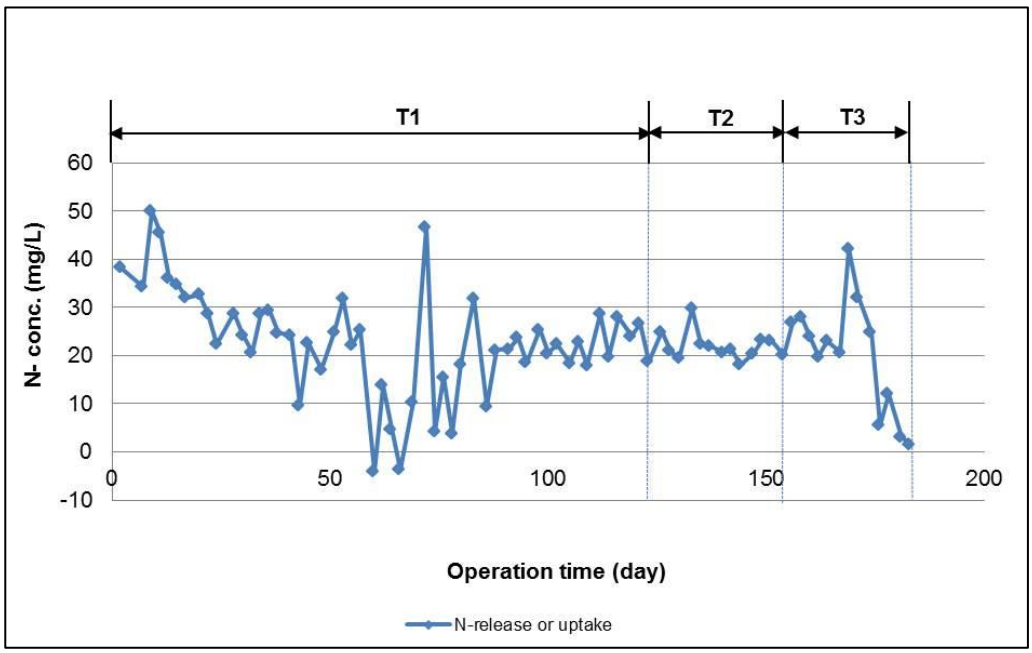

Fig. 6.13 :N-release or N-uptake

Fig. 6.13 clearly shows that most of the values are positive except two values in day 60 and day 66 meaning unidentified N has been occurred which could NO2¯N or other organic N. Further studies on this topic is neede.

6.3.6 O_2 concentration and consumption

6.3.6.1 Aeration rate vs dissolved oxygen (DO)

For aerobic MBR technology aeration is needed for creating cross-flow velocity (scouring purpose) and supplying dissolved oxygen (DO) for microorganisms. According to Drews and Kraume (2005) the MBR at low DO faces severely fouling problems (Section 5.6.6.1). The required level of DO 2-4 mg/L (Judd, S. 2006) for biomass can be achieved through air bubbling or pure oxygen supply by diffusers. As mentioned before, in this thesis work, oxygen transferred into the reactor was done with the help of an air-bubble diffuser.

The aeration rate supplied in MBR reactor for **T1** (Trial1) and **T2** (Trial2) were 1.0 ± 0.1 m^3/h and for **T3** (Trial3) it was 0.5 ± 0.05 with some fluctuations (Fig. 6.14). The corresponding dissolved oxygen (DO) were highly responsive to the supplied aeration rate as it is revealed strongly in **T3** where DO reduced from 2 – 6 mg/L with aeration rate of 1.0 ± 0.1 m^3/h to 2 – 4 mg/L with aeration rate of 0.5 ± 0.05 m^3/h.

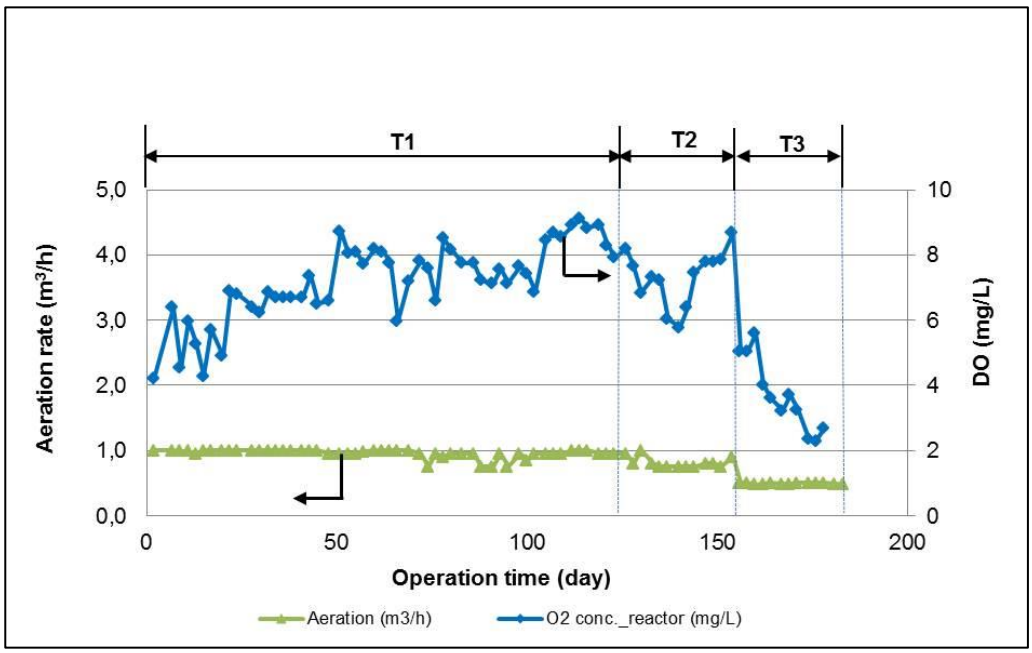

Fig. 6.14 : Effect of aeration rate and dissolved oxygen

The results presented in Fig. 6.14 defines that the required level of DO (e.g. 2-4 mg/L) can be achieved by adjusting the aeration rate in MBR.

6.3.6.2 O_2 uptake rate (OUR) vs dissolved oxygen (DO)

As reported in Fig. 6.15, the oxygen consumption in MBR reactor is highly responsive to DO with average O_2 consumption of 0.25 mg/L.min from **T1** (Trial1) until **T2** (Trial2). This consumption level is the half of the lower range of recommended in literature (Wastewater handbook (2013). This finding indicates that the microorganisms in the MBR reactor are very active and consume most of the available DO in the reactor from **T1** until **T2**. The rate of O_2 consumptions in **T3** (Trial3) were negligible with expected range of available DO (2 – 4 mg/L) but there was no effect on performances of microorganisms which was revealed by COD, TOC removal efficiencies (Section 6.3.3.1, section 6.3.3.4).

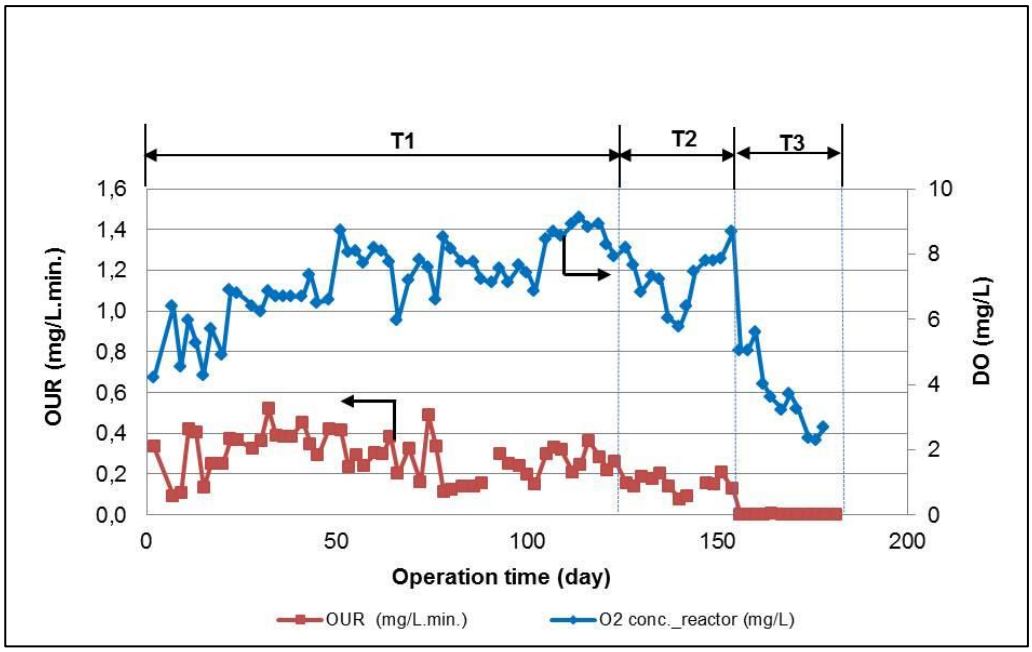

Fig. 6.15 : Effect of O2 consumption and DO

6.3.7 MLSS

6.3.7.1 MLSS in operation trials

According to Gunder (2001) and Krampe (2003), most MBR installations work at the MLSS level of 8 – 12 g/L while at higher MLSS value the MBR process loses its economical viability due to increased viscosity of the activated sludge and poor oxygen transportation efficiency. The range of MLSS in different operation trials in

this section were almost constant 6.5 to 8.5 g/L with little down grading values at the end of **T3** (Ttial3) as shown in Fig. 6.16. This might have happened due to less sludge generation in the reactor resulting from less availability of DO at reduced air supply in **T3**. Nevertheless, with these MLSS values the minimum recommended level of MLSS was possible to achieve.

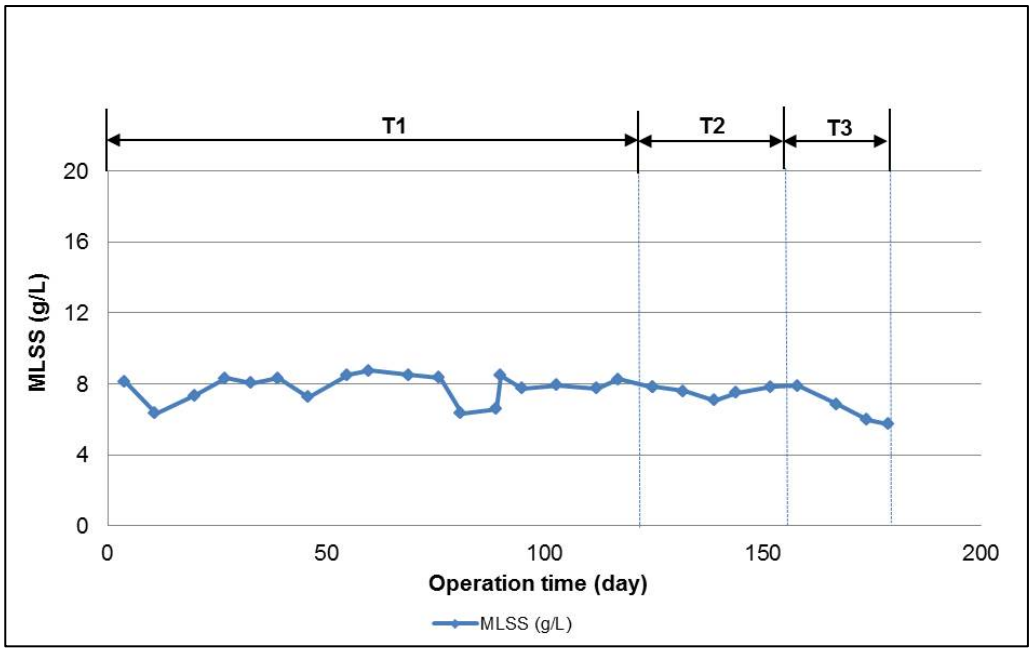

Fig. 6.16 : MLSS in different operation trials

6.3.7.2 Effect of MLSS in COD removal efficiency

Higher MLSS values might contribute to higher COD removal efficiency (Section 5.6.7.2). But in this section, MLSS values show irresponsive to COD removal efficiency as the reduced MLSS in **T3** (Trial3) had no effect on COD removal efficiency (Fig. 6.17).

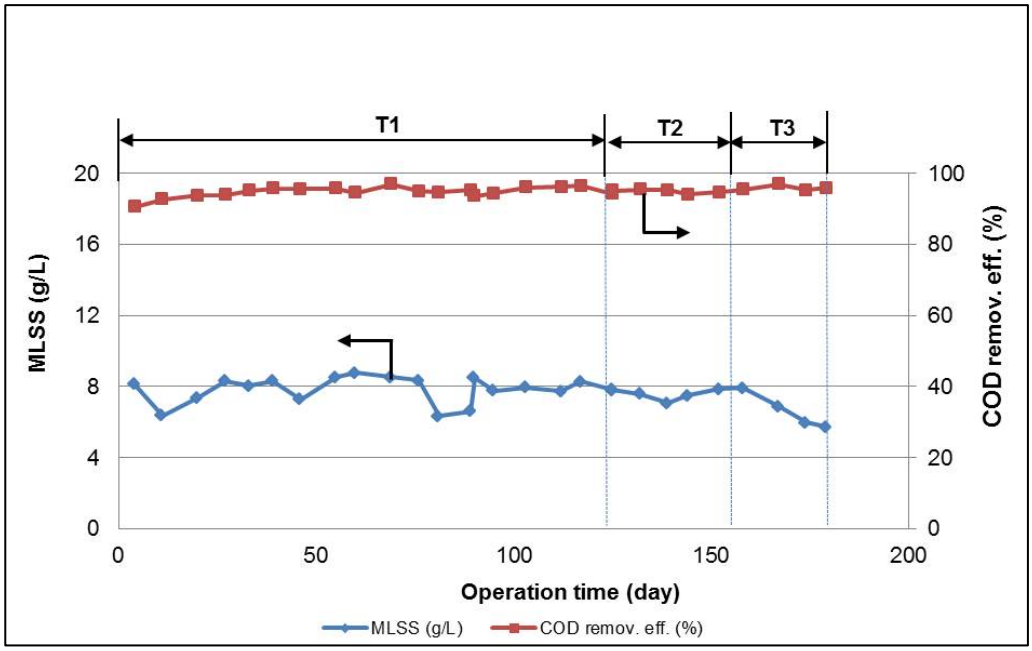

Fig. 6.17 : MLSS in COD removal efficiency

6.3.8 F/M ratio

The F/M ratio in MBR technology works as an indication of food supply for microorganisms (Section 5.6.8). The F/M ratio of the experiments carried out in **T1** (Trial1) is close to 0.1 Kg COD/Kg MLSS.d as shown in Fig. 6.18. Typical F/M ratio as reported in different literature is 0.3 Kg COD/Kg MLSS.d. The F/M ratio in **T2** (Trial2) and **T3** (Trial3) reduced to almost half of the values of **T1** but there was no effect on COD removal efficiency. So, the findings from the experiment conclude that the F/M ratio has no effect in MBR performance such as COD removal efficiency.

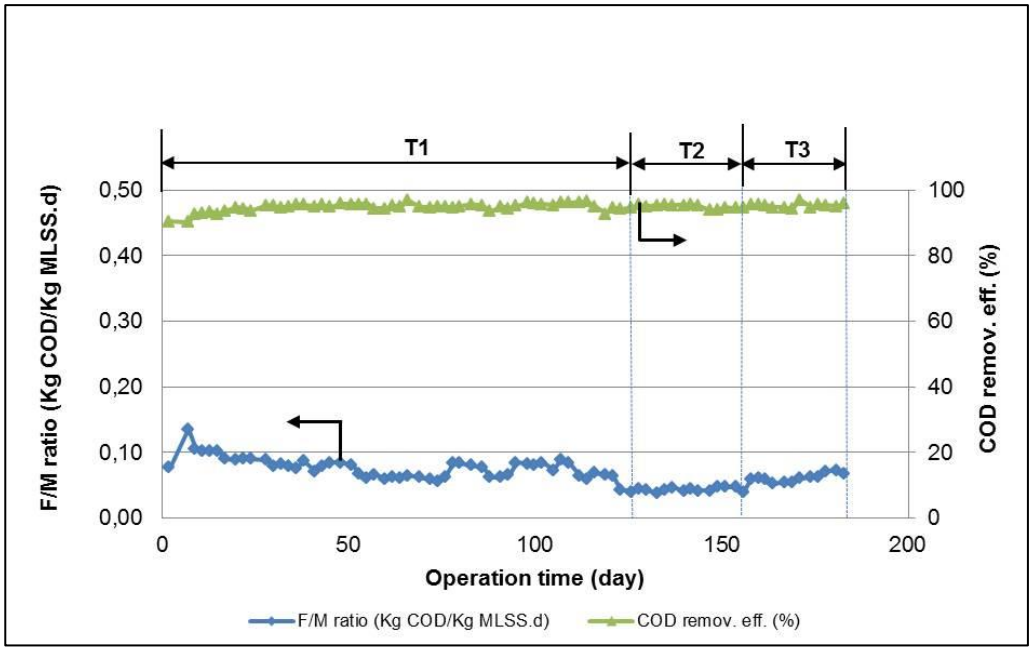

Fig. 6.18 : F/M ratio in COD removal efficiency

6.3.9 Chloride (Cl^-) concentration

The Cl^- concentration in permeate in **T1** through **T3** are in the range of 1800 to 2000 mg/L as shown in Fig. 7.19 which are close to the concentration of Cl_2 in MTDW (Calculated feed chloride concentration: 1717 mg/L). This indicates all of Cl^- has passed through the membrane due to its higher molecular weight. This means there is no accumulation of Cl^- in the MBR reactor which was expected. Some of the Cl_2 measurements from day 36 until day72 were not possible since these samples were thrown away mistakenly.

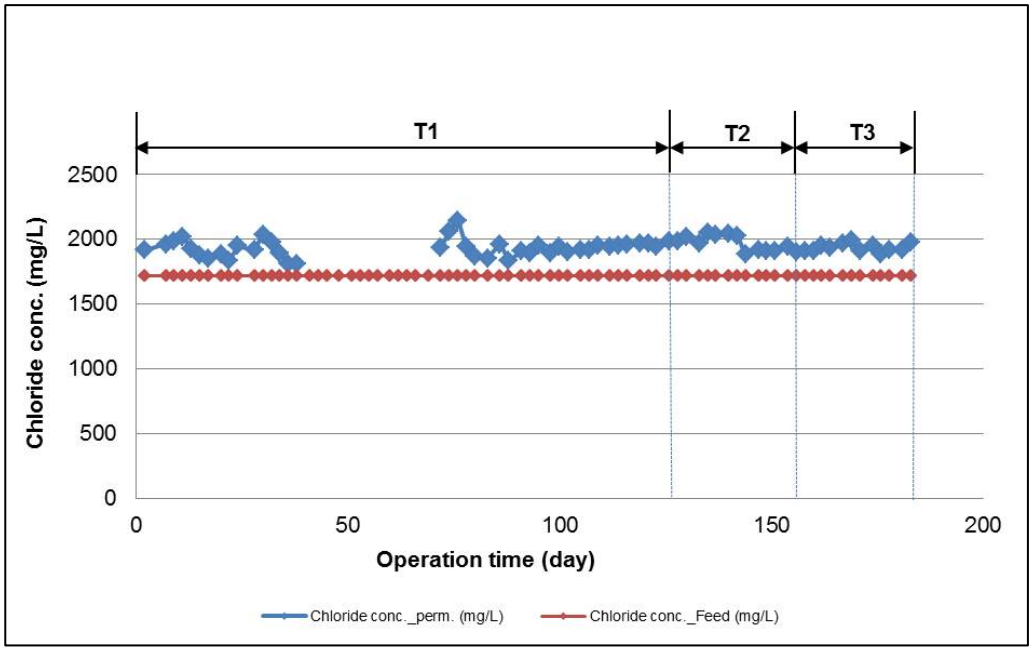

Fig. 6.19 : Cl^- concentration in permeate

6.3.10 Drying residue (DR) and Conductivity

Drying residue (DR) is the indicator of the amount of dissolved solid or salts in permeate (Section 5.6.10). The Fig. 6.20 showed that the DR in the permeate (3.5 g/L) kept almost constant during the entire experimental period with fluctuation in **T1** (Trial1). The difference of drying residue between the feed and permeate could be considered that some of the salts could be adsorbed or released by the biomass. Degradation could generate salts as well.

Conductivity is the indication of any salt accumulation in the reactor. Fig. 6.120 indicates that permeate conductivity is roughly in the range of 5.5 to 6.5 mS/cm which is in line with the conductivity of MTDW (Table 5.1).

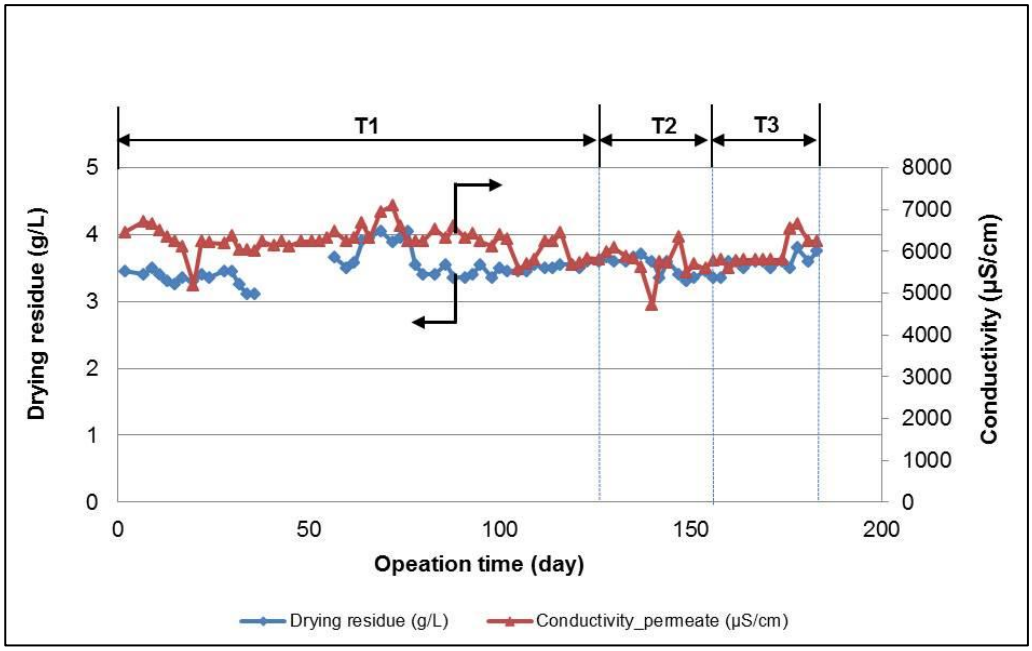

Fig. 6.20 : Permeate DR and conductivity

Fig. 6.20 represents the high correlation of DR and conductivity in different trials (**T1**-**T3**) except little fluctuation in day20 in **T1** (Trial1) and day140 in **T2** (Trial2). Some of the samples for DR analyses were missing as shown in T1 due to misuse of the samples.

6.3.11 pH and temperature

The Fig. 6.21 shows permeate pH which is similar to Feed pH. The designed experimental temperature was 20 ± 2 °C except a jump in **T3** (Trial1) which might have happened due to heat produced from some moving parts close to the experimental set up. The trial period of **T3** was the starting phase of summer. This also could contribute to the presented temperature rise but it had no significant effect in the results obtained (e.g COD, TOC removal efficiency).

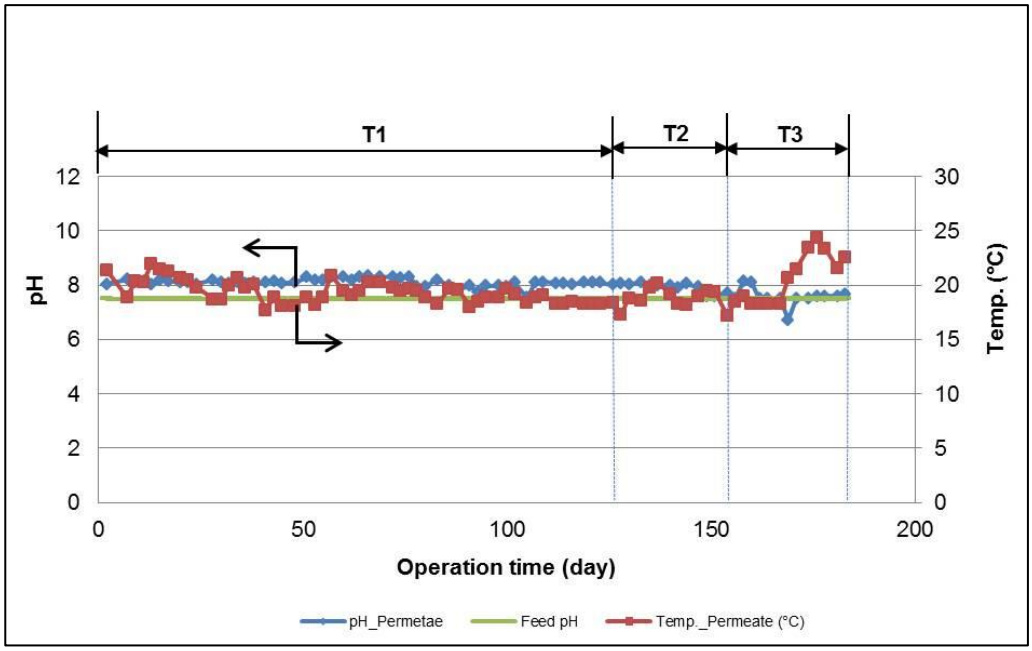

Fig. 6.21 : pH and temperature of permeate

6.3.12 Critical flux

Following a general protocol, the critical flux was measured (Section 5.6.12). The power of the suction pump was regulated to achieve step wise flux increase with corresponding TMP rise as shown in Table 6.3. The maximum limit of TMP for the applied PBM membrane module was considered as 350 mbar since this was the recommended value for PES membrane MBR module by the supplier (Microdyn-Nadir, Germany). The membrane was considered as fouled at above the TMP of 350 mbar.

Table 6.3 : Determination of critical flux in PBM membrane

Time interval (min.)	Applied voltage (V)	Flux (L/m^2.h)	TMP (mbar)
10	0.08	1.67	77.73
20	0.16	2.18	136.2
30	0.24	2.55	213.4
40	0.32	3.02	272
50	0.4	3.27	319.8
60	0.48	3.53	365.7
70	0.56	3.64	405.8
80	0.64	3.93	423.3
90	0.72	4.00	465.3
100	0.8	4.22	486.8

Since the membrane used for critical flux determination becomes blocked or fouled which might not be usable for further experiment, the critical flux of the applied PBM MBR module was determined at the end of the experiment. The critical flux of the applied PBM MBR module is shown in Fig.6.22.

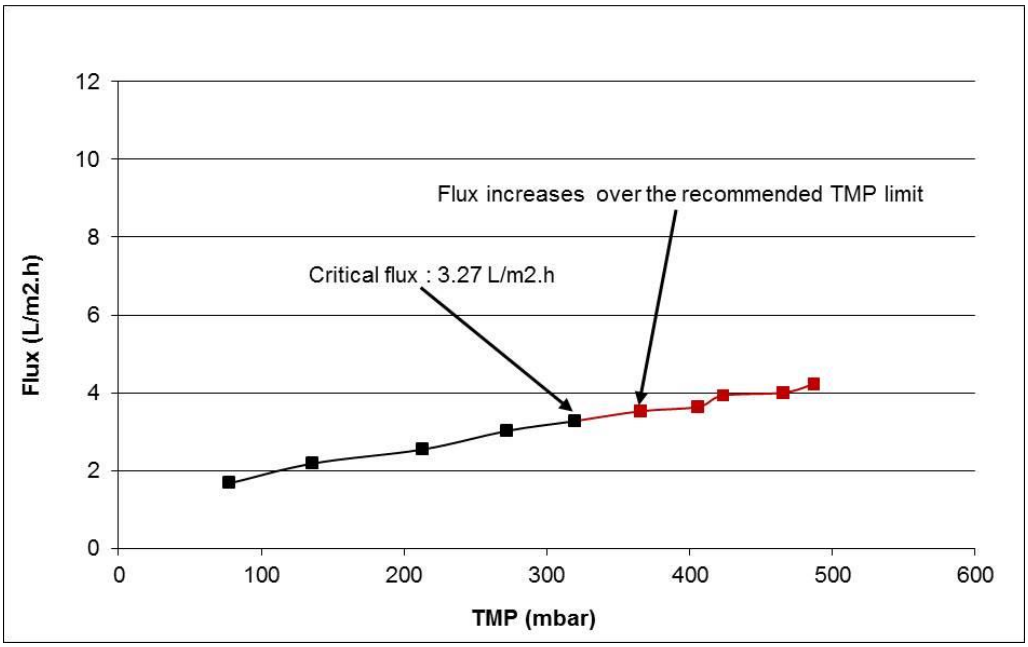

Fig. 6.22 : Critical flux of PBM membrane

Fig. 6.22 shows the flux 3.27 L/m^2.h and 3.53 L/m^2.h at TMP of 320 mbar and 365 mbar respectively. After that the flux increased a slightly but TMP increased significantly. According to commercial PES module manufacturing company Microdyn_Nadir above the TMP of 350, the membrane is considered

as fouled membrane. So, the critical flux of the membrane was determined as 3.5 L/m^2.h (considering slightly above the upper limit of TMP).

6.3.13 Membrane resistance model

As described in section 5.6.13, Darcy's Law establishes a relationship between TMP and flux which can be shown in Eq. (6.2)

$$J = \frac{TMP}{\mu R_t} \quad (6.2)$$

Where,

J = Membrane permeate flux (L/m^2.h)
TMP = Transmembrane pressure (mbar)
μ = Dynamic viscosity of permeate (N.s/m^2)
R_t = Total filtration resistance (1/m)

R_t can be expressed as the sum of individual resistances which can be varied based on the number and type of resistances considered (adapted from Jifeng et al., 2008). For this thesis, the expression of R_t was different based on the test media and experimental set up. R_t for model foulant humic acid, model textile dye wastewater and MBR sludge were defined as R_f, R_dye and R_mbr respectively and these are shown in Eq. (6.3) through Eq. (6.5).

$$Rt\_f = R_m + R_{ha} \quad (6.3)$$

$$Rt\_dye = R_m + R_{mtdw} \quad (6.4)$$

$$Rt_{mbr} = R_m + R_{sludge} \quad (6.5)$$

Where,

R_m = Constant resistance of the clean membrane (1/m)
R_{ha} = Fouling resistance due to humic acid (1/m)
R_{mtdw} = Fouling resistance due to MTDW (1/m)
R_{sludge} = Fouling resistance due to MBR sludge deposited on membrane surface (1/m)

Eq. (6.3) until Eq. (6.5) can be termed as resistance in membrane series (RIS) models based on different test media which are applied to describe membrane fouling mechanisms (Jifeng et al. 2008).

In this section of the thesis, the RIS model has been adapted according to applied experimental set ups and test media. The membrane resistances in different experimental set ups with varied test media have been calculated in the following sections.

a) Resistances in "UF_auto" set up with model foulant humic acid (HA)

The PBM membrane was tested with model foulant humic acid (HA) before applying in the MBR system to check the fouling behaviour of this modified membrane. The experimental set up used in this experiment was an auto-controlled UF cross-flow testing cell (Section 3.3, Fig. 3.5), termed as "UF-auto" in this section. The TMP of the experiment was 500 mbar and the obtained flux was 100.03 $L/m^2.h$ with DI water. Considering dynamic viscosity of the water as $1.002*10^{-3}$ at 20°C (Raymond, 1996), R_m was calculated using Eq. (6.2) to $1.79*10^{12}$ 1/m. In this calculation, dynamic viscosity of water was assumed to be equal to that of permeate.

Similarly, the fouling test was carried out with humic acid and membrane resistance was calculated using Eq. (6.3). In this case, flux of the experiment was 48.19 $L/m^2.h$ with TMP of 500 mbar. Using the same viscosity value, the calculated membrane resistance (denoted as R_{ha}) was $3.73*10^{12}$ 1/m. In summary, membrane resistance contributes around 30% to its total resistance where the rest of the 70% is contributed by humic acid.

b) Resistances in "UF_manu" set up with MTDW

The PBM membrane was also tested with model textile dayes to check the affinity of dyes to the membrane surface. The experimental set up used in this experiment was a manually -controlled UF cross-flow testing cell (Section 3.3, Fig.3.3), termed as "UF-manu" in this section. The TMP of the experiment was 1500 mbar and the obtained flux was 224.37 $L/m^2.h$ with DI water. Considering dynamic viscosity of the water as $1.002*10^{-3}$ at 20°C (Raymond, 1996), R_m was calculated using Eq. (6.2) to 2.4*10e12 1/m.

Similarly the membrane resistance was calculated using Eq. (6.4) after the test done with MTDW. In this case, flux of the experiment was 178.77 $L/m^2.h$ with

TMP of 1500 mbar. Using the same viscosity value, the calculated membrane resistance (denoted as R_{mtdw}) was $3.01*10^{12}$ 1/m. In summary, membrane resistance contributes around 45% to its total resistance where the rest of the 55% was contributed by MTDW.

c) Resistances in MBR experiment with biological sludge

In MBR experiment, firstly the test was carried out with DI water before the trial with biological sludge (Section 6.1). The TMP of the experiment was 30 mbar and the obtained flux was around 5.51 $L/m^2.h$ with DI water (Fig.6.1). Considering the same dynamic viscosity of the water as $1.002*10^{-3}$, R_m was calculated using Eq. (6.2) to $2.54*10^{12}$ 1/m.

After that the experiment was carried out in MBR set up for almost 183 days starting from **T1** until **T3** (Section 6.). In this case, the average flux of the entire experiment was 1.5 $L/m^2.h$ with average TMP of 51.88 mbar. Using the same viscosity value and Eq (6.5), the calculated membrane resistance (denoted as R_{sludge}) was $12.42*10^{12}$ 1/m. In summary, membrane resistance contributes around 17% to its total resistance where the rest of the 83% was contributed by biological sludge.

The summary of different resistances in different experiments is presented in Fig. 6.23 and Fig. 6.24. From Fig. 6.23, it is clear that the resistances with humic acid, MTDW and MBR have been increased significantly compared to their pure membrane resistances. But the increase of membrane resistance with MTDW is comparatively low. This indicates that HA and MBR sludge significantly contribute to membrane fouling. Fig. 6.24 indicates that percentage resistances of MBR bio sludge, humic acid and MTDW in their respective experiments are about 86%, 70% and 55% respectively and these values compared to their pure membrane resistances are significantly high.

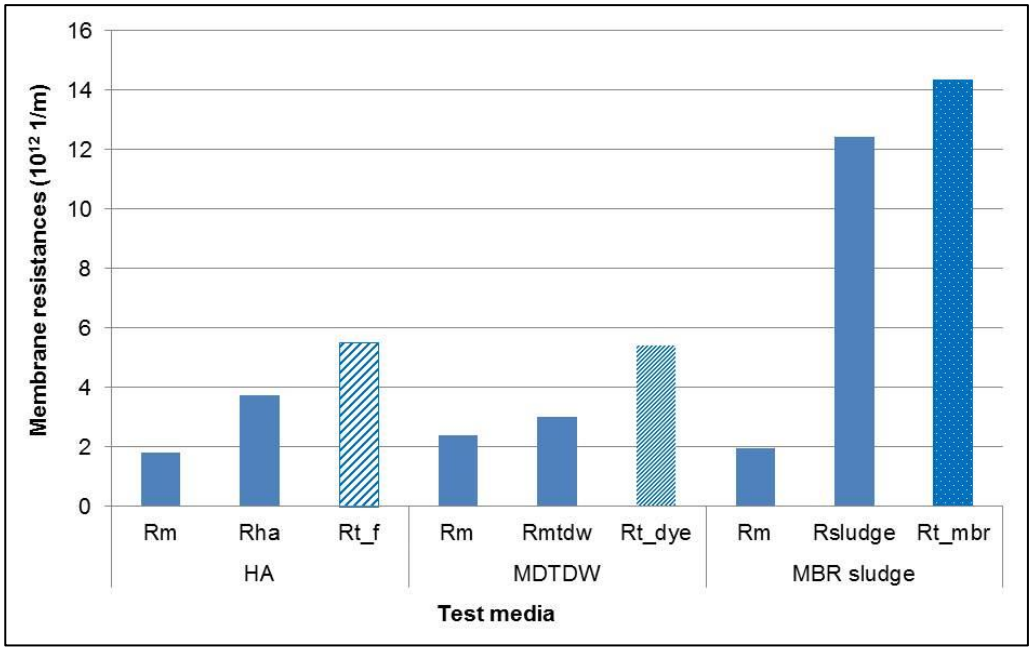

Fig. 6.23 : Numerical values of membrane resistances

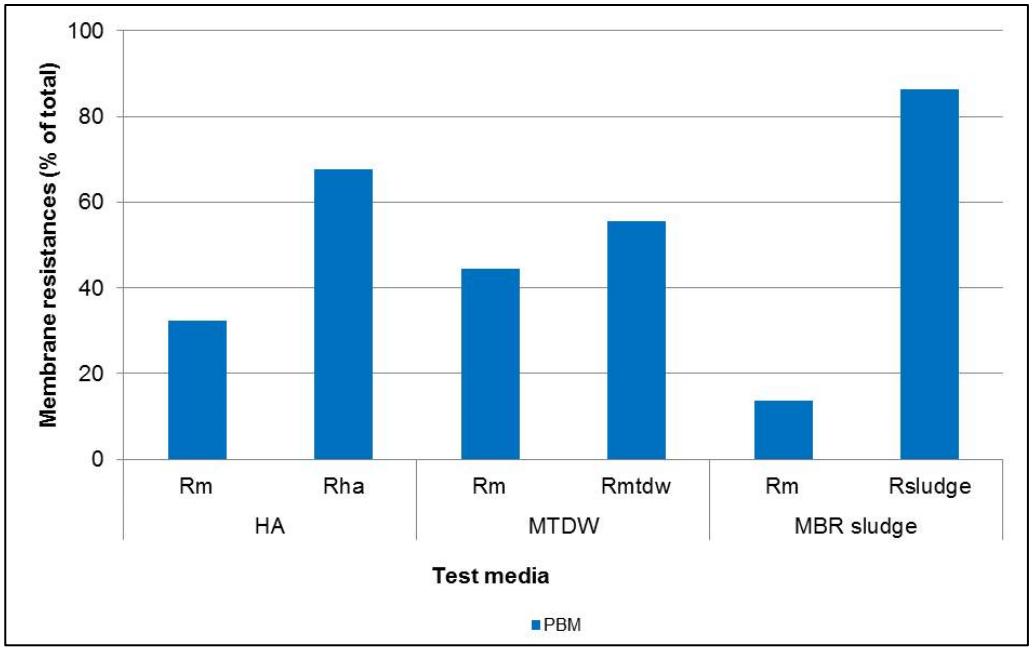

Fig. 6.24 : Individual contribution of membrane

References

Günder, B. (2001). "The Membrane Coupled-Activated Sludge Process in Municipal
Wastewater Treatment." Technomic Publishing Company Inc., Lancaster, USA

Huang, R.R., Hoinkis, J., Hu, Q., Koch, F. (2009), Treatment of dyeing wastewater by hollow fiber membrane biological reactor, J. Desalination and Water Treatment, 11, 1 - 6

Jifeng, G. X., Siqing, X, Rongchang, W. (2008), Study on Membrane Fouling of Submerged Membrane Bioreactor in Treating Bathing Wastewater, Journal of Environmental Sciences 20, 1158–1167

Judd, S. (2006), The MBR Book: Principles and Applications of Membrane Bioreactors in Water and Wastewater Treatment, editor, Elsevier

Krampe, J., and Krauth, K. (2003), Oxygen transfer into activated sludge with high MLSS concentrations. Water Science and Technology 47**,** 297-303.

Raymond A. Serway (1996). Physics for Scientists & Engineers (4th ed.). Saunders College Publishing. ISBN 0-03-005932-1

Viero, A.F., Sant' Anna Jr., G. L. (2008), Is hydraulic retentime an essential parameter for MBR performance?, Journal of Hazardous Materials 150, 185 – 186

Wastewater handbook (2013)
http://www.wastewaterhandbook.com/webpg/th_organics_34OUR.htm#3_4_1, accessed on November 24, 2013

7. Chapter 7 : Comparison of Performances between Commercial and Novel Membranes

The experiments with commercial UF PES MBR membrane module (denoted as Com1) have been carried out for 304 days and the results are presented in chapter 5. Subsequently under the same process conditions, experiments were carried out replacing the Com1 by novel coated MBR membrane module denoted as PBM for 183 days and the results are presented in chapter 6. After the experiments with PBM membrane, the similar experiments were performed for several 5 weeks using 2nd commercial UF PES MBR membrane module to check if the operating process conditions were similar to that of Com1. But the results obtained from the 2nd commercial UF PES MBR membrane module were not reliable due to some malfunctions of the experimental set up and these results were not used in this thesis. With expectation of reliable results, this module was replaced by another commercial UF PES MBR membrane module and experiments were carried out for 45 days. This module was denoted as Com2 and it has the similar characteristics of Com1. The results from the experiment with Com2 are reported in chapter 7 along with the experimental results of Com1 and PBM membranes. Table 7.1 depicts the applied membranes in different experiments that were carried out continuously.

Table 7.1 : Applied MBR membrane modules in different experiments

Experimental sequences	Applied membrane modules	Designation of the applied membranes	Duration of experiments	Experiments done in
Experiment1	1st commercial UF PES membrane module	Com1	304 days	Chapter 5
Experiment2	Commercial UF PES membrane module modified with novel PBM coatings	PBM	183 days	Chapter 6
Experiment3	2nd commercial UF PES membrane module	Com2	45 days	Chapter 7

The comparison of results obtained in three MBR processes (Com1-PBM-Com2) is described in this chapter with respect to different operating process conditions. The results obtained clearly define the benefits of PBM membrane in terms of product quality, degradation, fouling propensity, process robustness etc. which are described in the following sections.

7.1 Results

7.1.1 Water production

7.1.1.1 Flux and TMP

Fig. 7.1 indicates the flux & TMP of all the experiments carried out with Com1, PBM and Com2 membrane modules. The flux and TMP of Com1 and PBM have been described in sections 5.6.1.1 and 6.3.1.1 respectively. Additionally, the flux and TMP of Com2 are compared in this section.

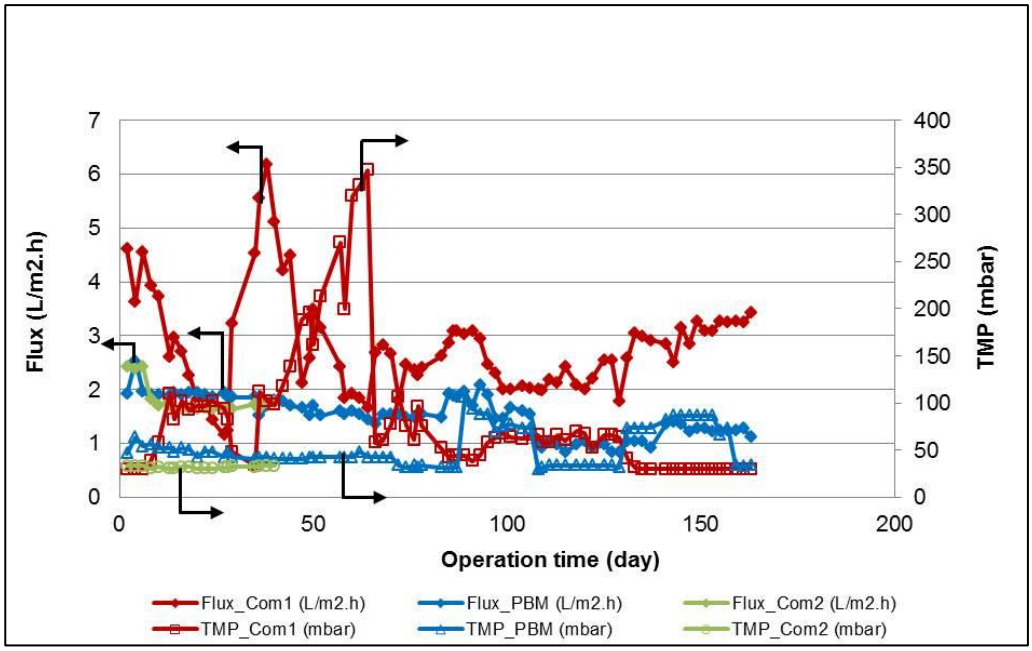

Fig. 7.1 : Flux and TMP of the (Com1_PBM_Com2) MBR experiments

Fig. 7.1 clearly shows that flux of the PBM membrane is lower than that of Com1 but the values were comparatively stable. This indicates the less sensitivity of PBM membrane to the varied process conditions. The flux of Com1 is very much fluctuating until day 66. This might be happened due to acclimation of the system since the feed composition was gradually adapted. The average flux and TMP of Com2 were similar to those of PBM and close to Com1. The flux of Com1 is typically higher than that of PBM module. Generally it can be

stated that all three experiments (Table 7.1) were carried out more or less under similar operating conditions.

7.1.1.2 Water permeability (WP)

Water permeabilities of all three experiments are presented in Fig. 7.2. The average water permeability of PBM membrane is 35 L/m^2.h.bar where this value of Com1 is around 60 L/m^2.h. Hence, the water permeability (WP) of PBM membrane is roughly half of Com1. But within the operation time of 189 days, Com1 membrane faced severely fouling problems on day 27 and day 189 and the modules needed to be replaced by new ones. PBM membrane faced no fouling problem nearly covering the same period except a slight WP drop on day 89 (probably due to mechanical blocking of the module which was visible after opening) and on day137 due to reduced aeration rate. The aeration is the main energy consumer in MBR technology for scouring of membrane and microorganisms. The aeration rate was reduced intentionally to observe the scouring effect of the membrane module. The result indicates that PBM has strong antifouling properties which might be economically viable due to reduced aeration rate reduced cleaning frequency. Generally the cleaning frequency for MBR module is 3 to 4 times in year. The cleaning frequency with PBM membrane could be reduced significantly. The WP of Com2 membrane module was around 57 L/m^2.h.bar which was close to that of Com1. This might represent the constant biological conditions of MBR reactors in different experimental sequences. The WP rise with PBM at the end of the experimental period can be neglected since the feed supplied to the MBR reactor became decomposed (anaerobic).

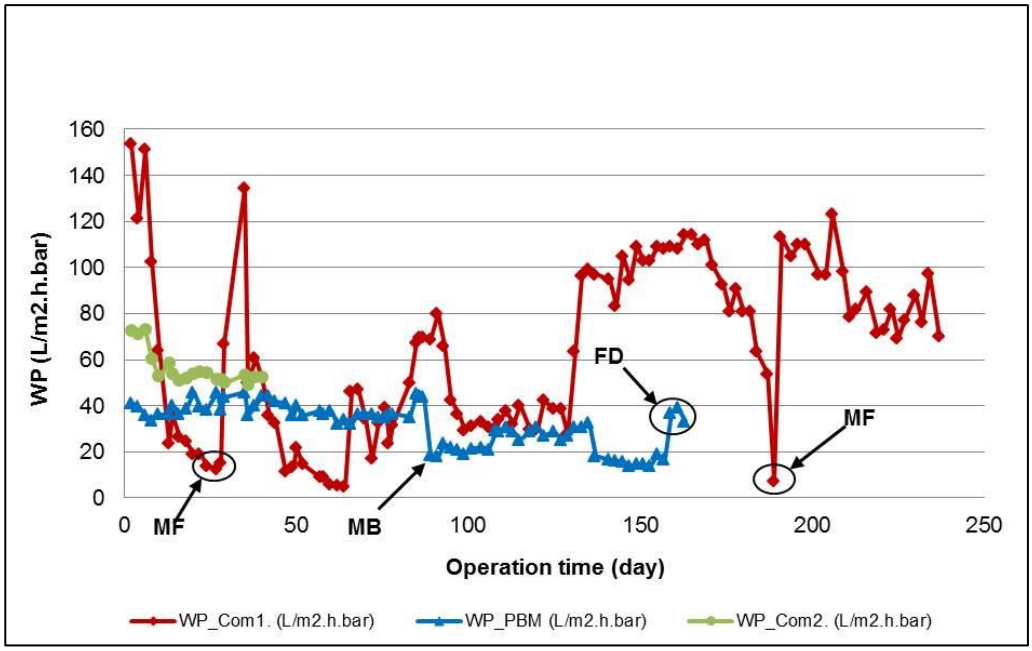

Fig. 7.2 : Water permeability of the (Com1-PBM_Com2) MBR experiments

N.B.:
MF: membrane fouled
MB: mechanically blocked
FD: feed decomposed

7.1.2 Hydraulic Residence Time (HRT)

Fig. 7.3, gives the HRT of all experiments with three different applied membrane modules. The average range HRTs of Com1, PBM and Com2 membrane modules were roughly 70 – 80 h, 100-110 h and 90-100 h. Generally, the HRT of these modules were similar except some high HRT period (day123-day156) with PBM MBR module. The HRT of PBM MBR module was raised to about 170 h from day108 to day137 to check if any nitrification takes place since high nitrification was found with the same MTDW applying in a side stream MBR at high HRT values of 167 h (not included in this thesis). But no nitrification even due to high HRT was found in this experiment.

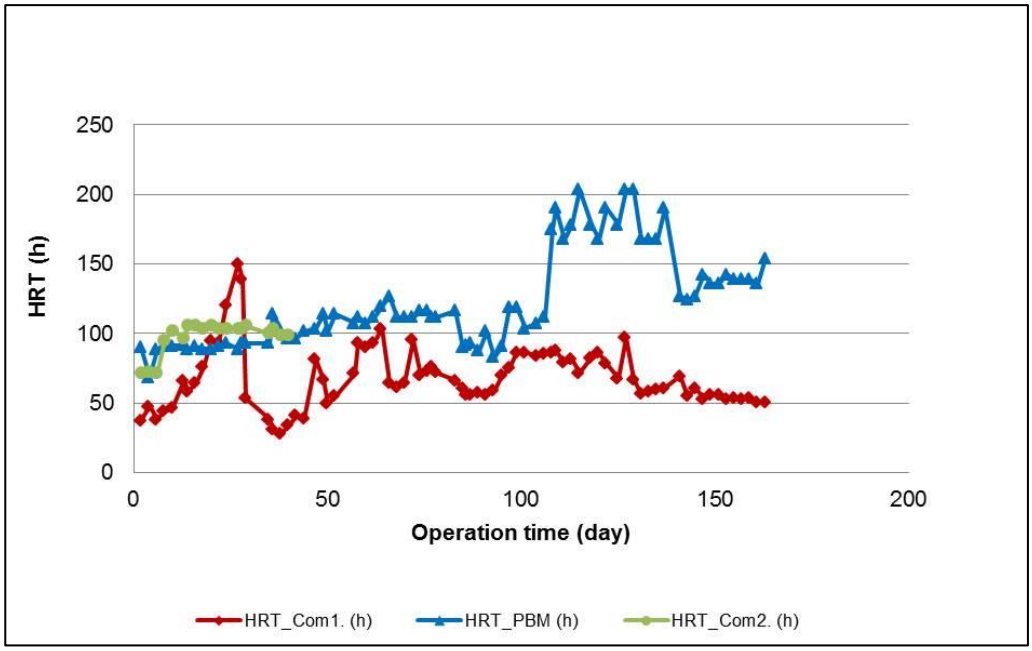

Fig. 7.3 : HRT of the (Com1_PBM_Com2) MBR experiments

7.1.3 COD and TOC

7.1.3.1 COD removal efficiency

The COD removal efficiency with PBM membrane is highly constant at 95% to 97% whereas this efficiency with Com1 membrane was fluctuating a lot with average values of around 90%. In total, PBM MBR module has roughly 7% higher COD removal efficiency. The results with Com2 membrane were similar to that of PBM module at the beginning of the experiment but tend to follow down grading values with 92% COD removal efficiency at the end. In this case, further continuations of the experiments with Com2 MBR module are recommended to observe long term effect.

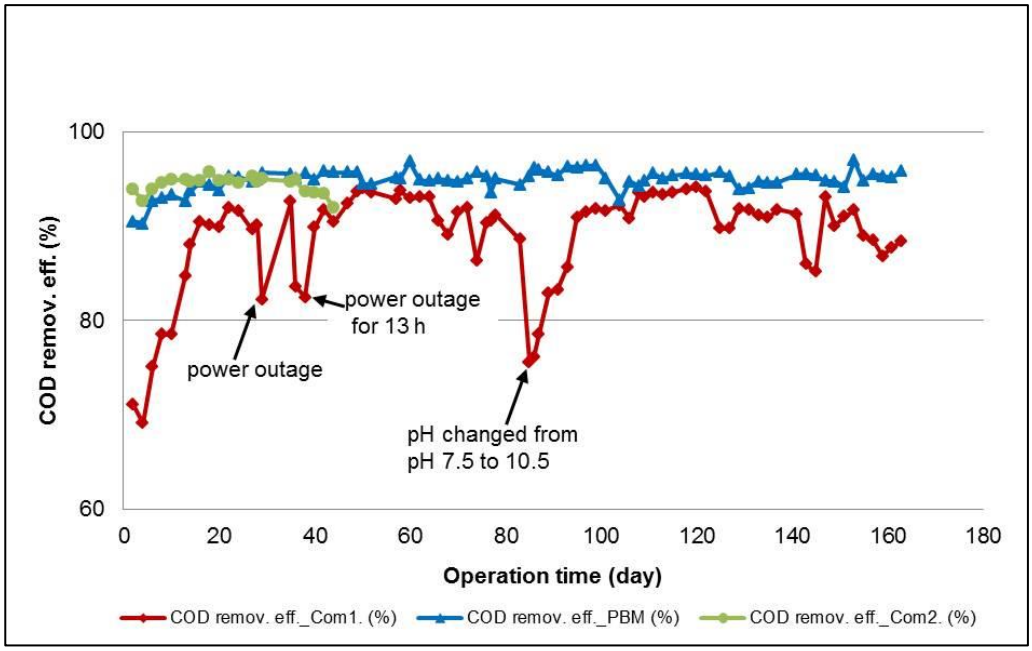

Fig. 7.4 : COD removal efficiencies with Com1_PBM_Com2 MBR modules

Some of the lower COD removal efficiencies occurred on day 29, day 38 and day 85 were due to power outages and pH change respectively. Because under such conditions, the microorganisms might have been under stress and performed poor degradation.

7.1.3.2 Effect of HRT on COD removal efficiency

In Fig. 7.5, the effect of HRT on COD removal efficiency is shown. In general, the HRT of Com1, PBM and Com2 are in the range of 80h to 110h with some fluctuations and except the high HRT period (day 108 – day 137). From the results of these experiments, it is revealed that HRT has no effect in COD removal efficiencies in any of the applied MBR modules. The COD removal efficiency at high HRT region of PBM MBR module was unchanged. This result is in line with the results found by Viero et al. (2008) where no influence of HRT on COD removal efficiency was found.

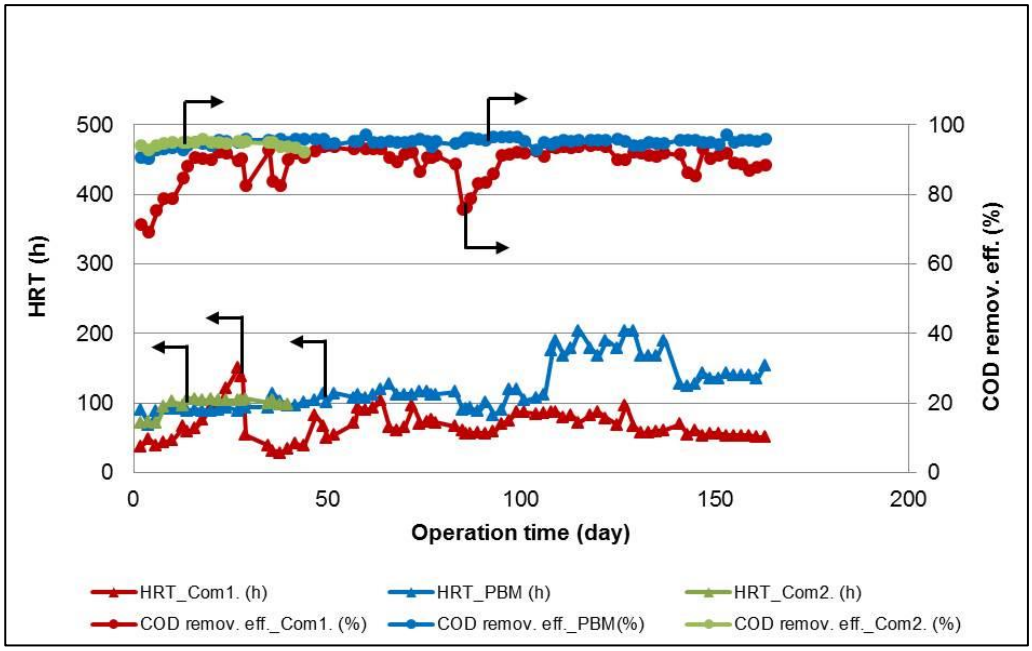

Fig. 7.5 : Effect of HRT on COD removal efficiency with Com1_PBM_Com2 MBR modules

7.1.3.3 COD and TOC relation

Fig. 7.6 shows that the TOC values are lower than the COD values which is logical. Theoretically, TOC and COD ratio is 0.25 to 0.3. The permeate TOC values are correlating with the respective permeate COD values in all three membranes modules. The calculated TOC/COD ratio of Com1, PBM and Com2 were 0.68, 0.23 and 0.18 suggesting that the PBM MBR process shows closer value close to the theoretical calculation. The results with PBM membrane module are less fluctuating compared to Com1 membrane module under different applied process conditions. The permeate TOC values of Com2 are in line with the TOC values of PBM. In general, the process with PBM membrane module in long term experiment shows as a robust process. The continuation of Com2 MBR module needs to be further investigated.

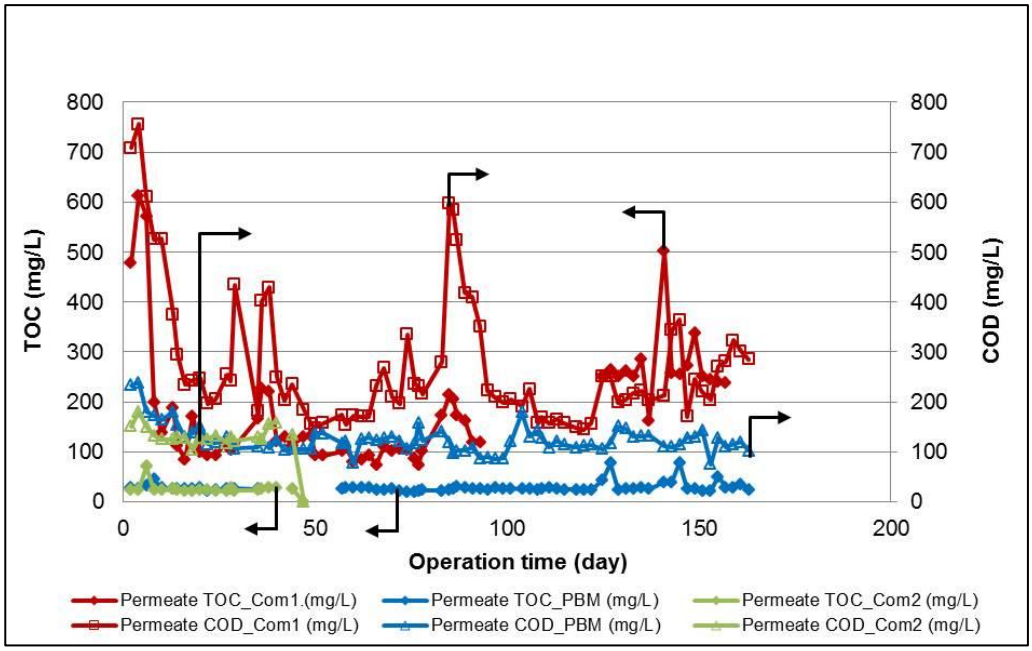

Fig. 7.6 : Relation between TOC and COD in Com1_PBM_Com2 MBR modules

7.1.3.4 TOC removal efficiency

The TOC removal efficiency with PBM MBR module is around 98% where these values with Com1 MBR module is 83% only though the results with Com2 MBR module is in line with that of PBM process. This result shows that in long term test PBM MBR module shows around 10% higher TOC removal efficiency compared to Com1 MBR module but it was the same with the experiment carried out with Com2. To be ensured of the higher performance of the PBM membrane, further tests with Com2 needs to be carried out.

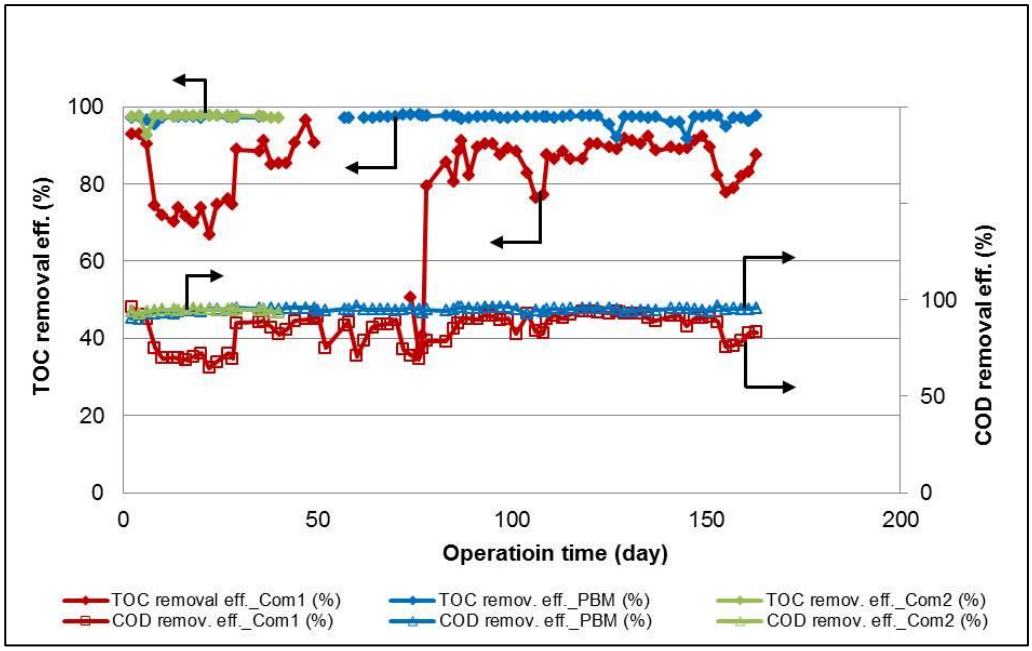

Fig. 7.7 : Comparison of COD and TOC removal efficiency in Com1_PBM_Com2 MBR modules

7.1.3.5 Permeate COD and reactor COD

The gap between permeate COD and reactor COD of PBM module is much lower and shows low fluctuation compared to those of Com1 and Com2 MBR modules as shown in Fig. 7.8. This means that less amount of COD have been accumulated in the reactor of PBM module compared to those of Com1 and Com2 modules. This shows that PBM module has higher degradation rate with less accumulation of COD in the reactor meaning less stress for microorganisms. This is a big advantage of the PBM module. On the other hand, if the widening of the gap with Com1 and Com2 modules is continued, more COD will be accumulated in the reactor which might be stressful for microorganisms. This can affect the performance of these modules. The trend of Com2 shows higher accumulation of COD in the reactor.

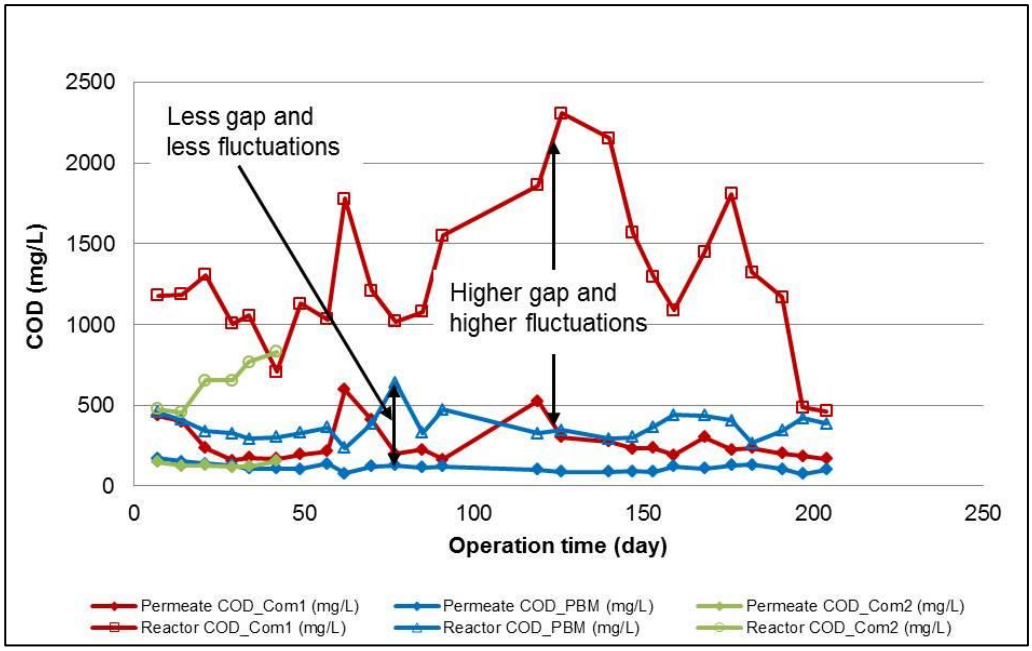

Fig. 7.8 : Comparison of permeate and reactor COD in Com1_PBM_Com2 modules

7.1.4 Dye removal efficiency

7.1.4.1 Red dye in permeate

The red dye removal efficiencies with Com1 and PBM membranes are highly fluctuating ranging from 20% to 70% with average values of around 40% (Fig. 7.9). The average red dye removal efficiency of Com2 membrane is 23% which is significantly lower with less fluctuation. Since the molecular weight of the red dye is 380.4 (Section 3.7) and the molecular weight cut off (MWCO) of Com1 and Com2 are 150 kDa, the undegreded red dye is supposed to pass through these membranes. The red dye removal efficiency of PBM membrane suggests that MWCO of the PBM membrane has not been reduced enough by novel coating to achieve significant removal efficiency (Section 4.2.4).

As described in section 4.2.8 and shown in Table 7.2 membranes (commercial PES and novel coated PBM) contributed to 25% of red dye rejection which might have occurred due to charge exclusion and the MBR systems (Com1 and PBM) contributed to 40%. The difference between these two values is 15% of

red dye rejection which might have occurred due to biological activity of microorganisms.

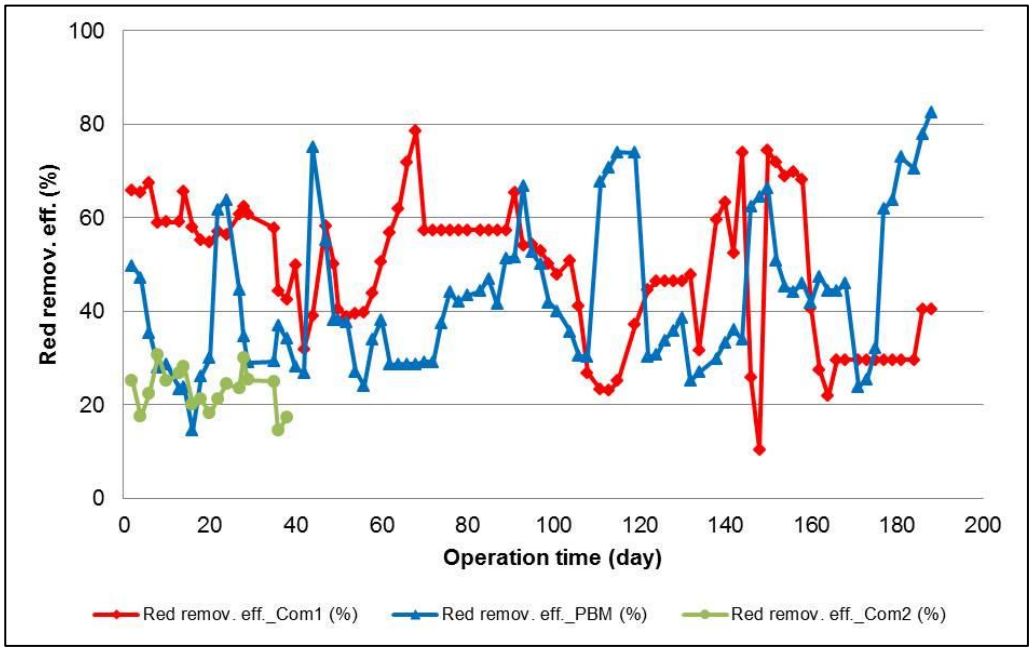

Fig. 7.9 : Red dye removal efficiencies in Com1_PBM_Com2 modules

Table 7.2 : Contributions of membrane and MBR system for red dye rejection

Test media	Red rejection (%)
Contribution of PES membrane	25
Contribution of PBM membrane	25
Contribution of Com1 and PBM	40

7.1.4.2 Blue dye in permeate

The blue dye removal efficiencies with Com1 and PBM membranes were fluctuating in the range of 40% until day 83 (Fig. 7.10). After the day 83, the blue dye removal efficiency with PBM membrane increased to around 60% where this efficiency with Com1 dropped to around 30. The blue removal efficiency with Com2 membrane was in line with the results of Com1. As described in section 4.2.8 and shown in Table 7.3, PES and PBM membranes contributed to 45% and 52% of blue dye rejections respectively which might have occurred

due to charge exclusion whereas the MBR systems (Com1 and PBM) contributed to 30% and 60% of blue dye rejection respectively. The difference between PES pure membrane and Com1 is -15% and this difference between PBM pure membrane and PBM MBR module is 8%. These results indicate that Com1 MBR system had no contribution in blue dye rejection whereas PBM MBR module contributed slightly (8%).

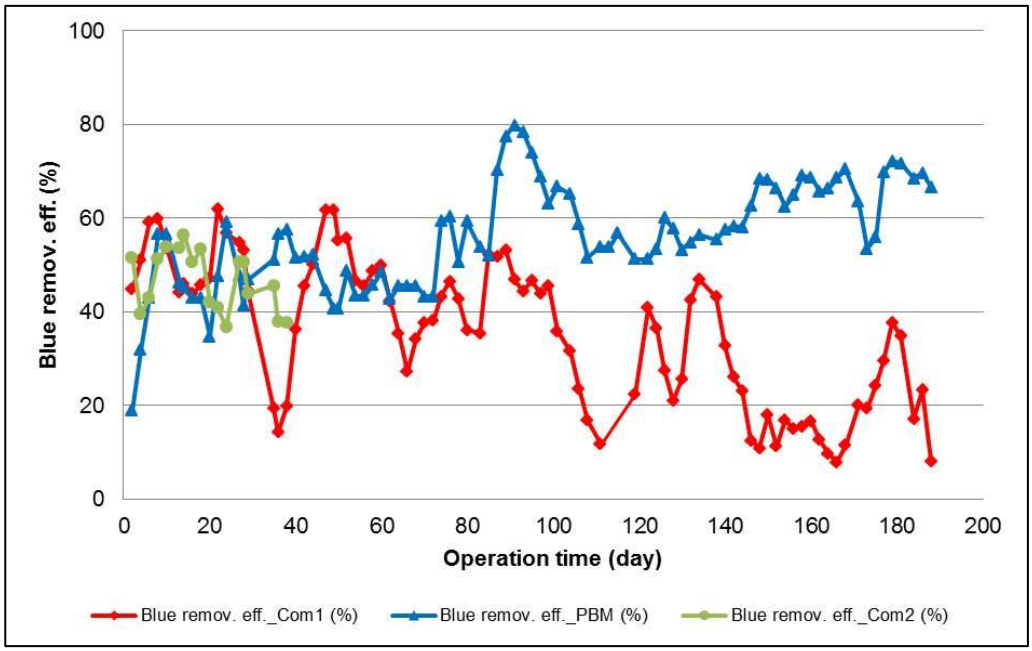

Fig. 7.10 : Blue dye removal efficiencies in Com1_PBM_Com2 modules

Table 7.3 : Contributions of membrane and MBR system for red dye rejection

Test media	Red rejection (%)
Contribution of PES membrane	45
Contribution of PBM membrane	52
Contribution of Com1 module	30
Contribution of PBM module	60

7.1.4.3 Red dye in reactor

Reactor red dye concentrations in all applied membranes processes (Com1, PBM and Com2) as shown in Fig.7.11 are lower than those of permeates dye

concentrations with strong fluctuations. The reactor dye concentrations are supposed to be equal or higher than the permeate dyes but the opposite behaviour of the results were noticed in all applied membrane processes as shown in Fig. 7.11. This might have occurred due to the sonication process (Section 3.9.5) applied to analysis the concentration of dyes in reactor samples. It was assumed that after sonication, the dyes adsorbed on the sludge will be released. Since dyes in permeate are lower than those of reactor, the dyes might have not released from the sludge. Further investigation on this work is needed. In general, no accumulation was noticed.

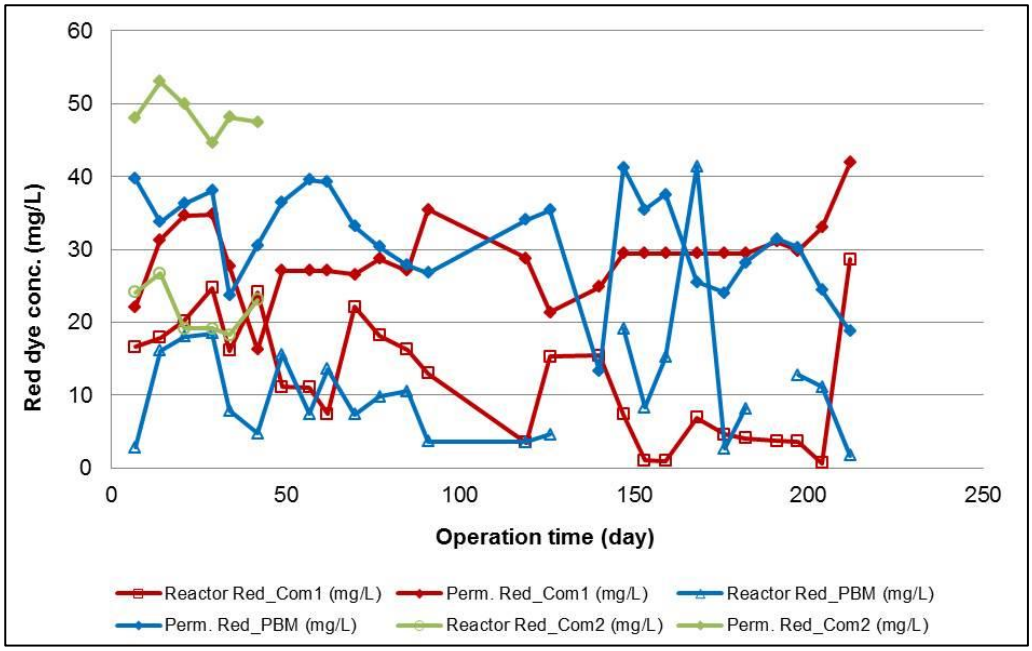

Fig. 7.11 : Comparison of permeate and reactor red dyes in Com1_PBM_Com2 modules

7.1.4.4 Reactor blue dyes

Reactor blue dyes in all applied membranes processes (Com1, PBM and Com2) as shown in Fig.7.12 are lower than those of permeate dyes. These were not expected and These might be happened due to sonication process (Section 3.8) applied to analysis the concentration of blue dyes in reactor samples. The difference between the concentrations of reactor blue dyes and permeate blue dyes in all of the applied membrane processes were almost constant which in-

dicates that no blue dyes were accumulated in the reactors. Some samples with PBM membrane were missing due to miss use.

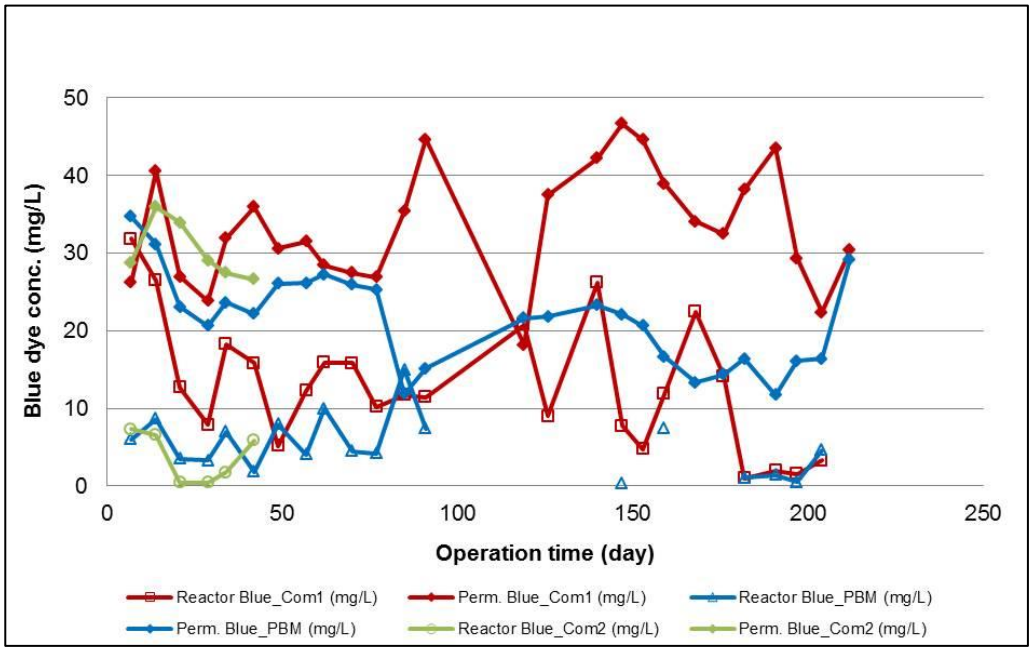

Fig. 7.12 : Comparison of permeate and reactor blue dyes in Com1_PBM_Com2 modules

7.1.5 N - Balance

The sources of total N (TN) for all membrane processes (Com1, PBM and Com2) are dyestuffs and NH_4Cl as described in section 5.6.5. Fig. 7.13 represents N-compounds in permeates and summarises the results on conversion of total-N (TN) into NH_4^+-N and NO_3^--N from feed to permeate.

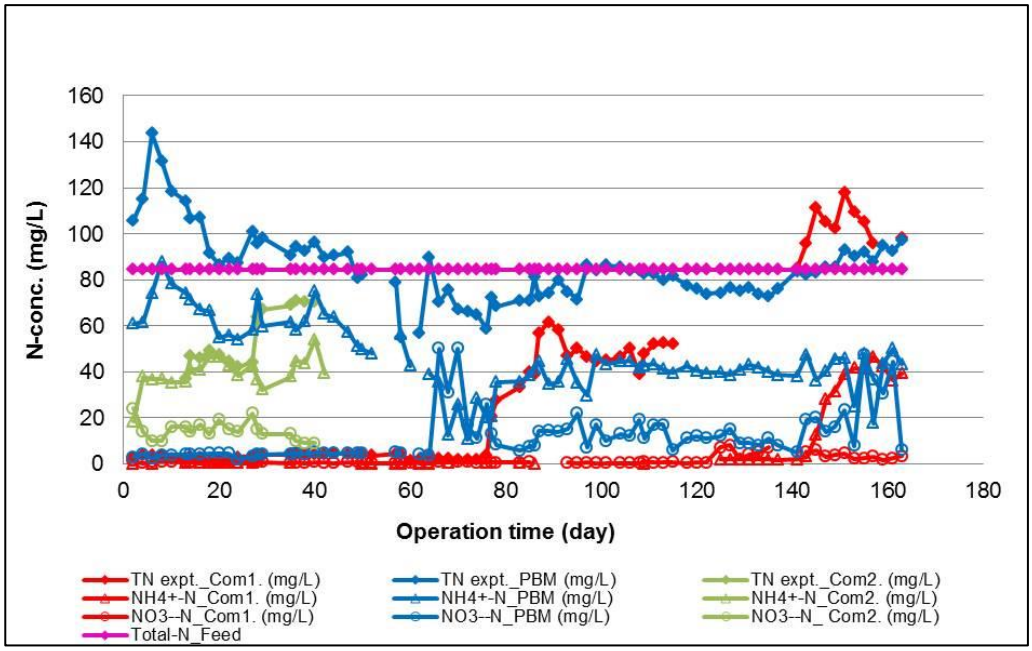

Fig. 7.13 : N- balance in Com1_PBM_Com2 modules

The TN with Com1 was very low until day140 and almost no nitrification was observed. After day140 as reported in Fig. 7.13, NH_4Cl at concentration of 300 mg/L was added to feed to have higher nutrient concentration reaching COD:N ratio to 30:1 which is close to the recommended value (Hach Lange, 2013) (Section 5.6.5). After this period, it can be noticed that the concentration of NO_3^--N in permeate was even very low and most of the TN remained as NH_4^+-N which means that no nitrification occurred. A different scenario was observed in N- compounds of permeate with PBM membrane. It can be calculated that the concentration of NO_3^--N and NH_4^+-N in permeate contribute to around 15% NO_3^--N conversion and 55% NH_4^+-N which concludes that partial nitrification was occurred with PBM module starting from after day 80. The similar results (15% NO_3^--N and 45% NH_4^+-N) were also found with Com2 membrane module. These result shows that the biological sludge might be adapted after long term experiments for partial nitrification. Generally, MBR application in textile wastewater gives higher nitrification (more than 90% NO_3^--N conversion) Huang et al. (2009) but it was not happened in this thesis. Further investigation on this topic is needed.

Difference between experimental TN and calculated TN

The concentration of total N in feed is 84.4 mg/L for all of the applied MBR modules as shown in Fig. 7.13 and the same concentration of TN in permeate can be expected after treatment if there is no accumulation or release. But Fig. 7.13 shows that sometimes the experimental total N crossed the maximum limit of 84.4 mg/L. This can be explained as release of total N by the permeate or uptake of total N in the permeate.

The difference between experimental TN (TN expt.) and calculated TN (summing up NO_3^-N, NH_4^+-N and N in dyes) can be termed as Diff._N and these values were calculated using Eq. (7.1) and Eq. (7.2).

$$Diff.\_N = Total.N_{perm}.expt. - Total.N_{perm}.calc \quad (7.1)$$

Where,

$$Total.N_{perm}.calc = NO_3^- - N + NH_4^- - N + Dye - N \quad (7.2)$$

Dye_N can be calculated by using Eq. (5.7b). Fig. 7.14 shows Diff._N of all applied membrane modules.

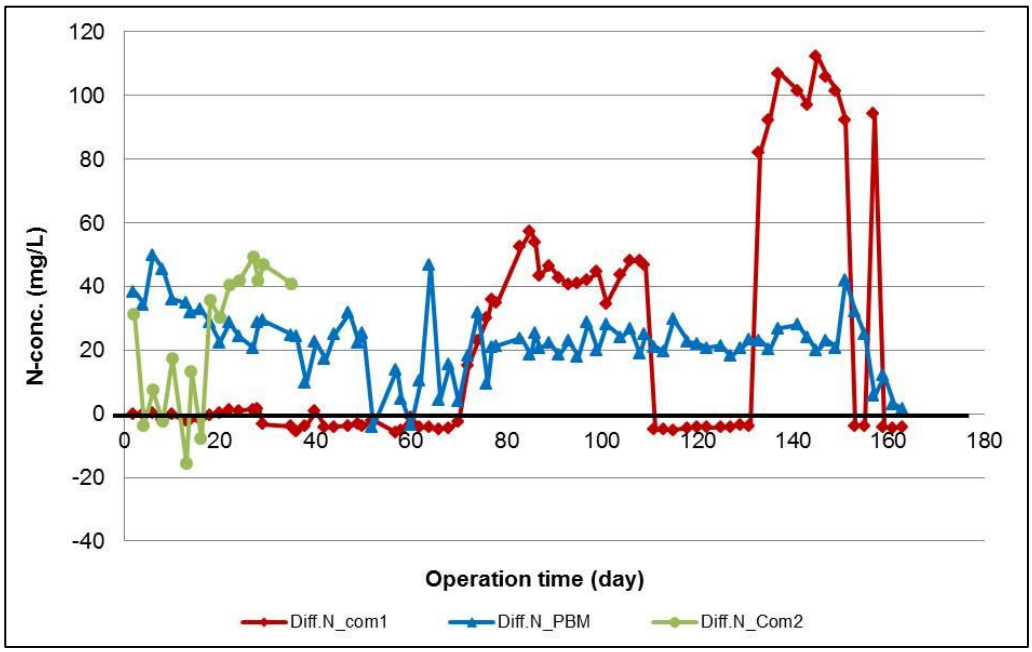

Fig.7.14 : N- concentration variations in Com1_PBM_Com2 modules

The result shows that Com1 process had negative values at the beginning which might have occurred from the measurement errors of NO_3^-N, NH_4^+-N

and N in dyes. The positive values of Diff.N with PBM process indicate that there is a unknown nitrogen source which could be $NO2^{-}N$ or organic nitrogen. Furhter studies on this topic is needed. Com2 process shows the similar trend of results like PBM meaning there is a unidentified nitrogen source in the samples.

7.1.6 O_2 concentration and consumption

7.1.6.1 Aeration rate vs dissolved oxygen (DO)

Fig. 7.15 gives the dissolved oxygen (DO) in Com1, PBM and Com2 membrane processes based on their respective air supply rate. The DO in the reactor with PBM is in the range of 6 to 8 mg/L where these values with Com1 and Com2 membranes are in the range of 2 to 6 mg/L. These results suggest that the more DO than required remained in the reactor with PBM membrane. So, the air supply could be reduced such as 0.5 m^3/h instead of 1 m^3/h which can be an economic advantage reducing the operation cost of the system. At reduced aeration rate of 0.5 m^3/h, the DO in PBM module was in the recommended level of 2-4 mg/L (Judd, 2006) while it went down in Com2 module under the same conditions. This suggests that aeration rate could be reduced in PBM module but it needs to be investigated further how it turns out with Com2 module.

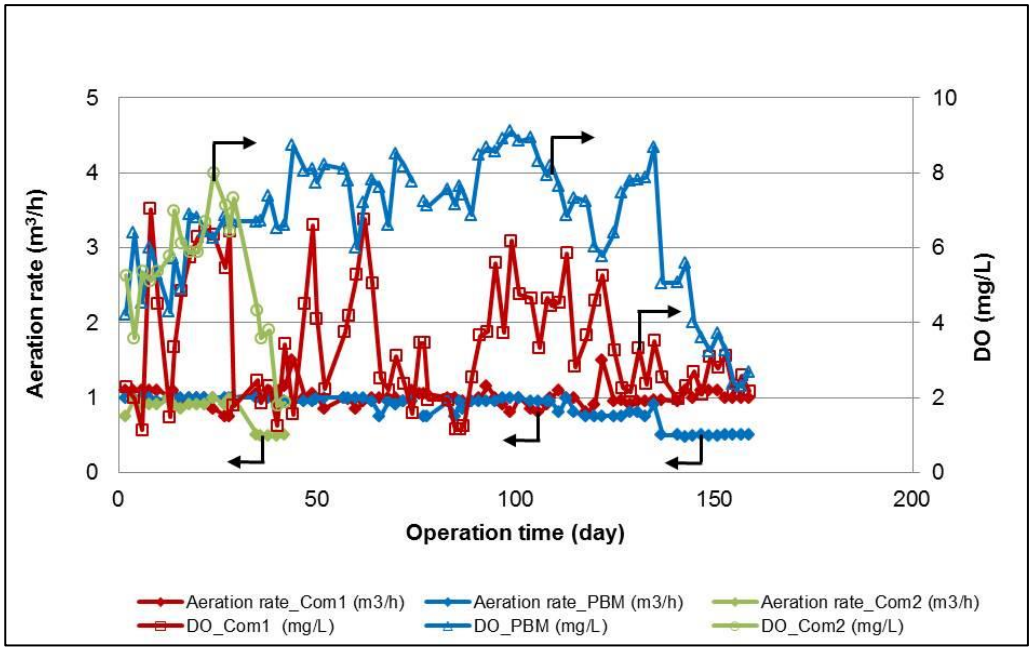

Fig. 7.15 : Effect of aeration rate and dissolved oxygen in Com1_PBM_Com2 modules

7.1.6.2 Oxygen uptake rate (OUR) vs dissolved oxygen (DO)

Fig. 7.16 shows that oxygen uptake rate (OUR) in PBM membrane process is less compared to available DO in the reactor. This might be happened due to lower activity of the activated sludge however the system was performing well in terms of COD removal efficiency, blue dye removal efficiency (Fig. 7.4, Fig. 7.10). The oxygen consumptions with Com1 membrane is close to that of PBM membrane but Com2 membrane shows 65% higher oxygen consumption compared to that of PBM membrane process. These results summarise that DO could be reduced in PBM process by reducing air supply rate which could save the operation cost.

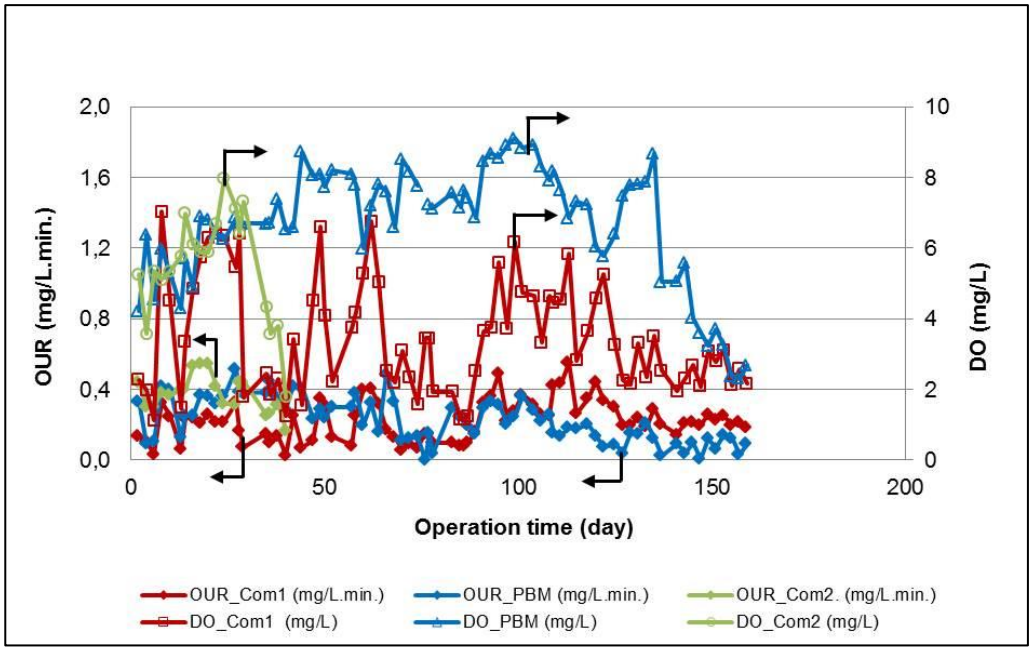

Fig. 7.16 : Effect of DO and OUR in Com1_PBM_Com2 modules

7.1.7 MLSS

7.1.7.1 MLSS in operation phases

The range of MLSS in PBM membrane were 6.5 to 8.5 g/L with little down grading values at the end where these values with Com1 were 10 to 12 g/L with little down grading values at the end as well (Fig. 7.17). The MLSS in Com2 process was close to that of Com1. As Gunder (2001) and Krampe (2003) reported that most MBR installations work at the MLSS level of 8 – 12 g/L while at higher MLSS value the MBR process loses its economical viability due to increased viscosity of the activated sludge and poor oxygen transportation efficiency, the minimum recommended values of the MLSS was reached by PBM membrane process while Com1 and Com2 were well balanced in the range. Even at minimum MLSS values, the PBM MBR membrane worked well. The trend of the Com2 shows higher grading values.

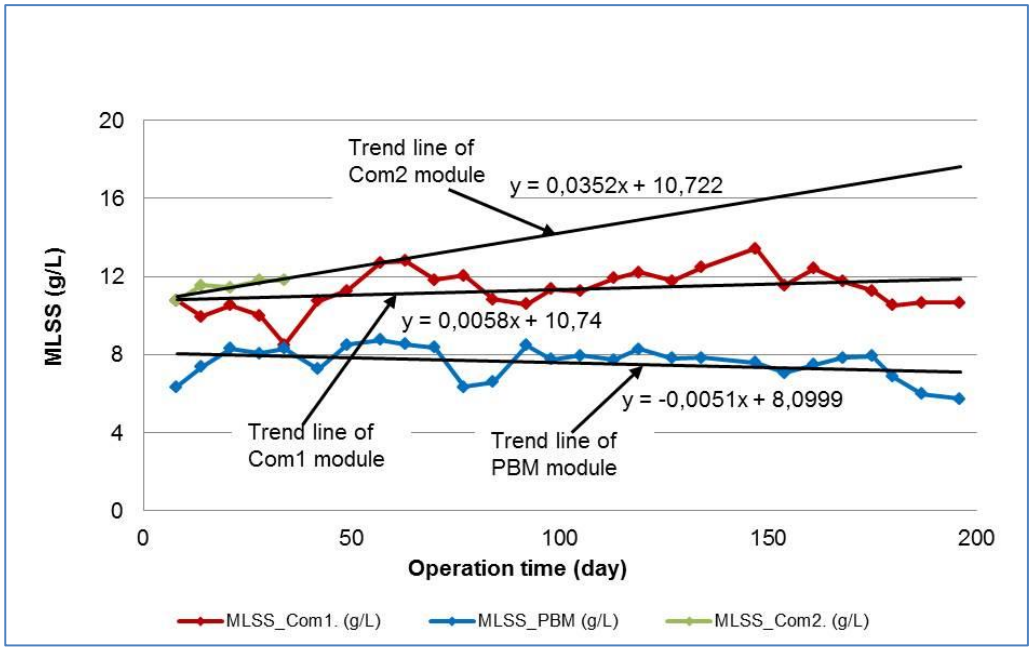

Fig. 7.17 : MLSS in different operation phases of Com1_PBM_Com2 modules

7.1.7.2 Effect of MLSS in COD removal efficiency

For MBR process it can be speculated that higher MLSS values could bring higher COD removal efficiency since higher population density of microorganisms can perform better degradation. But no effect of MLSS values in COD removal efficiency was noticed in any of the applied MBR modules especially at the end of operational phases where MLSS values were downward (Fig. 7.18).

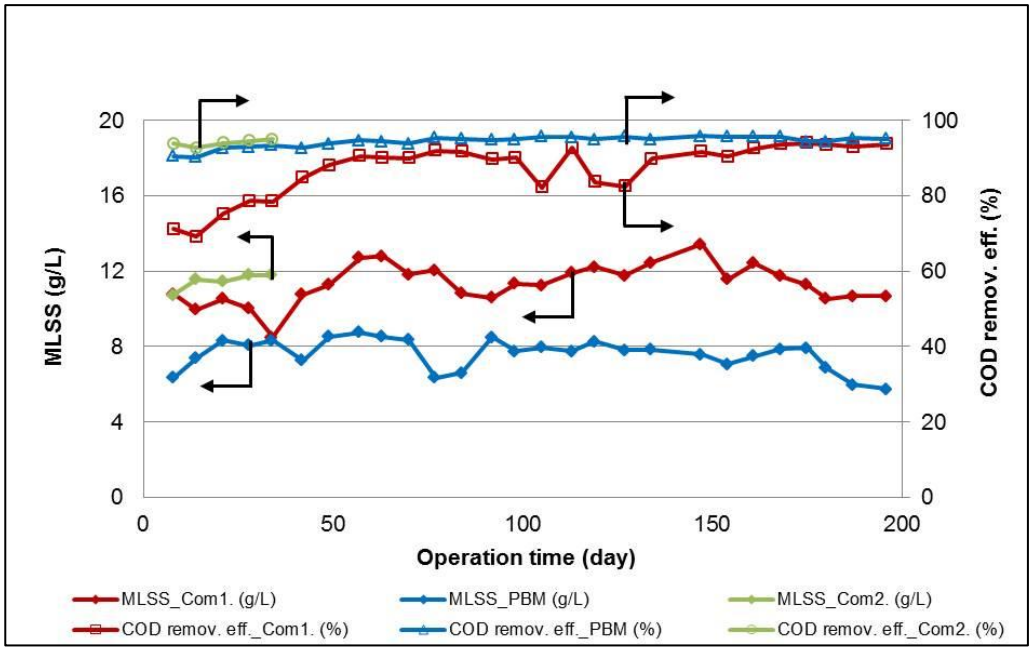

Fig. 7.18 : Effect of MLSS in COD removal efficiency in Com1_PBM_Com2 modules

7.1.8 F/M ratio

The F/M ratios of all the experiments were close to 0.1 Kg COD/Kg MLSS.d except a peak from day 29 to day 42 as shown in Fig.7.19. The F/M ratio with Com1 in day 38 increased to almost double of its normal values and the COD removal efficiencies was fluctuating accordingly. This happened due to coming out excess foam from the reactor which caused lower MLSS meaning higher F/M ratio. This fluctuation was very less and the COD removal efficiency also reduced. The Com1 started working well again after one week adapting the system. The F/M ratio with Com2 membrane was half of Com1 or PBM membrane modules but COD removal efficiency was not affected accordingly. In general, no significant influence of F/M ratio in COD removal efficiency was noticed.

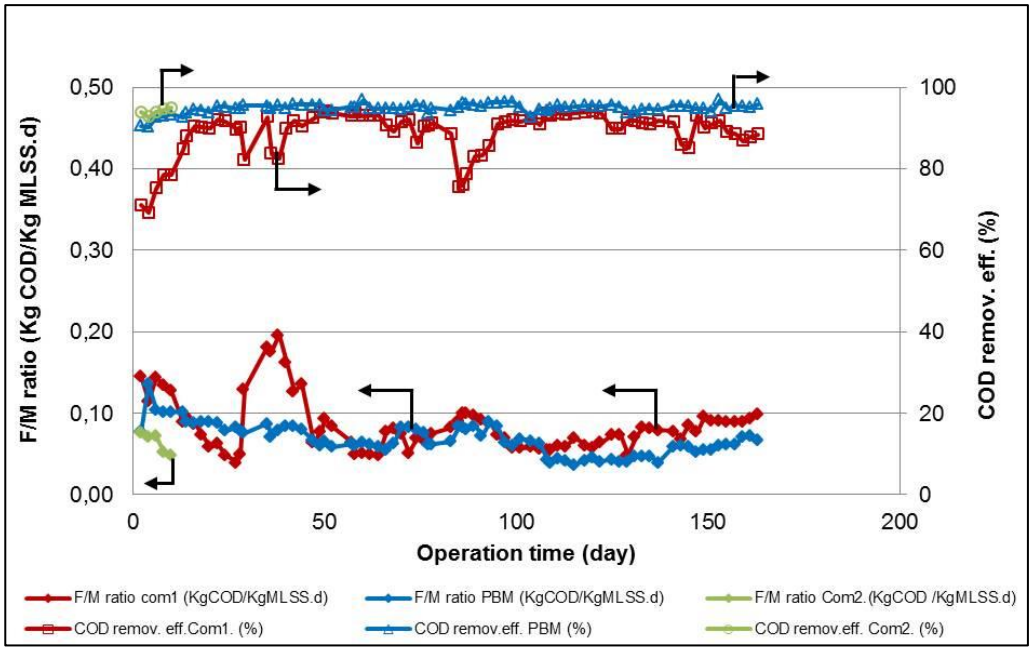

Fig. 7.19 : Effect of F/M ratio on COD removal efficiency in Com1_PBM_Com2 modules

7.1.9 Chloride (Cl^-) content

Fig. 7.20 represents the chloride concentration in Com1, PBM and Com2 membrane processes. The chloride concentration in the feed until day141 was around 1750 mg/L. Since the pore size of all of the applied membranes were not dense enough to retain Cl^-, the concentrations of Cl^- in the permeate were close to the concentration of feed which is shown in Fig.7.20. After day141, NH_4Cl was added in feed which raised the Cl^- concentration close to 2000 mg/L in the feed and the same value was also found in the permeates of Com1 and PBM membrane experimentally. The permeate Cl^- concentration in Com2 process shows the similar values like Com1 and PBM processes. These results suggest that no accumulation of Cl^- took place in the reactors.

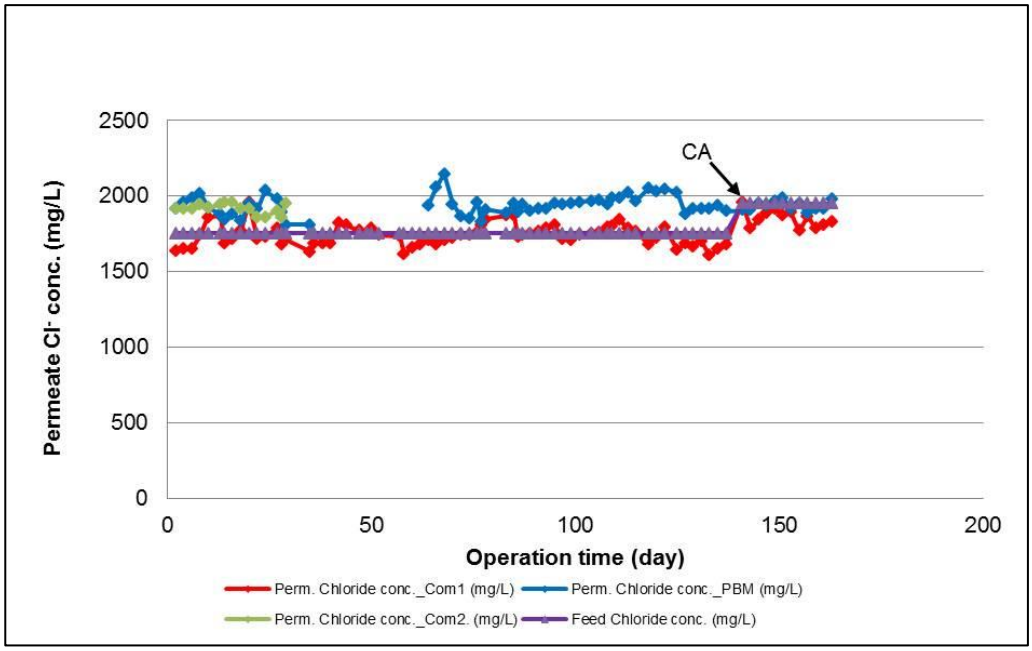

Fig. 7.20 : Cl_2 concentration in permeates of Com1_PBm_Com2 modules

N.B.:
CA: Chloride (NH_4Cl) added

7.1.10 Drying residue (DR) and electrical conductivity

Fig. 7.21 shows the drying residues (DR) and electrical conductivities of Com1, PBM and Com2 membrane processes. As DR contributes to conductivity values, it was noticed in the experiments especially with Com1 process where conductivity changed with corresponding values of DR. There were some fluctuating values with PBM and Com2 membranes which could be neglected since they were in the deviation range. In general all of these three processes show the same trend.

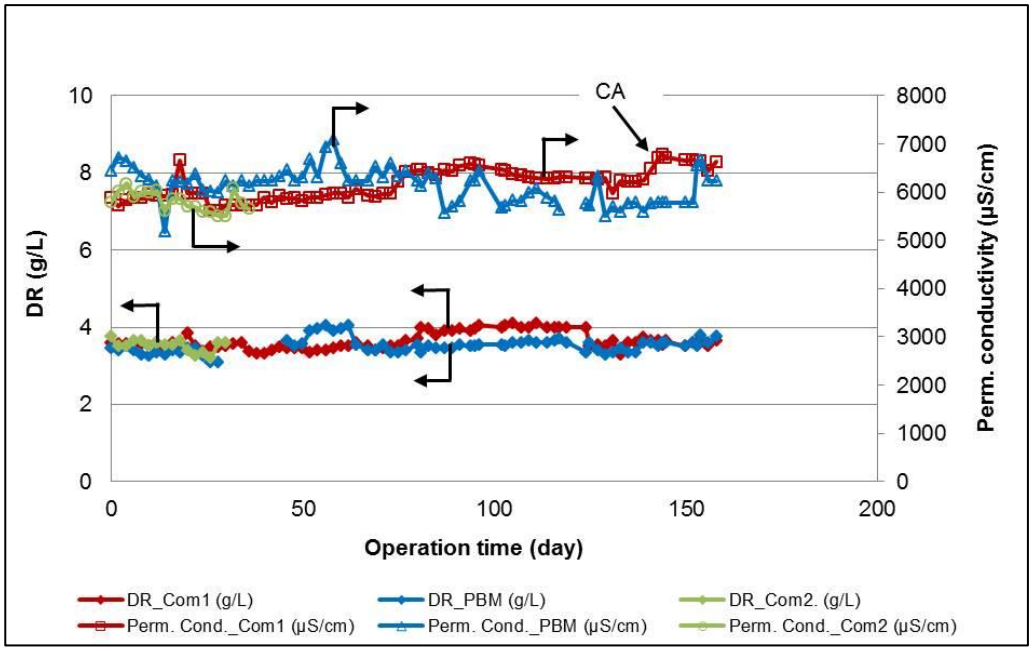

Fig. 7.21 : Permeate DR and conductivity in Com1_PBM_Com2 modules

7.1.11 pH and temperature

The Fig. 7.22, indicates permeate pH in the range of pH 7.5 to pH 8 for all of used MBR modules These pH range has been achieved through biological activities of microorganisms irrespective to feed pH values. The designed experimental temperature was 20 ± 2 °C except a little jump in Com1 process but it had no significant effect in the results obtained even at feed pH 10.5.

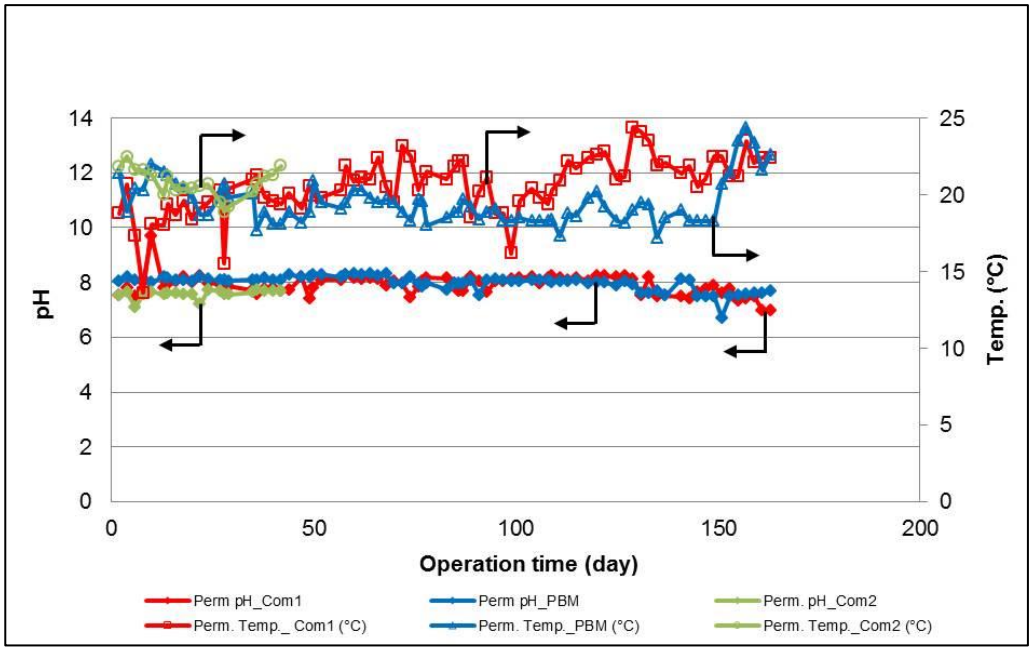

Fig. 7.22 : pH and temperature of permeates in Com1_PBM_Com2 modules

7.1.12 Critical flux (CF)

Logically critical flux is recommended to determine at the beginning of the experiment. But in this thesis critical fluxes were determined at the end of the experiments. Because, if the membrane especially the PBM module is clogged due to CF experiment, it might not be useable for further experiment.

Table 7.4 : Determination of critical flux in Com1 and PBM membranes

Time interval (min.)	Applied voltage (V)	TMP_Com1 (mbar)	Flux_Com1 (L/m².h)	TMP_PBM	Flux_PBM (L/m².h)
10	0.08	40.53	2.44	77.73	1.67
20	0.16	71.78	4.00	136.2	2.18
30	0.24	104	4.51	213.4	2.55
40	0.32	151.9	5.27	272	3.02
50	0.4	201.7	6.55	319.8	3.27
60	0.48	**247.6**	**6.73**	365.7	3.53
70	0.56	289.6	5.91	405.8	3.64
80	0.64	377.4	5.00	423.3	3.93
90	0.72	463.4	4.55	465.3	4.00
100	0.8	513.5	4.05	486.8	4.22

In this case, CF was determined following flux-step method (Bouhabila et al. 1998). To determine the critical flux (CF), the power of the suction pump (in terms of voltage) was increased gradually as shown in Table 7.4. This lead the flux increment gradually along with TMP rise. The Table 7.4 shows the obtained fluxes with TMPs in Com1 and PBM membranes.

The numerical values of flux and TMP from Table 7.4 have been transferred to graphical picture as shown in Fig. 7.23.

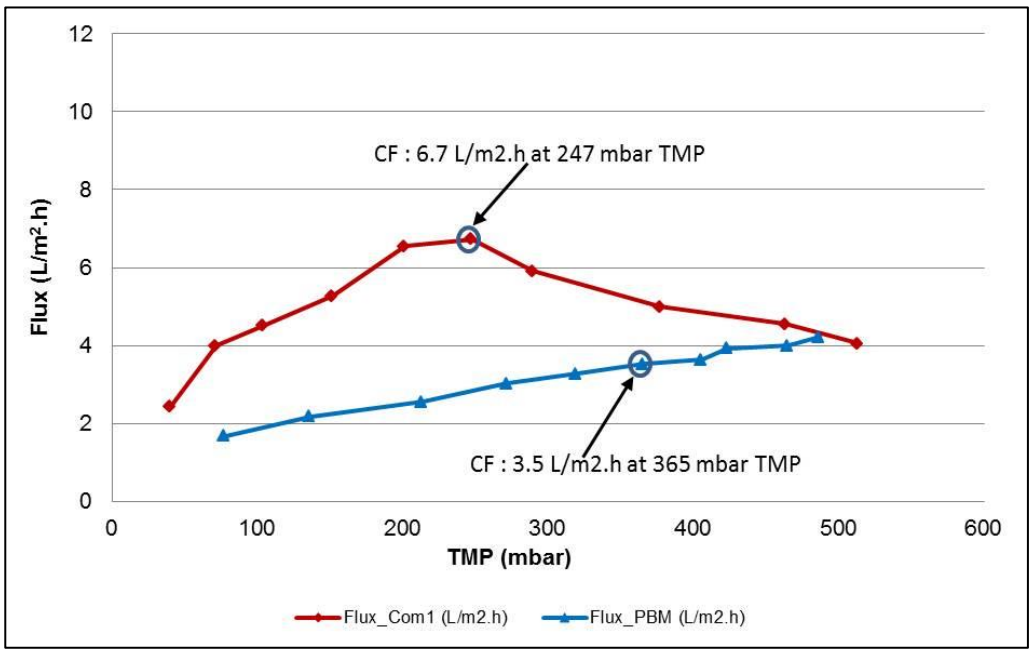

Fig. 7.23 : Critical fluxes of Com1 and PBM membranes

Fig. 7.23 shows that after maximum flux of 6.7 L/m^2.h with Com1 membrane, flux decreases with TMP beyond 350 mbar which indicates severe membrane fouling. On the other hand, flux increases with PBM beyond TMP 350 mbar but it was crossing the upper limit of TMP which was 350 mbar recommended by commercial MBR module manufacturing company Microdyn-Nadir (Germany). The maximum flux obtained experimentally with PBM membrane was 3.5 L/m^2.h with TMP close the maximum limit. So, CF of Com1 and PBM membranes were 3.5 L/m^2.h and 6.7 L/m^2.h respectively. The CF of Com2 was not determined since it was assumed that its value would be similar to that of Com1. Its worth to mention here that PBM membranes shows less prone to fouling.

7.1.13 Membrane resistance model

As described in section 5.6.13, Darcy's Law establishes a relationship between TMP and flux. In this section, the membrane in series (RIS) model has been applied in calculating membrane resistance and other resistances developing from the test media in different experimental set ups. This approach summarises the results obtained in chapter5 and chapter6 in terms of contribution of resistances to membrane fouling. The detailed description of the experimental set ups and test media have been discussed in the previous chapters (Chapter 5 and chapter6) for application of membrane resistance model. The applied total resistances of each individual test media such as humic acid (ha), model textile dye wastewater (mtdw) and MBR sludge (sludge) are given in Eq. /.1) through Eq. (7.3).

$$Rt\_f = R_m + R_{ha} \quad (7.1)$$

$$Rt\_dye = R_m + R_{mtdw} \quad (7.2)$$

$$Rt_{mbr} = R_m + R_{sludge} \quad (7.3)$$

Where,

R_m = Constant resistance of the clean membrane (1/m)
R_{ha} = Fouling resistance due to humic acid (1/m)
R_{mtdw} = Fouling resistance due to MTDW (1/m)
R_{sludge} = Fouling resistance due to MBR sludge deposited on membrane surface (1/m)

The respective resistances of both Com1 and PBM membranes were calculated using RIS model as described in section 5.6.13 and section 6.3.13 respectively. This section compares different resistances with Com1 and PBM with different test media as shown in Fig. 7.24.

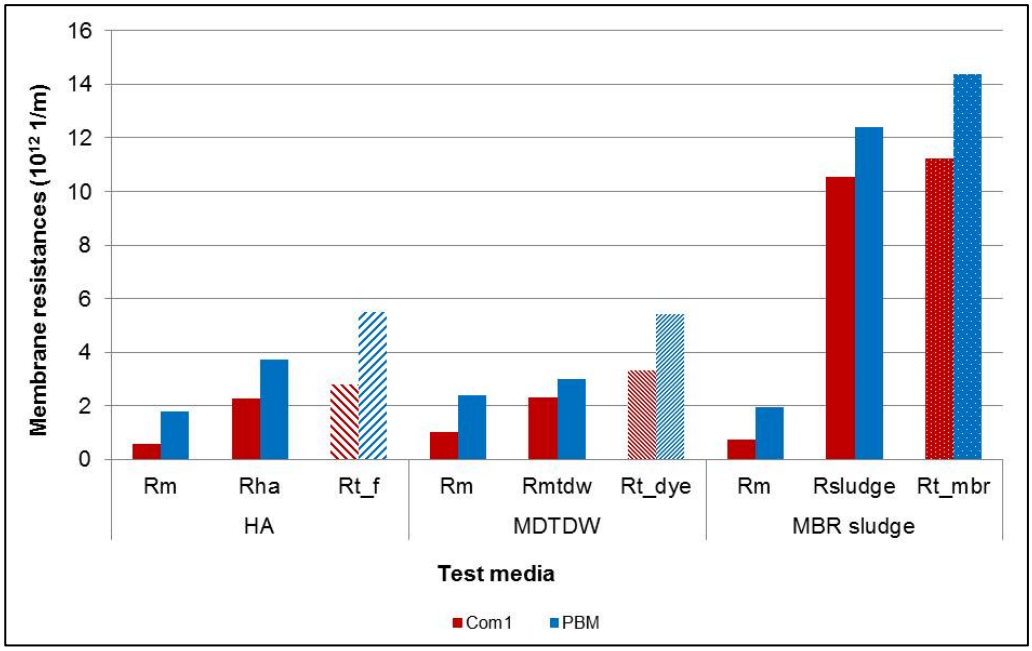

Fig. 7.24 : Numerical values of membrane resistances with different test media

The Fig. 7.24 indicates that pure membrane resistance with PBM membrane is higher compared to Com1 membrane due to its additional novel coating on it. The increase of resistances with Com1 membrane in model foulant HA, MTDW and MBR (biological) sludge are higher compared to those of PBM membranes. This indicates that PBM membrane has higher antifouling resistances. Fig.7.25 defines the individual contribution of membrane resistances to their total values in respective experiments with different test media.

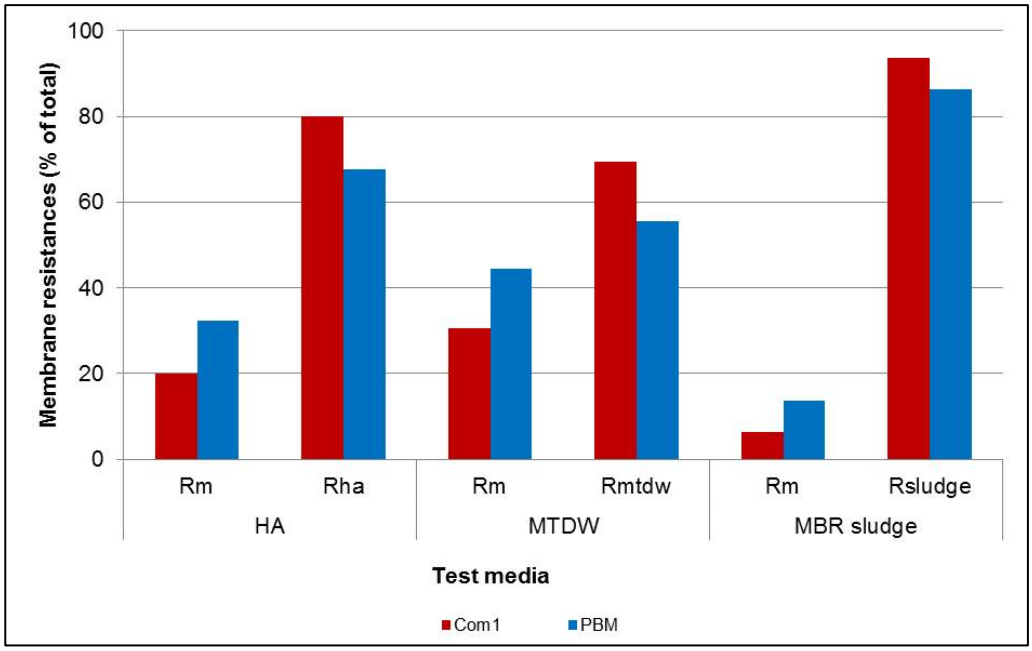

Fig. 7.25 : Individual contribution of membrane resistances with different test media

Fig. 7.25 shows that Com1 membrane contributes to 80%, 70% and 93% resistances of their total values with HA, MTDW and MBR sludge experiments respectively in their respective experiments where these values with PBM membranes are 67%, 55% and 86% respectively. This concludes that PBM membrane shows 13%, 15% and 7% less fouling resistances in HA, MTDW and MBR sludge experiment respectively. Considering the criticality of the applied test media which were responsible for membrane fouling, these can be arranged in a descending order such as MBR sludge, HA and MTDW. It suggests that MBR sludge is the most critical environment than HA and the least is the MTDW for membrane to be fouled. This finding summarises that in all of the experiments, the resistances of PBM membranes are less compared to those of Com1 which indicates that PBM membrane has higher antifouling effect.

7.2 Benefits of PBM membranes

7.2.1 Permeate quality

In terms of organic content, the higher COD/TOC reduction in permeate represents better permeate quality. The COD removal efficiencies in long term experiments with Com1 and PBM membranes were roughly 90% and 97% respectively (Fig. 7.4). On the other hand, dyes reduction in treated water is other criteria to define permeate quality. The higher is the dye rejection from permeate, the better is the permeate quality. Fig. 7.10 indicates that PBM membrane has 20% higher blue dye removal efficiency compared to PES membranes (Com1 and Com2) in the long term experiments. In terms of TOC reduction, PBM membrane shows 10% higher TOC removal efficiency compared to Com1 but it is similar with the result of Com2 which needs to be investigated for long term experiment. These outcomes conclude that PBM membrane, based on COD and dye removal efficiencies, represents better permeate quality compared to PES membrane.

7.2.2 Low fouling properties

7.2.2.1 Hydrophilicity

The contact angel of the PBM membrane reduced to 31% which was evident experimentally (Fig. 4.16). As it is described in section 2.1.3.2.3.1, reduction of contact angle indicates the higher hydrophilicity of the membrane. So, the increase of the hydrophilicity of the PBM membrane might have contributed to its low fouling properties.

7.2.2.2 Surface smoothness

The surface of the PBM membrane was very smooth which was revealed through AFM image analysis (Fig. 4.13) and root mean squared (RMS) roughness analysis (Fig. 4.14). The smoother surface of the PBM might have less prone to membrane fouling and the foulant cannot build up layer on its surface which was revealed by test with model foulant humic acid. The test with foulant HA (Section 4.2.7) represents that PBM membrane is less prone to membrane fouling with HA and it shows 59% fouling reversibility where PES membrane contributes to 11% only.

7.2.2.3 Contribution to fouling resistance

Fig. 7.25 demonstrates that the membrane resistance of PBM membrane, contributed by model foulant HA, MTDW and MBR (biological) sludge system,

are less compared to those of Com1 membrane. The results from all three experiments suggest that PBM membrane has low fouling propensity meaning high antifouling effect.

Analysing the results of MBR experiments carried out with commercial PES UF MBR module (Chapter5) and novel coated PBM MBR module (chapter6), it was found that commercial module faced severe fouling problems during the experimental period of 10 months and the modules were needed to replace by new ones. On the contrary, no replacement of novel coated PBM MBR module was needed almost for the same duration of experimental period. This finding suggests that PBM membrane has strong antifouling properties.

Since membrane fouling is regarded as the most important bottleneck for further development of MBR technology and is the main limitation for faster development, particularly when it leads to flux losses that cleaning can't restore (Howell, et al., 2004), the application of PBM membrane in MBR technology can improve the process with reduced fouling effect.

7.2.3 Antimicrobial properties

The antimicrobial properties of the PBM membrane, performed by prof. Altinkaya from Izmir Institute of Technology (IZTECH), Turkey (Section 4.2.9), which was not found in applied commercial PES UF membrane (e.g.Com1 membrane), can resist in forming Coliform Unit (CFU) on the membrane surface. This effect can reduce the cleaning cycle of the membrane and ultimately can increase the life cycle of the membrane resulting in reduced operation cost. After 6 months of MBR experiments with commercial PES MBR module and novel coated PBM MBR module, it was noticed that the commercial module was densely covered with biological sludge (Fig. 7.26) while the PBM module was comparatively clean (Fig. 7.27). It can be concluded that PBM membrane prevented microorganisms in creating bacterial colony on the membrane surface which might kept the surface clean.

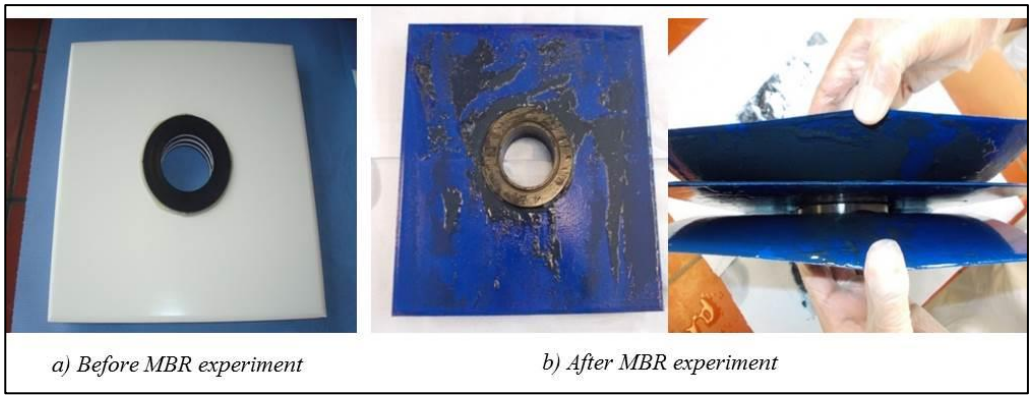

Fig. 7.26 : PES MBR modules

Fig. 7.27 : PBM MBR modules

Since the membrane surface may not covered by bacterial colony (in other words biological sludge), it may require less aeration intensity used for scouring purpose. This may also lead to reduced operation cost.

7.2.4 Process robustness

The PBM membrane developed by casting novel coating on the active surface of PES UF membrane is highly stable. This means, once the coating is polymerised, it becomes inseparable part of the PES UF membrane and can't be washed off under different operation conditions. After 6 months experiments with PBM MBR module in MBR technology, some analyses were done to check if the coating still exists. The root mean squared (RMS) roughness measurements by AFM analysis shows that RMS values of PES MBR mem-

brane and PBM MBR membrane are 24 nm and 10 nm respectively (Fig.7.28). These values are bit higher than those of unused membranes (Section 4.2.1, Fig. 4.14) which might have created due to biological sludge. If there would be no existence of novel coating with PBM MBR membrane after 6 months of experiments, its RMS values might have increased up to the similar value of PES MBR membrane but it didn't happen. It suggests that novel coating with PBM membrane still exists.

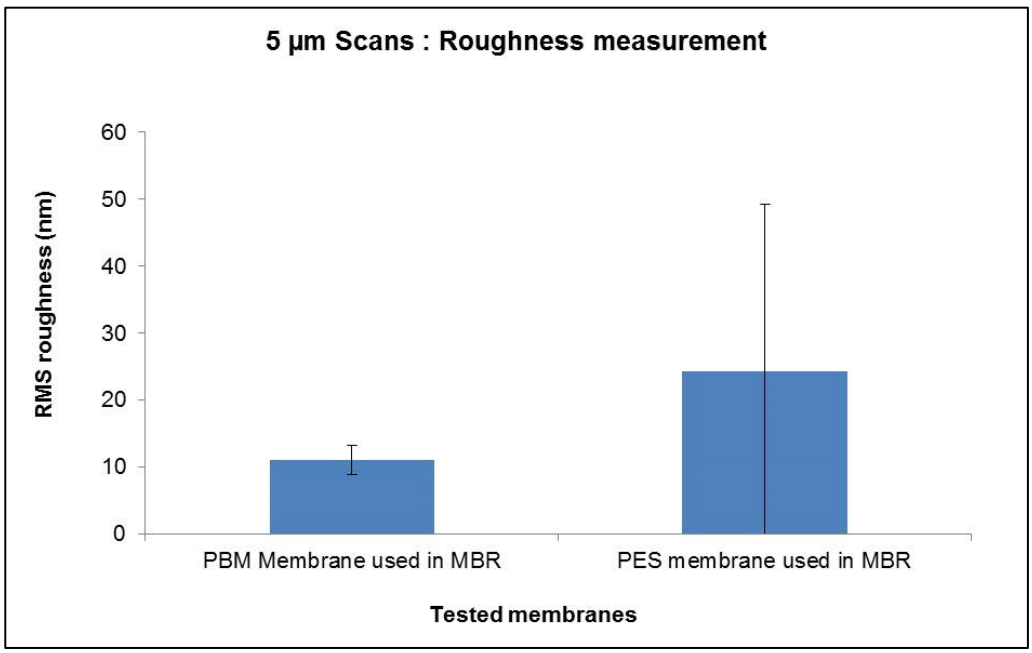

Fig. 7.28 : RMS roughness values (nm) of the used membranes in MBR application

Following the similar protocol as described in section 4.2.9, the antimicrobial activity of the used (used for 6 months in MBR experiments) PES and PBM membranes were tested. This test was performed by prof. Altinkaya from Izmir Institute of Technology (IZTECH), Turkey. Some portion of the used membranes, both from Com1 and PBM MBR modules, were subjected to 3 hours of pre-incubation with 60 CFU E.Coli bacteria and then incubated overnight on Mueller Hinton agar plates at 37°C. Though used PES UF membrane (Com1 membrane) didn't show any antimicrobial activity, it was used as a reference. The next step involved swabbing sample from the membrane surface after 24h incubation period with E. Coli bacteria and visualizing the collected sample on white cotton of the swab to determine whether bacterial growth has taken place or not. Due to dark blue colour of the used membranes, it was hard to count the

number of colonies, yet it was possible to observe whether bacterial layer exist or not (Fig. 7.29).

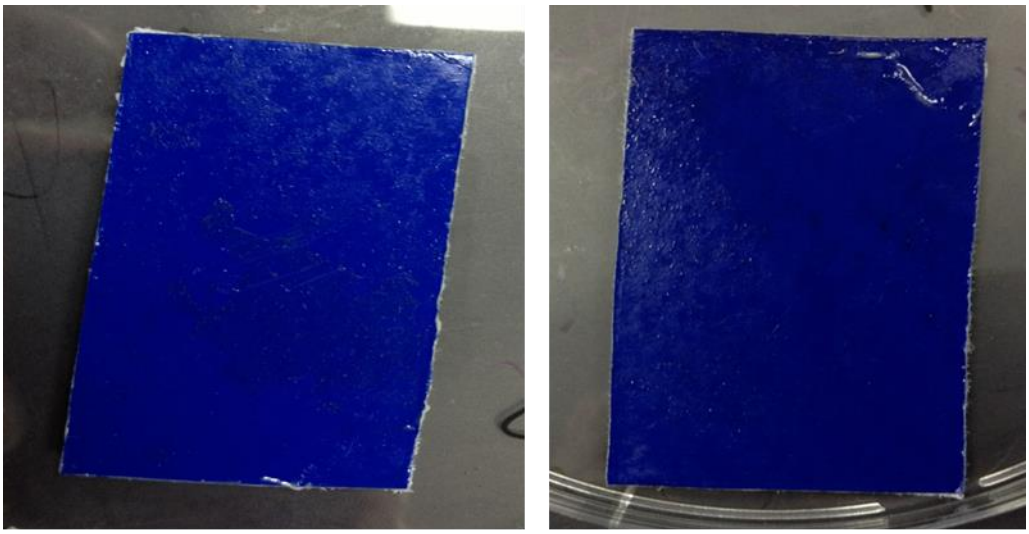

Fig. 7.29 : a) Used PES membrane presenting no antibacterial activity; b) Used PBM membrane presenting high antimicrobial activity

From this experiment it can be concluded that, the presence of bacteria on the surface of the used Com1 membrane was similar to that of clean Com1 membrane (Section 4.2.9) but no accumulation of bacteria was observed on the surface of the used PBM membrane. This finding suggests that PBM membrane was showing antibacterial properties like as pristine PBM. This gives the evidence that the coating still exists. In summary, the findings described here and including other performances such as constant high COD removal efficiency, antifouling properties, process stability etc. support the robustness of the PBM MBR process.

7.2.5 Energy consumption

The energy consumption for MBR process accounts for around 66% for aeration purpose splitting into 34% aeration for membrane scouring and 42% aeration for bioprocess (Hribljan, 2007). In addition, the aeration aims to perform two functions:

- Supplying oxygen to microorganisms
- Scouring membrane surface against fouling

The aeration rate can be varied based on the oxygen uptake rate (OUR) by microorganisms and scouring effect. Section 7.1.6 describes that the oxygen uptake rate by PBM membrane module was less compared to commercial PES MBR module (Com1 membrane) based on available dissolved oxygen (DO) which was contributed by the applied aeration rate. Fig. 7.15 shows that at aeration rate of 0.5 ± 0.05 m^3/h, the DO was in the range of 2 – 4 mg/L in PBM process and its performance (e.g. COD removal efficiency) was not affected. But the performance of Com2 membrane deteriorated (i.e. COD removal efficiency) at the aeration rate of 0.5 ± 0.05 m^3/h since its contributed DO might not be enough to perform the regular activities of bioprocess. This finding suggests that energy consumption in terms of air supply in PBM process might be reduced to 50%. This topic should be further studied.

On the other hand, since the PBM membrane showed antimicrobial properties; it was comparatively clean (Section 7.2.3). Therefore, the aeration rate could be reduced (not shown in this thesis) for scouring purpose which may reduce the energy in PBM process additionally.

In general, the areas of the membrane modules used for all experiments were 0.33 m^2. It was just used for initial experiment. For detailed discussion on energy saving the experiment with larger module is needed.

7.2.6 Techno-Economical analysis of the applied processes

Section 4.2.2 demonstrates that pore size was reduced with PBM membrane to 25% compared to its pristine PES membrane. The molecular weight cut off (MWCO) of the PBM membrane reduced to 64% compared to PES membrane as described in section 4.2.4. The pore size of the PBM membrane can be tuned by varying the temperature of microemulsion during polymerization and its chemical compositions. Following these process flexibilities PBM membranes with different pore size can be prepared based on their applications. Since the PBM layer is very thin (1 to 10 µm), a small amount of microemulsion was required to produce PBM coated membrane which is low in preparation but high in benefits. The cationic surfactant AUTEAB used in preparing PBM membrane shows antimicrobial properties which represents high resistant against biofouling especially in MBR applications. Due to very smooth and

hydrophilic surface of the PBM membrane, it has high antifouling effect as demonstrated by several tests with model foulant HA in a UF cross-flow testing cell (Section 4.2.7) and with MTDW in MBR experiments (Chapter 5 and Chapter 6). Due to low fouling and antimicrobial properties of the developed PBM membrane (Section 7.2.2, section 7.2.3), less cleaning frequency could be required and the membrane life span could be enhanced significantly. This could significantly reduce the operation cost. The constant trend of productivity (water permeability in this case) and higher rejection of organic compounds (e.g. COD rejection in this case) compared to applied PES membrane, were another benefit of the PBM membrane. The requirements of oxygen consumption by PBM incorporated MBR process in the long run operation was less than the PES MBR process without compromising its higher COD removal efficiency. This finding indicates the demand of less aeration which may save operation cost since aeration cost in MBR process contributes to the highest operation cost.

Table 7.5 : Benefits of PBM membrane over commercial PES membrane

Process parameters	Unit	Tested membranes		Comments
		PES	PBM	
Water permeability	L/m².h.bar	60	35	Roughly half of PES
COD removal efficiency	%	90	97	7% higher COD removal efficiency by PBM membrane
Low fouling properties		nil	- Higher hydrophilicity - Higher surface smoothness - Lower fouling resistances	PBM is a Low fouling novel membrane
Fouling reversibility	%	Very less (11%)	Very high (59%)	Life span of PBM could be increased
Process robustness		nil Two times membrane changed in 6 months operation	High No membrane replacement was needed for 6 month operations	PBM membrane could be less prone to membrane fouling and it is a Highly robust process
Antimicrobial effects		No antimicrobial properties	Highly antimicrobial properties and it exists even after 6 months of MBR experiments	PBM membranes shows high antimicrobial effects which might be benefited in low fouling properties
Energy consumption for membrane scouring		Reduced performance at reduced rate (0.5 m³/h)	Optimum performance even at reduced aeration rate (0.5 m³/h)	Energy for aeration supply with PBM membrane could be reduced
Aeration rate	m³/h	1	0.5	PBM membrane cane be operated at reduced air supply
Cleaning cycle		4 times per year	may be one time per year	Economic advantage with PBM membrane
Saving of maintenance cost	%	no saving	- 50% saving from aeration for scouring - 75% saving from membrane cleaning and replacement (estimated)	Maintenance cost in PBM membrane can be reduced significantly

7.3 Outlook for PBM membrane preparation

The process like preparing microemulsion, adding initiators, casting microemulsion etc used for preparing PBM membranes were not automated process but a hand-made operation. Since the hand-made operation can't be every time 100% reproducible, this may affect the properties of the prepared membrane and its performances. After adding initiators and before casting the microemulsion, the time frame (4-5 minutes) was critical. The viscosity of the microemulsion which increases rapidly based on the concentration of added initiators and temperature plays an important role in generating the morphology of the membrane. The viscosity increase was noticed only by eye estimation within the mentioned time frame and in considerable increased viscosity conditions microemulsion was casted. This part of the PBM membrane preparation was critical because several times microemulsion got polymerised inside the preparing flask within this time frame which might have occurred due to temperature increase in the microemulsion leading the quicker viscosity rise. Another factor is the application of the casting knife. It's really very hard to keep the speed of the casting knife movement constant each time the membrane is prepared. This option may affect the morphology of the prepared membrane and its performance. Because, if the speed of the casting knife movement is high, the coating thickness can be different than if the speed is reduced. Because, at the latter case, microemulsion can have more time to contribute in viscosity rise during polymerisation. After 3rd time cleaning of the PBM tested with model foulant humic acid (HA), it shows that some part is darker while others are lighter (Section 4.2.7.2, Fig. 4.22). This might have occurred due to non-homogeneity of the membrane surface. The effect of temperature rise in microemulsion viscosity also needs to be investigated in future research.

The membrane modules used in all of the experiments were small and these were used just for initial tests. If the membrane module is scaled-up to larger applications, those can't be prepared by hand made process due to some limitations as mentioned above. In this case, the processes like mixing chemicals for microemulsion, determining temperature and viscosity of the microemulsion, controlling the speed of the casting knife, controlling the rate of inert gas, checking the inertness of the casting chamber needs to be optimized through process automation.

References

Bouhabila, E.H., Aim, B. R., Buisson, H. (1998), Microfiltration of activated sludge using submerged membrane with air bubbling application to wastewater treatment, Desalination 118 (1998) 315 - 322

Günder, B. (2001). "The Membrane Coupled-Activated Sludge Process in Municipal
Wastewater Treatment." Technomic Publishing Company Inc., Lancaster, USA

Hach Lange, 2013, http://www.hachlange.ma, accessed on November 23, 2013

Hribljan, Michel J. (2007), Large MBR Design and Residuals Handling, WEF Webcast, June 12.

Howell, J.A., Chua, H.C., Arnot, T.C. (2004), In situ manipulation of critical flux in a submerged membrane bioreactor using variable aeration rates and effects of membrane history, Journal of Membrane Science, Vol 242 (2004) 13-19

Huang, R.R., Hoinkis, J., Hu, Q., Koch, F. (2009), Treatment of dyeing wastewater by hollow fiber membrane biological reactor, J. Desalination and Water Treatment, 11, 1 - 6

Judd, S. (2006), The MBR Book: Principles and Applications of Membrane Bioreactors in Water and Wastewater Treatment, editor, Elsevier

Krampe, J., and Krauth, K. (2003), Oxygen transfer into activated sludge with high MLSS concentrations. Water Science and Technology 47**,** 297-303.

8. Chapter 8 : Conclusion and Outlook

8.1 Conclusion

This PhD thesis deals with the development of membrane bioreactor (MBR) process based on novel low fouling membranes towards developing novel MBR process. As reported in different literature, there are several ways to develop hybrid/novel MBR process like integrating powdered activated carbon (PAC), biofilm carrier etc. to conventional MBR process and lifting their overall performance ((Mulder et al., 2007; Ravindran et al., 2009; Liu et al., 2010 and Yang et al., 2009). To achieve the novelty of the process in this thesis, the applied commercial membrane used in the MBR module was modified by nano-structured novel coating through polymerisable bicontinuous microemulsion (PBM) process. This results in higher antifouling, antimicrobial properties, higher COD and higher textile dye (blue) removal efficiency. The progress of the membrane bioreactor process development was subdivided into several phases:

- In the early stage of the research phase, a suitable option for modifying the commercial membrane was investigated. ITM-CNR, Italy did extensive research in this sector. After lot of investigations and scientific research, the process for preparing novel coating on a commercial PES UF membrane via polymerisable bicontinuous microemulsion (PBM) was developed (Chapter 4). Based on this developed process several novel coated membranes were prepared and characterised to select the right membranes for MBR module preparation. The ultimate goal was to compare the results between commercial MBR and novel coated MBR and to ascertain the novelty of the process.
- To reach the target, experiments with commercial MBR module (PES UF MBR module) were performed continuously in a lab-scale pilot plant for around 10 months (Chapter 5). This task was conducted in parallel with novel membrane preparations and characterisations. A model textile dye wastewater (MTDW) with the view of having constant compositions with respect to time was used as test media for all experiments. All the experiments were carried out with selected suitable operation conditions (Section 5.4).
- For the MBR experiments with the commercial PES UF MBR module, 6 sheets of novel coated membranes with size of 30 cm × 30 cm were

prepared and these were laminated to a 3 enveloped MBR module of 25 cm × 25 cm in size similar to the applied commercial MBR module with the support of membrane module manufacturing company, Microdyn-Nadir (Germany).

- After the MBR experiments with the commercial membrane were completed, the commercial MBR module was replaced by the novel coated MBR module and the experiments were carried out under the selected operating conditions for 6 months (Chapter 6).
- The results from two different kind of MBR modules in experimental sequences such as MBR with commercial membrane (Com1) →MBR with novel coated membrane (PBM) →again MBR with commercial membrane (Com2) were compared in terms of water permeability, permeate quality, COD/TOC removal efficiency, textile dye removal efficiency, antifouling/antimicrobial properties, N-balance, fouling resistance, process robustness and oxygen consumption (Chapter 7). The performance analysis showed that PBM incorporated novel coated MBR module compared to the commercial MBR module has 7% points higher COD removal efficiency, 20% points higher blue dye removal efficiency, high antifouling/antimicrobial properties, requires less energy in terms of aeration and economically viable highly robust process. In summary, all these benefits directs towards achieving the aim of the thesis, an upgraded MBR process due to application of novel low fouling membrane.

8.2 Outlook

Despite the demonstrated benefits of PBM coated MBR module, still process optimization is needed to achieve enhanced performances. The following recommendations can be made for further improvement of MBR process based on PBM coated membrane splitting into two sub-sections such as membrane coating process and MBR process:

MBR process

- The water permeability of PBM coated MBR module is roughly half of the applied commercial MBR module. After the coating the membrane resistance of PBM coated membrane increased to 3 times higher compared to commercial PES membrane (Section 5.6.13 and section 6.3.13). The extra coating of PBM membrane has created resistance resulting in lower permeability. The PBM coating was prepared by hand-

made process and the thickness of the coating was defined by casting knife. The hand-made casting process should be replaced by an automated one to achieve uniformity and reproducibility of the process. The thickness of the PBM coating should be kept as low as possible in order to keep water permeability high.

- The hydraulic retention time (HRT) of the carried out experiment was very high and it should be reduced in future work. The MBR process needs to be optimized varying the applied process. The poor nitrification was obtained in all applied MBR processes and a further study on this topic is needed.

Membrane coating process

- The quantification of the attached foulants (humic acid) needs to be done by XRD or other standard process. During the characterization of PBM coated membrane it was noticed that it has less attachment of model foulant (HA) compared to applied commercial membranes, which indicates the high antifouling properties of the coated membrane (Section 4.2.7.2). It was examined by eye assisted visualization (Fig. 4.22) and cross-sectional SEM image analysis (Fig. 4.23) to understand the fouling thickness layer but no element analysis was done
- The casting chamber needs to be 100% N_2-saturated excluding any trace of air/O_2 during polymerization because presence of air/O_2 hinders the polymerization process. Air/O_2 was excluded from the flask of microemulsion applying a stream of N_2 for 1 minute at 1 bar applied pressure (Fig. 4.8). For preparing PBM coated novel membrane in this thesis work, redox initiator was added to the microemulsion at the last stage of the preparation process and it was done outside of the casting chamber, though it lasts for few seconds. This step might have created the chance for microemulsion to become in contact with air/O_2. This might be a reason of varying polymerization time and performances that occurred sometimes (Section 7.3). The process for addition of redox initiators to microemulsion should be optimized in such a way that the trace of air/O_2 is excluded from the experimental set up.
- N_2 gas supplied for creating N_2-saturated environment in casting chamber was performed roughly for 1 minute at 1 bar pressure. It was assumed that the chamber was saturated with N_2 gas. This process needs to be optimized installing N_2 gas sensor/instrument to be ensured that the chamber is 100% N_2-saturated excluding air/oxygen.

- After adding redox initiator, the viscosity of the microemulsion increases. For preparing PBM coated membrane within this thesis, it was waited for 4 – 5 minutes after adding initiator to achieve suitable intermediate viscosity of the microemulsion. The development of viscosity increase was only monitored by naked eye; no instrument/sensor was used to quantify the value. Sometimes it happened that the microemulsion polymerized inside the flask of microemulsion or the microemulsion was too much liquid even in the same time frame. The reason of these occurrences needs to be investigated. This step of the preparation process also needs to be optimized using viscosity meter to define the right viscosity for casting process. The suitability of the application of UV photo initiator needs to be checked for scaled-up novel preparation process.

In summary, this thesis represents the development and application steps of a membrane bioreactor (MBR) with PBM coated novel low fouling membrane. The experiments with PBM coated MBR module were carried out for 6 months. After the experiment of this duration, the novel coating on the active surface of the commercial membrane still existed which was revealed by experimental investigations. The presented lab scale novel low fouling based MBR worked excellent in laboratory scale experiment and it can readily be deployed in industrial site to be tested with real test media. However, this technology can still be improved as recommended in this section to keep pushing the technology until expected achievements are reached.

References

Liu, Q, Wang, X.C., Liu, Y, Yuan, H., Du, Y. (2010), Performance of a hybrid membrane bioreactor in municipal wastewater treatment, Desalination 258, 143 - 147

Mulder, J. W., Braunersreuther, M., Schonewille, H., Jager, R. D. and Veraart, A. (2007), Hybrid MBR for industrial reuse of domestic wastewater in the Netherlands

Ravindran, V., Tsai, H.H., Williams, M.D., Pirbazari, M. (2009), Hybrid membrane bioreactor technology for small water treatment utilities: Process evaluation and primordial considerations, Journal of Membrane Science 244, 39 - 54

Yang Q., Y., Yang, T., Wang, H., J. and Liu, K. Q. (2009), Filtration characteristics of activated sludge in hybrid membrane bioreactor with porous suspended carriers (HMBR), Desalination 249, 507 - 514

Scientific activities of Shamim Ahmed Deowan

Academic experiences

Supervising:

Supervisor of the following theses/semester research projects in the field of Chemical Process Engineering at Karlsruhe University of Applied Sciences:

i) Lubna Jahan, (2013), Investigating the effects of Hydraulic Retention Time (HRT) and oxygen consumption in Membrane Bioreactor (MBR) towards developing novel MBR process, Master thesis, July, 2013, Karlsruhe Univesity of Applied Sciences, Germany

ii) Ting Yu, (2013), Treatment of Model Textile Dye Wastewater (MTDW) by Submerged Membrane Bioreactor (MBR) Technology, Master thesis, August, 2013, Karlsruhe Univesity of Applied Sciences, Germany

iii) Shahid Abbas, (2013), Measurement of Biochemical Oxygen Demand (BOD), Semester project2, March, 2013, Karlsruhe University of Applied Sciences, Germany

iv) Bernhard Wagner (2012), Membrane Bioreactor and Model Textile Dye Wastewater Treatment, Bachelor thesis, April, 2012, Karlsruhe Univesity of Applied Sciences, Germany

v) Lubna Jahan, (2012), Process of determining individual dye concentration from mixed solution of two different dyes, semester project2, October, 2012, Karlsruhe University of Applied Sciences, Germany

vi) Sachin Kalyanrao Mirkale (2012), Rejection of Textile Dye by Membrane Technology, October, 2012, Karlsruhe University of Applied Sciences, Germany

vii) Lubna Jahan, (2011), Determining chemical composition of model dye textile wastewater, semester project1, November, 2011, Karlsruhe University of Applied Sciences, Germany

viii) Abdelhakim El Fadil, (2011), Membrane Bioreactor (MBR) as an advanced technology for Olive Mill Wastewater (OMW) treatment, Master thesis, November, 2011, Karlsruhe University of Applied Sciences, Germany

Attendence to courses and conferences/Publications

Course attendence:

Attending to GRICU PhD National School 2011- Methematical Methods for Chemical Engineering/Nanotechnologies from 26th September, 2011 until 1st October, 2011, at Santa Margherita di Pula, Italy.

Publications:

Patent:

Alberto Figoli, Jan Hoinkis, Bartelo Gabriele, Giorgio De Luca, Francesco Galiano, **Shamim Ahmed Deowan**, worldwide patent titled as "BICONTINUOUS MICROEMULSION POLYMERIZED COATING FOR WATER TREATMENT", registration number IT GE2013A000096, filed on 27.09.2013.

Journal publications:

1. **Shamim Ahmed Deowan**, Francesco Galiano, Jan Hoinkis, Alberto Figoli, Enrico Drioli, Submerged Membrane Bioreactor (SMBR) for Treatment of Textile Dye Wastewater towards Developing Nobel MBR Process, APCBEE Procedia 5 (2013) 259-264
2. **S.A. Deowan**, B. Wagner, C. Arsipathi, J. Hoinkis, A. Figoli, E. Drioli et al, Treatment of model textile dye wastewater (MTDW) towards developing novel submerged membrane bioreactor process, Procedia Engineering 44(**2012**) 1768-1771
3. Jan Hoinkis, **Shamim A. Deowan**, Volker Panten, Alberto Figoli, Rong Rong Huang and Enrico Drioli, Membrane Bioreactor (MBR) Technology – A Promising Approach for Industrial Wastewater Reuse, Procedia Engineering 33 (**2012**) 234-241

Conference publications (Oral):

1. **S. A. Deowan**, F. Galiano, L. Jahan, C. Aresipathi, S.I. Bouhadjar, A. Figoli, J. Hoinkis, B. Gabriele, E. Drioli, (2013), Performances of Low Fouling Novel Submerged Membrane Bioreactor (NSMBR) in Textile Dye Wastewater Treatment, International Conference "Nanomemwater 2013", Izmir, Turkey, October 8th – October 10th, 2013

2. S.I.Bouhadjar, **S.A.Deowan**, F. Galiano, J. Hoinkis, M. Zenad, A. Figoli, (2013), Side-stream MBR for Model Textile Wastewater Treatment Using Commercial and Novel Membranes, International Conference "Nanomemwater 2013", Izmir, Turkey, October 8th – October 10th, 2013
3. A. Figoli, F. Galiano, **S.A. Deowan**, B. Gabriele, J. Hoinkis (2013), A New Class of Functional Membranes to Lower Fouling and Improve Rejections of Pollutants, International Conference "Nanomemwater 2013", Izmir, Turkey, October 8th – October 10th, 2013.
4. **S.A. Deowan**, F. Galiano, L. Jahan, S.I. Bouhadjar, C. Aresipathi, A. Figoli, J. Hoinkis, B. Gabriele, E. Drioli, (2013), SCMA 2013 Annual Conference" Water – In the Best of Times, In the Worst of Times" San Antonio, Texas, USA, July 31 – August, 2, 2013
5. **Shamim Ahmed Deowan**, Francesco Galiano, Jan Hoinkis, Alberto Figoli, Enrico Drioli, Submerged Membrane Bioreactor (SMBR) for Treatment of Textile Dye Wastewater towards Developing Nobel MBR Process, ICESD 2013, January 19-20, 2013, Dubai, UAE
6. F. Galiano, **S. A. Deowan**, Alberto Figoli1, J. Hoinkis, L. Veltri, B. Gabriele, Performance Test of Novel Membrane Regarding Water Permeability, Fouling Behavior and Dye Rejection, proceedings of the First International WATERBIOTECH Conference, October 9-11, 2012, National Research Center (NRC), Cairo, Egypt
7. **S.A. Deowan**, W. Korejba, C. Aresipathi, J. Hoinkis, A. Figoli, E. Drioli, R. Islam (2011) Design and testing of a pilot scale submerged membrane bioreactor (MBR) for textile wastewater treatment, ICChE 2011, December 29-30, 2011, BUET, Bangladesh

Conference Publications (Poster):

1. **S. A. Deowan**, F. Galiano, L. Jahan, S.E. Bouhadjar, C. Aresipathi, B. Gabriele, J. Hoinkis, A.Figoli, E. Drioli, Novel Nano-structured Membrane Materials for Membrane Bioreactor (MBR) Applications, BioNexGen 2nd training workshop, 15-17 May, 2013, Cetraro, Italy
2. F. Galiano, A. Figoli, **S. A. Deowan**, J. Hoinkis, L. Veltri, B. Gabriele, Novel hydrophilic membranes for wastewater treatment, BioNexGen 2nd training workshop, 15-17 May, 2013, Cetraro, Italy
3. C.Aresipathi, **S. A. Deowan**, J. Hoinkis, A.S.Beobide, J. Anastasopoulos, G. Voyiatzis, T. karachalios, K. Kouravelou, Membranes with Functionalized Carbon Nanotube pores: Synthesis, Characterization and application to model textile waste water, BioNexGen 2nd training workshop, 15-17 May, 2013, Cetraro, Italy

4. **S.A. Deowan**, B. Wagner, T. Yu, A. Zhao, L. Jahan, C. Aresipathi, J. Hoinkis, A. Figoli, E. Drioli Treatment of Model Textile Dye Wastewater (MTDW) towards Developing Novel Submerged Membrane Bioreactor Process, poster P3047 Euromembrane 2012, 23-27 September, Queen Elizabeth II Conference Centre, London, UK

Acknowledgement

I would like to acknowledge my profound indebtedness to my first supervisor Prof. Enrico Drioli, Department of Chemical Engineering, University of Calabria, Italy, for his continuous guidance and enormous assistance to implement this thesis and for providing informative suggestions to make this report a fulfilled one.

My endless gratefulness is to my second supervisor Dr. Alberto Figoli, a senior research scientist, Institute on Membrane Technology (ITM-CNR), Italy, to help me in creating an opportunity to carry out this cooperative PhD thesis under his supervision and to guide me through valuable suggestions and comments.

I am whole-heartedly life span owed to my third supervisor Prof. Jan Hoinkis, Deparment of Sensor Systems Technology, Faculty of Electrical Engineering and Electronics, Karlsruhe University of Applied Sciences, Germany who brought me from an industrial platform to an academic foreground and provided all kinds of assistances such as technical directions, valuable suggestions, critical comments, foreign research attachments, supports for conference attendance etc. needed for making this thesis works successful.

I would like to convey my special thanks to my colleague, PhD student Francesco Galiano, Institute on Membrane Technology (ITM-CNR), Italy for his endless supports in various fields starting from technical aspects (novel membrane developments, characterisation etc.) to social activities which made my research attachments in ITM-CNR technically sound and comfortable.

I am grateful to Dr. Daniel Johnson from Swansea University, UK; Prof. Alsoy Sacide Altinkaya from Izmir Institute of Technology (IZTECH), Turkey and Prof. Mauro Carraro and his research team from University of Padova, Italy for their supports in membrane characterisation and testing (partial) carried out for the thesis works.

I express my thankful attitude to the BioNexGen (grant agreement no. CP-FP-246039-2) EU-FP7/project for its financial support to carry out the thesis works.

I am grateful to my master thesis students (for whom I was the supervisor) Bernhard Wagner, Ting Yu and Lubna Jahan for their contributions in experiments and data generation.

I am also intended to thank the members of the research team in Karlsruhe University of Applied Sciences, Germany named as Dr. Catherine Aresipathi, PhD student Saadia Ilhem Bouhadjar, researcher Margaritta Aleksandrova, Aleksandrov Krazimir, Florian Fiedler, Michel Wartha, Torsten Kühle, the stuffs from the Institute on Applied Research (IAF) and the rest of the members from the department of sensor systems technology.

I would also like to express my thankfulness to the members of the research team in ITM-CNR, Italy namely Dr. Alessandra Criscuoli, Dr. Giorgio De Luca, PhD student Federica Bisignano, Dr. Lidietta Giorno and the rest of the members from ITM-CNR, Italy.

I am very much delightful to my wife, Shahin who constantly supported me with great patience for the progress of my thesis works and sometimes managed the pain of loneliness during my absences for attending conferences outside of our residing country. I would also like to express my gratefulness to my 6 year old lovely son Sablil who got limited leisure time from me due to the load of thesis works and missed me a lot during my absences for attending conferences. I would also like to thank my elder brother Babul Akter who supported me like as my father.

Finally, I would like to thank to all of my friends, relatives and the rest of my family members and all well-wishers to provide me mental support to be successful in this work.

As author I bear the responsibility for all interpretations, opinion and errors in this report.

Abbreviations

ADUF	Aerobic digester ultrafilration
AFM	Atomic force microscopy
anMBR	Anaerobic membrane bioreactor
AOP	Advanced Oxidation Process
APS	Ammonium persulfate
ASP	Activated sludge process
AUTEAB	Acryloyloxyundecyltriethyl ammonium bromide
BAC	Biologically activated carbon
BAT	Best available technology
BOD	Biochemical oxygen demand
CA	Cellulosic acetate
CAS	Conventional activated sludge
CF	Critical flux
CFV	Cross-flow velocity
CIA	Cleaning in air
CIP	Cleaning in place
COD	Chemical oxygen demand
Cl_2	Chloride
DI	Deionised
DR	Drying residue
DO	Dissolved oxygen
EGDMA	Ethylene glycol dimethacrylate
EPS	Extra-cellular polymeric substances
F/M	Food to microorganism ratio
FS	Flat sheet
GAC	Granular activated carbon
HA	Humic acid
HEMA	2-Hydroxylethyl methacrylate
HF	Hollow fibre
HRT	Hydraulic residence time
H_2O_2	Hydrogen peroxide

IC	Inorganic carbon
IDWTP	Integrated dyeing wastewater treatment plant
iMBR	Immersed MBR
kDa	Kilodalton
LiP	Lignin peroxidases
MBR	Membrane bioreactor
MLD	Million liters per day
MLSS	Mixed liquor suspended solids
MMA	Methyl methacrylate
MnP	Manganese dependent peroxidases
MnO_4	Permanganate
MPE	Membrane performance enhancer
MPR	Membrane photocatalytic reactor
MST	Membrane sewage treatment
MT	Multitubular
MTDW	Model textile dye wastewater
MW	Molecular weight
MWCO	Molecular weight cut off
NaOCl	Sodiumhypochloride
NF	Nanofiltration
NH_4^+–N	Nitrogen concentration in ammonia
NO_3^--N	Nitrogen concentration in nitrate
NO^{2-}-N	Nitrogen in nitrite
NOM	Natural organic matter
O_3	Ozone
OH	Hydroxide
PAC	Powdered activated carbon
PAN	Polyacrylonitrile
PBM	Polymerisable bicontinuous microemulsion
PE	Polyethylene
PES	Polythersulfone
PET	Polyethylene terephthalate
PVC	Polyvinylchloride
PVDF	Polyvinylidene difluoride
PP	Polypropylene

PS	Polysulfone
PTFE	Polytetrafluoroethelene
RIS	Resistance in membrane series
RO	Reverse osmosis
RO16	Reactive orange 16
SBR	Sequencing batch reactor
SEM	Scan electronic microscopy
SL	Sludge loading
sMBR	Side stream MBR
SMP	Soluble microbial products
SMPc	Soluble microbial products concentration
SRT	Sludge retention time
SSF	Solid state fermentation
TC	Total carbon
TOC	Total organic carbon
TMP	Transmembrane pressure
TMEDA	Tetramethylethylene diamine
TN	Total nitrogen
UF	Ultrafiltration
UV	Ultraviolet
WHO	World health organisation
WP	Water permeability
WWTPs	Wastewater treatment plant
ZW	ZeeWeed

Nomenclature

A	Absorbance
b	Path length or cuvette width (cm)
c	Concentration (mg/L)
C	Instant oxygen concentration (mg/L)
C_s	Saturated oxygen concentration (mg/L)
c_v	Coefficient of variation
d	Diameter of the pore (mm)
g	Acceleration due to gravity (m/s^2)
J	Membrane permeate flux ($L/m^2.h$)
K	The Kozeny-Carman constant
K_{La}	Mass transfer coefficient
N	The number of pores per square unit of membrane
Δp	Pressure difference (bar)
R_m	Membrane resistance for pure water filtration across the membrane (1/m)
R_e	Internal fouling resistance (1/m)
R_c	Cake layer resistance (1/m)
R_p	Resistance due to concentration polarizsation (1/m)
R_i	Resistance due to pore blocking (1/m)
R_t	Total filtration resistance (1/m)
S	The internal surface area (m^2)
s	Standard deviations
T	Temperatue (°C), a constant
α	Alpha factor
Δx	Pore length (mm)
$\bar{x}$	Mean value
η	Liquid viscosity
ε_s	Surface porosity
τ	Tortuosity facor
ε_v	The volume fraction or volume porosity of the pores
ρ	Density (kg/m^3)
η, μ	Dynamic viscosity of permeate ($N.s/m^2$)
ϵ	Molar absorptivity constant (L/cm. mg)
Φ	Typical constant, the values in the range of 1.015 to 1.040

Appendices

Appendix A	LabVIEW Control program
Appendix B	Formula for standard deviation and coefficient of variation (accuracy) calculation

Appendix A LabVIEW Control program

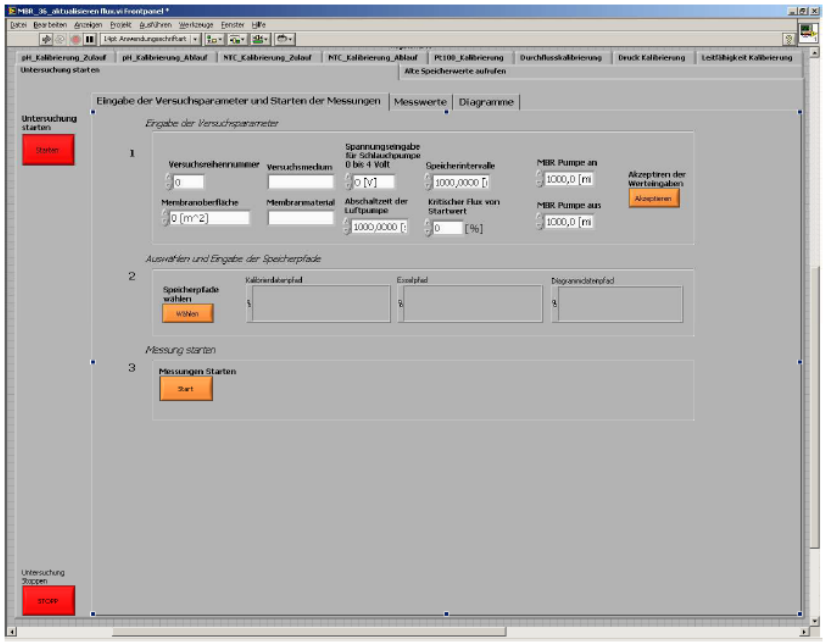

a) Data control sysstemw

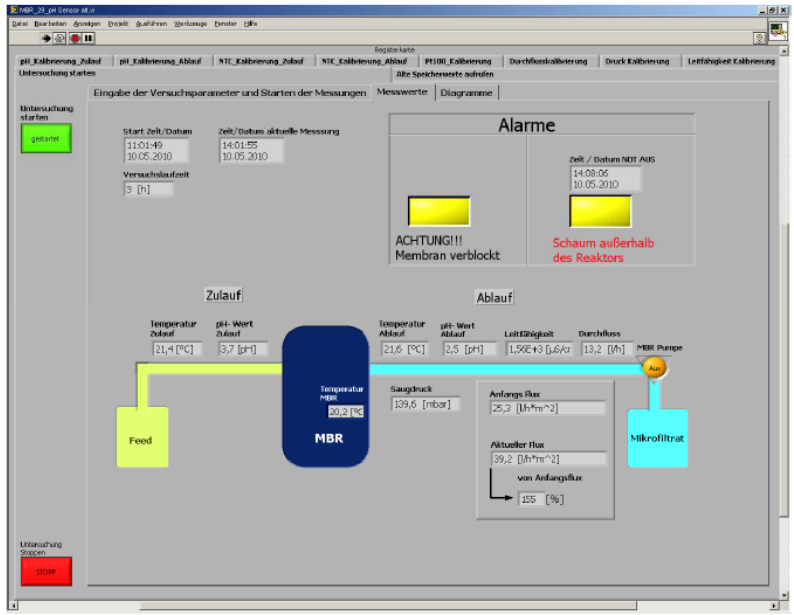

b) Process parameters displace

Figure: LabVIEW control system (Wlamir Korejba, 2010, Sectiion 3.4)

Appendix B

Formula for standard deviation and coefficient of variation (accuracy) calculation

Standard deviation

The most commonly used estimator is a modified version of standard deviation, the sample standard deviation. The following equation was consulted to obtain the standard deviation involved in error discussion. It is denoted as *s* and defined as (Kuester and Thiel, 1993):

$$s = \sqrt{\frac{1}{N-1}\sum_{\mathrm{i}=1}^{N}(x_{\mathrm{i}} - \bar{x})^2}$$

Where, x_1, x_2, x_3, …,x_n are the obtained values of analyses conducted and $\bar{x}$ is the mean value of this observations.

Coefficient of variation

The coefficient of variation c_v is a measure of a probability distribution. It is defined as the ratio of standard deviation *s* to the mean $\bar{x}$ (Kuester and Thiel, 1993):

$$c_v = \frac{s}{\bar{x}}$$

This equation consulted to estimate the coefficients of variation (Cv) in percentage regarding the error discussion. Here the C_v indicates the accuracy/error of the measuring instruments.